

PHYTOPATHOLOGIA MEDITERRANEA

Plant health and food safety

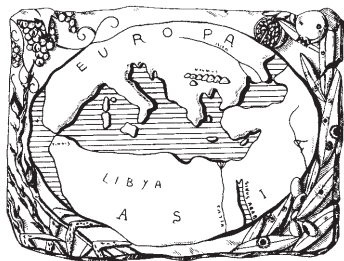
Volume 62 • No. 1 • April 2023

Isritto al Tribunale di Firenze con il n° 4923 del 5-1-2000 - Poste Italiane Spa - Spedizione in Abbonamento Postale - 70% DCB FIRENZE



The international journal of the
Mediterranean Phytopathological Union

FI
FIRENZE
UNIVERSITY
PRESS



PHYTOPATHOLOGIA MEDITERRANEA

Plant health and food safety

The international journal edited by the Mediterranean Phytopathological Union
founded by A. Ciccarone and G. Goidànich

Phytopathologia Mediterranea is an international journal edited by the Mediterranean Phytopathological Union. The journal's mission is the promotion of plant health for Mediterranean crops, climate and regions, safe food production, and the transfer of knowledge on diseases and their sustainable management.

The journal deals with all areas of plant pathology, including epidemiology, disease control, biochemical and physiological aspects, and utilization of molecular technologies. All types of plant pathogens are covered, including fungi, nematodes, protozoa, bacteria, phytoplasmas, viruses, and viroids. Papers on mycotoxins, biological and integrated management of plant diseases, and the use of natural substances in disease and weed control are also strongly encouraged. The journal focuses on pathology of Mediterranean crops grown throughout the world.

The journal includes three issues each year, publishing Reviews, Original research papers, Short notes, New or unusual disease reports, News and opinion, Current topics, Commentaries, and Letters to the Editor.

EDITORS-IN-CHIEF

Laura Mugnai – University of Florence, DAGRI, Plant pathology and Entomology section, P.le delle Cascine 28, 50144 Firenze, Italy
Phone: +39 055 2755861
E-mail: laura.mugnai@unifi.it

Richard Falloon – New Zealand Institute for Plant & Food Research (retired)
Phone: +64 3 337 1193 or +64 27 278 0951
Email: richardfalloon@gmail.com

CONSULTING EDITORS

A. Phillips, Faculdade de Ciências, Universidade de Lisboa, Portugal
G. Surico, DAGRI, University of Florence, Italy

EDITORIAL BOARD

I.M. de O. Abrantes, Universidad de Coimbra, Portugal
J. Armengol, Universidad Politécnica de Valencia, Spain
S. Banniza, University of Saskatchewan, Canada
A. Bertaccini, Alma Mater Studiorum, University of Bologna, Italy
A.G. Blouin, Plant & Food Research, Auckland, New Zealand
R. Buonauro, University of Perugia, Italy
R. Butler, Plant & Food Research, Christchurch, New Zealand
N. Buzkan, Imam University, Turkey
T. Caffi, Università Cattolica del Sacro Cuore, Piacenza, Italy
J. Davidson, South Australian Research and Development Institute (SARDI), Adelaide, Australia
A.M. D'Onghia, CIHEAM/Mediterranean Agronomic Institute of Bari, Italy
A. Eskalen, University of California, Davis, CA, United States
T.A. Evans, University of Delaware, Newark, DE, USA

A. Evidente, University of Naples Federico II, Italy
M. Garbelotto, University of California, Berkeley, CA, USA
L. Ghelardini, University of Florence, Italy
V. Guarnaccia, University of Turin, Italy
N. Iacobellis, University of Basilicata, Potenza, Italy
H. Kassemeyer, Staatliches Weinbauinstitut, Freiburg, Germany
P. Kinay Teksür, Ege University, Bornova Izmir, Turkey
A. Lanubile, Università Cattolica del Sacro Cuore, Piacenza, Italy
A. Moretti, National Research Council (CNR), Bari, Italy
L. Mostert, Faculty of AgriSciences, Stellenbosch, South Africa
J. Murillo, Universidad Publica de Navarra, Spain
J.A. Navas-Cortes, CSIC, Cordoba, Spain
L. Palou, Centre de Tecnologia Postcollita, Valencia, Spain
E. Paplomatas, Agricultural University of Athens, Greece

I. Pertot, University of Trento, Italy
A. Picot, Université de Bretagne Occidentale, LUBEM, Plouzané, France
D. Rubiales, Institute for Sustainable Agriculture, CSIC, Cordoba, Spain
J-M. Savoie, INRA, Villenave d'Ornon, France
A. Siah, Yncréa HdF, Lille, France
A. Tekauz, Cereal Research Centre, Winnipeg, MB, Canada
D. Tsitsigiannis, Agricultural University of Athens, Greece
J.R. Urbez Torres, Agriculture and Agri-Food Canada, Canada
J.N. Vanneste, Plant & Food Research, Sandringham, New Zealand
M. Vurro, National Research Council (CNR), Bari, Italy
A.S. Walker, BIOGER, INRAE, Thiverval-Grignon, France
M.J. Wingfield, University of Pretoria, South Africa

DIRETTORE RESPONSABILE

Giuseppe Surico, DAGRI, University of Florence, Italy
E-mail: giuseppe.surico@unifi.it

EDITORIAL OFFICE STAFF

DAGRI, Plant pathology and Entomology section, University of Florence, Italy
E-mail: phymed@unifi.it, Phone: ++39 055 2755861/862

EDITORIAL ASSISTANT - **Sonia Fantoni**

EDITORIAL OFFICE STAFF - **Angela Gaglier**

PHYTOPATHOLOGIA MEDITERRANEA

**The international journal of the
Mediterranean Phytopathological Union**

Volume 62, April, 2023

Firenze University Press

***Phytopathologia Mediterranea*. The international journal of the Mediterranean Phytopathological Union**

Published by

Firenze University Press – University of Florence, Italy

Via Cittadella, 7–50144 Florence–Italy

<http://www.fupress.com/pm>

Direttore Responsabile: **Giuseppe Surico**, University of Florence, Italy

Copyright © 2023 **Authors**. The authors retain all rights to the original work without any restrictions.

Open Access. This issue is distributed under the terms of the [Creative Commons Attribution 4.0 International License \(CC-BY-4.0\)](https://creativecommons.org/licenses/by/4.0/) which permits unrestricted use, distribution, and reproduction in any medium, provided you give appropriate credit to the original author(s) and the source, provide a link to the Creative Commons license, and indicate if changes were made. The Creative Commons Public Domain Dedication (CC0 1.0) waiver applies to the data made available in this issue, unless otherwise stated.



Citation: J. Jorben, A. Rao, S. Nagappa Chowluru, S. Tomar, N. Kumar, C. Bharadwaj, B. Siddanagowda Patil, K. Ram Soren (2023) Identification of multi-race Fusarium wilt resistance in chickpea (*Cicer arietinum* L.) using rapid hydroponic phenotyping. *Phytopathologia Mediterranea* 62(1): 3-15. doi: 10.36253/phyto-13352

Accepted: January 31, 2023

Published: April 6, 2023

Copyright: © 2023 J. Jorben, A. Rao, S. Nagappa Chowluru, S. Tomar, N. Kumar, C. Bharadwaj, B. Siddanagowda Patil, K. Ram Soren. This is an open access, peer-reviewed article published by Firenze University Press (<http://www.fupress.com/pm>) and distributed under the terms of the Creative Commons Attribution License, which permits unrestricted use, distribution, and reproduction in any medium, provided the original author and source are credited.

Data Availability Statement: All relevant data are within the paper and its Supporting Information files.

Competing Interests: The Author(s) declare(s) no conflict of interest.

Editor: Juan A. Navas-Cortes, Spanish National Research Council (CSIC), Cordoba, Spain.

ORCID:

JJ: 0000-0002-5978-1142
AR: 0000-0002-4317-2596
ST: 0000-0002-0292-3613
NK: 0000-0003-4908-2249
CB: 0000-0002-1651-7878
BSP: 0000-0001-5203-8244
KRS: 0000-0002-1604-7490

Jawahar Jorben and Apoorva Rao are joint first authors

Research Papers

Identification of multi-race Fusarium wilt resistance in chickpea (*Cicer arietinum* L.) using rapid hydroponic phenotyping

JAWAHAR JORBEN¹, APOORVA RAO¹, SRINIVASA NAGAPPA CHOWLURU², SAKSHI TOMAR², NEERAJ KUMAR¹, CHELLAPILLA BHARADWAJ^{1,*}, BASAVANAGOWDA SIDDANAGOWDA PATIL¹, KHELA RAM SOREN³

¹ Division of Genetics, ICAR-Indian Agricultural Research Institute (IARI), New Delhi, India

² Division of Plant Pathology, ICAR-Indian Agricultural Research Institute (IARI), New Delhi, India

³ ICAR-Indian Institute of Pulses Research (IIPR), Kanpur, India

*Corresponding author. E-mail: drchbharadwaj@gmail.com

Summary. Fusarium wilt, caused by *Fusarium oxysporum* f. sp. *ciceris* (Padwick) Matuo and K. Sato is a major cause for low productivity of chickpea. Presence of multiple pathogenic races makes it difficult for the breeder to screen for Fusarium wilt resistance. Twenty-two chickpea genotypes were grown in Hoagland solution and inoculated with five different *F. oxysporum* races two isolates of each race), including host and pathogens from the major chickpea growing region of India. The resistant chickpea line “WR 315” showed a “highly resistant” reaction, and the susceptible line “JG 62” showed a “highly susceptible” reaction across all pathogen races and isolates. However, the parent lines “Pusa 372” and “JG 11” showed “susceptible” reactions, while the marker-assisted backcrossing (MABC) lines of “Pusa 372” (IL.11,12,14) and “JG 11” (IL.15,16,17) were superior for assessed characters (lengths of roots and shoots, fresh and dry weights), and were highly resistant to most races. This is the first study to use race specific screening of MABC lines using hydroponic host culture in chickpea.

Keywords. Chickpea introgression lines, marker-assisted backcrossing, phenotyping.

INTRODUCTION

Chickpea (*Cicer arietinum* L.) is a major cool season grain legume of global importance grown in approx. 57 countries (Merga and Haji, 2019). *Cicer arietinum* is a diploid ($2n = 16$), annual, self-pollinated plant and with a genome size of approx. 738 Mb (Varshney *et al.*, 2013). The Middle East region between southeast Turkey, northwest Iran and parts of Syria, are the likely the primary centre of origin of this food crop plant. Chickpea is grown in a total of 13.7 million hectares (Mha) each year, with total grain production of world 14.3 million tons (MT) (FAOSTAT, 2020). In India, 8.35 M ha of chickpea are grown each year with 7.17 MT produced (DAFW, 2019). For

self-sufficiency in India, 16 to 17.5 MT production is required from the present 10.5 M ha area, and average required productivity of 1500 to 1700 kg ha⁻¹ (Dixit *et al.*, 2019, Hickey *et al.*, 2019).

Major constraints of chickpea production and productivity are biotic and abiotic stresses. Within biotic stresses, *Fusarium oxysporum* f. sp. *ciceris* (Padwick) Matuo and K. Sato (Foc), which causes Fusarium wilt, is the most important potential pathogen, which causes yield losses ranging from 10 to 100% (Jimenez-Diaz *et al.*, 1989, Sharma *et al.*, 2005). High pathogen variability makes development of disease resistant cultivars. Yellowing and wilting pathotypes of Foc have been reported based, on pathogenicity tests with eight physiological races (Haware and Nene, 1982; Trapero-Casas and Jimenez Diaz, 1985). Among them, race 0 and 1B/C cause host yellowing, and 1A, 2, 3, 4, 5, and 6 cause wilting, all the races have distinct geographical distributions (Jiménez-Díaz *et al.*, 2015). Foc isolates from chickpea growing in Indian states were highly variable compared to international isolates, with each state having more than one race. Chickpea cultivars tested on a new differential set revealed eight new Foc races in India (Dubey *et al.*, 2012). The soilborne pathogen can survive for many years in the absence of hosts, which poses serious drawbacks for cultivar phenotyping and Fusarium wilt management (Haware *et al.*, 1996). Pathogen variability and mutability result in losses of host resistance, and these remain the main hurdles for plant breeders aiming to develop effective disease resistance (Barve *et al.*, 2001).

Current assessments of host phenotype characteristics for disease resistance in breeding programmes mainly rely on visual scoring of disease under plot or micro plot, artificial inoculation conditions, and screening at disease hotspot locations. These methods are time-consuming, laborious, and expensive, and generate bias in recording of field data. Screening for Fusarium wilt under open field conditions is difficult, complex, inefficient, and unreliable, for screening large numbers of host lines, as results are influenced by environment, host and genetic factors. Effective and reliable phenotyping for *Fusarium* is therefore important to rapidly identify host resistance, and pathogen racial patterns, with limited environmental influences.

Hydroponics techniques have become the most efficient and reliable for screening large numbers of host germplasm lines (Amalraj *et al.*, 2019). These methods avoid dependency on soil to provide essential elements for host growth (Sheikh *et al.*, 2006). Using hydroponic systems, nutrition, pH, temperature, and dissolved oxygen can be closely controlled (Thompson *et al.*, 1998). As well, marker assisted backcross breeding can target

specific wilt resistance traits for selection against donor genomes in gene introgression, and can more effectively use molecular markers than conventional backcrossing (Varshney *et al.*, 2014; Bharadwaj *et al.*, 2021). Marker assisted backcrossing (MABC) is a precise and effective technique to introgress single loci that control traits of interest while retaining other important characteristics of recurrent parents (Collard and Mackill, 2008).

The present study was designed to use the hydroponic techniques for race specific screening of MABC lines against *Fusarium* race isolates, to identify levels of resistance in chickpea hosts at seedling stages.

MATERIALS AND METHODS

Plant material

An *in-planta* infection technique was used to screen chickpea lines for wilt resistance. This was carried out on hydroponically grown seedlings, which were inoculated with virulent Foc conidia. Twenty-two host genotypes were used in this study, including one resistant line “WR 315” (Millan *et al.*, 2006; Halila *et al.*, 2010), one susceptible line “JG 62” (Haware *et al.*, 1992; Ali *et al.*, 2002), two parents (JG 11 and Pusa 372) and their MABC introgression lines, along with the three genotypes ILCO (from Latvia), ILCO (from Czechoslovakia) and BGD112, were used in this study (Table 1). All of these introgression lines are advanced BC₃F₃ lines, which contain proposed lines for advanced varietal trial (AVT 1) of the All India Coordinated Research Program (AICRP) on Chickpea. A total of six SSR markers, including TA110, TA37, TR19, GA16, TA27, TA96 reported to be in the cluster containing genes conferring FW resistance on the linkage group CaLG02, were used to identify polymorphic markers for parental polymorphism (Millan *et al.*, 2006).

Pathogen multiplication and conidium production

Two representative isolates from each of five different Foc races, distributed across the major chickpea growing regions of India (Central zone, South zone, Northwest plain zone, and Northeast plain zone) were obtained from the Pulse Pathology laboratory, Division of Plant Pathology, ICAR-IARI New Delhi. These isolates were identified for each race and based on differential responses, and the isolates were characterized into five races based on a new set of differential cultivars (C 104, JG 74, CPS 1, BG 212, WR 315, KWR 108, GPF 2, DCP 92-3, Chaffa and JG 62). A total of 70 isolates of

Table 1. Chickpea genotypes, and introgression line numbers used in this study.

Sr. No.	Genotype	Introgression line No.
1	Pusa 372	-
2	WR 315	-
3	(*3Pusa 372///(Pusa 72/ WR 315)	1
4	(*3Pusa 372///(Pusa 72/ WR 315)	3
5	(*3Pusa 372///(Pusa 72/ WR 315)	5
6	(*3Pusa 372///(Pusa 72/ WR 315)	8
7	(*3Pusa 372///(Pusa 72/ WR 315)	9
8	(*3Pusa 372///(Pusa 72/ WR 315)	15
9	(*3Pusa 372///(Pusa 72/ WR 315)	18
10	(*3Pusa 372///(Pusa 72/ WR 315)	22
11	(*3Pusa 372///(Pusa 72/ WR 315)	25
12	(*3Pusa 372///(Pusa 72/ WR 315)	27
13	(*3Pusa 372///(Pusa 72/ WR 315)	28
14	(*3Pusa 372///(Pusa 72/ WR 315)	34
15	(*3JG 11///(JG 11/ WR 315)	37
16	(*3JG 11///(JG 11/ WR 315)	39
17	(*3JG 11///(JG 11/ WR 315)	42
18	JG 11	-
19	JG-62	-
20	ILCO (Czechoslovakia)	-
21	ILC0 (Latvia)	-
22	BGD 112	-

Foc were characterized, representing the pathogenic and morphological groups of 640 isolates which had been collected from the 13 important chickpea growing states in India. The common cultivars used by Jimenez-Diaz *et al.* (2015) and Dubey *et al.* (2012) were C104, G74, CPS1, BG212, WR315 and JG 62. Earlier studies based on old differentials showed the presence of eight races of the pathogen, of which only races 1A, 2, 3 and 4 were reported in India (Haware and Nene, 1982).

The international differentials developed during 1982, and these needed to be modified with a new set of chickpea cultivars, to keep up with the changed pathogen population (Dubey and Singh, 2008; Dubey *et al.*, 2010). Dubey *et al.* (2012) used a modified set of new differentials that categorised isolates into eight races instead of the four races reported in India by Haware and Nene (1982). Of these eight races, the five most virulent and widely distributed were used to screen genotypes in the present study. Previous research did not study virulence of different isolates to groups of differentials, and utilised molecular characterization which relied on information available in the literature correlated with molecular groups for which virulence infor-

Table 2. Races and origins of *Fusarium oxysporum* f. sp. *ciceris* used in this study, including regions of collection (Dubey *et al.*, 2012).

Race	Isolate code	Region (place of collection in India)
R1	118	ICRISAT, Hyderabad, Telangana
	121	Dharwad, Karnataka
R2	119	IIPR, Kanpur, Uttar Pradesh
	129	IIPR, Jhansi, Madhya Pradesh
R3	31	Faridkot, Punjab
	45	Ludhiana, Punjab
R4	153	JNKV, Jabalpur, Madhya Pradesh
	108	IARI, New Delhi
R5	4	RAS, Jaipur, Rajasthan
	6	RAS, Durgapur, Rajasthan

mation was available. These same sets of isolates were utilised for molecular characterization by four different molecular markers, including random amplified polymorphic DNA, universal rice primers, simple sequence repeats, and intersimple sequence repeats. These four sets of markers exhibited 100% polymorphism, and based on the unweighted paired group method with arithmetic average analysis, the isolates were in eight groups based on genetic similarities from 37 to 40% (Dubey *et al.*, 2012) (Table 2).

The isolates were each grown on Selective *Fusarium* Agar (SFA) in Petri dishes, and incubated at $28 \pm 2^\circ\text{C}$ for 7 d. Four SFA discs of each Foc race isolate were transferred into 20% (v/v) selective *Fusarium* broth for conidium production. Conidium concentration was assessed using a hemocytometer, and average concentrations of 3.2×10^6 conidia per mL^{-1} were used for inoculations.

Hydroponics and host growth conditions

Chickpea seeds were disinfected for 5 min in commercial bleach (0.042% (w/v) sodium hypochlorite) added to deionized water, and were rinsed well in running tap water. The seeds were then imbibed at 4°C for 48 h. Imbibed seeds were then germinated in 10% aerated nutrient solution on mesh in the dark for 3 d. Seven d-old seedlings were then transferred to continuously aerated 25% nutrient solution to grow the seedlings under sterile hydroponic conditions on floats in sterile water containing macro- and micro-nutrients (half-strength Hoagland's nutrient medium) (Hoagland and Arnon, 1950). For the first week, half strength nutrient solution was used, and was then gradually increased to full strength nutrient solution after 10 d. Control sets of seedlings were grown Hoagland's nutrient media to

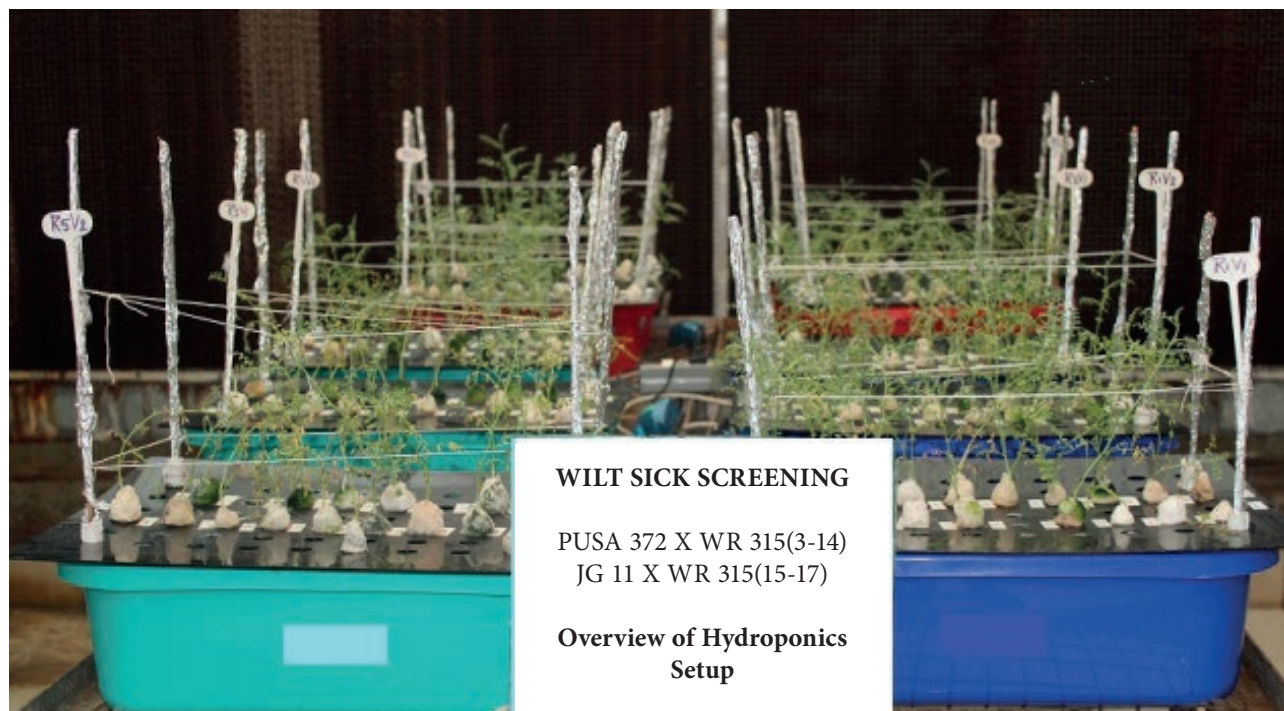


Figure 1. Hydroponics experimental set up used to screen chickpea lines for *Fusarium* wilt susceptibility.

compare disease incidence with wilt pathogen genotypes. The desired Foc conidium suspensions (3.2×10^6 conidia mL^{-1}) were added to each hydroponic tray, and 12 d-old seedlings were inoculated, and these were examined for wilt reactions (yellowing and wilting) for up to 30 d post inoculation. The nutrient media and conidium suspension of each pathotype/race were replenished at 4 d intervals during this period.

The inoculation experiment was carried out at the ICAR-Indian Agricultural Research Institute, New Delhi, India (Lat. 28.6377° N, Long. 77.1571° E) during 201920, in a temperature-controlled growth facility maintained at $20/14 \pm 2^\circ\text{C}$ day/night temperatures, with a daily photoperiod of 16 h and 45% relative humidity at germination, and then maintained $26 \pm 2^\circ\text{C}$ for effective infection (Figure 1).

Microscope observations, histopathological studies, disease assessments and disease progression

Microscope examinations of seedlings were carried out at 25 and 30 d after inoculation. The observations Growth and disease progression assessments were made for the resistant (“WR 315”) and susceptible (JG 62) controls, and all the MABC lines. Seedling roots were gently washed in tap water to remove adhered particles,

and were each hand sectioned into eight to ten 1-2 mm pieces of (cross and longitudinal sections), using a double-sided razor blade. The root pieces were then placed on glass microscope slides in drops of tryptophan blue or water, and then covered with cover slips for microscopic analyses. Single host genotypes were used in three replicates to study microscopic and histopathological characteristics, and for assessments of disease progression. For each assessed seedling, two hand sections were prepared and observed under a compound microscope at $\times 10$ magnification.

After inoculation, the plants were regularly monitored and scored every 3 d for disease symptoms and progression. Disease symptoms were scored using a six point (0-5) scale (modified from that described by Pouralibaba *et al.*, 2015), as follows:

- 0 = “no symptoms”- (0)-Immune,
- 1 = “tiny initiation on the leaf and yellowing in older leaves”- (0.1–10%) - Highly Resistant,
- 2 = “leaf showing complete yellowing of older and younger leaves”- (10.1–25%) - Resistant,
- 3 = “complete yellowing and falling of leaves”- (25.1–50%), Moderately susceptible,
- 4 = “wilted/curled/dried leaf, or defoliation”- (50–75%), Susceptible,
- 5 = “dried completely or killed plant” - (75.1-100%), Highly susceptible.

To represent all possible disease patterns in the plants, the disease scores were applied separately to each leaf. For effective comparison of resistance between the host genotypes, the disease score was developed for each complete plant. Considering n_1 , n_2 , n_3 , n_4 , and n_5 is the number of leaves showing, respectively, symptom types 1, 2, 3, 4 or 5, respectively, the formula used for calculating disease Index (DI)/disease score of each plant was:

$$DI = ((n_1 \times 0.10) + (n_2 \times 0.25) + (n_3 \times 0.5) + (n_4 \times 0.75) + (n_5 \times 1)/t) \times 100;$$

where 0.1, 0.25, 0.5, 0.75 and 1 are the indices that conform, respectively, to symptom categories y of 1, 2, 3, 4 or 5, and t represents the number of leaves in total including asymptomatic and fallen leaves due to disease. The absence of symptoms was scored as $DI = 0$ and dead plants as $DI = 100$ (Srinivasa *et al.*, 2019) (Figure 2).

The Foc inoculum was first used on seedlings that were 15 d-old, and relative progression of Fusarium wilt was observed at 10, 15, 18, 21, 24, 27, 30 d after inoculation to calculate the areas under the disease severity curves (AUDSC), using the formula $Y = \sum_{i=1}^{n-1} [(X_i + X_{i+1})/2] (t_{i+1} - t_i)$, where Y is the AUDPC, X_i is the disease incidence of the i th evaluation, and X_{i+1} is the disease incidence in next observation, and $(t_{i+1} - t_i)$ is the number of days between two observations (Gupta *et al.*, 2021). Final assessments were made 45-d-old seedlings.

Plant phenotypic characters

Sampling was carried out for each plant in all the three replications, and growth parameters were assessed, including root and shoot lengths, and root



Figure 2. Disease Indices (0–5) used for assessments of chickpea plants for severity of Fusarium wilt.

and shoot fresh and dry weights, to determine effects of Fusarium wilt (Foc) on plant phenotypes. Harvesting of roots and shoots were carried out separately, and to remove surface contamination, the roots were rinsed in distilled water for about 20s, followed by blotting to remove excess moisture. The dry weight of roots and shoots were determined by drying the plant parts at 80°C for 72 h. Genotypes with the lowest and highest disease scores were considered, respectively, to be highly resistant and susceptible to wilt. A completely randomized design was used in the experiment, and for phenotyping, single genotypes were used in each replication. These data were combined to determine means, descriptive analysis, correlations of root and shoot lengths, root and shoot dry and fresh weights, and mean wilt scores for each genotype.

Kruskal-Wallis rank-sum test for comparison of disease scores

The chickpea genotypes showing the lowest disease scores were considered to be resistant to Fusarium wilt, and those with high values were classified as susceptible. Disease scores and Kruskal Wallis tests gave comprehensive assessments of resistant and susceptible genotypes in this study (Supplementary Tables 3 and 4). The Kruskal Wallis test is non-parametric that does not assume that the data come from a particular distribution. Here ranks of the data values were used in the test rather than the actual data points.

Statistical analyses

Results were determined for different means, standard errors, standard deviations, and coefficients of variation. Statistically significant values were tested at $P = 0.05$, and Tukey's test was applied at this probability to assess significant differences between means. All the data including t tests were analysed using the STAR programme (Statistical Tool for Agricultural Research Version 2.0.1, 2014). A heat map was created using the R software 'stats' package, and correlation analyses were carried out using the "corrplot" package (version 0.84).

RESULTS

Histopathological observations

Presence of fungal mycelium was observed in the susceptible and resistant control plants. In the resist-

Table 3. Mean AUDPCs (\pm standard errors) for different chickpea genotypes (Sr. No.) inoculated with different races of *Fusarium oxysporum* f. sp. *ciceris*.

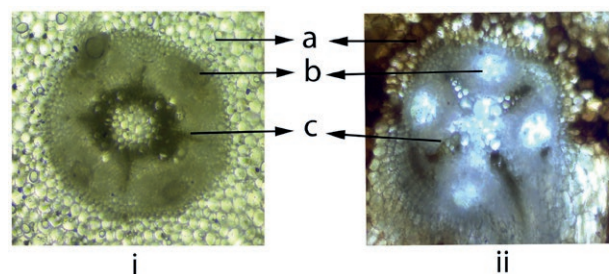
Sr. No.	Race 1	Race 2	Race 3	Race 4	Race 5
1	264.72 \pm 8.92	155.68 \pm 8.36	385.08 \pm 10.58	459.065 \pm 12.79	390.83 \pm 7.08
2	11.39 \pm 1.41	5.72 \pm 0.68	14.34 \pm 1.17	7.44 \pm 0.91	11.66 \pm 1.0
3	161.85 \pm 8.00	31.14 \pm 1.61	49.17 \pm 3.16	33.95 \pm 3.01	128.25 \pm 5.42
4	131.13 \pm 6.86	62.64 \pm 3.08	64.76 \pm 3.79	149.07 \pm 6.33	129.91 \pm 5.75
5	146.88 \pm 8.94	123.30 \pm 6.01	86.22 \pm 4.17	82.73 \pm 3.98	86.71 \pm 4.23
6	20.82 \pm 1.73	121.08 \pm 5.43	1.92 \pm 0.32	159.73 \pm 7.11	99.14 \pm 4.21
7	57.26 \pm 4.28	25.72 \pm 1.97	8.26 \pm 0.66	216.76 \pm 7.29	118.76 \pm 4.95
8	165.13 \pm 7.29	99.93 \pm 5.54	74.42 \pm 3.60	110.37 \pm 5.53	228.51 \pm 5.51
9	82.86 \pm 4.15	12.15 \pm 0.74	79.24 \pm 3.67	129.82 \pm 5.5	147.87 \pm 7.03
10	91.77 \pm 6.66	41.64 \pm 1.89	81.45 \pm 4.24	235.41 \pm 6.8	181.45 \pm 6.25
11	101.43 \pm 5.19	11.0 \pm 0.71	121.03 \pm 5.72	67.44 \pm 3.5	148.15 \pm 6.80
12	61.61 \pm 3.85	1.36 \pm 0.23	13.87 \pm 1.12	131.62 \pm 5.86	27.70 \pm 1.42
13	159.21 \pm 8.62	90.27 \pm 4.10	60.19 \pm 4.01	29.79 \pm 1.82	59.33 \pm 2.60
14	18.73 \pm 2.32	17.51 \pm 1.34	71.75 \pm 4.43	16.03 \pm 1.36	63.58 \pm 2.51
15	89.90 \pm 4.92	69.02 \pm 3.29	57.44 \pm 2.97	51.90 \pm 3.28	65.42 \pm 2.88
16	36.25 \pm 3.26	32.92 \pm 1.54	71.73 \pm 3.41	73.33 \pm 3.46	112.04 \pm 4.56
17	92.12 \pm 3.96	52.80 \pm 2.6	85.07 \pm 3.63	123.70 \pm 5.1	65.31 \pm 4.43
18	197.74 \pm 9.53	360.62 \pm 8.04	456.50 \pm 11.14	389.54 \pm 10.44	373.2 \pm 9.99
19	865.07 \pm 23.26	877.81 \pm 19.8	1053.49 \pm 16.06	1161.10 \pm 17.27	778.21 \pm 17.85
20	512.94 \pm 16.10	281.69 \pm 14.34	1200.07 \pm 19.11	493.61 \pm 13.71	159.68 \pm 8.23
21	109.92 \pm 5.05	123.75 \pm 6.09	68.06 \pm 2.73	170.06 \pm 7.65	311.16 \pm 9.85
22	202.22 \pm 4.44	110.11 \pm 5.23	133.95 \pm 5.81	51.56 \pm 3.32	77.32 \pm 3.59
t value	4.014***	3.0292***	2.8013***	3.6371***	4.7276***

Table 4. Descriptive statistics for seven chickpea plant traits analysed in this study.

Trait*	Min	Max	Range	Mean	SD	CV
SL	11.9	30.3	18.4	20.46	3.52	10.59
RL	8.9	29.3	20.4	16.07	3.82	4.97
SFW	0.47	1.64	1.17	0.87	0.23	7.61
SDW	0.044	0.16	0.0116	0.0873	0.02	6.71
RFW	0.35	1.56	1.21	0.79	0.267	4.92
RDW	0.036	0.172	0.136	0.0744	0.02	10.11
DS	0	100	100	15.6	18.4	13.3

*SL, shoot length; RL, root length; SFW, shoot fresh weight; SDW, shoot dry weight; RFW, root fresh weight, SDW, shoot dry weight. DS = Disease Score;

ant controls (WR 315) the xylem vessel discoloration was not prominent compared to the susceptible controls (JG 62), where xylem vessel discolorations and complete disruption were observed at the early stages of infection (Figure 3).

**Figure 3.** Example micrographs of chickpea root cross sections used in histopathological studies of Fusarium wilt. (i) resistant control host line WR 315, and (ii) susceptible control host JG 62. a, cortex; b, phloem; and c, xylem.

Identification of resistance against Fusarium wilt under a hydroponic system, based on in planta infection

Wilt symptoms were observed in the susceptible cultivar (JG 62) at 8 d after inoculation, but no symptoms were observed in the resistant genotype (WR 315). Parent Pusa 372 showed moderately susceptible responses against the Foc races 1, 3, 4, and 5, and showed resistant phenotype for race 2. JG 11 showed moderate susceptibility for

racess 2, 3, 4 and 5, and showed resistant phenotype for race 1. Eight host genotypes showed highly resistant reactions against five races of Foc. Among the 22 genotypes tested, four showed highly resistant responses to race 1, four were resistant to race 2, ten were resistant to race 3, seven were resistant to race 4, and seven genotypes were resistance to race 5. Fifteen MABC introgression lines of Pusa372 and JG 11 were tested against all five races s among which nine showed highly resistant response under hydroponic conditions. MABC introgression lines of Pusa 372 (IL.11,12,14) and JG 11 (IL.15,16,17) showed high resistance reactions to Fusarium wilt (Figures 4 and 5). ILC (CZ) showed varied reactions, with highly susceptible phenotypes for race 3, susceptible reaction to races 1 and 4, and moderately susceptible phenotypes for races 2 and 5. ILC (Lat) was highly resistant to races 1, 2 and 3, and moderately susceptible for races 4 and 5. The variety Pusa Green 112 (BGD 112) was resistant to races 2, 3, 4, and 5. Control plants grown in nutrient solution not show any disease symptoms during the experimental period.

Also, AUDPCs were calculated for all the host genotypes and with respect to all five Foc races under consideration. For race 1, AUDPC was greatest (865.07) for the susceptible control JG 62, was next greatest for ILCO (CZ), followed by parent Pusa 372 (264.72) and JG 11 (197.74). For MABC lines for race 1, the lowest AUDPC (18.73) was recorded for IL14, followed by IL6 (20.82) and IL16 (36.25). The resistant control WR 315 gave the lowest AUDPC value of 11.39. For race 2, AUDPC was greatest (877.81) for the susceptible control JG 62, next greatest (360.62) for JG11, followed by ILCO (CZ) (281.69 and parent Pusa 372 (155.68). For the MABC lines for race 2, the lowest AUDPC (1.36) was recorded for IL12, followed by IL11 (11.0) and IL9 (12.15). The resistant control WR 315 gave an AUDPC of 5.72. For race 3, AUDPC was greatest for ILCO (CZ) ((1053.49, followed by susceptible control JG 62 (1200.07), JG 11 (456.50) and parent Pusa 372 (385.08). For the MABC lines and race 3, the lowest AUDPC (1.92) was recorded for IL 6, followed by IL 7 (8.26) and IL12 (13.87). The resistant check WR 315 gave the lowest AUDPC of 14.34. Against race 4, AUDPC was greatest (1161.10) for the susceptible control JG 62, followed by ILCO (CZ) (493.61), and parent Pusa 372 (459.06) and JG11 (389.54). For MABC lines against race 3, the lowest AUDPC (16.03) was recorded for IL 14, followed by IL 13 (29.79) and IL3 (33.95). The resistant control WR 315 gave the lowest AUDPC value of 7.44. For race 5, AUDPC was greatest (778.21) for the susceptible control JG 62, followed by parent Pusa 372 (390.83), and JG11 (373.2). For the MABC lines against race 5, the lowest AUDPC (27.70) was recorded for IL 12, followed by IL 13 (59.33) and IL14 (63.58). The resistant control WR 315 gave the lowest AUDPC value of

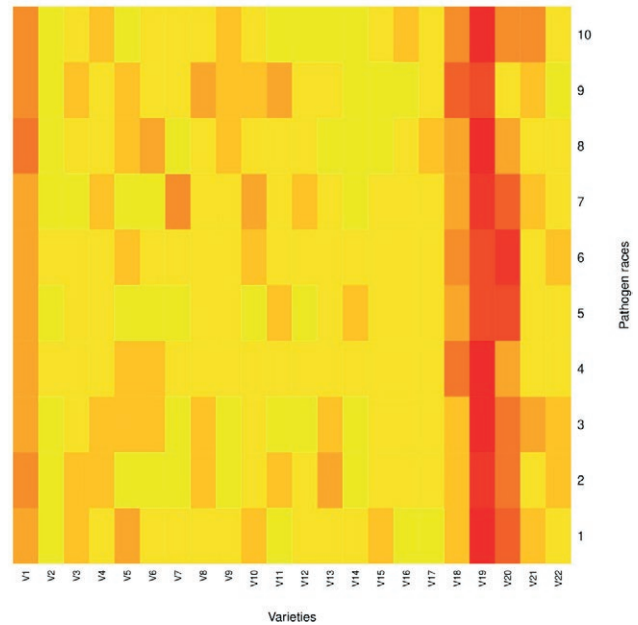


Figure 4. Heat map indicating Fusarium wilt severity scores for chickpea genotypes. from highly susceptible (red) to highly resistant (yellow) lines.



Figure 5. Differential responses of susceptible, resistant MABC lines, and resistance controls under Fusarium wilt stress (WS), and comparison with a very susceptible line (Control).

11.66. For AUDPCs, the susceptible check JG 64 gave the greatest value followed by parent Pusa 372, and the lowest AUDPC was recorded for the resistant control WR 315 (Table 3, Supplementary table 1). Results for AUDPC values for selected host genotypes are presented in Figure 6.

Host plant phenotypic traits measured under hydroponic conditions

The descriptive statistics for all seven host traits showed significant variations under wilt stress condi-

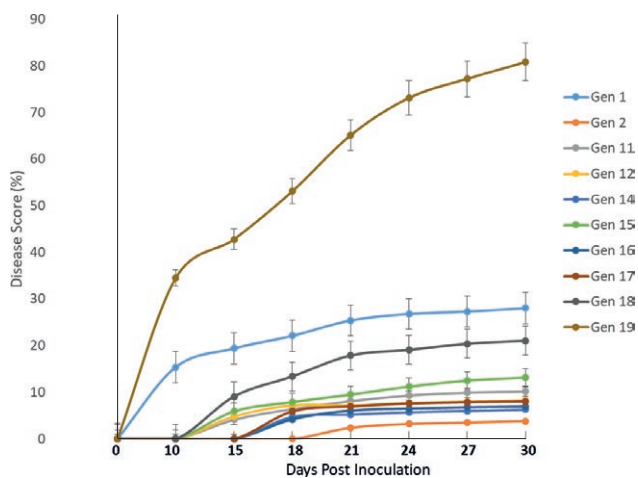


Figure 6. Disease progress curves for selected chickpea genotypes grown in hydroponic culture inoculated with *Fusarium oxysporum* f. sp. *ciceris* race 1.

tions, indicating considerable variation among the host genotypes (Table 4). Mean plant height under wilt stress was 20.5 cm, with a minimum of 11.9 cm (JG 62) and a maximum of 30.3 cm (IL.14). Mean root length under wilt stress was 20.0 cm, with a minimum of 8.9 cm (JG 62) and a maximum of 29.3 cm (IL.14). For mean shoot fresh and dry weights under wilt stress conditions were 0.87 g and 0.87 g, with respective minima of 0.47 g (JG 62) and 0.044 g (JG 62), and maxima of 1.64 g (IL.4) and 0.16 g (IL.6). Mean root fresh and dry weights were, respectively, maxima 1.56 g (IL.12) and 0.172 g (IL.13), and minima 0.79 and 0.07 and 0.35 (IL.20) and 0.036 (JG 62).

Correlations between host plant parameters

Correlation analyses were carried out for seven host plant traits (Figure 7). Correlations were statistically significant and strongly positive between the traits root fresh and dry weights (0.88), shoot fresh and dry weights (0.86), and root fresh weights and root lengths (0.53). Root and shoot weights were significantly and positively associated (0.44). Significant and negative associations occurred between disease scores and root lengths (-0.37) and root fresh weights (-0.33). Root fresh weights and shoot fresh weights (0.44) were positively related.

Reductions in host phenotypic traits

The greatest mean reductions in host plant parameters were observed for susceptible control plants of JG

62, with reductions of 47% in shoot length, 91% in root length, 34% in shoot fresh weight, 50% in shoot dry weight, 75% in root fresh weight, 56% in root dry weight, and an overall average 59% reduction across traits. Mean reductions for parent Pusa 372 were 35% for shoot length, 31% for root length, 31% for root length, 22% for shoot fresh weight, 19% for shoot dry weight, 54% for root fresh weight, 48% for root dry weight, and an overall average reduction across all traits of 35%. Mean proportional reductions for IL3 were 13% in shoot length, 38% in root length, 19% in shoot fresh weight, 11% in root dry weight, 23% in root fresh weight, 44% in root dry weight, with an overall average reduction across all traits of 25%. Mean reductions for IL11 were; 13% in shoot length, 21% in root length, 24% in shoot fresh weight, 37% in shoot dry weight, 40% in root fresh weight, 18% in root dry weight, with a 25% overall average reduction across all traits. Mean reductions for IL12 were; 10% in shoot length, 27% in root length, 24% in shoot fresh weight, 7% in shoot dry weight, 37% in root fresh weight, 17% in root dry weight, with a 20% overall reduction across all traits.

Greatest proportional reductions considering all host characters was measured for JG 62 (59%), then for Pusa 372 (35%) and JG 11 (32%), and the least reduction was for the resistant control WR 315 (11%) (Table 5, Supplementary Table 2).

Host parameters were affected differently by the different pathogen races. For shoot lengths, greatest reduction (21%) was measured for race 5, followed by race 3 (20%), race 2 (18%), race 1 (17%), and race 4 (12%) respectively. For root lengths, the greatest reduction was measured from race 5 (32%), followed by race 3 (32%), race 1 (23%), race 4 (20%), and race 2 (19%). For shoot fresh weights, the greatest reduction was from race 5 (47%), followed by race 1 (32%), race 3 (31%), race 2 (30%), and race 4 (22%). For shoot dry weights, the greatest reduction was measured from in race 5 (47%), followed by race 3 (26%), race 1 (24%), race 2 (23%), and race 4 (17%). For root fresh weights, the greatest reduction was from race 3 (40%), followed by race 5 (38%), race 4 (37%), race 1 (37%), and race 2 (33%). For root dry weights, the greatest reduction was from race 5 (43%), followed by race 1 (36%), race 2 (34%), race 3 (24%), and race 4 (14%). The results for the different races when subjected to "t" tests showed statistically significant differences among the host genotypes in responses host parameters assessed (Tables 5 and 6).

DISCUSSION

Screening of chickpea genotypes for susceptibility to Foc is usually carried out in wilt "sick" plots or

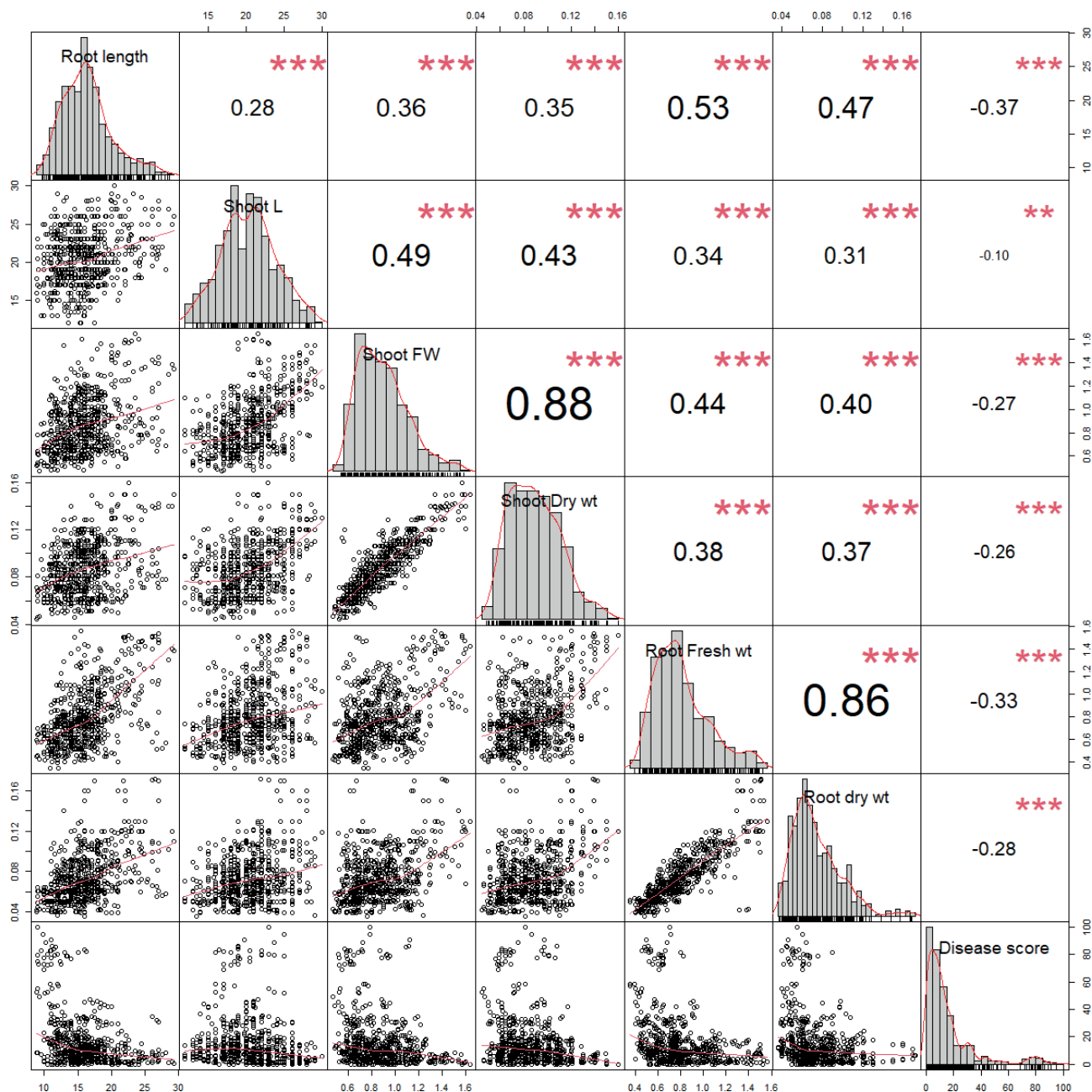


Figure 7. Correlations and distributions of six mean chickpea root parameters and mean Fusarium wilt scores, measured after hydroponic culture with *Fusarium oxysporum* f. sp. *ciceris*.

using pot culture techniques, which are environmentally sensitive, time consuming, involve complex inoculation methods, and where it is difficult to screen large numbers of host genotypes (Belaidi, 2016). Hydroponic screening for disease resistance has been reported for bean root rot (Anderson and Guerra, 1985), *Fusarium* sp. in banana (Zheng *et al.*, 2018), in *Medicago sativa* (Cong *et al.*, 2018), and screening for Phytophthora root

rot resistance in chickpea (Amalraj *et al.*, 2019). The present study is the first successful use of hydroponic culture for screening race-specific Fusarium wilt resistance in chickpea.

Histological distortions of vascular tissues in host roots and shoots in resistant and susceptible controls were observed. Formation of cavities were observed between phloem and xylem tissues, medulla and xylem,

Table 5. Average percentage reductions for different chickpea host lines (Sr. No.) for traits after inoculations with different races (R1 to R5) of *Fusarium oxysporum* f. sp. *ciceris*.

Sr. No	R1	R2	R3	R4	R5	Average
1	31	66	56	19	51	35
2	15	13	9	9	24	14
3	15	12	13	7	13	12
4	32	23	21	13	10	19
5	7	18	2	6	1	7
6	13	6	13	5	7	9
7	1	5	36	2	22	11
8	33	15	3	1	3	10
9	13	6.	18	10	8	11
10	18	7	36	12	22	18
11	10	17	16	10	9	12
12	12	0.8	14	11	12	10
13	9	11	8	6	0.9	7
14	29	12	5	10	16	14
15	18	19	10	4	24	15
16	3	21	38	7	41	20
17	0.3	54	21	14	24	20
18	31	19	36	29	31	29
19	30	40	50	35	91	46
20	16	9	11	9	1	9
21	2	21	8	24	12	13
22	17	2	14	2	33	12
t values	7.2896***	5.3361***	6.2446***	6.2377***	4.8384***	

Table 6. Percentage reduction of SL, RL, SFW, SDW, RFW and RDW with respect to five different races of *Fusarium oxysporum* f. sp. *ciceris*.

Sr.No.	Race 1	Race 2	Race 3	Race 4	Race 5	Average	t value
SL	16.56	18.49	20.32	11.70	21.15	16.49	6.9***
RL	22.87	19.35	31.99	20.11	32.16	23.75	6.79***
SFW	32.42	29.77	30.58	22.03	46.59	22.59	16.14***
SDW	24.31	22.67	26.47	16.86	46.98	24.52	6.50***
RFW	36.91	33.23	39.52	37.30	38.43	33.20	10.589***
RDW	36.31	34.03	24.12	14.64	43.04	27.83	7.62***

phloem and cells of cortical parenchyma, and proliferation of cells in vascular cambium was also observed. Stem cross sections revealed xylem colonization by the pathogen, while resistant plants showed normal development. The hydroponic system allowed effective assessments of compatible and incompatible interactions between chickpea races and resistant and susceptible cultivars (Jiménez-Fernández *et al.*, 2013). Similar results of xylem colonisation between resistant and suscepti-

ble cultivars were observed by Caballo *et al.* (2019) for race 5 of *Fusarium oxysporum* f. sp. *ciceris*. Obstruction of host water conduction systems affect photosynthesis due to closure of stomata induced by water deficit, and also affect functioning of RuBisCO (Pedrosa *et al.*, 2011). *Fusarium* wilt affects three crucial photosynthesis processes, including thylakoid electron transport, carbon reduction cycles, and CO₂ supply for stomata (Allen *et al.*, 1997).

Compatible interactions (susceptibility) of *Foc* infections inhibit plant growth through water stress and pathogen action. Therefore, increased root length in resistant plant genotypes is an efficient host defence mechanism against root-invading pathogens (Caballo *et al.*, 2019). Host leaves also lose turgidity, which leads decreased shoot and root dry weights (Jalali and Chand, 1992; Jimenez-Díaz *et al.*, 2015). Increased root length and fresh weight could be used as selection criteria for host resistance using hydroponic techniques. In the present study, negative and low correlations were observed between disease scores, shoot lengths, and shoot and root fresh and dry weights, indicating low variation among MABC lines for disease resistance. These are in advanced selection generations (AVT lines), and are near-isogenic for disease resistance.

Disease observations were taken by observing individual leaves, which increased accuracy of disease score calculation. These measurements showed that parent host lines (Pusa 372 and JG 11) were moderately susceptible to most of the assessed *Foc* races. The susceptible control (JG 62) was highly susceptible to all of the *Foc* races, and the resistant control (WR 315) was highly resistant to these races (Sharma *et al.*, 2005; Milan *et al.*, 2006). For all of the seven measured host physical characters and disease score, the parent Pusa 372 introgression lines (11, 12, 14) and JG 11 introgression line (17, 18) were generally superior for all characters, and were highly resistant to disease. Line ILC (CZ) showed varied reactions for different *Foc* races, and was moderately susceptible only to *Foc* races 5 and 2. ILC (Lat.) showed was highly resistant against all the tested *Foc* races, showing the potential for utilization of this landrace for diversification of resistant controls to other than WR 315. The variety Pusa Green 112 (BGD112) was resistant to all assessed races except race 1, and is therefore a potent donor source for *Fusarium* wilt resistance (Yadav *et al.*, 2004). Analysis of AUDPCs also showed that MABC lines had the lowest disease progression.

Reductions due to *Foc* were detected in growth traits of the resistant chickpea susceptible control, MABC lines, and the other varieties studied. Average plant parameter reductions were greatest after inocula-

tion with Foc race 5 (for shoot and root lengths, shoot fresh and weights, and root dry weight) and race 5 (for root fresh weight). For all the host phenotypic characters assessed, the greatest reductions were observed in root fresh weight (Table 5).

Average percentage reductions were 55% for MABC line 3, 25% for line 11, and 20% for line 12, and 35% for parent Pusa 372, 12% for donor parent WR 315, 31% for the national control JG 11, and 59% for the susceptible control JG 62. This indicates that in the case of MABC lines and a resistant check showed a lower percent reduction in the growth traits suggesting resistant response as compared to parents and susceptible check (Maitlo *et al.*, 2014). Punja and Rodriguez (2018) studied *Fusarium* species infecting roots of hydroponically grown marijuana plants, and observed reductions in root lengths and volumes, which were similar to reductions measured in the present study. This emphasizes how Foc can affect different host landraces, parents and MABC lines, and indicates the superiority of MABC lines over other genotypes.

MABC is regarded as a rapid method for developing host varieties that are resistant to Fusarium wilt (Varshney *et al.*, 2014). MABC development in chickpea has relied mostly on field or “wilt sick” plot screening for variety development (Mannur *et al.*, 2019; Roorkiwal *et al.*, 2020). Nevertheless, some of these varieties have become susceptible to Fusarium wilt, possibly due to changes in wilt incidence, pathogen genotype differences, and genotype/environment interactions (Neupane *et al.*, 2007; Sharma *et al.*, 2012). In the present study, race purity of Foc inocula was maintained under hydroponic culture, and the inoculated races were reisolated. This gave accurate, reproducible and reliable disease quantification, at an early stage of host infection. Screening using hydroponics based screening will increase accuracy and be useful for future MABC development programmes.

Hydroponic systems can be costly compared to traditional “sick plot” method, requiring specific skills, and host plants that are readily infected by pathogens. Many hosts require similar nutrient media, and hydroponic systems allow rapid inoculum spread (Pandey *et al.*, 2009; Sardare and Admane, 2013). Use of this method will aid current and future efforts in breeding for Fusarium wilt resistance in chickpea, as for genetic studies.

FUNDING INFORMATION

The senior author thanks the ICAR-Indian Agricultural Research Institute for an ICAR IARI-SRF Fellowship for PhD research support. Financial support

for research described in this paper was also provided by the Consortium Research Project (ICAR-CRP) for Chickpea and Functional Genomics (ICAR-NTPC).

AUTHOR CONTRIBUTIONS

CB and NS conceived this study. JJ and AR performed the experiments. JJ, ST and NK analysed the data. The manuscript was written by JJ, CB, KRS and BSP, with help from all the co-authors.

LITERATURE CITED

- Ali M.E.K., Inanaga S., Sugimoto Y., 2002. Sources of resistance to Fusarium wilt of chickpea in Sudan [*Cicer arietinum* L.]. *Phytopathologia Mediterranea* 41(3): 163–169.
- Allen D.J., McKee I.F., Farage P.K., Baker N.R., 1997. Analysis of limitations to CO₂ assimilation on exposure of leaves of two Brassica napus cultivars to UV-B. *Plant, Cell and Environment* 20(5): 633–640. doi: 10.1111/j.1365-3040.1997.00093.x
- Amalraj A., Taylor J., Sutton T., 2019. A hydroponics based high throughput screening system for Phytophthora root rot resistance in chickpea (*Cicer arietinum* L.). *Plant Methods* 15(1): 82. doi: 10.1186/s13007-019-0463-3
- Anderson A.J., Guerra D., 1985. Responses of bean to root colonization with *Pseudomonas putida* in a hydroponic system. *Phytopathology* 75(9): 992–995.
- Barve M.P., Haware M.P., Sainani M.N., Ranjekar P.K., Gupta V.S., 2001. Potential of microsatellites to distinguish four races of *Fusarium oxysporum* f. sp. *ciceris* prevalent in India. *Theoretical and Applied Genetics* 102: 138–147. doi : 10.1007/s001220051629
- Belaidi H., 2016. Screening of some chickpea germplasm accessions for resistance to two races of *Fusarium oxysporum* f. sp. *ciceris*, the causal of chickpea wilt disease. *American-Eurasian Journal of Agricultural & Environmental Sciences* 16: 1758–1763.
- Bharadwaj C., Tripathi S., Soren K.R., Thudi M., Singh R. K., ...Varshney R.K., 2021. Introgression of “QTL-hotspot” region enhances drought tolerance and grain yield in three elite chickpea cultivars. *The Plant Genome* 14(1). doi: 10.1002/tpg2.20076
- Caballo C., Castro P., Gil J., Millan T., Rubio J., Die J.V., 2019. Candidate genes expression profiling during wilting in chickpea caused by *Fusarium oxysporum* f. sp. *ciceris* race 5. *PlosOne* 14(10): e0224212. <https://doi.org/10.1371/journal.pone.0224212>

- Collard B.C., Mackill D.J., 2008. Marker-assisted selection: an approach for precision plant breeding in the twenty-first century. *Philosophical Transactions of the Royal Society B: Biological Sciences* 363(1491): 557–572.
- Cong L.L., Sun Y., Wang Z., Kang J.M., Zhang T.J., ... Yang Q.C., 2018. A rapid screening method for evaluating resistance of alfalfa (*Medicago sativa* L.) to Fusarium root rot. *Canadian Journal of Plant Pathology* 40(1): 61–69.
- DAFW, 2019. Agricultural Statistics at a Glance 2019, Department of Agriculture, Cooperation & Farmer's Welfare, Directorate of Economics and Statistics, Ministry of Agriculture and Farmers' Welfare, Government of India 2019.
- Dixit G.P., Srivastava A.K., Singh N.P., 2019. Marching towards self-sufficiency in chickpea. *Current Science* 116(2): 239–242. doi: 10.18520/cs/v116/i2/239-242.
- Dubey S.C., Singh S.R., 2008. Virulence analysis and oligonucleotide fingerprinting to detect diversity among Indian isolates of *Fusarium oxysporum* f. sp. *ciceris* causing chickpea wilt. *Mycopathologia* 165(6): 389–406.
- Dubey S.C., Priyanka K., Singh V., Singh B., 2012. Race profiling and molecular diversity analysis of *Fusarium oxysporum* f. sp. *ciceris* causing wilt in chickpea. *Journal of Phytopathology* 160(10): 576–587. doi: 10.1111/j.1439-0434.2012.01954.x
- FAOSTAT, 2020. FAO Statistics, Food and Agriculture Organization of the United Nations, Rome. Crops retrieved from <https://www.fao.org/faostat/en/#data/QC/visualize>
- Gupta D., Singh O.W., Basavaraj Y.B., Roy A., Mukherjee S.K., Mandal B., 2021. Direct Foliar Application of dsRNA derived from the full-length gene of NSs of groundnut bud necrosis virus limits virus accumulation and symptom expression. *Frontiers in Plant Science* 12: 734618.
- Halila I., Rubio J., Millán T., Gil J., Kharrat M., Marrakchi M., 2010. Resistance in chickpea (*Cicer arietinum*) to Fusarium wilt race "0". *Plant Breeding* 129: 563–566.
- Haware M. P., Nene Y. L., 1982. Races of *Fusarium oxysporum* f. sp. *ciceri*. *Plant Disease* 66(9): 809–810. doi: 10.1094/PD-66-809.
- Haware M.P., Nene Y.L., Pundir R.P.S., Rao J.N., 1992. Screening of world chickpea germplasm for resistance to Fusarium wilt. *Field Crops Research* 30(1–2): 147–154.
- Haware M.P., Nene Y.L., Natarajan M., 1996. The survival of *Fusarium oxysporum* f. sp. *ciceri* in the soil in the absence of chickpea. *Phytopathologia Mediterranea NUM*: 9–12.
- Hickey L.T., Hafeez A.N., Robinson H., Jackson S.A., Leal-Bertioli S.C., ... Wulff B.B., 2019. Breeding crops to feed 10 billion. *Nature Biotechnology* 37(7): 744–754. doi: 10.1038/s41587-019-0152-9.
- Hoagland D.R., Arnon D.I., 1950. The water-culture method for growing plants without soil. *Circular. California Agricultural Experiment Station* 347 (2nd edit).
- Jalali B.L., Chand H.A.R.I., 1992. Chickpea wilt. *Plant Diseases of International Importance*, Prentice Hall, Englewood Cliffs, New York, United States of America, 1: 429–444.
- Jimenez-Diaz R.M., Trapero-Casas A., de La Colina J.C., 1989. Races of *Fusarium oxysporum* f. sp. *ciceri* infecting chickpeas in southern Spain. In: *Vascular Wilt Diseases of Plants* (pp. 515–520). Springer, Berlin, Heidelberg. doi: 10.1007/978-3-42-73166-239
- Jiménez-Díaz R.M., Castillo P., del Mar Jiménez-Gasco M., Landa B.B., Navas Cortés J.A., 2015. Fusarium wilt of chickpeas: Biology, ecology and management. *Crop Protection* 73: 16–27. doi: 10.1016/j.cropro.2015.02.023.
- Jiménez-Fernández D., Landa B.B., Kang S., Jiménez-Díaz R.M., Navas-Cortés J.A., 2013. Quantitative and microscopic assessment of compatible and incompatible interactions between chickpea cultivars and *Fusarium oxysporum* f. sp. *ciceris* races. *Plos One* 8(4): e61360.
- Maitlo S.A., Syed R.N., Khanzada M.A., Rajput A.Q., Rajput N.A., Lodhi A.M., 2014. Host-response of chickpea cultivars to *Fusarium oxysporum* f. sp. *ciceris*. *Pakistan Journal of Phytopathology* 26(2): 193–199.
- Mannur D.M., Babbar A., Thudi M., Sabbavarapu M.M., Roorkiwal, ... Chamarthi S.K., 2019. Super Annigeri 1 and improved JG 74: two Fusarium wilt-resistant introgression lines developed using marker-assisted backcrossing approach in chickpea (*Cicer arietinum* L.). *Molecular Breeding* 39(1): 2. doi: 10.1007/s11032-018-0908-9.
- Merga B., Haji J., 2019. Economic importance of chickpea: production, value, and world trade. *Cogent Food Agriculture* 5(1): 1615718.
- Millan T., Clarke H.J., Siddique K.H., Buhariwalla H.K., Gaur P.M., ... Winter P., 2006. Chickpea molecular breeding: new tools and concepts. *Euphytica* 147(1): 81–103.
- Neupane R.K., Sharma M., Jha P., Rao J.N., Rao B.V., ... Pande S., 2007. Evaluation of chickpea genotypes for resistance to Fusarium wilt in Nepal. *Journal of SAT Agricultural Research* 5(1): 1–2.
- Pandey R., Jain V., Singh K.P., 2009. Hydroponics Agriculture: Its status, scope and limitations. *Division of*

- Plant Physiology, Indian Agricultural Research Institute, New Delhi, 20.*
- Pedrosa F.O., Monteiro R.A., Wassem R., Cruz L.M., Ayub R.A., ... Souza E.M., 2011. Genome of *Herbaspirillum seropedicae* strain SmR1, a specialized diazotrophic endophyte of tropical grasses. *PLoS Genetics* 7(5): e1002064.
- Pouralibaba H.R., Rubiales D., Fondevilla S., 2015. Identification of resistance to *Fusarium oxysporum* f. sp. *lentis* in Spanish lentil germplasm. *European Journal of Plant Pathology* 143(2): 399–405.
- Punja Z.K., Rodriguez G., 2018. *Fusarium* and *Pythium* species infecting roots of hydroponically grown marijuana (*Cannabis sativa* L.) plants. *Canadian Journal of Plant Pathology* 40(4): 498–513.
- R Core Team 2019. R: A language and environment for statistical computing. R Foundation for Statistical Computing, Vienna, Austria. <https://www.r-project.org/>
- Roorkiwal M., Bharadwaj C., Barmukh R., Dixit G. P., Thudi M., ... Varshney R.K., 2020. Integrating genomics for chickpea improvement: achievements and opportunities. *Theoretical and Applied Genetics* 133: 1703–1720. doi: 10.1007/s00122-020-03584-2.
- Rubio J., Hajj-Moussa E., Kharrat M., Moreno M.T., Millan T., Gil J., 2003. Two genes and linked RAPD markers involved in resistance to *Fusarium oxysporum* f. sp. *ciceris* race 0 in chickpea. *Plant Breeding* 122(2): 188–191.
- Sardare M.D., Admane S.V., 2013. A review on plant without soil-hydroponics. *International Journal of Research in Engineering and Technology* 2(3): 299–304.
- Sharma K.D., Chen W., Muehlbauer F.J., 2005. Genetics of chickpea resistance to five races of *Fusarium* wilt and a concise set of race differentials for *Fusarium oxysporum* f. sp. *ciceris*. *Plant Disease* 89(4): 385–390. doi: 10.1094/PD-89-0385.
- Sharma M., Babu T.K., Gaur P.M., Ghosh R., Rameshwar T., ... Pande S., 2012. Identification and multi-environment validation of resistance to *Fusarium oxysporum* f. sp. *ciceris* in chickpea. *Field Crops Research* 135: 82–88.
- Sheikh B.A., 2006. Hydroponics: key to sustain agriculture in water stressed and urban environment. *Pakistan Journal of Agriculture, Agricultural Engineering and Veterinary Sciences* 22(2): 53–57.
- Srinivasa N., Tusarkanti Bag., Dikshit H., Murulidhar Aski., 2019. Wilt disease of lentil and its management. *Wilt Diseases of Crops*, Indian Phytopathological Society, New Delhi, India, 355–399.
- STAR, version 2.0.1 2014. Biometrics and Breeding Informatics, PBGB Division, International Rice Research Institute, Los Baños, Laguna.
- Taiyun Wei., Viliam Simko., 2017. R package “corrplot”: Visualization of Correlation Matrix (Version 0.84). <https://github.com/taiyun/corrplot>.
- Thompson H.C., Langhans R.W., Both A.J., Albright L.D., 1998. Shoot and root temperature effects on lettuce growth in a floating hydroponic system. *Journal of the American Society for Horticultural Science* 123(3): 361–364.
- Trapero Casas A., Jiménez Díaz R.M., 1985. Fungal wilt and root rot diseases of chickpea in southern Spain. *Phytopathology* 75: 1146–1151.
- Varshney R.K., Mir R.R., Bhatia S., Thudi M., HuY., ... Luo M.C., 2014. Integrated physical, genetic and genome map of chickpea (*Cicer arietinum* L.). *Functional & Integrative Genomics* 14(1): 59–73. doi: 10.1007/s10142-014-0363-6
- Varshney R.K., Song C., Saxena R.K., Azam S., Yu S., ... Millan T., 2013. Draft genome sequence of chickpea (*Cicer arietinum*) provides a resource for trait improvement. *Nature Biotechnology* 31(3): 240. doi: 10.1038/nbt.2491.
- Varshney R.K., Thudi M., Nayak S.N., Gaur P.M., Kashiwagi J., ... Rathore A., 2014. Genetic dissection of drought tolerance in chickpea (*Cicer arietinum* L.). *Theoretical and Applied Genetics* 127(2): 445–462. doi: 10.1007/s00122-013-2230-6.
- Yadav S.S., Kumar J., Turner N.C., Berger J., Redden R., ... Bahl P.N., 2004. Breeding for improved productivity, multiple resistance and wide adaptation in chickpea (*Cicer arietinum* L.). *Plant Genetic Resources* 2(3): 181. doi: 10.1079/PGR200448.
- Zheng S.J., García-Bastidas F.A., Li X., Zeng L., Bai T., Xu S., ... Kema G.H., 2018. New geographical insights of the latest expansion of *Fusarium oxysporum* f. sp. *ubense* tropical race 4 into the greater Mekong sub-region. *Frontiers in Plant Science* 9: 457.



Citation: E. Maghrebi, O. Beldi, T. Ochi, B. Koopmann, H. Chaabane, B.A. Bahri (2023) First report of *Leptosphaeria maculans* and *Leptosphaeria biglobosa* causing blackleg disease of oilseed rape in Tunisia. *Phytopathologia Mediterranea* 62(1): 17-24. doi: 10.36253/phyto-13827

Accepted: December 12, 2022

Published: April 6, 2023

Copyright: ©2023 E. Maghrebi, O. Beldi, T. Ochi, B. Koopmann, H. Chaabane, B.A. Bahri. This is an open access, peer-reviewed article published by Firenze University Press (<http://www.fupress.com/pm>) and distributed under the terms of the Creative Commons Attribution License, which permits unrestricted use, distribution, and reproduction in any medium, provided the original author and source are credited.

Data Availability Statement: All relevant data are within the paper and its Supporting Information files.

Competing Interests: The Author(s) declare(s) no conflict of interest.

Editor: Jean-Michel Savoie, INRA Villenave d'Ornon, France.

ORCID:

EM: 0000-0002-9108-6158

OB: 0000-0002-1221-4845

TO: 0000-0002-0723-8025

BK: 0000-0001-5874-3067

HC: 0000-0002-0958-3818

BAB: 0000-0001-5905-5880

New or Unusual Disease Reports

First report of *Leptosphaeria maculans* and *Leptosphaeria biglobosa* causing blackleg disease of oilseed rape in Tunisia

ESSIA MAGHREBI^{1,*}, OLFA BELDI², TAHANI OCHI¹, BIRGER KOOPMANN³, HANENE CHAABANE¹, BOCHRA AMINA BAHRI^{1,4,*}

¹ Laboratory « Pests and Integrated Protection in Agriculture » (LR/BPIA), University of Carthage, National Agronomic Institute of Tunisia (INAT), Tunisia

² General Directorate of Protection and Quality Control of Agricultural Products, Tunisian Ministry of Agriculture, Water Resources and Fisheries, Tunisia

³ Plant Pathology and Crop Protection Division, Department of Crop Sciences, Georg-August-University Göttingen, Göttingen, Germany

⁴ Department of Plant Pathology, Institute of Plant Breeding, Genetics and Genomics, University of Georgia, Griffin, USA

*Corresponding authors. E-mail: maghrebi.essia@gmail.com; bbahri@uga.edu

Summary. Blackleg has been observed in oilseed rape in Tunisia since 2017. Morphological observations, pathogenicity tests, and sequencing of the internal transcribed spacer regions for four fungal isolates from affected plants confirmed the presence of *Leptosphaeria maculans* and *Leptosphaeria biglobosa*. These results provide the first record of *L. maculans* and *L. biglobosa* as causes of blackleg of oilseed rape in Tunisia.

Keywords. Blackleg disease, oilseed rape, fungal identification.

INTRODUCTION

Brassica napus L. is one of the most common domesticated *Brassica* crops for human and animal nutrition (Friedt *et al.*, 2018). Oilseed rape is estimated to occupy more than 35.6 million hectares (ha) of world agricultural area with average production of 71 million tons (t) in the 2021–2022 growing season (World Agricultural Production, 2022). The oilseed rape crops have been reintroduced into the Tunisian national cultivation systems since 2014 (Medimagh *et al.*, 2018), and average yields have increased from 1.3 t ha⁻¹ in 2014–2015 to 1.8 t ha⁻¹ in 2018–2019 (Maghreb Oléagineux, 2022). With more than 15,000 ha of current rapeseed crop area, these crops are important in Tunisia, especially in the northern regions of the country (Maghreb Oléagineux, 2022).

Five hybrid European spring varieties are currently subscribed in the Tunisian catalogue of varieties and dominate *Brassica napus* cultivation in Tunisia (Maghreb Oléagineux, 2022). Reductions in oilseed rape yields have

been noticed due to biotic stress (Wang *et al.*, 2020; Zheng *et al.*, 2020). Blackleg (Phoma stem canker) is an important fungal disease threat to international oilseed rape production (Howlett, 2004; Fitt *et al.*, 2006). *Leptosphaeria maculans* (Desm.) Ces. and de Not. (anamorph *Phoma lingam*) is the principal cause of this disease together with *L. biglobosa* Shoemaker and H. Brun (*L. biglobosa*) (Rouxel *et al.*, 1994; Shoemaker and Brun, 2001). *Leptosphaeria biglobosa* is considered to be less aggressive than *L. maculans*, and often attacks the upper parts of host plants (Williams, 1999; Shoemaker and Brun, 2001; Mendes-Pereira *et al.*, 2003). In 2017, symptoms similar to blackleg were observed in Beja, Bizerte, Nabeul and Manouba, the four main oilseed rape production areas of Tunisia.

The objective of the present study was to identify the causal agents responsible for the blackleg on oilseed rape in Tunisia. Cultural and morphological features, molecular sequencing of the internal transcribed spacer (ITS) region, phylogenetic analysis, and pathogenicity tests were performed for isolates of fungi obtained from oilseed rape crops.

MATERIALS AND METHODS

Isolation and morphological identification of causal agents

To isolate the causal agent, diseased oilseed rape plants were sampled from four northern regions of Tunisia (nine fields) during April and May 2018. The samples were conveyed to the Pests and Integrated Protection in Agriculture research laboratory in Tunisia. For each sample, five infected stem sections (5 cm length) were surface-sterilized in 1% sodium hypochlorite solution for 30 s, followed by 70% ethanol for 20 s, and three rinses in sterile water. The stem sections were then transferred into 90 mm diam. Petri dishes con-

taining V8 juice agar supplemented with 25 mg mL⁻¹ of chloramphenicol. After 15 d incubation under 12 h photoperiod at 20°C, serial dilutions were performed to obtain single conidium isolates that were then maintained on V8 juice agar at 20°C. From the initial isolate collection (Table 1), four isolates (obtained from four fields) were randomly selected for morphological and genetic identifications. Isolates L31 and L36 were from two fields in Manouba and isolates L48 and L50 were from two fields in Nabeul.

For macroscopic identification, 5 mm mycelium agar discs of each isolate were inoculated onto 90 mm diam. Petri dishes containing malt agar, V8 juice agar or potato dextrose agar (PDA). Colonies were photographed at 7 and 14 d after incubation at 20°C in complete darkness. For each isolate, colony colour, and conidium size and shape were analyzed under light microscope and then measured using ImageJ software (Schneider *et al.*, 2012).

Molecular and phylogenetic analyses of the causal agents

Genomic DNA was extracted from the four selected isolates using the CTAB protocol (Doyle and Doyle, 1987). PCR was performed to amplify the ITS region using the forward ITS1 (5'-TCCGTAGGTGAACCTGCGG-3') and the reverse ITS4 (5'-TCCTCCGCTTATTGATATGC-3') primer, as described by White *et al.* (1990). The amplifications were carried out using the Thermo Cycler 2720 (Applied Biosystems) in 25 µL reaction mixtures. PCR conditions were as follows: 4 min of initial denaturation at 94°C, followed by 30 cycles of denaturation each at 94°C for 1.5 min, 2 min of annealing at 55°C and 3 min of extension at 72°C, with a final elongation at 72°C for 10 min. A Sanger sequencing using both directions was carried out by CarthaGenomics Advanced Technologies (Tunis, Tunisia). The consensus ITS sequence of each

Table 1. Details of Tunisian regions from which *Leptosphaeria* spp. isolates were sampled in *Brassica napus* crops in 2018.

Region	Municipality	Commune	Field No.	Latitude	Longitude	Altitude (m)	Number of sampled isolates
Beja	Beja North	Ghyria	1	36.72900	9.135720	409	6
Beja	Beja North	Beja	2	36.72200	9.192360	245	1
Beja	Testour	Oued Zargua	3	36.66700	9.444870	169	2
Bizerte	Tinjah	Tinjah	4	37.17681	9.769790	4	4
Bizerte	Tinjah	Tinjah	5	37.15695	9.765250	15	3
Manouba	Tebourba	Chouigui	6	36.90000	9.850000	67	6 (<i>Inc. Isolate L36</i>)
Manouba	Tebourba	Eddekhila	7	36.89000	9.728000	74	5 (<i>Inc. Isolate L31</i>)
Nabeul	Menzel Bouzalfa	Menzel Bouzalfa North	8	36.69120	10.59816	58	3 (<i>Inc. Isolate L48</i>)
Nabeul	Menzel Bouzalfa	Errahma	9	36.71000	10.74000	133	4 (<i>Inc. Isolate L50</i>)

Table 2. Isolates of the *Leptosphaeria maculans* and *Leptosphaeria biglobosa* species complex used as references in the phylogenetic analyses.

Species	Subclade	Isolate name	IBCN number	Origin	Host	GenBank accession number	References	
<i>Leptosphaeria maculans</i>	'brassicae'	IRAN Br37	-	Iran	-	MG701143	Amirdehi <i>et al.</i> , 2017	
		Pk4	-	Iran	<i>B. napus</i>	MW444866	Zamanmirabadi <i>et al.</i> , 2022	
		UK7	-	UK	<i>B. napus</i>	DQ133891	Liu <i>et al.</i> , 2006	
		CBS 275.63	-	UK	-	MW810266	Zhao <i>et al.</i> , 2021	
	'lepidii'	Leroy / FSU428	80	Canada	<i>B. napus</i>	AJ550883		
		Lep-2 / FSU432	84	Canada	<i>Lepidium</i> sp.	AJ550890		
	'thlaspii'	92-01-2 / FSU373	65	Canada	<i>T. arvense</i>	AJ550891		
		CBS303.51	-	France	<i>Isatis tinctoria</i>	AJ550892		
	'australensis'	2.1 / FSU415	29	Australia	<i>B. napus</i>	AJ550869	Mendes-Pereira <i>et al.</i> , 2003;	
		PHW1268 / PHW126 / FSU471	91	USA	<i>B. oleracea</i>	AJ550870	Voigt <i>et al.</i> , 2005	
<i>Leptosphaeria biglobosa</i>	'erysimii'	Ery-2 / FSU431	83	Canada	<i>Erysimum</i> sp.	AJ550872		
		PL53	-	Poland	<i>B. napus</i>	AJ550865		
	'brassicae'	2379-4 / FSU437	89	Canada	<i>B. napus</i>	AJ550863		
		PHW1270 / PHW129 / FSU473	93	USA	<i>B. oleracea</i>	AJ550857		
		CBS127249	-	France	<i>B. juncea</i>	JF740199	De Gruyter <i>et al.</i> , 2012	
		HNO96	-	China	<i>B. napus</i>	MZ312591	-	
		UK5	-	UK	<i>B. napus</i>	DQ133890	Liu <i>et al.</i> , 2006	
		'americensis'	Phl002	-	USA	<i>B. rapa</i>	MG321243	Zou <i>et al.</i> , 2019
		'occiaustralensis'	UWA21-8	-	Australia	<i>B. napus</i>	AM410082	Vincenot <i>et al.</i> , 2008
			Lb1135	-	China	<i>B. napus</i>	MK335624	Luo <i>et al.</i> , 2021
'canadensis'	BJ-114 / FSU430	82	Canada	<i>B. juncea</i>	AJ550866	Mendes-Pereira <i>et al.</i> , 2003 Voigt <i>et al.</i> , 2005		

-. Unknown or not available information

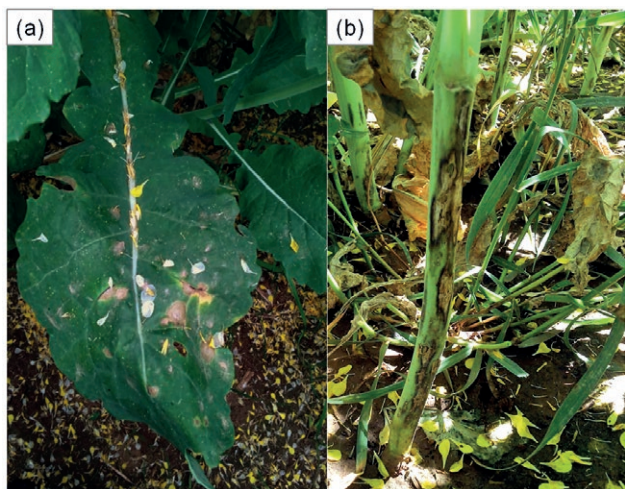


Figure 1. Blackleg (*Phoma* stem canker) symptoms on oilseed rape plants observed during field sampling in Tunisia in spring 2018. (a) Lesions observed on an upper leaf of the cv. PR45H73, in the Manouba region. (b) Severe symptoms on a stem of the cv. Trapper, in the Bizerte region.

isolate was then analyzed using the Basic Local Alignment Search Tool (BLAST) software on NCBI available from: <https://www.ncbi.nlm.nih.gov/>. The best match for each sequence with the lowest *E*-value and the highest query cover and percentage of identity was recorded. In addition, a phylogenetic analysis was carried out by aligning, using the ClustalW algorithm, the ITS sequences of the four isolates from Tunisia with available reference sequences of *L. maculans* and *L. biglobosa* in the GenBank database. Isolates from different countries of origin, representative of previously published *Leptosphaeria* subclades, were used in this assessment (Mendes-Pereira *et al.*, 2003, Voigt *et al.*, 2005, Liu *et al.*, 2006, Vincenot *et al.*, 2008, De Gruyter *et al.*, 2012, Amirdehi *et al.*, 2017, Zou *et al.*, 2019, Zhao *et al.*, 2021, Luo *et al.*, 2021, Zamanmirabadi *et al.*, 2022) (Table 2). A phylogenetic tree was obtained using the Maximum Likelihood method and the Tamura-Nei model (Tamura and Nei, 1993) with 1000 bootstrap replications, under the Mega XI software (Tamura *et al.*, 2021).

Pathogenicity tests

Seedlings of oilseed rape cv. Topas (which has no major resistance genes (Larkan *et al.*, 2016)) were grown under controlled conditions of 20°C, 90% relative humidity and 16 h light, 8 h dark cycles. Using the cotyledon assay for pathogenicity (Bonman *et al.*, 1980), nine plants were slightly wounded in each cotyledon lobe with a sterile needle, and were then each inoculated with a 10 µL spore suspension at 1×10^7 conidia mL⁻¹ (Winter and Koopmann, 2016; Alnajjar *et al.*, 2022). Mock inoculations with only sterile distilled water were also carried out in a similar manner. Each isolate and water controls were inoculated onto nine plants. Symptom evaluations were carried out 14 d post-inoculation using the IMASCORE rating scale (Volke, 1999; Balesdent *et al.*, 2001). *Leptosphaeria maculans* that gave sporulating grey-green tissue collapse in inoculated seedlings was re-isolated and morphologically identified, to assess Koch's postulates.

RESULTS AND DISCUSSION

In the northern visited oilseed rape fields of Tunisia, typical symptoms of blackleg were observed on the crop plants, that included large green to grey-coloured leaf spots and basal stem lesions, which were cream to pale brown thick dark brown borders. Lesions on living plants and on 2-month-old crop residues contained multiple pycnidia often releasing pink mucilage. Disease incidence was variable from one sampled field to another, but ranged between 48 and 100%. No severe attack leading to plant lodging was observed in the northern oilseed rape growing regions of Tunisia in 2018.

After 14 d of incubation, the fungal isolates L31, L36, and L50 had regular white-dark green colonies on PDA and white-brown mycelium on V8 agar, and irregular small brown to black colonies on malt agar. Colonies of isolate L48 varied from distinct brownish-yellow with yellow pigmentation on PDA and malt agar

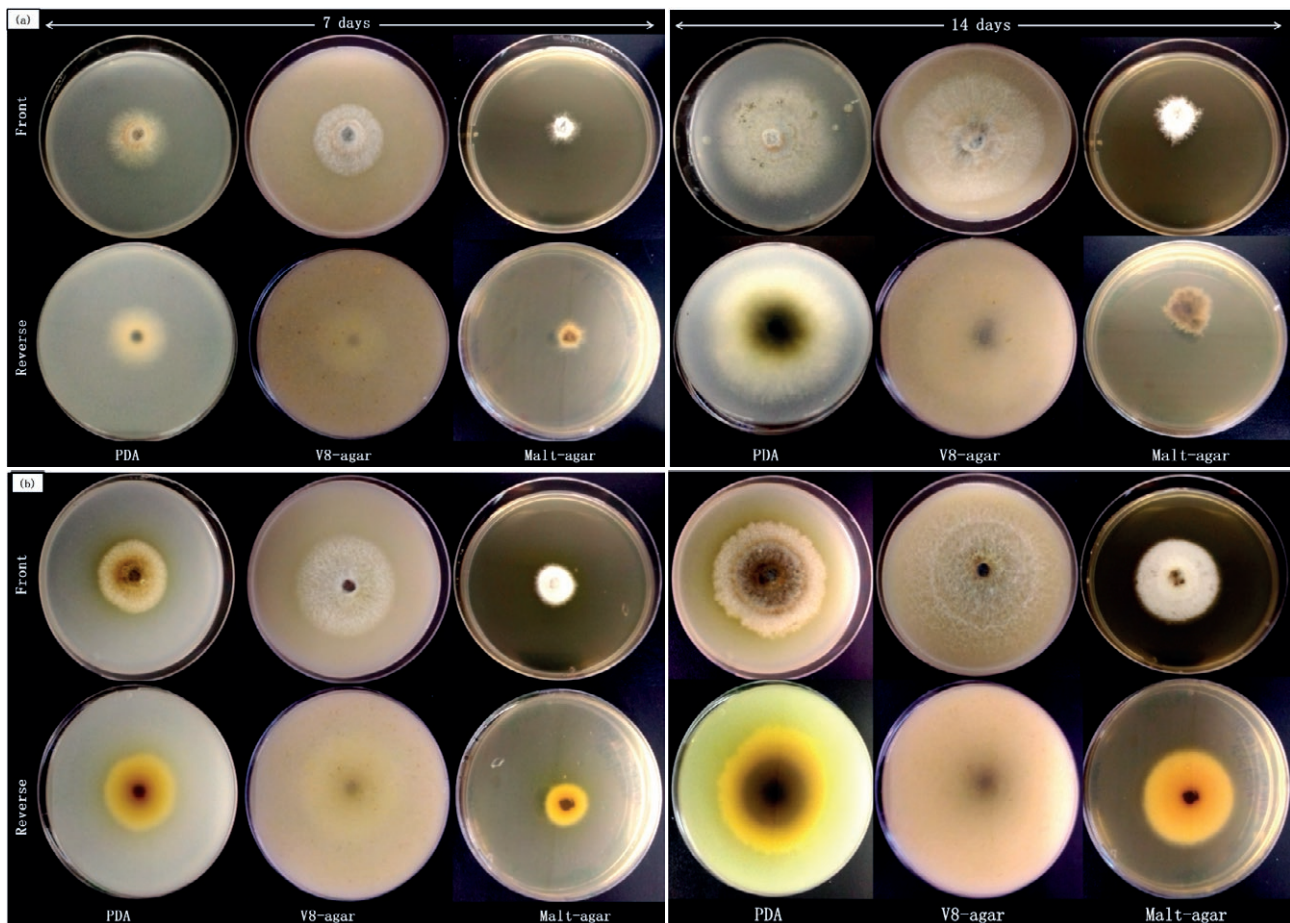


Figure 2. Front and reverse sides of cultures of *Leptosphaeria maculans* isolate L50 (a) and *Leptosphaeria biglobosa* isolate L48 (b), grown for 7 or 14 d at 20°C in the dark on Potato Dextrose agar (PDA), V8 agar or malt agar.

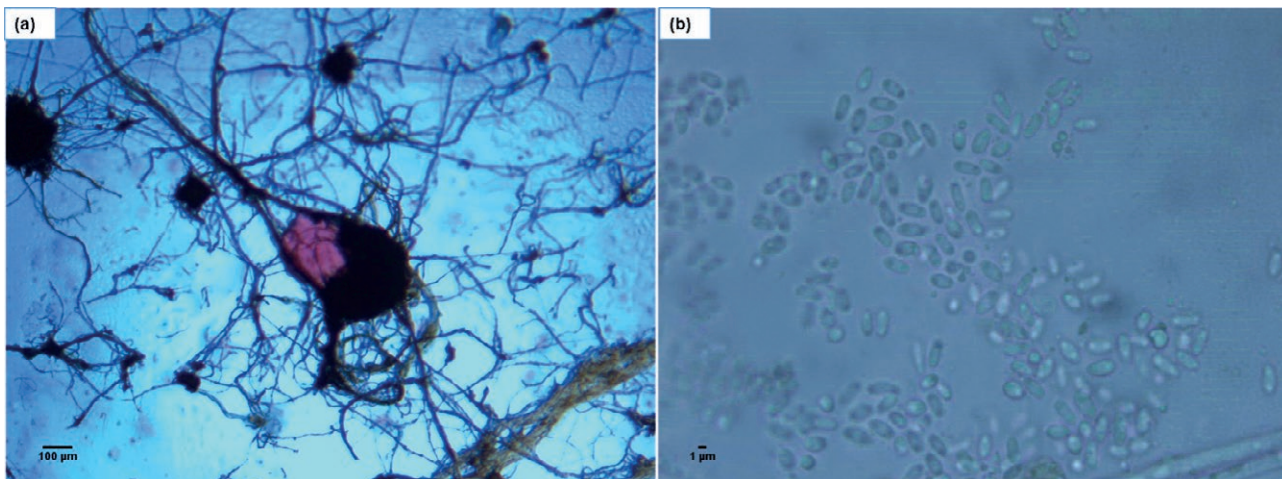


Figure 3. Micrographs of *Leptosphaeria maculans* isolate L50 after 21 d on V8 agar at 20°C in the dark. (a) Pycnidia with typical pinkish mucilage (40 ×), and (b) pycniospores (conidia) (100 ×).

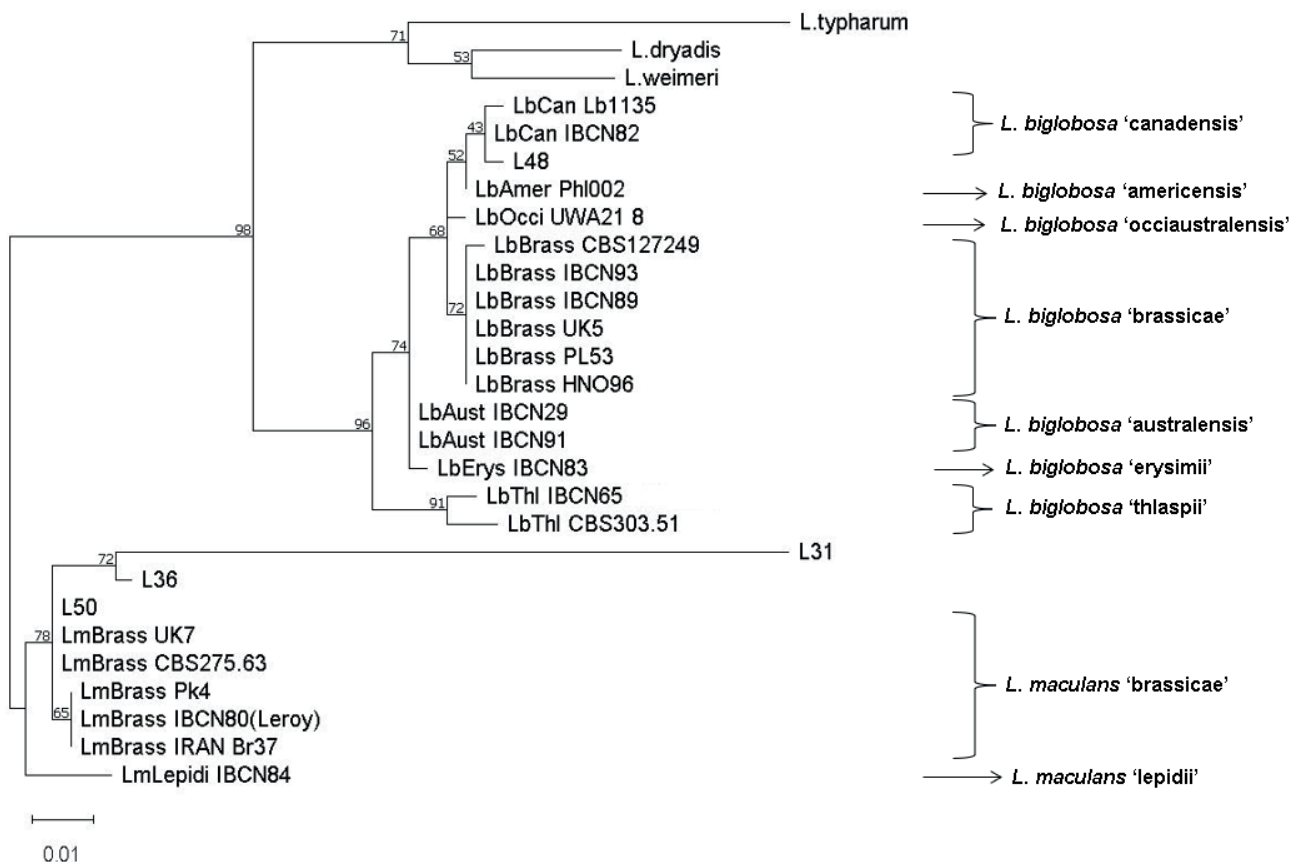


Figure 4. Phylogenetic tree of *Leptosphaeria maculans* and *Leptosphaeria biglobosa* isolates performed on the ITS sequenced region based on the Maximum Likelihood method and Tamura-Nei model. This analysis was carried out using Mega XI software (Tamura *et al.*, 2021), with 1000 bootstrap replications, and involved 28 nucleotide sequences of 327 final nucleotide positions [four sampled isolates from Tunisia, 21 other representative isolates of each subclade available in GenBank, and three different *Leptosphaeria* species (Cámara *et al.*, 2002): *L. typharum* (AF439465), *L. dryadis* (AF439461) and *L. weimeri* (AF439466)].

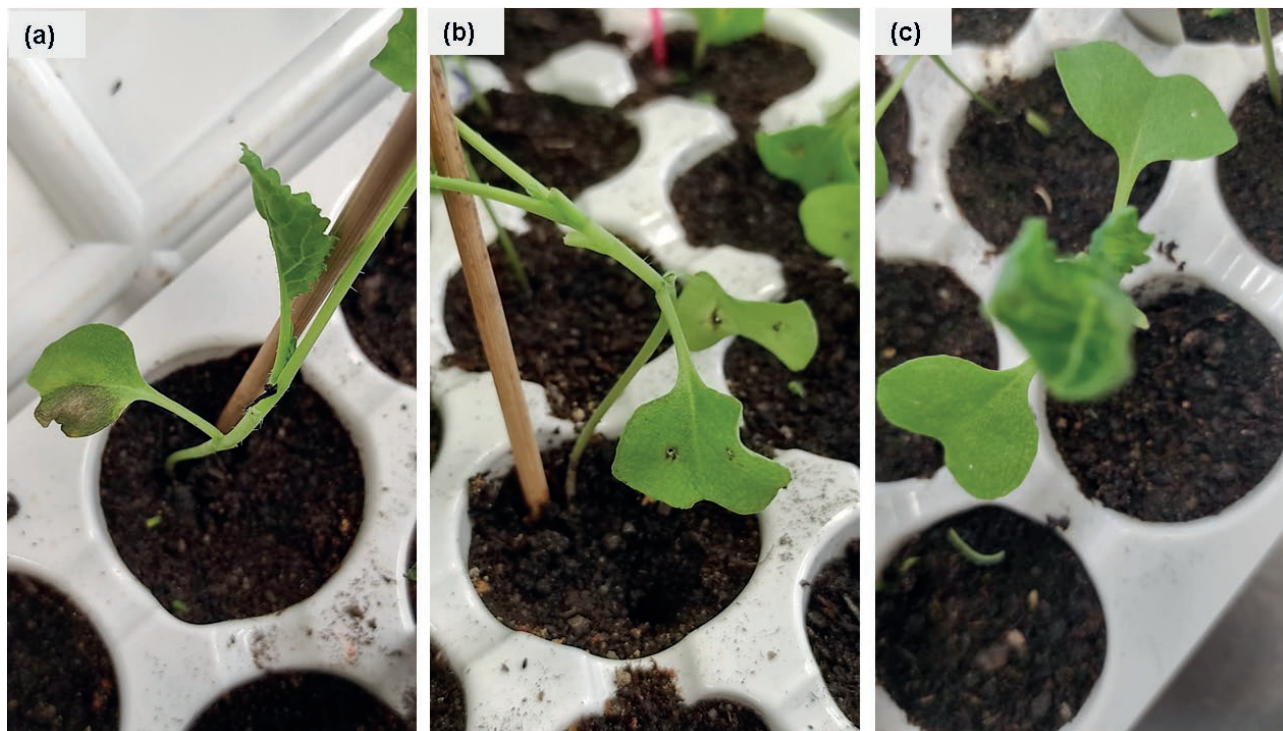


Figure 5. Leaf lesions on 14-d-old seedlings of oilseed rape cv. Topas (Larkan *et al.* 2016) inoculated with *Leptosphaeria maculans* isolate L50 (a) or *Leptosphaeria biglobosa* isolate L48 (b), under controlled conditions (20°C and 16 h dark 8 h light per day). Compatible (leaf spots) reactions were observed for L50 (a), and hypersensitive reactions were observed for L48 (b). No symptoms occurred on control plants inoculated with sterile water (c).

to white and dark-brown with notable aerial mycelium on V8 agar (Figure 2). Similar morphological characteristics have been previously reported, and supported identification of *L. maculans* for isolates L31, L36, and L50; and *L. biglobosa* for isolate L48 (Somda *et al.*, 1996; Howlett *et al.*, 2001; Chen *et al.*, 2010; Vakili Zarj *et al.*, 2017). The pycnidia in cultures were black and globose, and 200–500 µm in diameter. The pycnidia each had an ostiole, from which a conidial cirrhous protruded (Figure 3a). Each cirrhous had a mucilaginous texture and was light pink. No cirrhous colour variations toward bright red or “oxblood”, as described by Rouxel *et al.* (1994), were observed for the isolates. All conidia were single-celled, hyaline, ovoid to cylindrical, and of dimensions 2–4 × 1–2 µm (Figure 3b). The shape and size of the observed conidia and pycnidia for all four isolates corresponded to the descriptions for *Leptosphaeria* species (Somda *et al.*, 1996; Howlett *et al.*, 2001).

Sequenced ITS fragments for the four isolates were registered in GenBank under the accession numbers MZ542280 to MZ542283. Molecular analyses confirmed the identification of *L. maculans* and *L. biglobosa* from oilseed rape fields in Tunisia. Blast results of the ITS

sequences against the NCBI database showed that isolate L48 had 91% similarity with *L. biglobosa* subgroup ‘canadensis’ (GenBank number KJ574217). The remaining three isolates showed 86% (for L31), 93% (for L36), and 97% (for L50) similarity with *L. maculans* subgroup ‘brassicae’ (GenBank number KT225526).

The phylogenetic analyses using the ITS sequences of the four isolates from Tunisia and *L. maculans* reference isolates revealed that *L. maculans* isolates L31, L36 and L50 were most related to the reference isolate IBCN80 (GenBank number AJ550883) belonging to the *L. maculans* ‘brassicae’ subgroup (Figure 4). The *L. biglobosa* isolate L48 was closely related to all *L. biglobosa* ‘canadensis’ reference isolates, including IBCN63 (GenBank number AJ550868) and IBCN82 (GenBank number AJ550872).

The pathogenicity tests showed that for the three *L. maculans* isolates, typical host symptoms of grey-green tissue collapse with numerous pycnidia (IMASCORE = 6) were visible at 14 d post-inoculation (Figure 5a). For the *L. biglobosa* isolate L48, an hypersensitive reaction was developed (IMASCORE = 1) (Volke, 1999; Balesdent *et al.*, 2001) for all replicates (Figure 5b). These

phenotypic results were similar to those found by Zou *et al.* (2019), and confirmed the grouping of L48 to the subclade 'canadensis'. To fulfil Koch's postulates, *L. maculans* was re-isolated from the artificially inoculated plants. All control plants had no disease (Figure 5c).

This report is the first of *Leptosphaeria maculans* and *Leptosphaeria biglobosa* on oilseed rape in Tunisia, causing blackleg. *L. maculans* has been previously identified on wild radish (*Raphanus raphanistrum* L.) in Tunisia (Djebali *et al.*, 2009). The information from the present study will be useful for future blackleg diagnosis and disease management in oilseed rape in Tunisia.

REFERENCES

- Alnajjar D., von Tiedemann A., Koopmann B., 2022. Efficacy of blackleg major resistance genes in *B. napus* in Germany. *Pathogens, Multidisciplinary Digital Publishing Institute* 11: 461. DOI: 10.3390/pathogens11040461.
- Amirdehi E., Fotouhifar K.-B., Javan-Nikkhah M., 2017. Morphological and molecular study on some species of *Phoma* and related taxa in Iran. *Rostaniha, Agricultural Research, Education and Extension Organization (AREEO), Tehran, Iran* 18: 59–76. DOI: 10.22092/botany.2017.113235.
- Balesdent M.H., Attard A., Ansan-Melayah D., Delourme R., Renard M., Rouxel T., 2001. Genetic control and host range of avirulence toward *Brassica napus* cultivars Quinta and Jet Neuf in *Leptosphaeria maculans*. *Phytopathology* 91: 70–76. DOI: 10.1094/PHYTO.2001.91.1.70.
- Bonman J.M., Gabrielson R.L., Williams P.H., Delwiche P.A., 1980. Virulence of *Phoma lingam* to cabbage. *Proceedings 2nd Southeast Asian Symposium on Plant Diseases in the Tropics*, Bangkok, Thailand, 20-26 October 1980.
- Câmara M.P.S., Palm M.E., van Berkum P., O'Neill N.R., 2002. Molecular phylogeny of *Leptosphaeria* and *Phaeosphaeria*. *Mycologia* 94: 630–640. DOI: 10.1080/15572536.2003.11833191.
- Chen G.Y., Wu C.P., Li B., Su H., Zhen S.Z., An Y.L., 2010. Detection of *Leptosphaeria maculans* from imported canola seeds. *Journal of Plant Diseases and Protection* 117: 173–176. DOI: 10.1007/BF03356356.
- De Gruyter J., Woudenberg J.H.C., Aveskamp M.M., Verkley G.J.M., Groenewald J.Z., Crous P.W., 2012. Redisposition of phoma-like anamorphs in *Pleosporales*. *Studies in Mycology* 75: 1–36. DOI: 10.3114/sim0004.
- Djebali N., Scott J., Jourdan M., Souissi T., 2009. Fungi pathogenic on wild radish (*Raphanus raphanistrum* L.) in northern Tunisia as potential biocontrol agents. *Phytopathologia Mediterranea* 48: 205–213.
- Doyle J.J., Doyle J.L., 1987. A rapid DNA isolation procedure for small quantities of fresh leaf tissue. *Phytochemical Bulletin* 19: 11–15.
- Fitt B.D.L., Brun H., Barbetti M.J., Rimmer S.R., 2006. World-wide importance of phoma stem canker (*Leptosphaeria maculans* and *L. biglobosa*) on oilseed rape (*Brassica napus*). *European Journal of Plant Pathology* 114: 3–15. DOI: 10.1007/s10658-005-2233-5.
- Friedt W., Tu J., Fu T., 2018. Academic and economic importance of *Brassica napus* rapeseed. In: *The Brassica napus Genome* (S. Liu, R. Snowdon and B. Chalhouh, eds.), Cham, Springer International Publishing, 1–20.
- Howlett B.J., Idnurm A., Pedras M.S.C., 2001. *Leptosphaeria maculans*, the causal agent of blackleg disease of Brassicas. *Fungal Genetics and Biology* 33: 1–14. DOI: 10.1006/fgbi.2001.1274.
- Howlett B., 2004. Current knowledge of the interaction between *Brassica napus* and *Leptosphaeria maculans*. *Canadian Journal of Plant Pathology* 26: 245–252.
- Larkan N.J., Yu F., Lydiate D.J., Rimmer S.R., Borhan M.H., 2016. Single R gene introgression lines for accurate dissection of the *Brassica - Leptosphaeria* pathosystem. *Frontiers in Plant Science* 7: 1771. DOI: 10.3389/fpls.2016.01771.
- Liu S.Y., Liu Z., Fitt B.D.L., Evans N., Foster S.J., ... Lucas J.A., 2006. Resistance to *Leptosphaeria maculans* (phoma stem canker) in *Brassica napus* (oilseed rape) induced by *L. biglobosa* and chemical defence activators in field and controlled environments. *Plant Pathology* 55: 401–412. DOI: 10.1111/j.1365-3059.2006.01354.x.
- Luo T., Li G., Yang L., 2021. First report of *Leptosphaeria biglobosa* 'canadensis' causing blackleg on oilseed rape (*Brassica napus*) in China. *Plant Disease, Scientific Societies* 105: 3760. DOI: 10.1094/PDIS-12-20-2735-PDN.
- Maghreb Oléagineux, 2022. Présentation du programme Maghreb Oléagineux Tunisie. Available at: <http://maghreboleagineux.com/le-programme/>. Accessed June 26, 2022.
- Medimagh S., Mechri M., Mastouri M., Ben H., Khamassi K., 2018. Genetic variability studies for morphological and qualitative attributes among spring rapeseed (*Brassica napus* L.) varieties under rainfed conditions of Tunisia. In: *Proceedings International Congress on Oil and Protein Crops*. Moldova Academy of Science, Chisinau, Moldova. 20-24 May 2018 41.
- Mendes-Pereira E., Balesdent M.-H., Brun H., Rouxel T., 2003. Molecular phylogeny of the *Leptosphaeria macu-*

- lans*- *L. biglobosa* species complex. *Mycological Research* 107: 1287–1304. DOI: 10.1017/S0953756203008554.
- Rouxel T., Gall C., Balesdent M., 1994. Du polymorphisme au complexe d'espèces : combien d'agents pathogènes sont impliqués dans la nécrose du collet du colza ? *Agronomie* 14: 413–432.
- Schneider C.A., Rasband W.S., Eliceiri K.W., 2012. NIH Image to ImageJ: 25 years of image analysis. *Nature Methods, Nature Publishing Group* 9: 671–675. DOI: 10.1038/nmeth.2089.
- Shoemaker R.A., Brun H., 2001. The teleomorph of the weakly aggressive segregate of *Leptosphaeria maculans*. *Canadian Journal of Botany* 79: 412–419. DOI: 10.1139/b01-019.
- Somda I., Renard M., Brun H., 1996. Morphology, pathogenicity and isozyme variation amongst French isolates of *Leptosphaeria maculans* recovered from *Brassica juncea* cv. Picra. *Plant Pathology* 45: 1090–1098. DOI: 10.1046/j.1365-3059.1996.d01-190.x.
- Tamura K., Nei M., 1993. Estimation of the number of nucleotide substitutions in the control region of mitochondrial DNA in humans and chimpanzees. *Molecular Biology and Evolution* 10:512-526.
- Tamura K., Stecher G., Kumar S., 2021. MEGA 11: Molecular Evolutionary Genetics Analysis Version 11. *Molecular Biology and Evolution*. Available at: <https://doi.org/10.1093/molbev/msab120>.
- Vakili Zarj Z., Rahnama K., Nasrollanejad S., Yamchi A., 2017. Morphological and molecular identification of *Leptosphaeria maculans* in canola seeds and flowers collected from the north Iran. *Archives of Phytopathology and Plant Protection* 50: 526–539. DOI: 10.1080/03235408.2017.1339986.
- Vincenot L., Balesdent M.H., Li H., Barbetti M.J., Sivasithamparam K., Gout L., Rouxel T., 2008. Occurrence of a new subclade of *Leptosphaeria biglobosa* in western Australia. *Phytopathology* 98: 321–329. DOI: 10.1094/PHYTO-98-3-0321.
- Voigt K., Cozijnsen A.J., Kroymann J., Pöggeler S., Howlett B.J., 2005. Phylogenetic relationships between members of the crucifer pathogenic *Leptosphaeria maculans* species complex as shown by mating type (MAT1-2), actin, and β -tubulin sequences. *Molecular Phylogenetics and Evolution* 37: 541–557. DOI: 10.1016/j.ympev.2005.07.006.
- Volke, b. 1999. *Leptosphaeria maculans*, der Erreger der Wurzelhals- und Stengelfäule an Raps: Verbreitung verschiedener Pathogenitätsgruppen in Europa, Quantifizierung des Befalls und Schadwirkung im Freiland. Ph.D. thesis, University of Göttingen, Germany.
- Wang Y., Strelkov S.E., Hwang S.-F., 2020. Yield losses in canola in response to blackleg disease. *Canadian Journal of Plant Science* 100: 488–494. DOI: 10.1139/cjps-2019-0259.
- White T.J., Bruns T., Lee S., Taylor J., 1990. Amplification and direct sequencing of fungal ribosomal RNA genes for phylogenetics. In: *PCR Protocols* (M.A. Innis, D.H. Gelfand and J.J.S.J. White, eds.), Academic Press, San Diego, United States of America, 315–322.
- Williams, Fitt, 1999. Differentiating A and B groups of *Leptosphaeria maculans*, causal agent of stem canker (blackleg) of oilseed rape. *Plant Pathology* 48: 161–175. DOI: 10.1046/j.1365-3059.1999.00333.x.
- Winter M., Koopmann B., 2016. Race spectra of *Leptosphaeria maculans*, the causal agent of blackleg disease of oilseed rape, in different geographic regions in northern Germany. *European Journal of Plant Pathology* 145: 629–641. DOI: 10.1007/s10658-016-0932-8.
- World Agricultural Production, 2022, Rapeseed production by country- World Agricultural Production 2021/2022. Available at: <https://www.worldagricultural-production.com/crops/rapeseed.aspx>, Accessed June 26, 2022.
- Zamanmirabadi A., Hemmati R., Dolatabadian A., Batley J., 2022. Genetic structure and phylogenetic relationships of *Leptosphaeria maculans* and *L. biglobosa* in northern regions of Iran. *Archives of Phytopathology and Plant Protection*, Taylor & Francis 55: 1062–1081. DOI: 10.1080/03235408.2022.2081653.
- Zhao P., Crous P.W., Hou L.W., Duan W.J., Cai L., Liu F., 2021. Fungi of quarantine concern for China I: Dothideomycetes. *Persoonia - Molecular Phylogeny and Evolution of Fungi* 47: 45–105. DOI: 10.3767/persoonia.2021.47.02.
- Zheng X., Koopmann B., Ulber B., von Tiedemann A., 2020. A global survey on diseases and pests in oilseed rape: Current challenges and innovative strategies of control. *Frontiers in Agronomy* 2: 2:590908. DOI: 10.3389/fagro.2020.590908.
- Zou Z., Zhang X., Parks P., du Toit L.J., Van de Wouw A.P., Fernando W.G.D., 2019. A new subclade of *Leptosphaeria biglobosa* identified from *Brassica rapa*. *International Journal of Molecular Sciences* 20: 1668. DOI: 10.3390/ijms20071668.



Citation: E. Troiano, G. Parrella (2023)
First report of tomato leaf curl New
Delhi virus in *Lagenaria siceraria*
var. *longissima* in Italy. *Phytopatho-*
logia Mediterranea 62(1): 25-28. doi:
10.36253/phyto-14147

Accepted: February 9, 2023

Published: April 6, 2023

Copyright: ©2023 E. Troiano, G. Parrella.
This is an open access, peer-reviewed
article published by Firenze Univer-
sity Press (<http://www.fupress.com/pm>)
and distributed under the terms of
the Creative Commons Attribution
License, which permits unrestricted
use, distribution, and reproduction
in any medium, provided the original
author and source are credited.

Data Availability Statement: All re-
levant data are within the paper and its
Supporting Information files.

Competing Interests: The Author(s)
declare(s) no conflict of interest.

Editor: Arnaud G Blouin, Institut des
sciences en production végétale IPV,
DEFRA, Agroscope, Nyon, Switzerland.

ORCID:

ET: 0000-0001-7755-4915

GP: 0000-0002-0412-4014

New or Unusual Disease Reports

First report of tomato leaf curl New Delhi virus in *Lagenaria siceraria* var. *longissima* in Italy

ELISA TROIANO, GIUSEPPE PARRELLA*

*Institute for Sustainable Plant Protection of the National Research Council (IPSP-CNR),
Piazzale Enrico Fermi 1 – 80055 Portici (NA), Italy*

*Corresponding author. E-mail: giuseppe.parrella@ips.cnr.it

Summary. During 2022, a new disease of bottle gourd, causing leaf mosaic and yellowing symptoms, was observed in a private garden in the Campania region, Southern Italy. Incidence of disease was high (up to 80% of plants with symptoms). Polymerase chain reaction (PCR) with coat protein specific primers to tomato leaf curl New Delhi virus (ToLCNDV) indicated association of a begomovirus with the disease. The sequence comparison and phylogenetic analysis of the complete DNA genome further revealed the virus as within ToLCNDV-ES strain. Nevertheless, phylogenetic relationships showed two distinctive subgroups among ToLCNDV-ES isolates, with subgroup I composed only of ToLCNDV-ES isolates identified in the Campania region, including the isolate found in bottle gourd. The possible evolutionary forces that determined evolution of the two subgroups within the ToLCNDV-ES strain, including the role of the vector and cultural practices, are briefly analyzed and discussed.

Keywords. ToLCNDV-ES, ToLCNDV-In, bottle gourd, begomoviruses, subgroups division.

During field monitoring for cucurbit viruses carried out in 2022 in the Campania region of Southern Italy, an unusual disease was noted on some bottle gourd plants (*Lagenaria siceraria* (Molina) Standl.) of the *longissima* variety, growing in a private garden. Symptoms consisted of stunting, reduced leaf area and severe bright-yellow mosaic of the younger leaves and yellowing of the oldest leaves (Figure 1). The flowers were also affected, with deformations and anomalies such as blistering, fraying and reduced size. Fruit development was stunted, many turned necrotic and dropped a few days from fruit set. In many plants production was completely compromised. Incidence of the disease was high with 80% of the plants affected (n = 23). The insect vector *Bemisia tabaci* (Gennadius) (Hemiptera: Aleyrodidae) was found associated to the bottle gourd plants inspected, and the genotype of ten specimens of the vector was identified as previously described (Parrella *et al.*, 2012; Parrella *et al.*, 2014). Only the Q2 variants of the Mediterranean (MED) species were found on the plants.

To identify the putative virus(es) associated with the syndrome observed, ten symptomatic plants were chosen, and one leaf per plant was sampled. The



Figure 1. Symptoms associated to tomato leaf curl New Delhi virus (ToLCNDV) infections in bottle gourd (*Lagenaria siceraria* var. *longissima*): severe bright-yellow mosaic of young leaves and yellowing of oldest leaves.

samples were analyzed by double antibody sandwich ELISA using commercial kits (Bioreba AG) for cucumber mosaic virus (CMV), and by indirect plate trapped antigen ELISA for potyviruses (potygroup test). No positive reactions were observed for all the samples analyzed by ELISA. Loop-mediated isothermal amplification (LAMP)-based kit (Enbitech), including positive and negative controls specific for tomato leaf curl New Delhi virus (ToLCNDV, genus *Begomovirus*, family *Geminiviridae*), was then used to check samples for ToLCNDV infections. Results showed that all samples tested positive for this virus.

DNA was extracted from all symptomatic leaf samples, and from leaves of a healthy and a ToLCNDV-infected zucchini plant, and was used in PCR reactions with primer pair TLCNDVCP1 (5'-CTCCAAGAGATTGAGAAGTCC-3') and TLCNDVCP2 (5'-TCTG-GACGGGCTTACGCCCT-3'), designed to amplify a 1.0 kb fragment encompassing the AV1 (coat protein) gene of ToLCNDV. The expected amplicon was obtained only from symptomatic plants, indicating the presence of ToLCNDV in the bottle gourd samples (Figure 2). The identity of the virus was further confirmed by sequencing 3 out of 10 amplicons. The three sequences showed 100% nucleotide sequence similarity among them, and the greatest level of similarity (99.8%) with the Italian ToLCNDV pepper isolate Caa-164/16 (GenBank no. MK732932), identified in 2019 in the Campania region (Luigi *et al.*, 2019).

The full-length genome sequence (DNA-A and DNA-B) was determined from two ToLCNDV-infected bottle gourd plants. DNA from these plants was used for rolling-circle amplification using ϕ 29 DNA polymer-

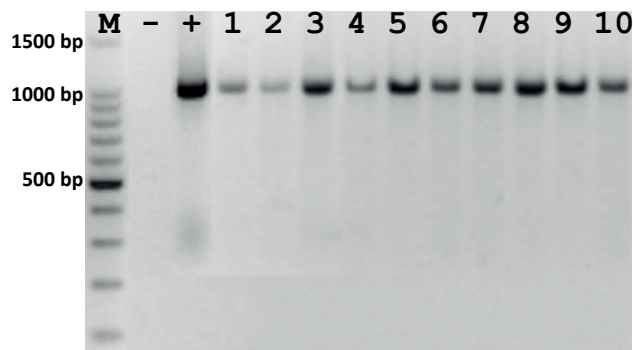


Figure 2. PCR detection of ToLCNDV in symptomatic bottle gourd (*Lagenaria siceraria* var. *longissima*) plants. Lanes M, 100 bp DNA ladder; -, negative control (healthy bottle gourd plant); +, positive control (ToLCNDV infected zucchini plant); 1-10, symptomatic bottle gourd plants.

ase (TempliPhi kit, GE Healthcare) and digested with a set of restriction endonucleases (Haible *et al.*, 2006). The two samples yielded amplification products with identical restriction patterns. One sample was selected to clone the putative DNA-A and DNA-B begomovirus genome components using single *Bam*HI or *Nco*I sites. Inserts of two clones, one corresponding to DNA-A and the other to DNA-B, were completely sequenced.

The DNA-A sequence (2738 nt, GenBank no. OP588911) showed the greatest nucleotide similarity (99.4%) with the DNA-A of the Italian isolates Som-166/16, Caa-164/16 and Cum-45/16 (GenBank nos. MN782303, MK732932 and MF688670, respectively), whereas the DNA-B sequence (2,686 nt, GenBank no. OP588912) showed greatest nucleotide similarity (99.5%) with the DNA-B of the Italian isolate Cum-45/16 (GenBank no. MF688671). Phylogenetic and molecular evolutionary analyses were performed with MEGA version 11, using both Maximum Likelihood and Neighbor-Joining methods and Tamura-Nei model (Tamura *et al.*, 2021).

Phylogenetic reconstructions placed all the ToLCNDV isolates from the Campania region in a distinct subgroup within the ToLCNDV-ES phylogenetic group (Figure 3).

ToLCNDV European isolates belong to the ToLCNDV-ES strain, which are particularly adapted to cucurbits and poorly infectious in other hosts, including tomato (Fortes *et al.*, 2016). In addition, a pumpkin ToLCNDV-ES isolate, belonging to the subgroup I of Italian ToLCNDV isolates and identified in continental Italy (Campania region), has been shown to infect tomatoes only when coinfecting with TYLCV, which may complement functions (e.g. virus movement within hosts) that are blocked in the ToLCNDV-ES-tomato interaction (Vo *et al.*, 2022).

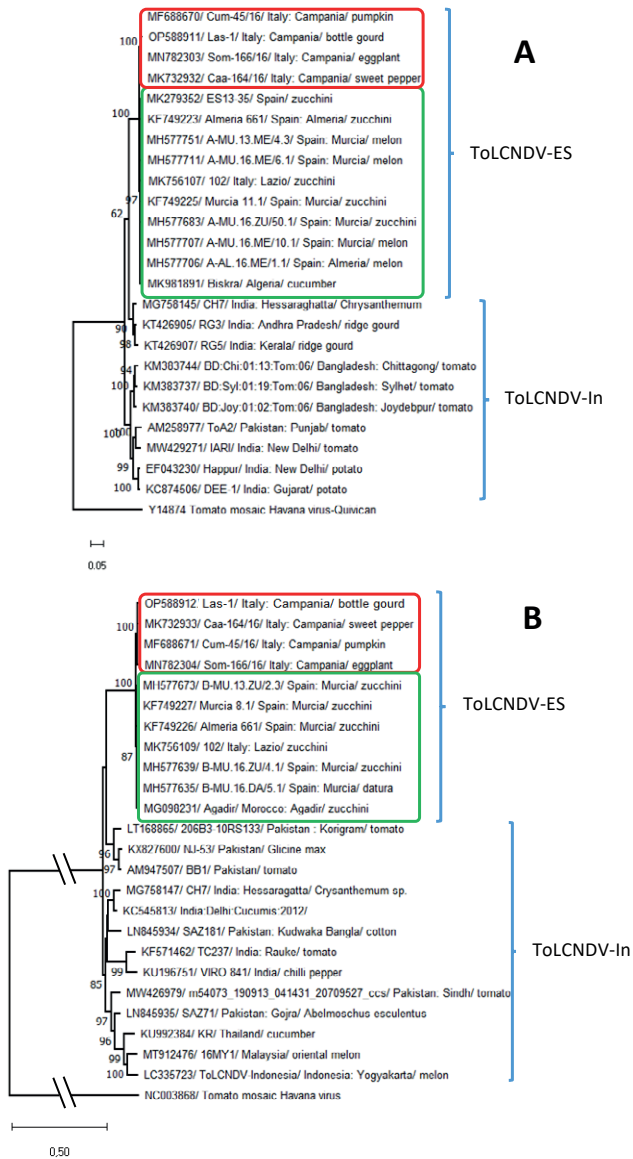


Figure 3. Phylogenetic analyses based on the complete nucleotide sequences of ToLCNDV DNA-A (A) and B (B) components of different virus isolates from the Mediterranean area (ToLCNDV-ES) and Asian continent (ToLCNDV-In). Evolutionary analyses were conducted in MEGA X (Kumar *et al.*, 2018), using the Maximum Likelihood method and Tamura-Nei model (Tamura and Nei, 1993), with 1000 bootstrap replicates. The percentage of trees in which the associated taxa clustered together is shown next to the branches for values >75%. In both trees, the ToLCNDV isolate from bottle gourd (*Lagenaria siceraria* var. *longissima*) Las-1 groups together with the other three isolates identified in the same Italian region (Campania), thus forming a distinct subgroup, the subgroup I (red box), within the ToLCNDV-ES major clade. The green box groups the ToLCNDV isolates belonging to subgroup II (isolates from Spain and Lazio, central Italy) within the ToLCNDV-ES major clade.

The results of the present study highlight the poor adaptation of ToLCNDV-ES isolates to tomato, at least those belonging to subgroup I. In this apparent specialization of ToLCNDV-ES isolates to infect cucurbits, the MED-Q2 genotype of *B. tabaci* may have played a role. The MED-Q2 strain is widespread in the Campania region, especially on intensive cultivation of zucchini that overlaps from spring to autumn-winter. The MED-Q2 populations characterized in this region are also extremely invasive, characterized by abundant populations and high numbers of annual generations, due to an unbalanced sex ratio in favour of females, apparently correlated with an almost fixed infection of the *Rickettsia* sp. as secondary endosymbionts (Parrella *et al.*, 2018).

The combination of these factors may have contributed to the emergence, selection and spread of ToLCNDV isolates that are highly adapted to cucurbits. In addition, from a phylogenetic point of view, within the ToLCNDV-ES major clade and both considering the coat protein (Panno *et al.*, 2019) or the whole genome (the present study), the ToLCNDV-ES isolates identified in Campania group together, forming a distinct subgroup, both for the DNA A and DNA B sequences (Figure 3). Therefore, the phylogenetic relationships among ToLCNDV-ES isolates correlated with their different biological features.

This report represents the first finding of ToLCNDV in bottle gourd in Italy, confirming the widespread occurrence of this virus in different cucurbit crops in Italy. Although *Lagenaria siceraria* has been already reported as a host of ToLCNDV in Thailand (by Ito *et al.*, 2008) and India (by Sohrab *et al.*, 2010), both publications described symptoms of stunting and very small, yellow or chlorotic, slightly curled leaves, that are different from the symptoms we observed on bottle gourd in Italy and reported here (Figure 1). Genetic differences both of the virus strains, spreading in the two continents (Fortes *et al.*, 2016), and of the bottle gourd varieties cultivated in Europe and Asia (Levi *et al.*, 2009) could explain these differences.

Based on the evidence collected in the field during several years of monitoring in the Campania region, relating to the constant and abundant presence of the MEDQ2 variant of *B. tabaci* and to the absence of ToLCNDV infection in tomato, further research on the possible contribution in ToLCNDV evolution by this *B. tabaci* genotype would be appropriate.

LITERATURE CITED

Bertin S., Luigi M., Parrella G., Davino S., Tomassoli L., 2018. Survey of the distribution of *Bemisia tabaci*

- (Hemiptera: Aleyrodidae) in Lazio region (Central Italy): a threat for the northward expansion of tomato leaf curl New Delhi virus (*Begomovirus: Gemini-viridae*). *Phytoparasitica* 46: 171–182.
- Fortes I.M., Sánchez-Campos S., Fiallo-Olivé E., Díaz-Pendón J.A., Navas-Castillo J., Moriones E., 2016. A novel strain of tomato leaf curl New Delhi virus has spread to the Mediterranean Basin. *Viruses* 8: 307.
- Haible D., Kober S., Jeske H., 2006. Rolling circle amplification revolutionizes diagnosis and genomics of geminiviruses. *Journal of Virological Methods* 135: 9–16.
- Ito T., Sharma P., Kittipakorn K., Ikegami M., 2008. Complete nucleotide sequence of a new isolate of tomato leaf curl New Delhi virus infecting cucumber, bottle gourd and muskmelon in Thailand. *Archives of Virology* 153: 611–613.
- Kumar S., Stecher G., Li M., Knyaz C., Tamura K., 2018. MEGA X: Molecular evolutionary genetics analysis across computing platforms. *Molecular Biology and Evolution* 35: 1547–1549.
- Levi A., Thies J., Ling K.-S., Simmons A.M., Kousik C., Hassell R., 2009. Genetic diversity among *Lagenaria siceraria* accessions containing resistance to root-knot nematodes, whiteflies, ZYMV or powdery mildew. *Plant Genetic Resources*, 7: 216–226.
- Luigi M., Bertin S., Manglli A., Troiano E., Davino S., Tomassoli L., Parrella G., 2019. First report of tomato leaf curl New Delhi virus causing yellow leaf curl of pepper in Europe. *Plant Disease* 103: 2970.
- Panno S., Caruso A.G., Troiano E., Luigi M., Manglli A., Vatrano T., ... Davino S., 2019. Emergence of tomato leaf curl New Delhi virus in Italy: estimation of incidence and genetic diversity. *Plant Pathology* 68: 601–608.
- Parrella G., Scassillo L., Giorgini M., 2012. Evidence for a new genetic variant in the *Bemisia tabaci* species complex and the prevalence of the biotype Q in southern Italy. *Journal of Pest Science* 85: 227–238.
- Parrella G., Nappo A.G., Manco E., Greco B., Giorgini M., 2014. Invasion of the Q2 mitochondrial variant of Mediterranean *Bemisia tabaci* in southern Italy: possible role of bacterial endosymbionts. *Pest Management Science* 70: 1514–1523.
- Parrella G., Troiano E., Formisano G., Accotto G.P., Giorgini M., 2018. First report of tomato leaf curl New Delhi virus associated with severe mosaic of pumpkin in Italy. *Plant Disease* 102: 459.
- Sohrab S.S., Mandal B., Ali A., Varma A., 2010. Chlorotic curly stunt: a severe begomovirus disease of bottle gourd in northern India. *Indian Journal of Virology* 21: 56–63.
- Tamura K., Nei M., 1993. Estimation of the number of nucleotide substitutions in the control region of mitochondrial DNA in humans and chimpanzees. *Molecular Biology and Evolution* 10: 512–526.
- Tamura K., Stecher G., Kumar S., 2021. MEGA11: Molecular evolutionary genetics analysis version 11. *Molecular Biology and Evolution* 38: 3022–3027.
- Vo T.T.B., Troiano E., Lal A., Hoang P.T., Kil E.-J., Lee S., Parrella G., 2022. ToLCNDV-ES infection in tomato is enhanced by TYLCV: Evidence from field survey and agroinoculation. *Frontiers in Microbiology* 13: 954460.



Citation: J.N. Rodríguez-Vázquez, K. Ammar, I. Solís, F. Martínez-Moreno (2023) Virulence of *Puccinia triticina* and *Puccinia tritici-duri* on durum wheat in southern Spain, from 2020 to 2022. *Phytopathologia Mediterranea* 62(1): 29-34. doi: 10.36253/phyto-14227

Accepted: February 28, 2023

Published: April 6, 2023

Copyright: © 2023 J.N. Rodríguez-Vázquez, K. Ammar, I. Solís, F. Martínez-Moreno. This is an open access, peer-reviewed article published by Firenze University Press (<http://www.fupress.com/pm>) and distributed under the terms of the Creative Commons Attribution License, which permits unrestricted use, distribution, and reproduction in any medium, provided the original author and source are credited.

Data Availability Statement: All relevant data are within the paper and its Supporting Information files.

Competing Interests: The Author(s) declare(s) no conflict of interest.

Editor: Andy Tekauz, Cereal Research Centre, Winnipeg, MB, Canada.

ORCID:

JNR-V: 0000-0002-6352-6793

KA: 0000-0003-2436-9200

IS: 0000-0003-4807-1070

FMM: 0000-0001-5852-1851

Short Notes

Virulence of *Puccinia triticina* and *Puccinia tritici-duri* on durum wheat in southern Spain, from 2020 to 2022

JAIME NOLASCO RODRÍGUEZ-VÁZQUEZ^{1,*}, KARIM AMMAR², IGNACIO SOLÍS¹, FERNANDO MARTÍNEZ-MORENO¹

¹ Department of Agronomy, University of Seville, ETSIA, Ctra de Utrera km 1, 41013 Seville, Spain

² CIMMYT, Carretera México-Veracruz, km. 45, El Batán, Texcoco 56237, Mexico

*Corresponding author. E-mail: jnrodriguez@agrovegetal.es

Summary. Leaf rust is a major wheat disease in southern Spain, where durum wheat is an important crop. Until the 2019/2020 season, this disease was effectively managed, as the most widely planted cultivars in southern Spain had effective resistance genes. A problem arose in the spring of 2020, when every farm field and durum wheat trial examined displayed leaf rust symptoms. Leaves had few but large uredinal pustules, different from those of the normal leaf rust caused by *Puccinia triticina*, and telia developed rapidly after only a few days. The symptoms clearly fitted with *P. tritici-duri*, another wheat leaf rust species already reported in the western Mediterranean Basin. This species is not new in southern Spain but has never been observed at such high severity on almost every durum wheat cultivar grown in that region. Leaf rust severity was assessed in durum wheat field trials in the 2020, 2021 and 2022 growing seasons in four provinces of southern Spain. During 2020 and 2021, 13 single pustule isolates of leaf rust were also collected from different cultivars of durum wheat. Inoculation of the isolates on a differential host set showed that four different races were present, two being of *P. tritici-duri*. Only cultivar Calero showed consistent resistance to the races of *P. tritici-duri* employed in this study.

Keywords. Leaf rust, virulence, resistance, telia.

INTRODUCTION

Durum wheat (*Triticum turgidum* L. subsp. *durum* (Desf.) Husn.) is an especially important crop in the Mediterranean Basin, sown on 13.14 Mha. In Spain, it is an important crop in the southern region of Andalusia, with a sown area of 180 Kha (in 2019–2020), representing approx. 60% of the durum area in the country (MAPA, 2022). Leaf rust, caused by *Puccinia triticina* Eriks., is one of the main biotic constraints of wheat in Spain. From 1998 to 2005, leaf rust outbreaks on durum wheat were quite frequent in Andalusia, which forced farmers to apply fungicides, and breeders to develop resistant cultivars. In the spring of 2020, leaf rust uredia (or pustules)

were observed in west Andalusia on previously resistant durum wheat cultivars, such as the popular Don Ricardo known to harbour the leaf rust resistance genes *Lr27+Lr31*. The pustules were scarce but larger than usual, with a tendency to rapidly form telia on the abaxial sides of the pustules. The atypical symptoms observed were consistent with leaf rust caused by *Puccinia tritici-duri* V. Bourgin that had already been reported in Morocco, Portugal, and Spain. This species has *Anchusa azurea* Mill. (*Boraginaceae*) as the alternate host, instead of *Thalictrum speciosissimum* (*Ranunculaceae*), the alternate host of *P. triticina* (Ezzahiri and Roelfs, 1992; Anikster *et al.*, 1997).

The objectives of the present study were to determine the severity of this newly emerged leaf rust species on a group of important Spanish durum wheat cultivars, and to characterize the virulence spectra of isolates of *P. triticina* and *P. tritici-duri* collected in four locations of southern Spain in 2020, 2021 and 2022.

MATERIALS AND METHODS

Five durum wheat cultivars popular in southern Spain, namely Amilcar (susceptible check), Don Ricardo, Athoris, Euroduro, and Calero, were sown in field trials, each with three replications (plots each of 8 rows and measuring 1.4 × 5 m) in the locations of Ecija (near Seville), Conil de la Frontera (near Cadiz), Cordova, Escacena del Campo (near Huelva), and Jerez de la Frontera (near Cadiz). Natural leaf rust infections occurred during all three seasons the experiments were conducted. Leaf rust severity was assessed using the modified Cobb scale at the time of maximum infection (Roelfs *et al.*, 1992). Samples of infected durum wheat leaves were obtained from four locations (Conil, Escacena, Ecija, and Cordova), in 2020 and 2021. Infected leaves were collected from plant breeder plots and commercial fields. Single pustule isolates (six in 2020, seven in 2021) were inoculated and grown on the susceptible check Atil/Local Red. A set of 20 near isogenic lines of



Figure 1. Symptoms of *Puccinia tritici-duri* in durum wheat field trials in southern Spain, showing large but sparse pustules (left panel).

the bread wheat cultivar Thatcher was used to determine the virulence spectrum and nomenclature of the 13 collected single pustule isolates (Kolmer and Hughes, 2017). The susceptible checks Thatcher and Atil/Local Red, the cultivar Gatcher, two additional Thatcher isogenic lines, plus 14 durum wheat cultivars with known resistance genes were also inoculated. Four plants of each genotype were grown in trays (60 × 40 × 10 cm) containing (3:1 peat:sand), in a greenhouse of the University of Seville (Spain). The plants were inoculated at two different stages, onto fully developed but young leaves (the first leaf (seedling) and the fifth leaf of each plant), by blowing a mix of uredospores and talcum powder (1:50) (approx. 0.2 mg per genotype). Inoculated plants were placed in a dark dew chamber for 14 h at 20°C, and 100% relative humidity. Twelve days after inoculation, the plants were evaluated for rust development. Infection types were scored using the 0–4 scale described by Stakman *et al.* (1962).

RESULTS AND DISCUSSION

During the 2019–2020 season, leaf rust infections were observed in the field on all durum wheat cultivars tested except Calero (Table 1). The symptoms observed were considered atypical because of the abundance of telia and because the five host cultivars had previously and repeatedly displayed reactions in farmers' fields ranging from complete resistance (Don Ricardo) to intermediate resistance (Amilcar). Rust severity varied among the cultivars and site-years, ranging from 5 to 65% in the susceptible cultivar Amilcar. The variability can be accounted for by different annual weather patterns, and because the sites such as Conil and Jerez were near the ocean where relative humidities are high day-night thermal oscillations are small. However, the relative rankings of the cultivars remained the same throughout.

Data of infection types of the 20-line differential set showed that the 13 isolates corresponded to four different races (Table 2). Two of the races were *Puccinia triticina* and two were *P. tritici-duri*. *Puccinia triticina* differed



Figure 2. Uredia of *Puccinia triticina* (left) and uedia and telia of *P. tritici-duri* uredia+telia (right) on infected durum wheat leaves in a greenhouse 30 d after inoculation

Table 1. Mean leaf rust severity (%) on five durum wheat cultivars grown in replicated field trials at five locations of southern Spain from 2019/20 to 2021/22.

Cultivar / Location-year	Ecija 2020	Jerez 2020	Conil 2020	Cordova 2020	Conil 2021	Escacena 2022
Amilcar	18 a*	50 a	65 a	5 b	17 a	6 a
Don Ricardo	10 b	23 c	25 c	1 c	7 b	3 a
Athoris	10 b	32 bc	40 b	7 b	10 b	4 ab
Euroduro	18 a	37 b	53 ab	12 a	15 a	11 a
Calero	1 c	1 d	5 d	1 c	1 c	1 b

*Duncan test. Within each column, means accompanied by a common letter are not different ($P \leq 0.05$). Disease severities shown are means of single ratings taken for each of the three replicated plots per cultivar.

from *P. tritici-duri* in its avirulence on *Lr1*, *Lr3ka*, *Lr9*, *Lr17*, and virulence on *Lr18*, *Lr20*, whereas *P. tritici-duri* gave a constant mesothetic reaction on almost all the Thatcher near isogenic lines, except for those with *Lr24*, *Lr26* and *Lr28* genes. The mesothetic reaction of *P. tritici-duri* was also common when this pathogen was inoculated onto the additional set of durum wheat cultivars, including cultivars considered resistant to *P. triticina* (Camayo, Storlom). Another difference between the two rust species was the speed with which they developed telia under our greenhouse conditions, with *P. tritici-duri* doing so 26 d after inoculation, much more rapidly than the 45 d for *P. triticina*.

Puccinia tritici-duri has been present in the western Mediterranean Basin for a long time (D'Oliveira and Samborski, 1966; Anikster *et al.*, 1997), in countries such as Morocco, Portugal and Spain with traditions of planting durum wheat. Rust-infected *Anchusa azurea* (the alternate host of *P. tritici-duri*) was observed in southern Spain before 1918 (González-Fragoso, 1918), but all *A. azurea* plants inspected at different locations in Andalusia during 2020 and 2021 were free of rust. It is likely that *P. tritici-duri* had coexisted with *P. triticina* for a long time, infecting durum wheat fields. From 1992 to 2005, durum wheat acreage increased in Andalusia and other regions of Spain, due to subsidies from the European Union, and leaf rust became a serious problem beginning in 1998. Until that time, the host resistance mainly relied on two genes globally, namely *Lr72* and *Lr14a*. However, development of virulent races against these two genes made *P. triticina* a major disease in durum wheat worldwide, including Spain, where virulence to *Lr14a* was first reported in 2013 (Martínez-Moreno and Solís, 2019). By 2005, new *P. triticina* resistant cultivars were released in southern Spain, likely providing *P. tritici-duri* with enhanced opportunities to infect durum wheat.

Given the almost general and variable levels of susceptibility observed in the relatively small sets of durum

wheat germplasm evaluated in southern Spain against *P. tritici-duri*, and the very limited host options available with known *R*-genes to provide complete resistance to *P. triticina*, breeders and pathologists will need to explore and find new sources of suitable resistance in wider and more diverse sets of germplasm. These resistance discovery activities will have to be conducted under conditions that ensure the exclusive presence of *P. tritici-duri*, without the confounding effects of *P. triticina*. However, before such costly initiatives are taken, it is important to accurately assess the likelihood of *P. tritici-duri* becoming a major and yield-limiting pathogen in southern Spain, and to determine the actual yield losses and economic impacts when this pathogen is present on cultivars that are otherwise resistant to *P. triticina*.

ACKNOWLEDGMENTS

The authors thank F. Ruiz and J.A. Muñoz (Agrovegetal S.A.) for their technical support in field trial management, disease monitoring, and leaf rust sample collecting.

AUTHOR CONTRIBUTIONS

FMM and ISM conceived the manuscript and designed the research. JNRV and FMM took and analyzed the data and wrote the manuscript. All authors reviewed the manuscript.

LITERATURE CITED

Anikster Y., Bushnell W.R., Eilam T., Manisterski J., Roelfs A.P., 1997. *Puccinia recondita* causing leaf rust on cultivated wheat, wild wheat, and rye. *Canadian Journal of Botany* 75: 2082–2096.

Table 2. Distribution of leaf rust infection phenotypes at seedling and fifth leaf stages on 22 near-isogenic Thatcher lines, Thatcher, Gatcher, Atil/Local Red, and 14 durum wheat cultivars with known *R*-genes, that were inoculated with the four leaf rust races collected in this study.

Resistance gene	Virulence of races and infection type ^a			
	<i>Puccinia tritici-duri</i> 1	<i>P. tritici-duri</i> 2	<i>P. triticina</i> 1	<i>P. triticina</i> 2
Race nomenclature	PBDSS	BBBBB	DBBSJ	DBBTJ
Inoculations	Seedling/5th leaf	Seedling/5th leaf	Seedling/5th leaf	Seedling/5th leaf
Thatcher	4 / 3	X / 2	4 / 4	3 / 3
Thatcher- <i>Lr1</i>	4 / 3	X / 3	1 / ;	2 / 1
Thatcher- <i>Lr2a</i>	1 / 1	1 / 1	2 / 1	2 / 1
Thatcher- <i>Lr2c</i>	3 / 3	X / 1	3 / 3	3 / 3
Thatcher- <i>Lr3</i>	3 / 3	X / 2	1 / ;	1 / 1
Thatcher- <i>Lr9</i>	1 / 2	1 / 1	0 / 0	0 / 0
Thatcher- <i>Lr16</i>	2 / 2	X / 2	1 / 2	1 / 3
Thatcher- <i>Lr24</i>	; / ;	; / ;	; / ;	; / 1
Thatcher- <i>Lr26</i>	; / ;	; / ;	; / ;	; / 1
Thatcher- <i>Lr3ka</i>	1 / 2	1 / 1	0 / 0	0 / 0
Thatcher- <i>Lr11</i>	X / 3	1 / 1	1 / 1	1 / 1
Thatcher- <i>Lr17</i>	3 / 3	X / 2	; / ;	1 / 1
Thatcher- <i>Lr30</i>	2 / 2	1 / 2	2 / 2	2 / 1
Thatcher- <i>LrB</i>	4 / 3	2 / 2	3 / 3	3 / 3
Thatcher- <i>Lr10</i>	3 / 4	X / 2	3 / 2	3 / 3
Thatcher- <i>Lr14a</i>	4 / 3	X / 2	3 / 4	3 / 3
Thatcher- <i>Lr18</i>	X / 2	X / 2	2 / 2	3 / 3
Thatcher- <i>Lr3bg</i>	3 / 3	X / 1	1 / ;	1 / 1
Thatcher- <i>Lr14b</i>	4 / 2	X / 2	3 / 4	3 / 3
Thatcher- <i>Lr20</i>	3 / 3	X / 2	3 / 2	3 / 3
Thatcher- <i>Lr28</i>	; / ;	1 / ;	1 / ;	1 / 1
Thatcher- <i>Lr19</i>	1 / 2	; / 1	; / ;	; / 0
Thatcher- <i>Lr23</i>	3 / 3	2 / 2	2 / 2	3 / 3
Gatcher (<i>Lr27+Lr31</i>)	X / 3	X / 1	4 / 4	4 / 4
Atil/Local Red	4 / 3	4 / 4	4 / 4	4 / 4
Gallareta (<i>LrAltar</i>)	X / X	X / 3	3 / 3	4 / 3
Somateria (<i>Lr14a</i>)	X / X	X / X	3 / 4	3 / 3
Camayo (<i>LrCam</i>)	X / X	X / X	1 / ;	1 / ;
Colosseo (<i>Lr14a+</i>)	X / 3	X / X	4 / 4	3 / 3
Don Jaime (<i>Lr14a</i>)	X / X	X / X	4 / 4	3 / 3
Don Ricardo (<i>Lr27+Lr31</i>)	X / X	X / X	1 / ;	1 / ;
Don Javier	X / 3	X / X	2 / 2	2 / 3
Storlom (<i>Lr3</i>)	X / X	X / X	; / ;	0 / ;
Jupare (<i>Lr27+Lr31</i>)	X / X	X / X	1 / ;	1 / ;
Guayacán (<i>Lr61</i>)	X / X	X / X	; / ;	; / ;
Aconchi- <i>Lr19</i>	X / X	X / X	0 / 0	0 / 0
Aconchi- <i>Lr47</i>	X / X	X / X	; / ;	0 / ;
Cirno	X / X	X / X	1 / 1	1 / ;
Calero	1 / 1	1 / 1	1 / 1	; / ;
No. isolates	6	3	2	2

^a Infection type assessment according to the 0–4 scale of Stakman *et al.* (1962). 0 = no macroscopic signs of infection, ; = no uredinia with hypersensitive necrotic flecks present, 1 = small uredinia surrounded by necrosis, 2 = small to medium-size uredinia surrounded by necrosis, X = mesothetic response, few but big uredinia surrounded by some necrosis, accompanied by small necrotic spots, 3 = medium-size uredinia with or without chlorosis, 4 = large uredinia without chlorosis or necrosis.

D'Oliveira B., Samborski D.J., 1966. Aecial stage of *Puccinia recondita* on *Ranunculaceae* and *Boraginaceae* in Portugal. Pp. 133–150. *Proceedings of Cereal Rusts Conferences*, Cambridge, United Kingdom.

Ezzahiri B., Roelfs A.P., 1992. *Anchusa italica* as an alternate host for wheat leaf rust in Morocco. *Plant Disease* 76:1185. DOI: 10.1094/PD-76-1185A.

González-Fragoso R., 1918. *La Roya de los Vegetales*. Pub-

- lisher: Junta para Ampliación de Estudios e Investigaciones Científicas (Imp. de Fortanet, Libertad 29), Madrid, Spain, 267 pp.
- Kolmer J.A., Hughes M.E. 2017. Physiologic specialization of *Puccinia triticina* on wheat in the United States in 2015. *Plant Disease* 107: 1496–1506.
- MAPA (Ministerio de Agricultura, Pesca y Alimentación), 2022. Available at: <https://www.mapa.gob.es/es/>. Accessed February 23, 2023.
- Martínez–Moreno F., Solís I., 2019. Wheat rust evolution in Spain: an historical review. *Phytopathologia Mediterranea* 58(1): 3–16. doi: 10.13128/Phytopathol_Mediterr-22561
- Roelfs A.P., Singh R.P., Saari E.E., 1992. *Rust Diseases of Wheat: Concepts and Methods of Disease Management*. CIMMYT, Mexico D.F., Mexico, 81 pp.
- Stakman E.C., Stewart D.M., Loegering W.Q., 1962. *Identification of Physiologic Races of Puccinia graminis var. tritici*. United States Department of Agriculture, Agricultural Research Service, E617, Minnesota, USA, 54 pp.



Citation: V. Moreira, M.J. Carbone, P. Mondino, S. Alaniz (2023) *Colletotrichum* infections during flower development and fruit ripening in four olive cultivars. *Phytopathologia Mediterranea* 62(1): 35-46. doi: 10.36253/phyto-14087

Accepted: February 15, 2023

Published: April 6, 2023

Copyright: © 2023 V. Moreira, M.J. Carbone, P. Mondino, S. Alaniz. This is an open access, peer-reviewed article published by Firenze University Press (<http://www.fupress.com/pm>) and distributed under the terms of the Creative Commons Attribution License, which permits unrestricted use, distribution, and reproduction in any medium, provided the original author and source are credited.

Data Availability Statement: All relevant data are within the paper and its Supporting Information files.

Competing Interests: The Author(s) declare(s) no conflict of interest.

Editor: Epaminondas Paplomatas, Agricultural University of Athens, Greece.

ORCID:

VM: 0000-0001-5784-5918

MJC: 0000-0003-1845-9277

PM: 0000-0002-4494-5271

SA: 0000-0002-6530-7279

Research Papers

Colletotrichum infections during flower development and fruit ripening in four olive cultivars

VICTORIA MOREIRA*, MARIA JULIA CARBONE, PEDRO MONDINO, SANDRA ALANIZ

Departamento de Protección Vegetal, Facultad de Agronomía, Universidad de la República, Av. Garzón 780 12900, Montevideo, Uruguay

*Corresponding author. E-mail address: vmoreira@fagro.edu.uy

Summary. Olive anthracnose, caused by *Colletotrichum*, is an important disease in olive-growing regions, with the most destructive symptoms being fruit rot and blossom blight. Susceptibility of fruit to *Colletotrichum* increases with maturity, but differences between cultivars and *Colletotrichum* species have been reported, still information on flower susceptibility during development is scarce. The susceptibility of the olive cultivars Arbequina, Coratina, Frantoio and Picual was evaluated during flower development and fruit maturity to *Colletotrichum acutatum* s.s., *C. nymphaeae*, *C. fioriniae*, *C. theobromicola* and *C. alienum*. Susceptibility to anthracnose begins in early stages during flower development and increases during blossoming. Flowers of Arbequina, Coratina and Picual were susceptible, whereas those of Frantoio were moderately susceptible. Green fruit developed less anthracnose than mature fruit. At the green fruit stage, Arbequina and Frantoio were the most susceptible, Coratina was intermediate, and Picual was moderately susceptible, while no differences were found among the cultivars at mature fruit stages. No mayor differences were found among the *Colletotrichum* species with exception of *C. theobromicola*, which caused greatest severity at the green fruit stage. Future research should focus on developing anthracnose management strategies to minimize the disease progress from early stages of flower development and fruit ripening, especially in the most susceptible olive cultivars.

Keywords. Olive anthracnose, cultivar susceptibility, blossom blight, soapy rot.

INTRODUCTION

Anthracnose is an important olive disease in olive-growing regions (Cacciola *et al.*, 2012; Moral *et al.*, 2014; Talhinhos *et al.*, 2018; Azevedo-Nogueira *et al.*, 2020), especially in those with humid climates such as South Africa (Gorter, 1956), Australia (Sergeeva *et al.*, 2008), Brazil (Filoda *et al.*, 2021) and Uruguay (Moreira *et al.*, 2021). Eighteen *Colletotrichum* species of the species complexes *C. acutatum*, *C. gloeosporioides* and *C. boninense* have been reported to be associated with this disease (Talhinhos *et al.*, 2011; Schena *et al.*, 2014; Chattaoui *et al.*, 2016; Moral *et al.*, 2017; Talhinhos *et al.*, 2018; Moreira

et al., 2021). In Uruguay, *C. acutatum* s.s. was found as the prevalent species, followed by *C. nymphaeae* and *C. fioriniae* belonging to the *C. acutatum* species complex, and *C. theobromicola* and *C. alienum* belonging to the *C. gloeosporioides* species complex (Moreira et al., 2021).

The most common host symptom caused by anthracnose is fruit rot at the ripening stage. Fruit rot causes yield losses and deterioration in oil quality (Moral et al., 2014; Leoni et al., 2018). Infections can also occur from flowering to fruit ripening. During bloom, species of *Colletotrichum* can infect host plant calices, petals, stamens, and pistils causing flower collapse known as blossom blight (Moral et al., 2009; Talhinhos et al., 2018; Filoda et al., 2021; Moreira et al., 2021). Each infected flower is usually covered with an orange gelatinous mass of *Colletotrichum* conidia (Sergeeva et al., 2008; Moreira et al., 2021). If the flower is not destroyed, *Colletotrichum* infects the fruit set, remaining as latent until fruits ripen, when the typical soapy fruit is expressed (Moral et al., 2009; Talhinhos et al., 2018), although the importance of these infections for yield losses is unknown.

Infected fruits show depressed brown lesions that are rapidly covered with abundant orange gelatinous masses of *Colletotrichum* conidia. Fruits can be infected from green stages, and these infections remain latent infections until fruit maturation. The infected fruit can fall or remain mummified on trees, serving as a primary inoculum sources for subsequent infections in the next year (Moral et al., 2008; 2014; Mosca et al., 2014; Talhinhos et al., 2018).

The Uruguayan climate is characterized by persistent high humidity, frequent rainfall (approx. 1,100 mm per year) and moderate temperatures (Leoni et al., 2018; Conde-Innamorato et al., 2019). These conditions favour olive anthracnose development. In addition, 50% of the plantations (currently 2788 ha) are of the Arbequina cultivar (MGAP-DIEA, 2021), which is moderately susceptible to this disease (Moral, et al., 2014; 2017; Leoni et al., 2018). The remaining 50% of olive groves is planted mostly with cultivars such as Coratina, Picual and Frantoio, which have shown no resistance under these climatic conditions (Leoni et al., 2018). These cultivars are mainly used for oil production for export (MGAP-DIEA, 2020).

Studies have shown that susceptibility of olive cultivars to anthracnose can be variable (Moral and Trapero, 2009; Cacciola et al., 2012; Moral et al., 2014; 2017), and depends on the *Colletotrichum* species (Talhinhos et al., 2015). Fruit susceptibility varies according to developmental stage (Moral et al., 2008; Moral and Trapero, 2009; Talhinhos et al., 2015; Moral et al., 2017). Nevertheless, information is limited on the susceptibility of different fruit maturity stages and different cultivars to *Colletotrichum*. Although flowers can be infected

by *Colletotrichum* (Moral et al., 2014; Kolainis et al., 2020; Moreira et al., 2021), there have been no studies that indicate when in flower differentiation the flowers become susceptible. Knowing when the first infections occur at flowering and their potential incidence is important so anthracnose management strategies can be developed, including those based on fungicides.

The present study focused on evaluating the susceptibility to five *Colletotrichum* species of the Arbequina, Coratina, Picual and Frantoio olive cultivars, the major cultivars produced in Uruguay. The study concentrated on flower development and fruit ripening host stages.

MATERIAL AND METHODS

Plant and fungal material

Apparently healthy olive flower panicles and fruit were collected from commercial orchards of the cultivars Arbequina, Coratina, Picual and Frantoio with scarce anthracnose. The panicles were collected at three different flowering stages, 1- swollen bud (BBCH51), 2- final differentiation (BBCH55), or 3- beginning of flowering (BBCH61), and fruits were collected at two physiological maturity stages, 1- green fruit (BBCH80) or 2- ripe fruit (BBCH89) (Sanz-Cortes et al., 2002). The collected samples were stored in nylon bags in coolers until processing in the laboratory.

Fifteen *Colletotrichum* isolates belonging to *C. acutatum* s.s (eight isolates), *C. nymphaeae* (three), *C. fioriniae* (one), *C. theobromicola* (two) and *C. alienum* (one isolate) were used in this study (Table 1). The previously identified isolates were selected from the olive *Colletotrichum* collection and deposited at the Plant Protection Department, Facultad de Agronomía, Universidad de la República, Uruguay (Moreira et al., 2021).

For inoculum preparation, each isolate was grown on Potato Dextrose Agar (Oxoid Ltd) at 24°C under near UV-light with a 12-h photoperiod. After 7 d incubation, colony surfaces in culture plates were each flooded with 10 mL of sterile distilled water (SDW), and the scraped with a sterile spatel. The resulting conidium suspensions were filtered through layers of cheesecloth, and conidium concentration was adjusted to 1×10^6 conidia mL⁻¹ with a hemacytometer.

Flower inoculation

Flowers in either the Stage 1- swollen bud (BBCH51) or Stage 2- final differentiation (BBCH55) were each surface-disinfected by dipping for 1 min in 1.0% NaClO

Table 1. Uruguayan *Colletotrichum* isolates used to evaluate the susceptibility of four olive cultivars at different phenological stages during flower development and fruit ripening.

Species Complex	Fungal species	Isolate	Olive cultivar	Geographical origin		Organ
<i>C. acutatum</i> species complex	<i>C. acutatum</i>	OL18	Arbequina	Maldonado	Garzón	Flower
		OL36	Arbequina	Montevideo	Melilla	Flower
		OL42	Arbequina	Treinta y Tres	Mendizabal	Flower
		OL51	Arbequina	Rocha	Nuevo Manantial	Leaf
		OL53	Arbequina	Rocha	Nuevo Manantial	Branch
		OL74	Picual	Rocha	Nuevo Manantial	Fruit
		OL92	Coratina	Maldonado	Garzón	Fruit
	<i>C. nymphaeae</i>	OL97	Arbequina	Montevideo	La Paz	Fruit
		OL28	Arbequina	Treinta y Tres	Mendizabal	Flower
		OL96	Arbequina	Montevideo	La Paz	Fruit
		OL113	Arbequina	Canelones	Las Brujas	Fruit
		OL23	Arbequina	Montevideo	La Paz	Flower
	<i>C. gloeosporioides</i> species complex	<i>C. theobromicola</i>	OL110	Manzanilla	Canelones	Las Brujas
OL112			Arbequina	Canelones	Las Brujas	Fruit
<i>C. alienum</i>		OL98	Arbequina	Montevideo	Melilla	Fruit

solution, and then rinsed three times with SDW. For the Stage 3- beginning of flowering (BBCH61) flowers, surface disinfection was not possible due the sensitivity of flower petals to NaClO. After air-drying, the flowers were dipped in respective isolate conidium suspensions for 30 s, placed in transparent plastic trays containing moistened filter paper, and then incubated at 24°C with a 12 h photoperiod. Control treatments inoculated with SDW were included for each cultivar and flower phenological stage. Three repetitions for each cultivar, phenological stage and *Colletotrichum* isolate were used. Each repetition consisted of at least eight swollen buds for Stage 1, two panicles each with at least 15 undeveloped flower buds for Stage 2, and two panicles with at least ten open or semi-open flowers for Stage 3. Each experiment was performed using a completely randomized design with factorial arrangement.

Anthracoze incidence was assessed periodically until the plant material was destroyed or until 100% incidence was achieved, after 12 d for swollen buds, 6 d for final differentiation, or days for beginning of flowering. Incidence was calculated as the percentage of affected buds or flowers in the total number of buds or flowers evaluated. In each evaluation, the initial symptoms and their evolution was recorded as the number of necrotic buds or flowers, and the presence of gelatinous mass of *Colletotrichum* conidia.

Fruit inoculation

Fruits at the Stage 1- green fruit (BBCH80) or Stage 2- ripe fruit (BBCH89) were surface-disinfected by dip-

ping for 3 min in 1% NaClO solution, and then rinsed three times with SDW. After air-drying, the fruits were dipped in respective isolate conidium suspensions for 30 s, and were then placed into plug seedling trays, one fruit in each hole. The plug seedling trays were enclosed in moistened transparent nylon bags, and were then incubated at 24°C with a 12 h photoperiod. Control treatments inoculated with SDW were included for each cultivars and fruit phenological stages. Four repetitions of fruits per cultivar, phenological stages and *Colletotrichum* isolates were used. Each repetition consisted of five fruits, and each experiment was carried out using a completely randomized design with factorial arrangement.

Anthracoze severity was periodically assessed during 50 d for green fruit and 18 d for mature fruit. The 0–5 scale proposed by Moral *et al.*, (2008) was used, where 0 = no visible lesions, 1 = visible lesions affecting <25% of the fruit surface, 2 = 25–49%, 3 = 50–74%, 4 = 75–100% of fruit surface, and 5 = soapy fruit (fruit completely covered with gelatinous mass of *Colletotrichum* spores). Presence of gelatinous masses of *Colletotrichum* conidia was also recorded.

Statistical analyses

Flower anthracnose incidence was plotted for the three flower phenological stages of the four olive cultivars. A regression curve was fitted considering the significance of the regression and the coefficient of determination (R^2), based on average incidence of the 15 *Colletotrichum* isolates and evaluation time. Anthrac-

nose incidence values were also used to calculate the area under the disease progress curve (AUDPC) for each *Colletotrichum* species, using the following formula:

$$AUDPC_i = \sum_{i=1}^n [(I_{i+1} + I_i) / 2] (t_{i+1} - t_i),$$

where I = incidence (%) at i th observation, t_i = time (d) at the i th observation, and n = the total of number of observations.

The AUDPC data were analyzed for normality with the Shapiro-Wilk test, and for homogeneity with the Levene test. These data were subjected to ANOVA with a factorial arrangement, with olive cultivar and *Colletotrichum* species as factors. The treatments means were compared using Tukey's test ($P \leq 0.05$).

Fruit anthracnose severity values were used to calculate the McKinney's Index (Moral *et al.*, 2017), using the following formula:

$$McKinney's\ Index = \frac{\sum(n_i \times i)}{5 \times N} \times 100$$

where i = the severity of symptoms (0 to 5), n_i = the number of fruits with the severity of i , and N = the total number of evaluated fruits.

The McKinney's Index values at the two maturity stages and for the four olive cultivars were plotted. A regression model was adjusted for each *Colletotrichum* species considering the statistical significance of the regression and the coefficient of determination (R^2). Anthracnose severity values were used to calculate the AUDPC for each *Colletotrichum* species using the formula outlined above. The AUDPC data were analyzed for normality with the Shapiro-Wilk test, and for homogeneity with the Levene test. The AUDPC was transformed to when necessary, to comply with normality assumptions. Then, the AUDPC data were subjected to ANOVA, with a factorial arrangement, with olive cultivar and *Colletotrichum* species as factors. The treatments means were compared using by Tukey's test ($P \leq 0.05$). Statistical analyses were carried out using the programs InfoStat version 2016 (<http://www.infostat.com.ar>) and SigmaPlot version 12.0 (<http://www.sigmaplot.co.uk>).

RESULTS

Flower infections

Typical anthracnose symptoms and signs developed in flowers at the three phenological stages in the four cultivars inoculated with the *Colletotrichum* species. No symptoms were observed in control treatments (Figure

1, a to c). Initial symptoms consisted of brownish colouration of the swollen buds or the flower buds at final differentiation, and necrotic lesions on flower petals (Figure 1, a.2 to c.2). The affected organs then quickly blighted, and were covered with orange-salmon coloured gelatinous masses containing abundant *Colletotrichum* conidia (Figure 1, a.3 to c.3). Accelerated detachment of swollen buds, flower buds and open flowers was observed in comparison with the control treatments, where the buds or flowers remained attached for longer periods.

Almost all graphs of blossom blight incidence fitted exponential curves (Figure 2 and Supplementary Table 1). For the AUDPC variables, statistically significant interactions were found between olive cultivars and *Colletotrichum* species inoculated in the three flowering phenological stages (Table 2). The lowest anthracnose incidence was observed at the swollen bud stage, and no major differences were recorded among the four olive cultivars. In this stage, the first symptoms appeared approx. 4 to 7 d after inoculation, whereas the greatest anthracnose incidence was recorded at 12 d, and ranged between 20 and 40% (Figure 2).

At final differentiation stage, the first symptoms were observed at 3 d after inoculation, with the least average incidence (2.0%) in the Frantoio cultivar and the greatest (17%) in the Arbequina cultivar. Incidence then progressed rapidly, and 6 d after inoculation reached 59 for Frantoio and 100% for Arbequina. At Stage 3-beginning flowering greatest anthracnose incidence was recorded. Two d after inoculation, incidence ranged from 8% for Frantoio to 50% for Picual, and 2 d later between 45% for Frantoio and 91% for Arbequina (Figure 2, Table 3).

Except for *C. alienum* inoculated onto cv. Arbequina at bud swollen stage, all five *Colletotrichum* species infected flowers at all three phenological stages. Nevertheless, in some specific species-cultivar-phenological stage combinations, anthracnose symptoms were not visible until the second evaluation, for example, the cultivars Coratina and Picual inoculated with all *Colletotrichum* species at the swollen bud stage (Figure 2).

Fruit infections

Characteristic anthracnose symptoms and signs developed in fruits at the two phenological stages (green and ripe) of the four inoculated cultivars, and also in some fruit not inoculated with *Colletotrichum* species (Figure 1, d and e). Symptoms in uninoculated fruits could have been from natural latent *Colletotrichum* infections. At the green fruit stage, initial symptoms consisted of small, depressed, 1-2 mm necrotic lesions scattered

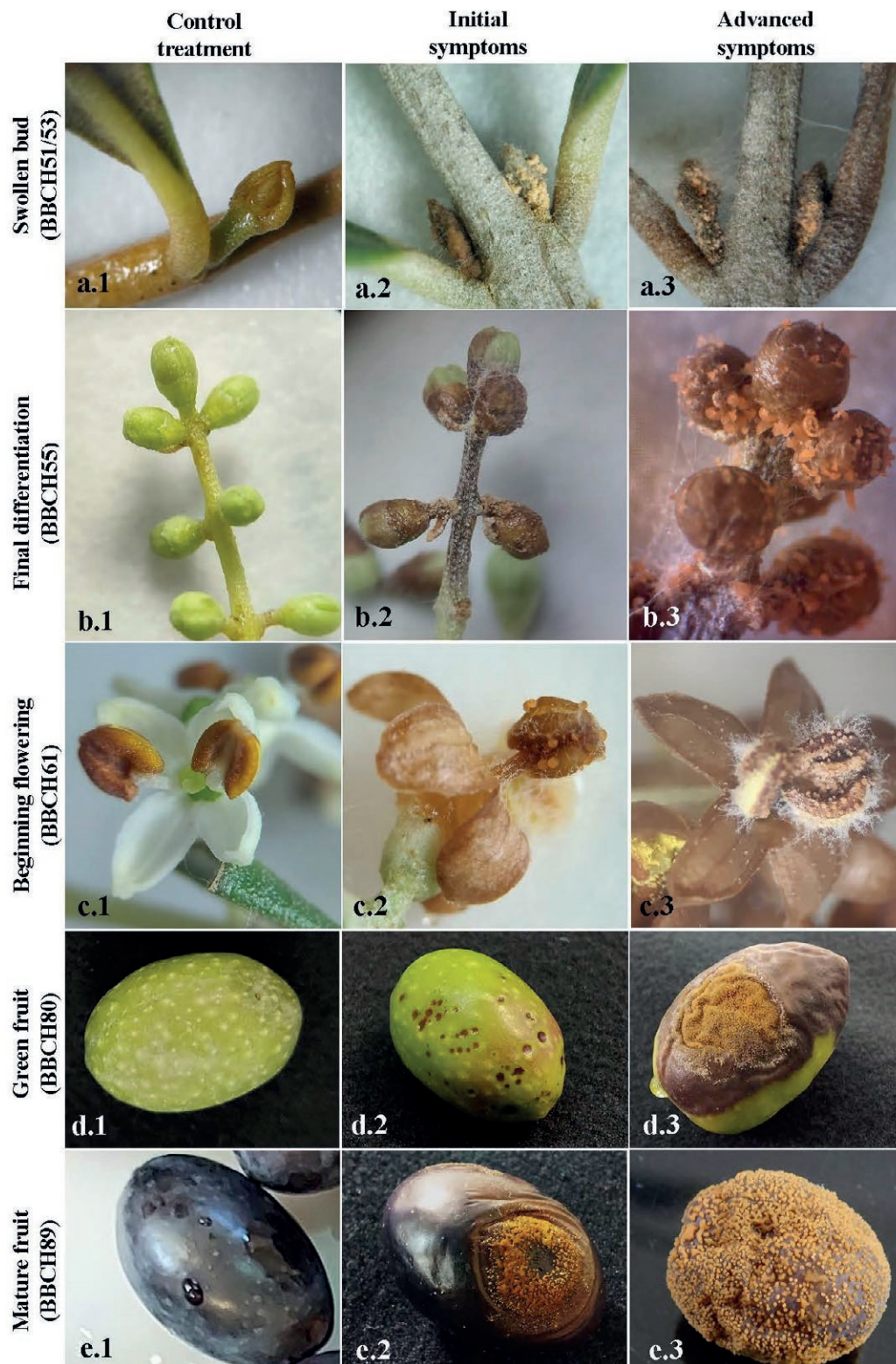


Figure 1. Initial and advanced anthracnose symptoms developed on olive flower and fruits at different phenological stages, after inoculation with species of *Colletotrichum*. **a**, swollen buds (BBCH51/53) 7 and 12 d after inoculation. **b**, final differentiation (BBCH55), 3 and 6 d after inoculation. **c**, beginning of flowering (BBCH61), 2 and 4 d after inoculation. **d**, green fruit (BBCH80) 7 and 26 d after inoculation. **e**, mature fruit (BBCH89) 6 and 12 d after inoculation.

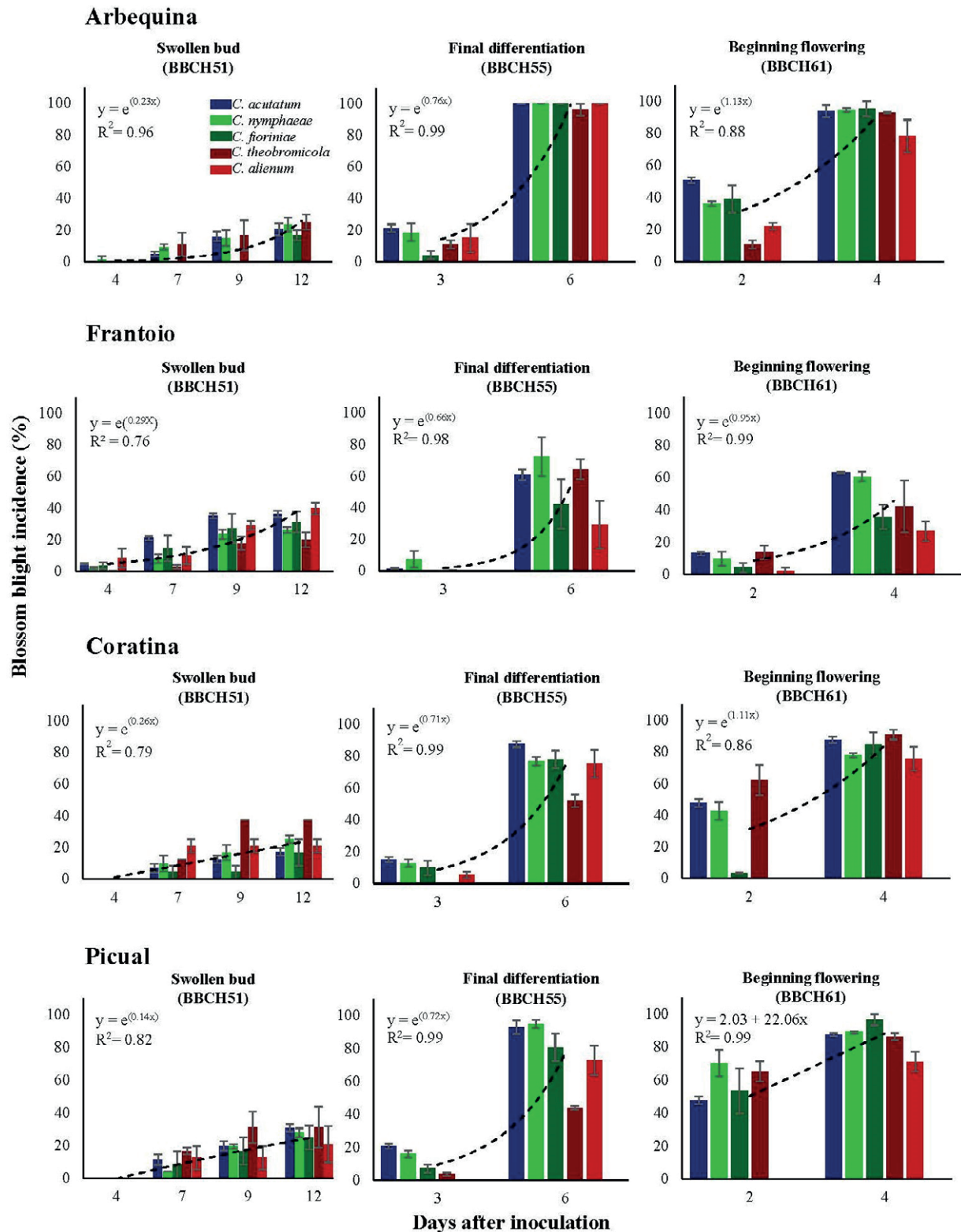


Figure 2. Mean incidences of olive blossom blight in flowers of four olive cultivars inoculated with five *Colletotrichum* species, at swollen buds (BBCH51/53), final differentiation (BBCH55), and beginning of flowering (BBCH61). Vertical bars indicate standard errors of means, each calculated from three replicates. Trend curves were graphed based on the average incidence at each evaluation time. The R^2 and estimations of the trend curves were obtained using SigmaPlot version 12.0 software.

throughout each fruit (Figure 1, d.2). Symptoms then progressed into depressed brown lesions, which were quickly covered with orange gelatinous masses of *Colletotrichum* conidia, known as “soapy fruit” (Figure 1, d.3). On ripe fruit, symptoms developed more quickly and consisted of typical soapy fruit (Figure 1, e.2 and e.3).

Table 2. Analysis of variance of data of Areas Under Disease Progress Curves (AUDPCs) estimated based on anthracnose incidence and severity developed in olive flower and fruits, for four olive cultivars inoculated with five *Colletotrichum* species. The flowers were inoculated at three phenological stages and fruits at two stages.

Source	SS ¹	df	MS	F	P-value	CV
<i>Swollen bud (BBCH51/53)</i>						
Model	441.44	19	23.23	3.77	0.0003	42.61
Cultivar	118.23	3	39.41	6.4	0.0013	
Species	103.16	4	25.79	4.18	0.0068	
Cultivar × species	211.8	12	17.65	2.86	0.0069	
Error	228.01	37	6.16			
Total	669.45	56				
<i>Final differentiation (BBCH55)</i>						
Model	4518.11	19	237.8	14.51	<0.0001	17.46
Cultivar	2425.35	3	808.45	49.31	<0.0001	
Species	1264.55	4	3160.14	19.28	<0.0001	
Cultivar × species	828.22	12	69.02	4.21	0.0003	
Error	655.76	40	16.39			
Total	5173.87	59				
<i>Beginning flowering (BBCH61)</i>						
Model	15598.22	19	820.96	23.28	<0.0001	16.92
Cultivar	8356.56	3	2785.5	78.99	<0.0001	
Species	2926.24	4	731.56	20.75	<0.0001	
Cultivar × species	4315.43	12	356.62	10.2	<0.0001	
Error	1410.57	40	35.26			
Total	17008.79	59				
<i>Green fruit (BBCH80)</i>						
Model	2.1	19	0.11	138.49	<0.0001	5.34
Cultivar	1.08	3	0.36	451.37	<0.0001	
Species	0.84	4	0.21	261.74	<0.0001	
Cultivar × species	0.17	12	0.01	18.18	<0.0001	
Error	0.04	53	8.0E-04			
Total	2.14	72				
<i>Mature fruit (BBCH89)</i>						
Model	5114.24	19	269.17	8.51	<0.0001	15.98
Cultivar	924.51	3	308.17	9.74	<0.0001	
Species	1593.17	4	398.29	12.59	<0.0001	
Cultivar × species	2453.88	12	204.49	6.49	<0.0001	
Error	1866.42	59	31.63			
Total	6980.66	78				

¹ SS: sum of squares, df: degrees of freedom, MS: mean squares, F: teste F, CV: coefficient of variation.

Fruit anthracnose severity at both green and ripe fruit phenological stages, fitted sigmoidal curves (Figure 3 and Supplementary Table 1). For AUDPC variables, significant interactions were found between olive cultivars and inoculated *Colletotrichum* species inoculated, at both green and ripe fruit phenological stages (Table 2). On green fruit, the first symptoms were observed between 5 and 14 d after inoculation. In this stage, Arbequina and Frantoio reached severity values close to 50% at 30 d after inoculation, and Coratina 35 d after inoculation, whereas Picual reached 50% severity at 50 d after inoculation (Figure 3). At the mature fruit stage, the first symptoms were observed 4 d after inoculation. Anthracnose evolution occurred more quickly compared to that at the green fruit stage. For all cultivars and *Colletotrichum* species, severity was an average of 77% at 12 d after inoculation, and 92% at 18 d after inoculation (Figure 3).

The five *Colletotrichum* species were able to infect fruits at two phenological stages in the four olive cultivars. *Colletotrichum theobromicola* caused the greatest AUDPC values at the green fruit stage (Table 3). Green fruit inoculated with this species developed symptoms earlier (5 d after inoculation) compared with the other *Colletotrichum* species (14 d after inoculation), and reached almost 100% severity about 15 d earlier than those inoculated with the other *Colletotrichum* spp. (Figure 3). In ripe fruit, the behaviour among the five *Colletotrichum* species was similar. Anthracnose indices close to 100% were reached at about 15 d after inoculation, except for the cultivars Arbequina and Frantoio inoculated with *C. alienum*, where severity indices were close to 50%.

DISCUSSION

This study assessed anthracnose susceptibility during flower development and fruit ripening in the four main olive cultivars grown in Uruguay, Arbequina, Frantoio, Coratina and Picual. That study used artificial inoculations with five *Colletotrichum* species, of detached olive panicles and fruits. The results indicated that the four olive cultivars assessed were susceptible to *Colletotrichum* at all the evaluated phenological stages, although differences in phenological stages, olive cultivars, and *Colletotrichum* species were detected.

The swollen bud stage was susceptible to *Colletotrichum* species. Although susceptibility of this phenological stage to anthracnose was low, we demonstrated that *Colletotrichum* can infect flowers from early stages during flower development. In later stages of flower develop-

Table 3. Mean Areas Under Disease Progress Curves (AUDPCs) estimated based on anthracnose incidence and severity developed in flower and fruits of four olive cultivars inoculated with five *Colletotrichum* species. The flowers were inoculated at three phenological stages and fruits at two stages.

Cultivar	Species	Phenological stage				
		Flowers			Fruit	
		Swollen bud (BBCH51/53) ¹	Final differentiation (BBCH55)	Beginning flowering (BBCH61)	Green Fruit (BBCH80)	Mature Fruit (BBCH89)
Arbequina	<i>C. acutatum</i>	4.66 abcd ²	35.62 h	48.93 cde	35.94 ef	41.44 de
	<i>C. nymphaeae</i>	5.35 abcd	34.29 gh	34.47 bcd	29.28 de	38.90 cde
	<i>C. fiorinia</i>	1.39 ab	27.09 defgh	43.40 cde	46.70 gh	44.38 e
	<i>C. theobromicola</i>	5.94 abcd	29.53 efgh	31.16 bc	67.78 j	44.30 e
	<i>C. alienum</i>	0.00 a	32.49 fgh	47.90 cde	36.26 fg	13.05 a
Frantoio	<i>C. acutatum</i>	11.94 d	15.83 abcd	22.23 ab	24.77 cd	43.24 de
	<i>C. nymphaeae</i>	6.85 abcd	21.82 bcdefg	20.13 ab	35.72 ef	37.72 bcde
	<i>C. fiorinia</i>	4.58 abcd	10.62 ab	11.06 a	23.60 cd	44.44 e
	<i>C. theobromicola</i>	4.55 abcd	16.31 abcd	17.44 ab	61.98 ij	37.72 bcde
	<i>C. alienum</i>	6.66 abcd	4.90 a	7.85 a	17.97 cd	26.5 abc
Coratina	<i>C. acutatum</i>	4.11 abcd	29.91 efgh	45.75 cde	30.04 de	32.13 bcde
	<i>C. nymphaeae</i>	5.75 abcd	25.59 defgh	40.91 cde	29.28 de	31.33 bcde
	<i>C. fiorinia</i>	2.55 abc	24.49 cdefgh	22.27 ab	20.04 bc	40.72 cde
	<i>C. theobromicola</i>	10.07 cd	13.00 abc	53.81 e	51.39 hi	40.59 cde
	<i>C. alienum</i>	7.52 abcd	21.58 bcdef	18.95 ab	16.96 bc	39.88 cde
Picual	<i>C. acutatum</i>	6.90 abcd	34.62 h	55.61 e	6.26 a	23.11 ab
	<i>C. nymphaeae</i>	5.60 abcd	31.72 fgh	56.98 e	11.95 b	31.35 bcde
	<i>C. fiorinia</i>	5.56 abcd	23.75 cdefgh	50.89 de	4.56 a	31.55 bcde
	<i>C. theobromicola</i>	9.26 bcd	12.84 abc	54.24 e	34.13 ef	31.35 bcde
	<i>C. alienum</i>	7.82 abcd	18.21 bcde	17.78 ab	5.64 a	23.22 bcd

¹ Phenological scale according to Sanz-Cortes *et al.* (2002).

² In each column, mean values followed by the same letter are not significantly different (Tukey's HSD test; $P = 0.05$).

ment, susceptibility increased, and symptoms and signs progressed rapidly. Symptoms included brown colouration of the flower organs that progressed to collapse of inflorescences, known as blossom blight. Affected organs were rapidly covered by typical orange-salmon coloured gelatinous masses, corresponding to *Colletotrichum* conidia (Sergeeva *et al.*, 2008; Iliadi *et al.*, 2018; Moreira *et al.*, 2021).

Results of the present study are similar to those of Kolainis *et al.*, (2020), who observed that in the olive cultivars Koroneiki and Kalamon, the first anthracnose symptoms appeared 2 d after inoculation of detached flowers at beginning of flowering stage. In contrast, Moral *et al.*, (2009) inoculated flowers of Arbequina, Hojiblanca and Picual cultivars at the same phenological stage, but the first symptoms were visible 5 d after inoculation. These differences could be because Moral *et al.*, (2009) utilized attached flowers, whereas in the present study and that of Kolainis *et al.* (2020), detached flowers were used.

For the four olive cultivars evaluated, some differences were observed in anthracnose susceptibility at different flowering stages. No major variations were observed at the swollen bud stage, but at final differentiation and beginning of flowering, Frantoio was the least susceptible cultivar to *Colletotrichum*, Arbequina was the most susceptible, and Coratina and Picual were of intermediate susceptibility. Similar results were obtained by Moral *et al.*, (2009), who found that Arbequina was more susceptible than Hojiblanca and Picual when inoculated at the beginning of flowering.

In previous research, we demonstrated that species *C. acutatum* s.s., *C. nymphaeae*, *C. fiorinia*, *C. theobromicola* and *C. alienum* caused typical blossom blight at beginning of flowering (Moreira *et al.*, 2021). In the present study, although the incubation period could be variable, isolates of these five *Colletotrichum* species infected olive from the early stages of flower development.

Results recorded here for behaviour of inoculated green and ripe olive fruit were generally in agreement

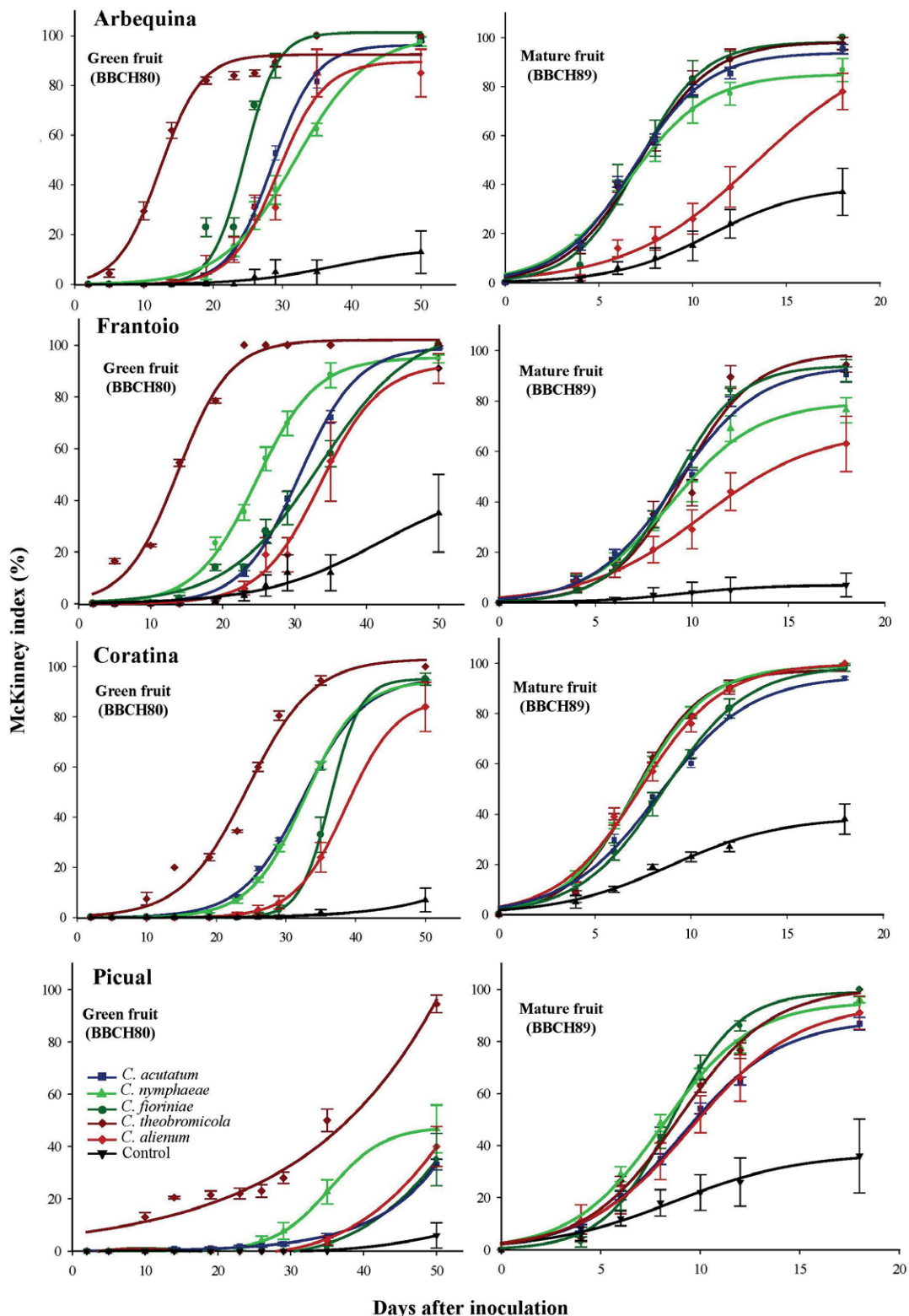


Figure 3. Mean anthracnose severity indices in fruit of four olive cultivars inoculated with five *Colletotrichum* species at green (BBCH80) and ripe fruit (BBCH89) phenological stages. Severity values were used to calculate the McKinney indices. The incidence registered in the control treatments can be attributable to the latent infection of *Colletotrichum* spp. expression. Vertical bars correspond are standard errors of the means calculated based on four replicates. The R^2 and the estimations of trend curves were obtained using SigmaPlot version 12.0 software.

with previous research. Olive fruits can be infected by *Colletotrichum* at different stages during fruit ripening, but the susceptibility increases with ripening (Moral *et al.*, 2008; 2009; Sergeeva, 2014; Chattaoui *et al.*, 2016; Moral *et al.*, 2017). We also observed differences in symptom development. While on ripe fruit the typical soapy fruit symptoms were observed from the beginning, on green fruit initial symptoms consisted of small and depressed necrotic lesions that later progressed into the typical soapy fruit. In addition, at the green stage, the first symptoms were visible between 5 and 7 d after inoculation, whereas on ripe fruit symptoms were seen earlier, between 1 and 5 d post inoculation. Similar results were obtained by Moral *et al.*, (2008), who observed first symptoms at 7 d on detached leaves, and at 4 d on ripe fruit, after *Colletotrichum* inoculation.

For susceptibility of the different olive cultivars, at the green fruit stage Picual was the least susceptible and Arbequina and Frantoio were the most susceptible cultivars to *Colletotrichum* spp., while Coratina developed disease with intermediate susceptibility. These results are similar to other studies, where Arbequina was susceptible to moderately susceptible, Coratina was moderately susceptible (Andres 1991; Moral and Trapero, 2009; Bartolini and Cerreti, 2013), and Picual was moderately resistant or resistant to anthracnose (Moral and Trapero, 2009; Talhinhos *et al.*, 2015; Moral *et al.*, 2017).

On mature fruit, the four olive cultivars were all highly susceptible to anthracnose. These results showed some discrepancies with other studies, where Frantoio was found to be highly resistant to anthracnose in Spain (Moral *et al.*, 2008; Moral and Trapero, 2009; Moral *et al.*, 2017). Nevertheless, in accordance with the present results, Frantoio showed high susceptibility to anthracnose in Argentina (Andres, 1991) and Italy (Loprieno and Tenerini, 1960).

Although the differences in anthracnose susceptibility found among cultivars at the green fruit stage were not recorded for ripe fruit, this was not surprising. Moral and Trapero (2009) reported that green fruits were more resistant to *Colletotrichum* than ripe fruit, probably because of greater concentrations of phenolic compounds in green than ripe fruits. However, when maturity is reached, all olive cultivars can become diseased, and develop complete rot regardless of their early fruit susceptibilities (Moral *et al.*, 2008).

Colletotrichum theobromicola differed substantially from the other *Colletotrichum* species inoculated in this study, being the most aggressive pathogen at the green fruit stage. This was surprising since this species, together with *C. alienum*, was isolated from a low proportion

of olives with typical anthracnose symptoms in Uruguay (Moreira *et al.*, 2021). In Australia, inoculated detached green stage fruit was more affected by *C. theobromicola* and *C. gloeosporioides* s.s than *C. aenigma*, *C. cigarro*, *C. queenslandicum*, *C. siamense* and *C. karstii* (Schena *et al.*, 2014). Regarding the international occurrence of *C. theobromicola*, This pathogen has been reported affecting olive in Argentina, Australia, and Uruguay (Schena *et al.*, 2014; Lima *et al.*, 2020; Moreira *et al.*, 2021), but not in countries of the Mediterranean basin, where most olives are cultivated. Schena *et al.*, (2014) mentioned that new diseases are expected to emerge as consequence of climate change, and suggested that *C. theobromicola* could play an important role in olive anthracnose disease with these changes.

For ripe fruit, behaviour of the five *Colletotrichum* species was similar, except for *C. alienum* which was less aggressive when it was inoculated on the cultivars Arbequina and Frantoio. In Portugal, Talhinhos *et al.*, (2015) found that *C. acutatum* s.s. and *C. nymphaeae* were more aggressive than *C. gloeosporioides* s.s. and *C. rhombiforme* on ripe fruit. In Italy Schena *et al.* (2017) observed that *C. acutatum* s.s. was more aggressive than *C. godetiae* on ripe fruit. In this work, *C. acutatum* s.s., *C. nymphaeae* and *C. fiorinae* were of similar aggressiveness.

The present study is the first in which anthracnose susceptibility has been evaluated at different host flower development stages. Based on these results, the risk of anthracnose occurrence starts at early stages of flower development. This would allow development of improved disease management decisions. For example, the most opportune time to initiate preventive fungicide applications should be at early stages of flower development, to minimize yield losses caused by olive anthracnose. For olive cultivars, Frantoio was moderately susceptible to anthracnose, whereas Picual, Coratina and Arbequina were susceptible cultivars during flowering. However, the present study results indicate that at the green fruit stage, Frantoio and Arbequina were the most susceptible cultivars, Coratina had an intermediate susceptibility, and Picual was least susceptible. In mature fruit, no differences were found among the assessed cultivars. In this study we confirmed that Arbequina, the main olive cultivar produced in Uruguay, was one of the most susceptible to *Colletotrichum* during flowering and fruit ripening. Future research should focus on improving anthracnose management strategies to minimize the impacts of this disease during flower development and fruit maturity, especially in those olive cultivars that are most susceptible to this disease.

ACKNOWLEDGEMENTS

The authors thank the Agencia Nacional de Investigación e Innovación (ANII; POS_NAC_2017_1_140485) and Comisión Académica de Posgrado (CAP) for financial support of this research.

AUTHOR CONTRIBUTIONS

VM was responsible for performing the assays, data analyses and drafted the manuscript of this paper. MJC assisted in experimental assays, data analyses, and made contributions to the manuscript. PM and SA supervised the assays, interpretation of the results, and performed critical revisions of the manuscript. All authors approved the final manuscript.

LITERATURE CITED

- Andrés F., 1991. *Enfermedades y Plagas del Olivo*. 2nd Ed. Riquelme y Vargas Ediciones, S.L., Jaén
- Azevedo-Nogueira F., Martins-Lopes P., Gomes S., 2020. Current understanding of *Olea europaea* L. – *Colletotrichum acutatum* interactions in the context of identification and quantification methods. *Crop Protection* 132, 105106. <https://doi.org/10.1016/j.cropro.2020.105106>
- Bartolini G., Cerreti S., 2013. Olive germplasm (*Olea europaea* L.). Available at: <http://www.oleadb.it> Accessed on January 20, 2022.
- Cacciola S.O., Faedda R., Sinatra F., Agosteo G.E., Schena L., Frisullo S., San Lio G., 2012. Olive anthracnose. *Journal of Plant Pathology* 94: 29-44p. <http://dx.doi.org/10.4454/JPPFA2011001>
- Chattaoui M., Raya M.C., Bouri M., Moral J., Pérez-Rodríguez M., ... Rhouma A., 2016. Characterization of a *Colletotrichum* population causing anthracnose disease on olive in northern Tunisia. *Journal of Applied Microbiology* 120: 1368–1381. <https://doi.org/10.1111/jam.13096>
- Conde-Innamorato P., Arias-Sibillotte M., Villamil J.J., Bruzzone J., Bernaschina Y., ... Leoni C., 2019. It is feasible to produce olive oil in temperate humid climate regions. *Frontiers in Plant Science* 10: 1544. <https://doi.org/10.3389/fpls.2019.01544>
- Filoda P.F., Arellano A.D.V., Dallagnol L.J., Chaves F.C., 2021. *Colletotrichum acutatum* and *Colletotrichum nymphaeae* causing blossom blight and fruit anthracnose on olives in southern Brazil. *European Journal Plant Pathology* 161: 993–998 <https://doi.org/10.1007/s10658-021-02372>
- Gorter G.J., 1956. Anthracnose fungi of olives. *Nature* 178: 1129–1130.
- Iliadi M.K., Tjamos E., Antoniou P., Tsitsigiannis D.I., 2018. First report of *Colletotrichum acutatum* causing anthracnose on olives in Greece. *Plant Disease* 102: 820. <https://doi.org/10.1094/PDIS-09-17-1451-PDN>
- Kolainis S., Koletti A., Lykogianni M., Karamanou D., Gkizi D., ... Aliferis K.A., 2020. An integrated approach to improve plant protection against olive anthracnose caused by the *Colletotrichum acutatum* species complex. *PLOS One* 15:15. <https://doi.org/10.1371/journal.pone.0233916>
- Leoni C., Bruzzone J., Villamil J.J., Martínez C., Montelongo, M.J., Bentancur O., Conde-Innamorato P., 2018. Percentage of anthracnose (*Colletotrichum acutatum* s.s.) acceptable in olives for the production of extra virgin olive oil. *Crop Protection* 108: 47–53. <https://doi.org/10.1016/j.cropro.2018.02.013>
- Lima N.B., Pastor S.E., Maza C.E., Conforto C., Vargas-Gil S., Roca M., 2020. First report of Anthracnose of olive fruit caused by *Colletotrichum theobromicola* in Argentina. *Plant Disease* 104: 589. <https://doi.org/10.1094/PDIS-06-19-1207-PDN>
- Loprieno N., Tenerini I., 1960. Indagini sul *Gloeosporium olivarum* Alm., agente della “lebbra” delle olive. *Phytopathology* 39: 262–290.
- MGAP–DIEA, 2020. Censo de productores de olivos 2020. Serie de trabajos especiales n° 364 Available at: https://www.gub.uy/ministerio-ganaderia-agricultura-pesca/sites/ministerio-ganaderia-agricultura-pesca/files/2021-03/PUBLICACION_Olivos2020_Final.pdf Accessed on January 20, 2023.
- MGAP–DIEA, 2021. Encuesta a productores de olivos 2021. Available at: https://www.gub.uy/ministerio-ganaderia-agricultura-pesca/sites/ministerio-ganaderia-agricultura-pesca/files/documentos/noticias/Comunicado_encuesta%20olivos%202021_0.pdf Accessed on January 20, 2023.
- Moral J., Bouhmidi K., Trapero A., 2008. Influence of fruit maturity, cultivar susceptibility, and inoculation method on infection of olive fruit by *Colletotrichum acutatum*. *Plant Disease* 92(10): 1421–1426. <https://doi.org/10.1094/PDIS-92-10-1421>
- Moral J., Trapero A., 2009. Assessing the susceptibility of olive cultivars to anthracnose caused by *Colletotrichum acutatum*. *Plant Disease* 93: 10.
- Moral J., de Oliveira R., Trapero A., 2009. Elucidation of disease cycle of olive anthracnose caused by *Colletotrichum acutatum*. *Phytopathology* 99: 548–556.
- Moral J., Xaviér C., Roca L.F., Romero J., Moreda W., Trapero A., 2014. La Antracnosis del olivo y su efec-

- to en la calidad del aceite. *Grasas Aceites* 65: 2. Doi: <http://dx.doi.org/10.3989/gya.110913>.
- Moral J., Xavier V.J., Roca L.F., Caballero J., Trapero A., 2017. Variability in susceptibility to anthracnose in the world collection of olive cultivars of Cordoba (Spain). *Frontiers in Plant Science* 8: 1892. <https://doi.org/10.3389/fpls.2017.01892>
- Moreira V., Mondino P., Alaniz S., 2021. Olive anthracnose caused by *Colletotrichum* in Uruguay: symptoms, species diversity and pathogenicity on flowers and fruits. *European Journal Plant Pathology* 160: 663–668. <https://doi.org/10.1007/s10658-021-02274-z>
- Mosca S., Nicosia M.G., Cacciola S.O., Schena L., 2014. Molecular analysis of *Colletotrichum* species in the carposphere and phyllosphere of olive. *PLoS One* 9: e114031. <https://doi.org/10.1371/journal.pone.0114031>
- Sanz-Cortés F., Martínez-Calvo J., Badenes, Bleiholder H., Hack H., Llacer G., Meier U., 2002. Phenological growth stages of olive trees (*Olea europaea*). *Annals of Applied Biology* 140: 151–157. <https://doi.org/10.1111/j.1744-7348.2002.tb00167.x>
- Schena L., Mosca S., Cacciola S.O., Faedda R., Sanzani S.M., ... San Lio G.M., 2014. Species of the *Colletotrichum gloeosporioides* and *C. boninense* complexes associated with olive anthracnose. *Plant Pathology* 63: 437–446. <https://doi.org/10.1111/ppa.12110>
- Schena L., Abdelfattah A., Mosca S., Li Destri Nicosia M.G., Agosteo G.E., Cacciola S.O., 2017. Quantitative detection of *Colletotrichum godetiae* and *C. acutatum sensu stricto* in the phyllosphere and carposphere of olive during four phenological phases. *European Journal Plant Pathology* 149: 337–347 <https://doi.org/10.1007/s10658-017-1185-x>
- Sergeeva V., Nair N.G., Spooner-Hart R., 2008 Evidence of early flower infection in olives (*Olea europaea*) by *Colletotrichum acutatum* and *C. gloeosporioides* causing anthracnose disease. *Australasian Plant Disease Notes* 3: 81–82. <https://doi.org/10.1071/DN08032>
- Sergeeva V., 2014. The Role of Epidemiology Data in Developing Integrated Management of Anthracnose in Olives - a Review. VII International Symposium on Olive Growing, ISHS *Acta Horticulturae* 1057. 6p
- Talhinhas P., Mota-Capitão C., Martins S., Ramos A.P., Neves- Martins J., ... Oliveira H., 2011. Epidemiology, histopathology and etiology of olive anthracnose caused by *Colletotrichum acutatum* and *C. gloeosporioides* in Portugal. *Plant Pathology* 60: 483–495. <https://doi.org/10.1111/j.1365-3059.2010.02397.x>
- Talhinhas P., Gonçalves E., Sreenivasaprasad S., Oliveira H., 2015. Virulence diversity of anthracnose pathogens (*Colletotrichum acutatum* and *C. gloeosporioides* species complexes) on eight olive cultivars commonly grown in Portugal. *European Journal Plant Pathology* 142: 73–83
- Talhinhas P., Loureiro A., Oliveira H., 2018. Olive anthracnose: A yield- and oil quality-degrading disease caused by several species of *Colletotrichum* that differ in virulence, host preference and geographical distribution. *Molecular Plant Pathology* 8: 1797–1807. <https://doi.org/10.1111/mpp.12676>.



Citation: A. Fiorenza, G. Gusella, L. Vecchio, D. Aiello, G. Polizzi (2023) Diversity of *Botryosphaeriaceae* species associated with canker and dieback of avocado (*Persea americana*) in Italy. *Phytopathologia Mediterranea* 62(1): 47-63. doi: 10.36253/phyto-14057

Accepted: February 27, 2023

Published: May 8, 2023

Copyright: ©2023 A. Fiorenza, G. Gusella, L. Vecchio, D. Aiello, G. Polizzi. This is an open access, peer-reviewed article published by Firenze University Press (<http://www.fupress.com/pm>) and distributed under the terms of the Creative Commons Attribution License, which permits unrestricted use, distribution, and reproduction in any medium, provided the original author and source are credited.

Data Availability Statement: All relevant data are within the paper and its Supporting Information files.

Competing Interests: The Author(s) declare(s) no conflict of interest.

Editor: Alan J.L. Phillips, University of Lisbon, Portugal.

ORCID:

AF: 0000-0002-5824-8936

GG: 0000-0002-0519-1200

DA: 0000-0002-6018-6850

GP: 0000-0001-8630-2760

Research Papers

Diversity of *Botryosphaeriaceae* species associated with canker and dieback of avocado (*Persea americana*) in Italy

ALBERTO FIORENZA, GIORGIO GUSELLA*, LAURA VECCHIO, DALIA AIELLO, GIANCARLO POLIZZI

Dipartimento di Agricoltura, Alimentazione e Ambiente, University of Catania, 95123, Via S. Sofia 100, Catania, Italy

*Corresponding author. E-mail: giorgio.gusella@unict.it

Summary. Increased branch canker and dieback were observed in commercial avocado (*Persea americana*) orchards in Sicily, Italy. Surveys were conducted in 2021 and 2022 on 11 orchards to investigate etiology of the disease. Seventy-five plants from four orchards, showing branch canker and dieback, were sampled. Isolations from woody diseased tissues revealed the presence of fungi (*Botryosphaeriaceae*). Identification of the isolates was achieved by morphological and multi-loci phylogenetic analyses (Maximum Parsimony and Maximum Likelihood) of the ITS, *tefl-α*, and *tub2* loci. *Botryosphaeria dothidea*, *Lasiodiplodia citricola*, *Macrophomina phaseolina*, *Neofusicoccum cryptoaustrale*, and *Neofusicoccum luteum* were identified. Representative isolates collected from the orchards, characterized based on the *tub2* locus and identified as *N. parvum*, were excluded from this study, since this species has already been reported in our territory. Pathogenicity tests were conducted on potted, asymptomatic, 2-year-old avocado trees using mycelial plugs. These tests showed that all the *Botryosphaeriaceae* species characterized in this study were pathogenic to avocado. This is the first report of *L. citricola*, *M. phaseolina* and *N. cryptoaustrale* causing canker and dieback on avocado trees, and is the first record of these fungi causing branch disease on avocado in Italy.

Keywords. Fungal diseases, *Botryosphaeria*, *Lasiodiplodia*, *Macrophomina*, *Neofusicoccum*, phylogeny.

INTRODUCTION

Avocado (*Persea americana* L.) is a tree native to Mexico and has spread to many tropical and subtropical regions (Bost *et al.*, 2013). Consumption of avocado fruit and new plantings of avocados has considerably increased (Bost *et al.*, 2013). The greatest production is in Mexico, followed by Colombia and the Dominican Republic (FAOSTAT, 2022). In Europe, Spain was the first country to develop commercial production of avocados (Pérez-Jiménez, 2008). In Italy, avocado production is spread in the Southern regions, mainly in Sicily, where the cultivated area has increased in the last 10 years (Migliore

et al., 2017). In Sicily, avocado provides good agricultural diversification as an alternative crop to citrus (Guarnaccia et al., 2016).

Several diseases can affect avocados, and several fungi taxa have been associated with different symptoms. Traditionally, root diseases have been considered the most important limiting factors for avocado production. Among these, those caused by *Phytophthora cinnamomi* and *Rosellinia necatrix* are considered the most important and widespread diseases of avocado, leading to serious losses, especially in the Mediterranean regions where avocado production is well established (Zentmyer, 1980; López-Herrera and Melero-Vara, 1992; Fiorenza et al., 2021). In recent years, species of *Nectriaceae* have also been shown to be important, especially in Australia where different taxa have been associated with crown root rot disease (Parkinson et al., 2017). In Italy, recent studies have shown the presence of *Nectriaceae* spp. causing a complex of root symptoms (Vitale et al., 2012; Aiello et al., 2020b).

In recent decades, increased research has been carried out on canker diseases of fruit and nut crops (Moral et al., 2019; Guarnaccia et al., 2022a). These diseases have been re-discovered as important and limiting for perennial crops, especially because they cause polyetic epidemics, a complex of pathogen taxa are involved, and most of the causal agents are polyphagous and live as latent pathogens. Among the taxa associated and responsible for shoot, branch and trunk cankers and dieback, *Botryosphaeriaceae* is a widely investigated group of fungi (Batista et al., 2021). *Botryosphaeriaceae* includes fungi that can be pathogens, saprobes and endophytes (Slippers and Wingfield, 2007; Phillips et al., 2013), and can be severe threats to fruit, nut, ornamental and forest trees (Slippers and Wingfield, 2007; Moral et al., 2019). DNA-based tools, especially multi-locus phylogeny, have shown that many genera and species within the *Botryosphaeriales* have been described, synonymized, and re-accommodated (Zhang et al., 2021).

On avocado, despite sporadic reports of *Diaporthe* species associated with cankered tissues (Guarnaccia et al., 2016; Torres et al., 2016; Mathioudakis et al., 2020), different *Botryosphaeriaceae* have been extensively reported worldwide causing canker and dieback on woody tissues and fruit rots, including: *Botryosphaeria dothidea*, *Diplodia aromatica*, *D. dominicana*, *D. mutila*, *D. pseudoseriata*, *D. seriata*, *Dothiorella iberica*, *Lasi-diplodia laeliocattleyae*, *L. pseudotheobromae*, *L. theobromae*, *Neofusicoccum australe*, *N. luteum*, *N. mangiferae*, *N. mediterraneum*, *N. nonquaesitum*, *N. parvum*, and *N. stellenboschiana* (Peterson, 1978; Hartill, 1991; Hartill and Everett, 2002; Zea-Bonilla et al., 2007; McDon-

ald et al., 2009; Ni et al., 2009; McDonald and Eskalen, 2011; Ni et al., 2011; Dann et al., 2013; Auger et al., 2013; Twizeyimana et al., 2013; Carrillo et al., 2016; Valencia et al., 2019; Arjona-Girona et al., 2019; Tapia et al., 2020; Guarnaccia et al., 2020; Wanjiku et al., 2020; Qiu et al., 2020; Rodríguez-Gálvez et al., 2021; Avenot et al., 2022). On avocado, canker and dieback symptoms can appear on shoots, branches, and trunks. Usually, reddish sap that became white/beige with the age has been associated with cankers. The tree bark can be friable or sunken and necrotic, showing cracking, with external dark discolouration. Internally, infected wood becomes brown with characteristic wedge-shaped discolourations affecting the xylem. Under high disease pressure, severe xylem colonization may be observed, with associated wilting of shoots and leaves, that remain attached.

In Italy, the first investigations of avocado branch and trunk canker were reported in 2016, showing the presence of *Botryosphaeriaceae* (*N. parvum*), *Diaportheaceae* (*D. foeniculacea* and *D. sterilis*) and *Glomerellaceae* (*Colletotrichum gloeosporioides* and *C. fructicola*) (Guarnaccia et al., 2016). Studies on avocado canker diseases in Italy have continued, and in 2018, a new species *Neocosmospora persea* was described, causing branch and trunk canker, which was also later reported in Greece (Guarnaccia et al., 2018, 2022b). More recently, the new species *Neopestalotiopsis siciliana* and *Ne. rosae* were reported as causing stem lesions and dieback on avocado (Fiorenza et al., 2021).

An increased incidence of shoot and branch canker has been observed in Sicilian avocado orchards since 2016. The present study has investigated the diversity of *Botryosphaeriaceae* associated with symptomatic trees. The aims of the study were: (i) to characterize the *Botryosphaeriaceae* recovered from symptomatic avocado samples, and (ii) to test their pathogenicity to this host.

MATERIALS AND METHODS

Field surveys and fungal isolation

Surveys were conducted in Sicily (Italy) during 2020 and 2021 in the main avocado production areas (Catania, Messina, and Siracusa provinces). Eleven orchards were investigated and selected for sampling. Samples (three to ten plants from each site) of symptomatic branches, trunks and shoots were collected, and brought to the Plant Pathology laboratory, Dipartimento di Agricoltura, Alimentazione e Ambiente, Sezione di Patologia Vegetale, University of Catania. Small sections (0.5 cm²) of symptomatic tissues were surface disinfected for 1 min in 1.5% sodium hypochlorite solution (NaOCl),

rinsed in sterile distilled water, dried on sterile absorbent paper and placed on potato dextrose agar (PDA; Lickson) amended with 100 mg L⁻¹ of streptomycin sulphate (Sigma-Aldrich) to prevent bacterial growth, and incubated at 25±1°C for 7 d. Isolation frequency of *Botryosphaeriaceae* was calculated using the formula: $F = (N_{Bot}/N_{Tot}) \times 100$, where F is the frequency of *Botryosphaeriaceae*; N_{Bot} is the number of woody fragments from which *Botryosphaeriaceae* were isolated; and N_{Tot} is the total number of woody fragments from which fungi were isolated. Single hyphal tip cultures on PDA were obtained. These isolates are maintained in the Plant Pathology collection of the University of Catania.

Morphological and culture characters of isolates

Representative isolates of each morphologically different group of isolates were transferred onto Technical Agar (AT, 1.2% Agar Technical, Biolife) supplemented with autoclaved pine needles (Smith *et al.*, 1996), and were incubated at room temperature under UV light. The size, colour, and shape of conidia produced by the isolates were examined. After 14 d, pycnidia were observed with a stereoscope, and were mounted in 100% lactic acid. Fifty conidia from each representative isolate were measured (length and width), using an Olympus-BX61 fluorescence microscope coupled to an Olympus DP70 digital camera. Measurements were captured using the software analySIS 3.2 (Soft Imaging System GmbH). Dimensions are reported here as averages.

DNA extraction and PCR analyses

The representative isolates were cultivated on PDA for 7 d, and genomic DNA was extracted using the Wizard Genomic DNA Purification Kit (Promega Corporation) following the manufacturer's protocol. The quality of the DNA was determined using a Nanodrop Lite Spectrophotometer (Thermo Fisher Scientific), and was diluted to 5 ng µL⁻¹ with nuclease-free water. The internal transcriber spacer region (ITS) of the nuclear ribosomal RNA operon was amplified with primers ITS5 and ITS4 (White *et al.*, 1990), and the primers EF1-728F and EF1-986R (Carbone and Kohn, 1999) were used to amplify part of the translation elongation factor 1 alpha locus (*tef1-α*), and primer sets Bt2a and Bt2b (Glass and Donaldson, 1995) were used for the partial beta tubulin locus (*tub2*). The amplifications were each carried out in a final volume of 25 µL using One Taq® 2× Master Mix with Standard Buffer (BioLabs), according to the manufacturer's instructions, on an Eppendorf Mastercycler

(AG 22331). The PCR consisted of initial 30 s at 94°C, followed by 35 cycles at 94°C for 30 s, 50–52°C (ITS), 57–59°C (*tef1-α*), or 52°C (*tub2*) for 1 min, followed by 68°C for 1 min, and 5 min at 68°C. All PCR products were visualized on 1% agarose gels (90 V for 40 min), stained with GelRed®, purified, and sequenced by Macrogen Inc. Forward and reverse DNA sequences were assembled and edited using AliView software (Larsson, 2014), and were submitted to GenBank. Sixty-two isolates were sequenced (amplifying the *tub2* locus only), and based on these preliminary results only 23 representative isolates were considered for further locus sequencing and phylogenetic analyses.

Phylogeny

Sequences were read, assembled, and edited using MEGAX: Molecular Evolutionary Genetics Analysis across computing platforms (Kumar *et al.*, 2018). The ITS, *tub2* and *tef1-α* DNA sequence datasets were aligned using MEGAX. For comparison, 57 additional sequences were selected according to the most recent taxonomic classification of *Botryosphaeriaceae* genera and species involved in this study (Table 1). Two analyses were performed. Maximum parsimony analysis (MP) was performed in PAUP* (Phylogenetic Analysis Using Parsimony) version 4.0a (Swofford, 2002). The analysis of the combined dataset (ITS + *tub2* + *tef1-α*) was obtained with the heuristic search function and tree bisection and reconstruction (TBR) as branch swapping algorithms with the branch swapping option set on 'best trees' only. Gaps were treated as 'missing', the characters were unordered and of equal weight, and Maxtrees were limited to 100. Tree length (TL), consistency index (CI), retention index (RI), and rescaled consistency index (RC) were calculated. A total of 1000 bootstrap replicates were performed to test the robustness of the tree topologies. The best-fit model of nucleotide evolution for each locus, according to the Akaike information criterion (AIC), was evaluated using MrModeltest v. 2.4 (Nylander, 2004). The Maximum Likelihood analysis (ML) of the combined loci was performed in GARLI v.0.951 (Zwickl, 2006), and clade support was assessed by 1000 bootstrap replicates. *Phyllosticta ampelici* (CBS 111645) and *Phyllosticta citricarpa* (CBS 102374) served as the outgroup taxa in both analyses.

Pathogenicity test

A pathogenicity test was conducted in a greenhouse, February to April 2022. Five 2-year-old asymptomatic avocado plants 'Hass' grafted on 'Zutano' rootstocks

Table 1. Information of fungal isolates used in the phylogenetic analysis and their corresponding GenBank accession numbers. Isolates in bold font are from this study. The “T” superfix identifies type material.

Species	Isolate ID	Host	Country	GenBank accession No.		
				ITS	<i>tefl-α</i>	<i>tub2</i>
<i>Botryosphaeria agaves</i>	CBS 133992 = MFLUCC 11-0125 ^T	Agave sp.	Thailand	JX646791	JX646856	JX646841
<i>Botryosphaeria agaves</i>	CBS 141505 = CPC 26299	Agave sp.	France	KX306750	MT592030	MT592463
<i>Botryosphaeria corticis</i>	CBS 119047 ^T CAP 197	<i>Vaccinium corymbosum</i>	New Jersey, USA	DQ299245	EU017539	EU673107
<i>Botryosphaeria corticis</i>	CBS 119048 = CAP 198	<i>Vaccinium corymbosum</i>	New Jersey, USA	DQ299246	EU017540	MT592464
<i>Botryosphaeria dothidea</i>	CBS 115476 = CMW 8000 ^T	<i>Prunus</i> sp.	Switzerland	AY236949	AY236898	AY236927
<i>Botryosphaeria dothidea</i>	CBS 110302 = CAP 007	<i>Vitis vinifera</i>	Portugal	AY259092	AY573218	EU673106
<i>Botryosphaeria dothidea</i>	AB2	<i>Persea americana</i>	Catania, Sicily, Italy	OP654490	OP764459	OP764436
<i>Botryosphaeria dothidea</i>	AB4	<i>Persea americana</i>	Catania, Sicily, Italy	OP654491	OP764460	OP764437
<i>Botryosphaeria dothidea</i>	AB5	<i>Persea americana</i>	Catania, Sicily, Italy	OP654492	OP764461	OP764438
<i>Botryosphaeria dothidea</i>	AC5	<i>Persea americana</i>	Catania, Sicily, Italy	OP654493	OP764462	OP764439
<i>Botryosphaeria dothidea</i>	AC7	<i>Persea americana</i>	Catania, Sicily, Italy	OP654494	OP764463	OP764440
<i>Botryosphaeria dothidea</i>	AC9	<i>Persea americana</i>	Catania, Sicily, Italy	OP654495	OP764464	OP764441
<i>Botryosphaeria dothidea</i>	AC10	<i>Persea americana</i>	Catania, Sicily, Italy	OP654496	OP764465	OP764442
<i>Botryosphaeria dothidea</i>	AC11	<i>Persea americana</i>	Catania, Sicily, Italy	OP654497	OP764466	OP764443
<i>Botryosphaeria fabierciana</i>	CBS 118831 = CMW 14009	<i>Syzygium cordatum</i>	South Africa	DQ316084	MT592032	MT592468
<i>Botryosphaeria fabierciana</i>	CBS 127193 = CMW 27094 ^T	<i>Eucalyptus</i> sp.	China	HQ332197	HQ332213	KF779068
<i>Botryosphaeria kuwatsukai</i>	CGMCC 3.18007 ^T	<i>Malus</i> sp.	China	KX197074	KX197094	KX197101
<i>Botryosphaeria kuwatsukai</i>	CGMCC 3.18008	<i>Amygdalus</i> sp.	China	KX197075	KX197095	KX197102
<i>Botryosphaeria qingyuanensis</i>	GERC 2946 = CGMCC 3.18742 ^T	<i>Eucalyptus hybrid</i>	China	KX278000	KX278105	KX278209
<i>Botryosphaeria qingyuanensis</i>	GERC 2947 = CGMCC 3.18743	<i>Eucalyptus hybrid</i>	China	KX278001	KX278106	KX278210
<i>Botryosphaeria ramosa</i>	GERC 2001 = CGMCC 3.187396	<i>Eucalyptus hybrid</i>	China	KX277989	KX278094	KX278198
<i>Botryosphaeria ramosa</i>	CBS 122069 = CMW 26167 ^T	<i>Eucalyptus camaldulensis</i>	Australia	EU144055	EU144070	KF766132
<i>Lasioidiplodia citricola</i>	CBS 124706 = IRAN 1521C	<i>Citrus</i> sp.	Iran	GU945339	GU945339	KU887504
<i>Lasioidiplodia citricola</i>	CBS 124707 = IRAN 1522C ^T	<i>Citrus</i> sp.	Iran	GU945354	GU945340	KU887505
<i>Lasioidiplodia citricola</i>	CGMCC 3.19022	<i>Vaccinium corymbosum</i>	China	MH330318	MH330327	MH330324
<i>Lasioidiplodia citricola</i>	AC20	<i>Persea americana</i>	Catania, Sicily, Italy	OP654498	OP764481	OP764444
<i>Lasioidiplodia euphorbiaceicola</i>	CGM 3609 ^T	<i>Jatropha curcas</i>	Brazil	KF234543	KF226689	KF254926
<i>Lasioidiplodia euphorbiaceicola</i>	CMW 33268	<i>Adansonia</i> sp.	Senegal	KU887131	KU887008	KU887430
<i>Lasioidiplodia mahajangana</i>	CBS 124925 = CMW 27801 ^T	<i>Terminalia catappa</i>	Madagascar	FJ900595	FJ900641	FJ900630
<i>Lasioidiplodia mahajangana</i>	CBS 124926 = CMW 27818	<i>Terminalia catappa</i>	Madagascar	FJ900596	FJ900642	FJ900631
<i>Lasioidiplodia mediterranea</i>	CBS 137783 = BL 1 ^T	<i>Quercus ilex</i>	Italy	KJ638312	KJ638331	KU887521
<i>Lasioidiplodia mediterranea</i>	CBS 137784 = BL 101	<i>Vitis vinifera</i>	Italy	KJ638311	KJ638330	KU887522
<i>Lasioidiplodia parva</i>	CBS 456.78 ^T	<i>Cassava</i>	Colombia	EF622083	EF622063	KU887523
<i>Lasioidiplodia parva</i>	CBS 494.78	<i>Cassava</i>	Colombia	EF622084	EF622064	EU673114

(Continued)

Table 1. (Continued). Isolates in bold font are from this study. The “T” suffix identifies type material.

Species	Isolate ID	Host	Country	GenBank accession No.		
				ITS	<i>tefl-α</i>	<i>tub2</i>
<i>Lasiodiplodia viticola</i>	CBS 128313 = UCD 2553AR ^T	<i>Vitis vinifera</i>	USA	HQ288227	HQ288269	HQ288306
<i>Lasiodiplodia viticola</i>	CBS 128314 = UCD 2604MO	<i>Vitis vinifera</i>	USA	HQ288228	HQ288270	HQ288307
<i>Macrophomina eufhorbiicola</i>	CMM4134 / CCMF-CNPA 288 ^T	<i>Ricinus communis</i>	Brazil	KU058936	KU058906	MF457658
<i>Macrophomina eufhorbiicola</i>	CMM4145 / CCMF-CNPA 289	<i>Ricinus communis</i>	Brazil	KU058937	KU058907	MF457659
<i>Macrophomina phaseolina</i>	CBS 227.33 ^T	<i>Zea mays</i>		KF531825	KF531804	KF531806
<i>Macrophomina phaseolina</i>	KARE1339	<i>Pistacia vera</i>	USA	MN097202	MN106057	MN106087
<i>Macrophomina phaseolina</i>	AC28	<i>Persea americana</i>	Catania, Sicily, Italy	OP654499	OP764467	OP764445
<i>Macrophomina phaseolina</i>	AC29	<i>Persea americana</i>	Catania, Sicily, Italy	OP654500	OP764468	OP764446
<i>Macrophomina phaseolina</i>	AC51	<i>Persea americana</i>	Catania, Sicily, Italy	OP654501	OP764469	OP764447
<i>Macrophomina phaseolina</i>	AC52	<i>Persea americana</i>	Catania, Sicily, Italy	OP654502	OP764470	OP764448
<i>Macrophomina pseudophaseolina</i>	CPC 21417	<i>Arachis hypogaea</i>	Senegal	KF951791	KF952153	KF952233
<i>Macrophomina pseudophaseolina</i>	CPC 21524	<i>Hibiscus sabdariffa</i>	Senegal	KF951799	KF952161	KF952240
<i>Macrophomina tecta</i>	BRIP 70781 ^T	<i>S. bicolor</i>	Chinchilla, Qld	MW591684	MW592271	MW592300
<i>Macrophomina tecta</i>	BRIP 71603	<i>S. bicolor</i>	Chinchilla, Qld	MW591631	MW592218	MW592301
<i>Macrophomina vaccinii</i>	CGMCC 3.19503 ^T	<i>V. corymbosum</i> × <i>V. darrowii</i>	China	MK687450	MK687426	MK687434
<i>Macrophomina vaccinii</i>	CGMCC 3.19504	<i>V. corymbosum</i> × <i>V. darrowii</i>	China	MK687451	MK687427	MK687435
<i>Neofusicoccum australe</i>	CBS 139662 = CMW 6837 ^T	<i>Acacia</i> sp.	Victoria, Australia	AY339262	AY339270	AY339254
<i>Neofusicoccum australe</i>	CBS 113220 = CMW 6853	<i>Sequoiadendron</i>	Australia	AY339263	AY339271	AY339255
<i>Neofusicoccum cryptoaustrale</i>	CBS 122813 = CMW 23785 ^T	<i>Eucalyptus</i> sp.	South Africa	FJ752742	FJ752713	FJ752756
<i>Neofusicoccum cryptoaustrale</i>	AVORAM1	<i>Persea americana</i>	Catania, Sicily, Italy	OP654508	OP764476	OP764454
<i>Neofusicoccum cryptoaustrale</i>	AVORAM2	<i>Persea americana</i>	Catania, Sicily, Italy	OP654509	OP764477	OP764455
<i>Neofusicoccum cryptoaustrale</i>	AVORAM3	<i>Persea americana</i>	Catania, Sicily, Italy	OP654510	OP764478	OP764456
<i>Neofusicoccum cryptoaustrale</i>	AVORAM4	<i>Persea americana</i>	Catania, Sicily, Italy	OP654511	OP764479	OP764457
<i>Neofusicoccum cryptoaustrale</i>	AVORAM5	<i>Persea americana</i>	Catania, Sicily, Italy	OP654512	OP764480	OP764458
<i>Neofusicoccum lummitzeriae</i>	CBS 139674 = CMW 41469 ^T	<i>Lummitzera racemosa</i>	South Africa	KP860881	KP860724	KP860801
<i>Neofusicoccum lummitzeriae</i>	CBS 139675 = CMW 41228	<i>Lummitzera racemosa</i>	South Africa	MT587480	MT592193	MT592685
<i>Neofusicoccum luteum</i>	CBS 110497 = CPC 4594 = CAP 037	<i>Vitis vinifera</i>	Portugal	EU673311	EU673277	EU673092
<i>Neofusicoccum luteum</i>	CBS 110299 = LM 926 = CAP 002 ^T	<i>Vitis vinifera</i>	Portugal	AY259091	KX464688	DQ458848
<i>Neofusicoccum luteum</i>	AVF3	<i>Persea americana</i>	Catania, Sicily, Italy	OP654503	OP764471	OP764449
<i>Neofusicoccum luteum</i>	AVF5	<i>Persea americana</i>	Catania, Sicily, Italy	OP654504	OP764472	OP764450
<i>Neofusicoccum luteum</i>	AVF6	<i>Persea americana</i>	Catania, Sicily, Italy	OP654505	OP764473	OP764451
<i>Neofusicoccum luteum</i>	AVF7	<i>Persea americana</i>	Catania, Sicily, Italy	OP654506	OP764474	OP764452
<i>Neofusicoccum luteum</i>	AVF8	<i>Persea americana</i>	Catania, Sicily, Italy	OP654507	OP764475	OP764453
<i>Neofusicoccum mediterraneum</i>	CBS 121558	<i>Olea europea</i>	Italy	GU799463	GU799462	GU799461
<i>Neofusicoccum mediterraneum</i>	CBS 121718 = CPC 13137 ^T	<i>Eucalyptus</i> sp.	Greece	GU251176	GU251308	GU251836

(Continued)

Table 1. (Continued). Isolates in bold font are from this study. The “T” superfix identifies type material.

Species	Isolate ID	Host	Country	GenBank accession No.		
				ITS	<i>tefl-α</i>	<i>tub2</i>
<i>Neofusicoccum protearum</i>	CBS 114176 = CPC 1775 = JT 189 ^T	<i>Leucadendron salignum</i> × <i>L. lauroolum</i>	South Africa	AF452539	KX464720	KX465006
<i>Neofusicoccum protearum</i>	CBS 115177 = CPC 4357	<i>Protea magnifica</i>	South Africa	FJ150703	MT592239	MT592731
<i>Neofusicoccum stellenboschiana</i>	CBS 110864 = CPC 4598	<i>Vitis vinifera</i>	South Africa	AY343407	AY343348	KX465047
<i>Neofusicoccum terminaliae</i>	CBS 125263 = CMW 26679 ^T	<i>Terminalia sericea</i>	South Africa	GQ471802	GQ471780	KX465052
<i>Neofusicoccum terminaliae</i>	CBS 125264 = CMW 26683	<i>Terminalia sericea</i>	South Africa	GQ471804	GQ471782	KX465053
<i>Neofusicoccum ursorum</i>	CBS 122811 = CMW 24480 ^T	<i>Eucalyptus</i> sp.	South Africa	FJ752746	FJ752709	KX465056
<i>Neofusicoccum ursorum</i>	CBS 122812 = CMW 23790	<i>Eucalyptus</i> sp.	South Africa	FJ752745	FJ752708	KX465057
<i>Neofusicoccum viticlavatum</i>	CBS 112878 = CPC 5044 = JM 86 ^T	<i>Vitis vinifera</i>	South Africa	AY343381	AY343342	KX465058
<i>Neofusicoccum viticlavatum</i>	CBS 112977 = STE-U 5041	<i>Vitis vinifera</i>	South Africa	AY343380	AY343341	KX465059
<i>Phyllosticta ampelcida</i>	CBS 111645	<i>Taxus baccata</i>	Netherlands	FJ824766	FJ824773	FJ824779
<i>Phyllosticta citricarpa</i>	CBS 102374	<i>Citrus aurantium</i>	Brazil	FJ824767	FJ538371	FJ824778

were selected for each tested fungal species. Inoculations were each carried out using a mycelium plug (0.5 cm²) from a 10-d-old culture of each of *Botryosphaeria dothidea* (AC7), *Lasiodiplodia citricola* (AC20), *Macrophomina phaseolina* (AC29), *Neofusicoccum crypto-aurale* (AVORAM4), and *Neofusicoccum lutem* (AVF5). Each inoculation site was first surface disinfected with a 70% ethanol solution. Two points of inoculation for each plant were made on the stem after removing a piece of bark with a sterile scalpel blade, placing the isolate mycelium plug onto the wound and covering it with Parafilm® (American National Can) to prevent desiccation. Three 2-year-old asymptomatic avocado plants were inoculated with sterile PDA plugs to serve as inoculation controls. The plants were moved to a greenhouse and regularly watered. Temperature in the greenhouse ranged from 18 to 27°C and humidity from 70 to 80%. The inoculated plants were monitored weekly for symptom development, and a final assessment was conducted 63 d after the inoculations. Lesion length measurements were recorded, and were statistically analyzed in Statistix 10 (Analytical Software, 2013) using analysis of variance (ANOVA). Mean differences were compared with the Fisher's protected least significant difference (LSD) test at $\alpha = 0.05$. To fulfill Koch's postulates, re-isolations were carried out following the procedure described above, and each re-isolated fungus was identified through observation of morphological characteristics.

RESULTS

Field surveys and fungal isolations

Disease was observed on 2 to 10-year-old avocado plants 'Hass', grafted on different rootstock cultivars ('Zutano', 'Duke 7', and 'Dusa') in Sicily (Italy). All the sampled plants showed symptoms of shoot and branch canker, and dieback emerging within the green canopies (Figure 1 A to D). Occasionally, a white powder was present on the surfaces of the lesions (Figure 1 E). It was also possible to observe the infections starting from pruning wounds (Figure 1 F and G). The bark of cankered shoots was cracked, darkly discoloured, and/or slightly sunken (Figure 1 H). Cankers were reddish-brown under the bark, and variable in shape. Necrotic lesions and internal discoloration were observed at the grafting points of young plants (Figure 1 I). Isolations frequently (41%) yielded Botryosphaeriaceae-like fungi, and *Botryosphaeriaceae* were detected in all the samples analyzed.

A total of 106 *Botryosphaeriaceae* isolates were collected and stored. Of these, 62 isolates (59%) were processed for DNA extraction, PCR, and sequencing. A

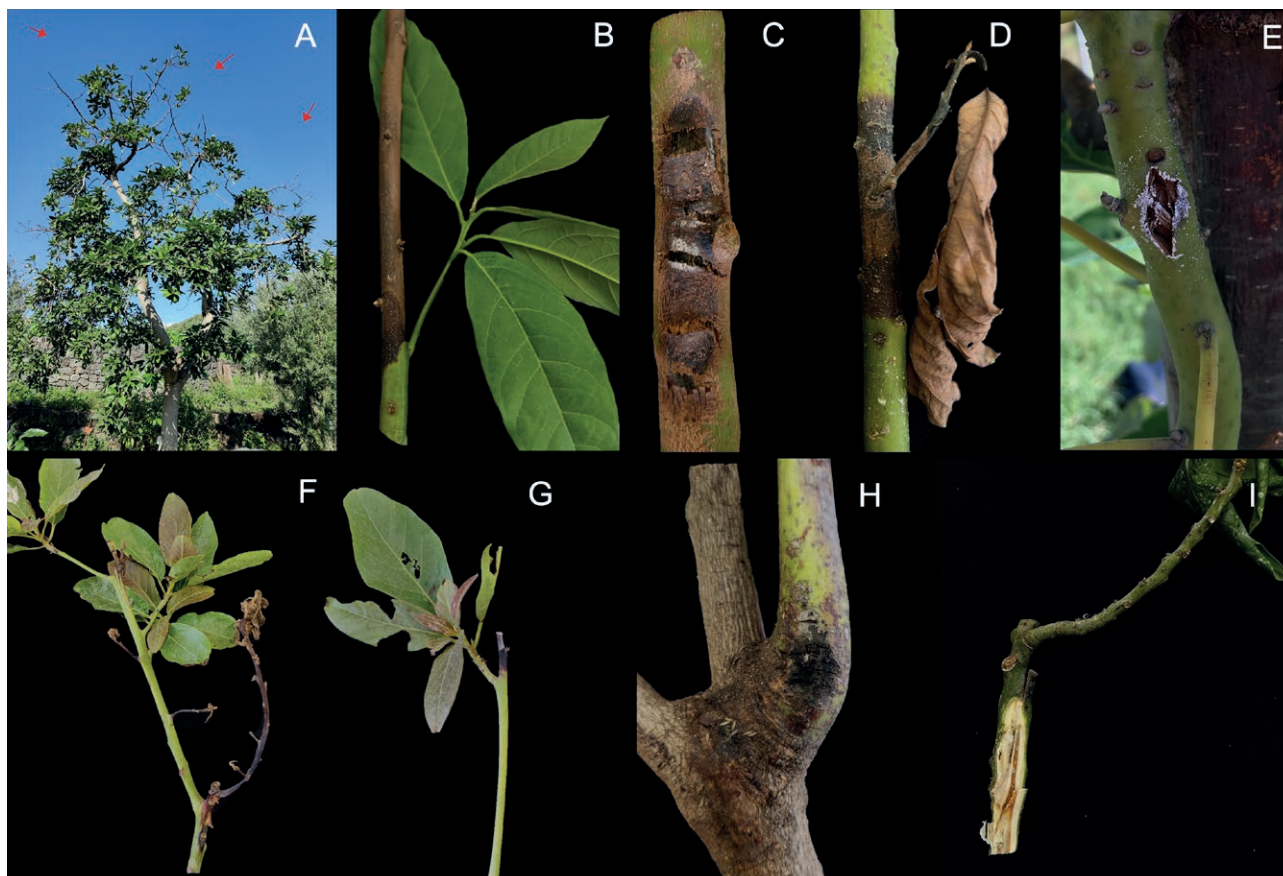


Figure 1. Symptoms of *Botryosphaeriaceae* on avocado trees observed in the field. **A**, Shoot dieback in the host canopy. **B**, Branch dieback. **C** and **D**, External canker (shoot canker). **E**, Canker with white powdery exudation. **F** and **G**, Infection originating from pruned wounds. **H**, bark cracking. **I**, infected grafting point.

preliminary screening based on the *tub2* locus was conducted on all 62 isolates, and this showed that representative isolates from seven orchards (orchard numbers 5 to 11, Table 2) were *N. parvum*. Since this fungal species was already characterized and reported in a preliminary study (Guarnaccia *et al.*, 2016), these isolates were excluded from further locus sequencing and phylogenetic analyses, but the *N. parvum* isolates were collected and stored, since the present investigation showed that this fungus predominated in Sicilian avocado orchards. A total of 23 isolates derived from four orchards (orchards numbers 1 to 4) were fully characterized, as these isolates were previously unreported in Italy. These 23 isolates were from 75 young (2 to 4-year-old) plants showing typical symptoms of canker and dieback. More details of the collected and characterized isolates are summarized in Table 2.

Phylogeny

The MP analysis of the combined dataset showed that of 3,116 characters, 464 were parsimony-informative, 239 were parsimony-uninformative, and 2,413 were constant. A total of 100 trees were retained. Tree length was equal to 1,178, CI = 0.771, RI = 0.953, and RC = 0.735. The best-fit model of nucleotide evolution based on the AIC resulted GTR + I + G for ITS, HKY + G for *tub2* and GTR + G for *tef1- α* . The ML analysis showed that of 3,116 total characters, 2,413 were constant characters and 564 were parsimony informative. Isolates AB2, AB4, AB5, AC5, AC7, AC9, AC10 and AC11 strongly clustered within the clade of *B. dothidea* (81% MP bootstrap support and 81% ML bootstrap support). Isolate AC20 strongly grouped within the clade of *Lasiodiplodia citricola*, (74/85). Isolates AC28, AC29,

Table 2. Information on fungal isolates collected and processed in this study from 11 avocado orchards. * identifies the representative isolates preliminarily identified based on the *tub2* locus. † identifies the isolates fully characterized (ITS + *tub2* + *tef1-c*) and included in the phylogenetic analyses. × indicates that the representative isolates were excluded from the phylogenetic analyses, because they were identified as *Neofusicoccum parvum* in the preliminary *tub2* locus characterization.

Orchard No.	Location (Province)	Tree age	Symptoms	Collected <i>Botryosphaeriaceae</i>	No. of representative isolates*	No. of chosen isolates†	Species
1	Fiumefreddo (Catania)	-	Dieback	9	8	5	<i>N. luteum</i> (5), <i>N. parvum</i> (3)
2	Ramacca (Catania)	2-3 yrs.	Dieback	5	5	5	<i>N. cryptoaustrale</i> (5)
3	Riposto (Catania)	2-4 yrs.	Canker	5	5	5	<i>B. dothidea</i> (5)
4	Mascali (Catania)	2-3 yrs.	Canker, dieback, grafting point canker	26	10	8	<i>B. dothidea</i> (3), <i>L. citricola</i> (1), <i>M. phaseolina</i> (4), <i>N. parvum</i> (2)
5	Agnone Bagni (Siracusa)	2-4 yrs.	Canker, dieback, grafting point canker	8	8	×	<i>N. parvum</i> (8)
6	Fiandaca (Catania)	-	Canker, dieback	5	2	×	<i>N. parvum</i> (2)
7	Acireale (Catania)	-	Dieback, grafting point canker	7	4	×	<i>N. parvum</i> (4)
8	Messina (ME)	-	Discolouration	3	2	×	<i>N. parvum</i> (2)
9	Noto (SR)	2 yrs.	Canker, dieback, grafting point canker	17	9	×	<i>N. parvum</i> (9)
10	Giarre (Catania)	Mature trees	Canker, dieback	9	1	×	<i>N. parvum</i> (1)
11	Riposto (Catania)	3 yrs.	Canker	12	8	×	<i>N. parvum</i> (8)

AC51 and AC52 grouped in the clade of *Macrophomina phaseolina* (73/81). Regarding *Neofusicoccum*, for isolates AVORAM1 to 5 the bootstrap support was 52 for the MP analysis and 60 for the ML analysis. These isolates were accommodated within *Neofusicoccum cryptoaustrale*. Isolates AVF3, AVF5, AVF6, AVF7, AVF8 were strongly supported (99/99) within the clade of *Neofusicoccum luteum*.

According to these results, five species isolated from avocado in this study were identified, including: *B. dothidea*, *L. citricola*, *M. phaseolina*, *N. cryptoaustrale*, and *N. luteum* (Figure 2). The ITS, *tub2*, and *tef1-α* sequences generated in this study were deposited in GenBank (Table 1).

Morphological and cultural characteristic of the isolates

Observing pure cultures on PDA, a total of six groups of *Botryosphaeriaceae*-like fungi were observed:

Isolate AC5 (*B. dothidea*) had olivaceous colonies that became grey with black reverse sides. Conidia were hyaline, fusiform and measured $23.2 \times 5.6 \mu\text{m}$.

Lasiodiplodia citricola AC20 had colonies with abundant aerial mycelium that became smoke grey to olivaceous-grey or iron-grey on the surfaces and greenish grey to dark slate blue on the reverse sides. Conidia were initially hyaline, aseptate, ellipsoid to ovoid and becoming pigmented, verrucose and ovoid, and measured $21.3 \times 13.1 \mu\text{m}$.

Macrophomina phaseolina isolate AC29 had grayish fluffy aerial mycelium on the colony surfaces, which were purplish grey on the reverse sides. Abundant microsclerotia were produced on pine needles in AT medium. Conidia were $25.0 \times 10.5 \mu\text{m}$.

The colonies of isolate AVORAM4 (*N. cryptoaustrale*) were initially white with fluffy aerial mycelium, changing to straw-yellow after 3 d incubation and then to pale olivaceous-grey. Conidia were hyaline, smooth with granular contents, aseptate, fusiform, and measured $20.0 \times 6.0 \mu\text{m}$.

Isolate AVF5 (*N. luteum*) was initially white with fluffy aerial mycelium and changed to yellow after 3-4 d incubation, after which the colour changed to pale olivaceous-grey from the middle of the colonies to the irregular margins. Conidia were hyaline, thin walled, aseptate, smooth, ellipsoidal, and measured $19.5 \times 5.5 \mu\text{m}$.

Isolates of *N. parvum* had white fluffy aerial mycelium that became grey and then black with the age. Conidia were hyaline, non-septate, and subglobose, with obtuse apices, and measured $18.2 \times 6.1 \mu\text{m}$.

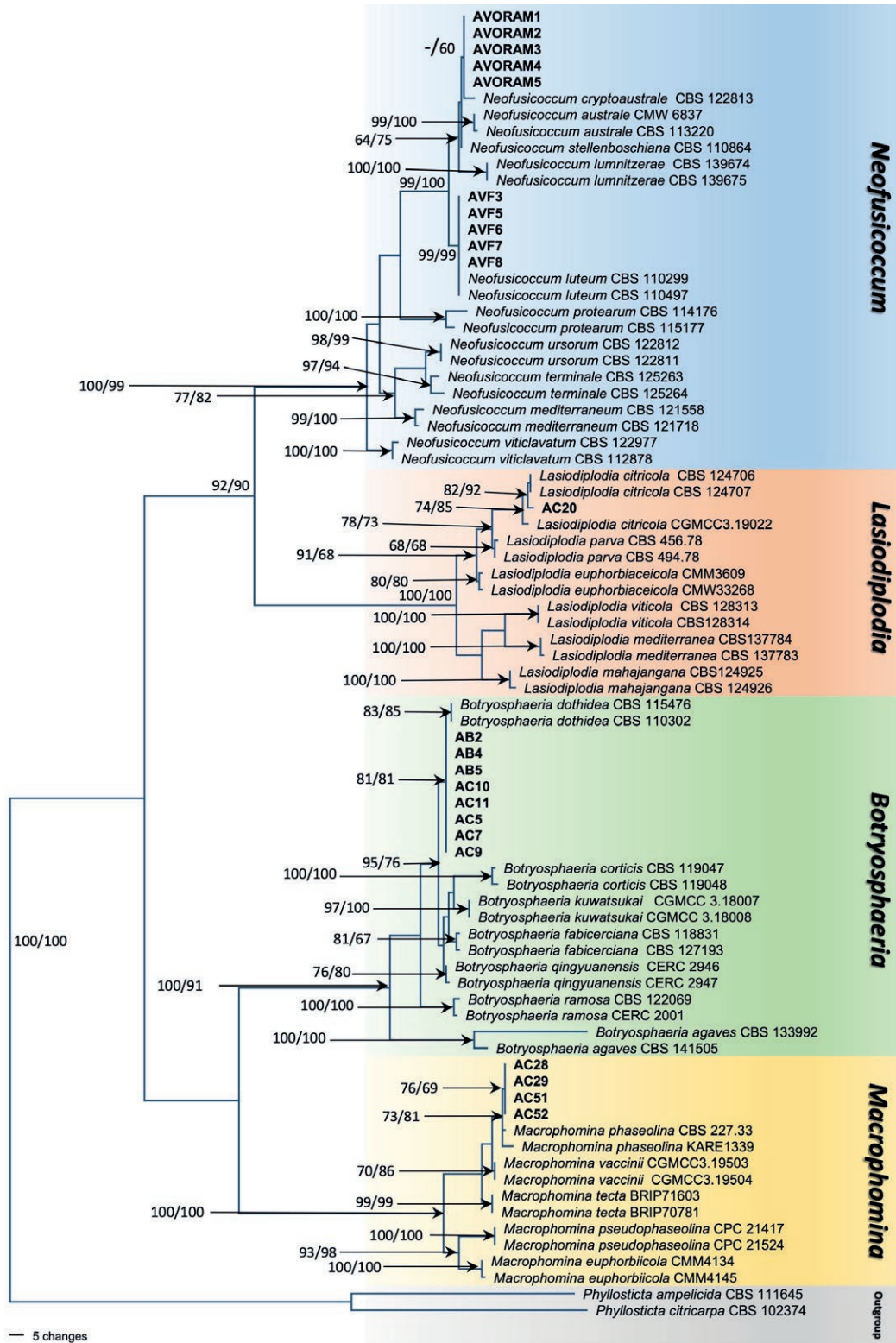


Figure 2. One of 100 equally most parsimonious trees generated from maximum parsimony analysis of three-loci (ITS + *tub2* + *tef1-α*) combined dataset of *Botryosphaeriaceae* species. Numbers before after slashes represent, respectively, parsimony and likelihood bootstrap values from 1,000 replicates. *Phyllosticta ampelicida* (CBS 111645) and *Phyllosticta citricarpa* (CBS 102374) were the outgroup taxa in both analyses. Isolates in bold font were generated in the present study. Bars indicate the numbers of nucleotide changes.

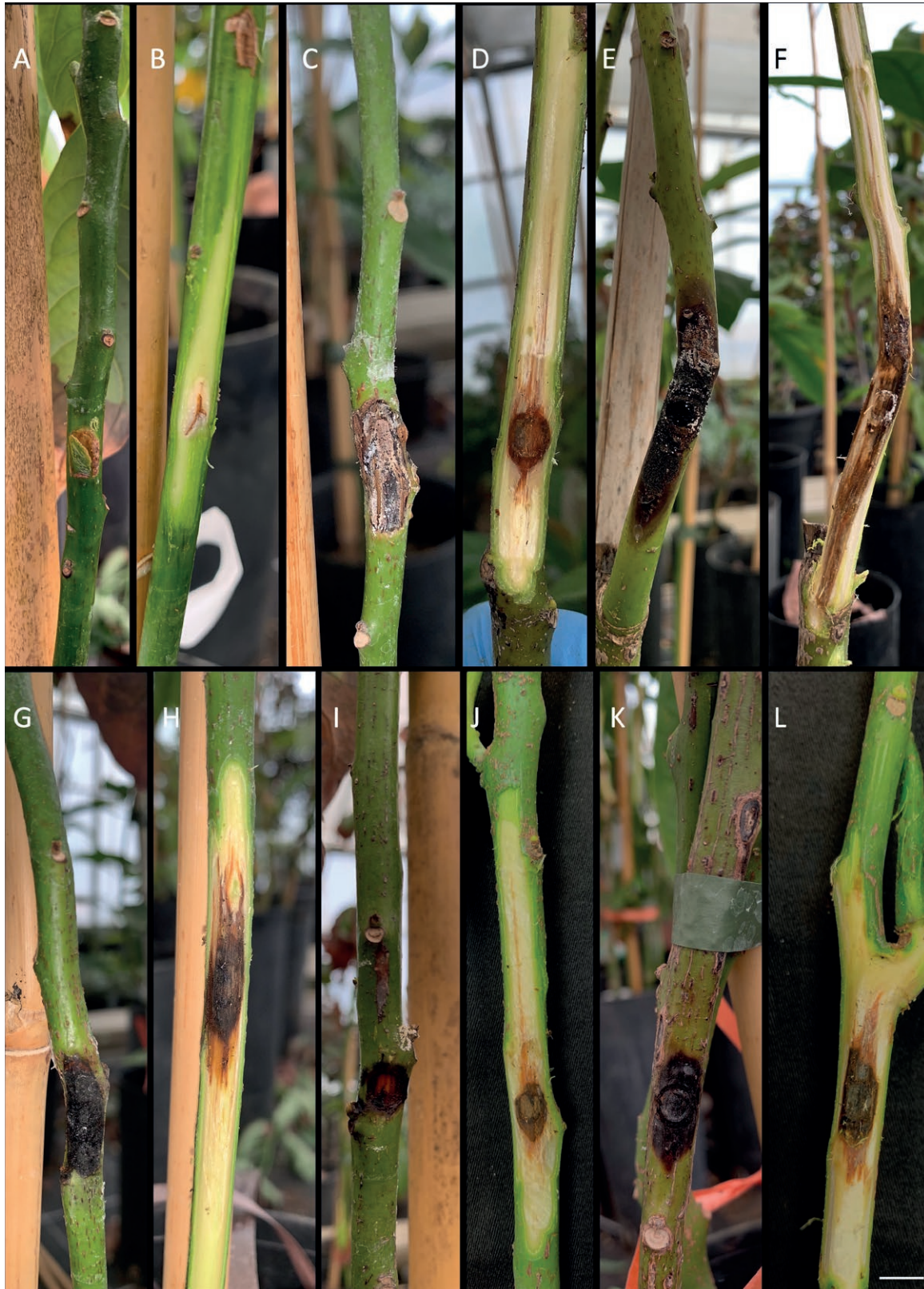


Figure 3. Result of the pathogenicity test after 63 days. A-B, Control. C-D, Shoots inoculated with *Botryosphaeria dothidea*. E-F, *Neofusicoccum luteum*. G-H, *Neofusicoccum cryptoaustrale*. I-J, *Lasiodiplodia citricola*. K-L, *Macrophomina phaseolina*. Scale bar: 2 cm.

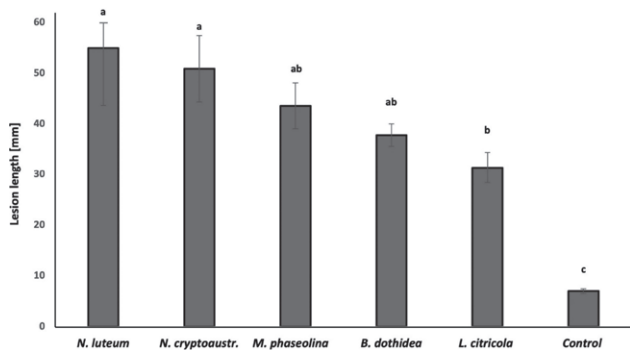


Figure 4. Mean lesion lengths (mm) resulting from the pathogenicity test of *Botryosphaeria dothidea*, *Lasiodiplodia citricola*, *Macrophomina phaseolina*, *Neofusicoccum cryptoaustrale*, and *N. luteum* on potted plants. Values are each for two inoculation points per plant for each fungal species. Control consisted of the same number of inoculation points. Vertical bars represent standard errors of the means. Bars accompanied with different letters indicate means that were significantly different (Fisher's protected LSD test; $\alpha = 0.05$).

Pathogenicity test

The pathogenicity showed that all the *Botryosphaeriaceae* species in this study were pathogenic to avocado plants, and produced similar symptoms to those observed in the field. All the inoculated species produced external and internal discolouration lesions. The inoculation controls did not show any symptoms (Figure 3). After 15 d, all the inoculated trees showed dark discolouration of the outer layers of bark. In detail, *N. luteum* isolate AVF5 produced the longest lesions (mean = 55.0 mm), followed by *N. cryptoaustrale* isolate AVO-RAM4 (50.9 mm), *M. phaseolina* isolate AC29 (43.6 mm), *B. dothidea* isolate AC7 (37.8 mm) and *L. citricola* isolate AC20 (31.4 mm). All the inoculated fungi produced lesion lengths that were statistically different from the controls ($P < 0.05$), and only lesions from *Neofusicoccum* sp. were significantly different compared to those from *L. citricola* (Figure 4). Re-isolations showed gave colonies with the morphological characteristics the same as the inoculated species, fulfilling Koch's postulates.

DISCUSSION

This study has elucidated the diversity of *Botryosphaeriaceae* species causing avocado canker and dieback in commercial orchards in Italy. The species characterized were *B. dothidea*, *L. citricola*, *M. phaseolina*, *N. cryptoaustrale*, and *N. luteum*. *Neofusicoccum parvum* was also constantly encountered during field surveys. This species had been characterized in a previous study

(Guarnaccia *et al.* 2016), and was here characterized only on the basis of *tub2* locus, and excluded from the phylogenetic analysis. This research confirms that *N. parvum* was the predominant *Botryosphaeriaceae* species associated with canker and dieback symptoms of avocado in Sicilian orchards.

Botryosphaeria dothidea is the type species of *Botryosphaeria* (Marsberg *et al.*, 2017), and has been reported from many plant species with broad global distribution. There are 1,260 fungus-host records for *B. dothidea* and its synonyms listed in the Fungal Database (Farr and Rossman, 2022). However, some of these reports are outdated causing taxonomic confusion. Batista *et al.* (2021) report that *B. dothidea* was associated with 403 hosts in 66 countries. McDonald and Eskalen (2011) reported fungi belonging to the *Botryosphaeriaceae*, including *B. dothidea* (*Fusicoccum aesculi*), have been associated with avocado branch cankers in California. Previous field surveys conducted in Sicily on different perennial crops, including pistachio, walnut and *Ficus* spp., recorded presence of *B. dothidea* and other *Botryosphaeriaceae* (Gusella *et al.*, 2020; 2022; Fiorenza *et al.*, 2022a). In the present study, within *Lasiodiplodia*, the *L. citricola* was occasionally isolated from symptomatic avocado branches, as were *M. phaseolina* and *B. dothidea*. The pathogenicity test confirmed the aggressiveness of *L. citricola* on avocado woody tissues. Different species of *Lasiodiplodia*, including *L. citricola*, have been reported to cause diseases in multiple fruit and nut tree hosts (Úrbez-Torres *et al.*, 2008, 2010; Chen *et al.*, 2013a, 2013b, 2013c; 2014; Carlucci *et al.*, 2015; Rodríguez-Gálvez *et al.*, 2017). In Sicily, *L. citricola* was recently identified as a serious threat to *Acacia* spp. causing dieback (Costanzo *et al.*, 2022). On avocado, recent studies have described *L. laeliocattleyae*, *L. pseudotheobromae* and *L. theobromae* as etiological agents of fruit stem-end rot and dieback (Garibaldi *et al.*, 2012; Qui *et al.*, 2020; Rodríguez-Gálvez *et al.*, 2021; Avenot *et al.*, 2022).

Macrophomina phaseolina is widely distributed and is a serious threat to different crops (Baird *et al.*, 2003; Sarr *et al.*, 2014). This pathogen causes charcoal rot of soybean (Sarr *et al.*, 2014), chickpea (Dell'Olmo *et al.*, 2022), sunflower (Bokor, 2007), sorghum (Sharma *et al.*, 2014), and strawberry (Koike, 2008). It has also been reported to cause diseases on woody hosts, such as grapevine (González and Tello, 2011; Nouri *et al.*, 2018), olive (Sergeeva *et al.*, 2005), pistachio (Nouri *et al.*, 2020), and almond (Inderbitzin *et al.*, 2010). *Macrophomina phaseolina* was thought to be one of the pathogens causing avocado root rot in Australia (Poudel *et al.*, 2021), but it has not been recorded as causing canker on this host. Based on previous studies in Italy, on fruit and

ornamental hosts showing typical symptoms of *Botryosphaeriaceae*, including canker and dieback of woody tissues, *M. phaseolina* has not been previously isolated. This is the first report of *M. phaseolina* on avocado. Further investigations are required need to clarify the geographic extent this species in Italy, and its association with different host plants.

Neofusicoccum cryptoaustrale was detected in only one of the sampled avocado orchards. This fungus was first described Eucalyptus trees in South Africa (Crous *et al.*, 2013; Pavlic-Zupanc *et al.*, 2017), and was reported on ornamental and fruit crops, including *Pistacia lentiscus* (Linaldeddu *et al.*, 2016), *Olea europea* (van Dyk *et al.*, 2021; Hernández-Rodríguez *et al.*, 2022), and mangrove species (Osorio *et al.*, 2017). This fungus formed a cryptic sister species with *N. australe* (Crous *et al.*, 2013). Results of the present study showed that the isolates from avocado clustered with the type isolate of *N. cryptoaustrale* (CBS 122813), close to the well supported clade of *N. australe*. We do not exclude that the present study isolates identified as *N. cryptoaustrale* could be re-accommodated following progress with multi-locus phylogeny. *Neofusicoccum luteum* is well known as a canker pathogen of avocado, and has been reported to cause branch canker and stem-end rot on avocado in California (McDonald *et al.*, 2009; 2011; Twizeyimana *et al.*, 2013; Avenot *et al.*, 2022), Australia (Tan *et al.*, 2019), New Zealand (Hartill, 1991; Hartill and Everett 2002), and Chile (Tapia *et al.*, 2020). This fungus was also identified in California as the main cause of stem-end rot in harvested avocado fruit (Twizeyimana *et al.*, 2013).

Despite of the diversity of *Botryosphaeriaceae* identified in the present study, *N. parvum* was the most prevalent species associated with canker and dieback of avocado, since it was detected from seven sampled locations with a high isolation frequency, as was previously reported in Italy by Guarnaccia *et al.* (2016) and in Spain by Arjona-Girona *et al.* (2019). *Neopestalotiopsis* also came from symptomatic tissues showing cankers and discolouration, but was not included in this study since it was already reported and described by Fiorenza *et al.* (2022b). Pathogenicity tests showed that representative isolates caused lesions on healthy plants. These data demonstrated that all the inoculated fungi were pathogenic to avocado, and that the isolates characterized as *N. cryptoaustrale* and *N. luteum* were the most virulent compared those of *B. dothidea*, *M. phaseolina*, and *L. citricola*.

Botryosphaeriaceae species have been reported as pathogens of the ornamentals to the agricultural crops in Italy, especially in Sicily (Ismail *et al.*, 2013; Guarnaccia *et al.*, 2016; Aiello *et al.*, 2020a, 2022; Gusella *et al.*, 2020, 2021, 2022; Bezerra *et al.*, 2021; Fiorenza *et*

al., 2022a; Costanzo *et al.*, 2022). Of the studies in Italy, *Botryosphaeriaceae* have been commonly encountered in different hosts and environments. Presence of contiguous susceptible hosts and the polyphagous behaviour of this pathogen family can guarantee inoculum survival in nurseries, open fields, and urban areas. The fungi characterized in the present study have also been described on other hosts. *Botryosphaeriaceae* (including those detected in this study) are endophytes, able to induce latent infections (Slippers and Wingfield, 2007). It is possible to detect the levels of latent infections using qPCR (Luo *et al.*, 2017; 2019; 2020; 2021).

The orchards investigated in the present study contained mainly young avocado trees (2 to 4-year-old). Presence of *Botryosphaeriaceae* spp. within the tissues in young trees indicates that most of the infections may originate nurseries, and then spread once the trees are transplanted in open fields. In Sicily, avocado trees are imported from other Mediterranean countries, because there are no nurseries specialized in avocado propagation. For these reasons, monitoring of latent infections, and attention during nursery propagation, are needed to avoid or limit *Botryosphaeriaceae* infections and new sources of inoculum.

This study presents updated results on the association of *Botryosphaeriaceae* species causing canker and dieback on avocado in Italy. The surveys and analyses have elucidated the diversity of this group of fungi involved in avocado canker diseases. Further studies are required to elucidate the epidemiology, control, and latent pathogenic status of *Botryosphaeriaceae* on avocado. This study is also the first to report *L. citricola*, *M. phaseolina* and *N. cryptoaustrale* causing canker and dieback on avocado trees, and is the first report of the recorded fungi causing branch disease on avocado in Italy.

FUNDING

Programma Ricerca di Ateneo MEDIT-ECO UNICT 2020-2022 Linea 2-University of Catania (Italy); SUPER-AVOCADO-Avocado biologico siciliano: superfood per la valorizzazione delle aree ionico-tirreniche” CUP: G79J21005580009

LITERATURE CITED

Aiello D., Guarnaccia V., Costanzo M.B., Leonardi G.R., Epifani F., Perrone G., Polizzi, G., 2022. Woody Canker and Shoot Blight Caused by *Botryosphaeriaceae* and *Diaporthaceae* on Mango and Litchi in Italy.

- Horticulturae* 8: 330. <https://doi.org/10.3390/horticulturae8040330>
- Aiello D., Gusella G., Fiorenza A., Guarnaccia V., Polizzi G., 2020a. Identification of *Neofusicoccum parvum* causing canker and twig blight on *Ficus carica* in Italy. *Phytopathologia Mediterranea* 59: 213–218. <https://doi.org/10.14601/Phyto-10798>
- Aiello D., Gusella G., Vitale A., Guarnaccia V., Polizzi G., 2020b. *Cylindrocladiella peruviana* and *Pleiocarpon algeriense* causing stem and crown rot on avocado (*Persea americana*). *European Journal of Plant Pathology* 158: 419–430. <https://doi.org/10.1007/s10658-020-02082-x>
- Arjona-Girona I., Ruano-Rosa D., López-Herrera C.J., 2019. Identification, pathogenicity and distribution of the causal agents of dieback in avocado orchards in Spain. *Spanish Journal of Agricultural Research* 17: e1003–e1003. <http://orcid.org/0000-0002-3539-0163>
- Auger J., Palma F., Pérez I., Esterio M., 2013. First report of *Neofusicoccum australe* (*Botryosphaeria australis*), as a branch dieback pathogen of avocado trees in Chile. *Plant Disease* 97: 842–842. <https://doi.org/10.1094/PDIS-10-12-0980-PDN>
- Avenot H.F., Vega D., Arpaia M.L., Michailides T.J., 2022. Prevalence, Identity, Pathogenicity, and Infection Dynamics of *Botryosphaeriaceae* causing Avocado Branch Canker in California. *Phytopathology* First Look <https://doi.org/10.1094/PHYTO-11-21-0459-R>
- Baird R. E., Watson C.E., Scruggs M., 2003. Relative longevity of *Macrophomina phaseolina* and associated mycobiota on residual soybean roots in soil. *Plant Disease* 87: 563–566. <https://doi.org/10.1094/PDIS.2003.87.5.563>
- Batista E., Lopes A., Alves A., 2021. What do we know about *Botryosphaeriaceae*? An overview of a worldwide cured dataset. *Forests* 12: 313. <https://doi.org/10.3390/f12030313>
- Bezerra J.D.P., Crous P.W., Aiello D., Gullino M.L., Polizzi G., Guarnaccia V., 2021. Genetic diversity and pathogenicity of *Botryosphaeriaceae* species associated with symptomatic citrus plants in Europe. *Plants* 10: 492. <https://doi.org/10.3390/plants10030492>
- Bokor P., 2007. *Macrophomina phaseolina* causing a charcoal rot of sunflower through Slovakia. *Biologia* 62: 136–138. <https://doi.org/10.2478/s11756-007-0020-9>
- Bost J.B., Smith N.J.H., Crane J.H., 2013. History, distribution and uses. In: *The Avocado: Botany, Production and Uses* (Schaffer, B., Wolstenholme, B. N. and Whitley, A. W. ed.), CABI International Press, Wallingford, UK, 10–30.
- Carbone I., Kohn L.M., 1999. A method for designing primer sets for speciation studies in filamentous ascomycetes. *Mycologia* 91: 553–556. <https://doi.org/10.1080/00275514.1999.12061051>
- Carlucci A., Cibelli F., Lops F., Raimondo M.L., 2015. Characterization of *Botryosphaeriaceae* species as causal agents of trunk diseases on grapevines. *Plant Disease* 99: 1678–1688. <https://doi.org/10.1094/PDIS-03-15-0286-RE>
- Carrillo J.D., Eskalen A., Rooney-Latham S., Scheck H.J., 2016. First report of *Neofusicoccum nonquaesitum* causing branch canker and dieback of avocado in California. *Plant Disease* 100: 1778–1778. <https://doi.org/10.1094/PDIS-11-15-1357-PDN>
- Chen S.F., Fichtner E., Morgan D.P., Michailides T.J., 2013a. First report of *Lasiodiplodia citricola* and *Neoscytalidium dimidiatum* causing death of graft union of English walnut in California. *Plant Disease* 97: 993–993. <https://doi.org/10.1094/PDIS-10-12-1000-PDN>
- Chen S.F., Morgan D.P., Hasey J.K., Michailides T.J., 2013b. First report of *Lasiodiplodia citricola* associated with stem canker of peach in California, USA. *Journal of Plant Pathology* 95.
- Chen S.F., Morgan D., Beede R. H., Michailides T.J., 2013c. First report of *Lasiodiplodia theobromae* associated with stem canker of almond in California. *Plant Disease* 97: 994–994. <http://dx.doi.org/10.4454/JPP.V95I3.019>
- Chen S.F., Morgan D.P., Michailides T.J., 2014. *Botryosphaeriaceae* and *Diaporthaceae* associated with panicle and shoot blight of pistachio in California, USA. *Fungal Diversity* 67: 157–179. <https://doi.org/10.1007/s13225-014-0285-6>
- Costanzo M.B., Gusella G., Fiorenza A., Leonardi G.R., Aiello D., Polizzi G., 2022. *Lasiodiplodia citricola*, a new causal agent of *Acacia* spp. dieback. *New Disease Reports* 45: e12094. <https://doi.org/10.1002/ndr2.12094>
- Crous P.W., Wingfield M.J., Guarro J., Cheewangkoon R., Van der Bank M., ... Groenewald J.Z., 2013. Fungal Planet description sheets: 154–213. *Persoonia-Molecular Phylogeny and Evolution of Fungi* 31: 188–296. <https://doi.org/10.3767/003158513X675925>
- Dann E.K., Ploetz R.C., Coates L.M., Pegg K.G., 2013. Foliar, fruit and soilborne diseases. In: *The avocado: botany, production and uses* (Schaffer, B., Wolstenholme, B. N. and Whitley, A. W. ed.), CABI International Press, Wallingford, UK, 380–422. <https://doi.org/10.1079/9780851993577.0299>
- Dell'Olmo E., Tripodi P., Zaccardelli M., Sigillo, L., 2022. Occurrence of *Macrophomina phaseolina* on Chickpea in Italy: Pathogen Identification and Characterization. *Pathogens* 11: 842. <https://doi.org/10.3390/pathogens11080842>

- FAOSTAT, 2022. Food and Agriculture Organization, Statistical Database (<https://www.fao.org/faostat/en/#home>)
- Farr D.F., Rossman, A.Y., 2022. Fungal Databases, U.S. National Fungus Collections, ARS, USDA. Retrieved October 7, 2022. Available at: <https://nt.ars-grin.gov/fungaldatabases>.
- Fiorenza A., Aiello D., Leonardi G.R., Continella A., Polizzi G., 2021. First Report of *Rosellinia necatrix* Causing White Root Rot on Avocado in Italy. *Plant Disease* PDIS-02. <https://doi.org/10.1094/PDIS-02-21-0412-PDN>
- Fiorenza A., Aiello D., Costanzo M.B., Gusella G., Polizzi G., 2022a. A New Disease for Europe of *Ficus microcarpa* Caused by *Botryosphaeriaceae* Species. *Plants* 11: 727. <https://doi.org/10.3390/plants11060727>
- Fiorenza A., Gusella G., Aiello D., Polizzi G., Voglmayr H., 2022b. *Neopestalotiopsis siciliana* sp. nov. and *N. rosae* Causing Stem Lesion and Dieback on Avocado Plants in Italy. *Journal of Fungi* 8: 562. <https://doi.org/10.3390/jof8060562>
- Garibaldi A., Bertetti D., Amatulli M.T., Cardinale J., Gullino M.L., 2012. First report of postharvest fruit rot in avocado (*Persea americana*) caused by *Lasiodiplodia theobromae* in Italy. *Plant Disease* 96:460–460. <https://doi.org/10.1094/PDIS-10-11-0886>
- Glass N.L., Donaldson G.C., 1995. Development of primer sets designed for use with the PCR to amplify conserved genes from filamentous ascomycetes. *Applied and environmental microbiology* 61: 1323–1330. <https://doi.org/10.1128/aem.61.4.1323-1330.1995>
- González V., Tello M.L., 2011. The endophytic mycota associated with *Vitis vinifera* in central Spain. *Fungal Diversity* 47: 29–42. <https://doi.org/10.1007/s13225-010-0073-x>
- Guarnaccia V., Vitale A., Cirvilleri G., Aiello D., Susca A., ... Polizzi, G., 2016. Characterisation and pathogenicity of fungal species associated with branch cankers and stem-end rot of avocado in Italy. *European Journal of Plant Pathology* 146: 963–976. <https://doi.org/10.1007/s10658-016-0973-z>
- Guarnaccia V., Sandoval-Denis M., Aiello D., Polizzi G., Crous P.W., 2018. *Neocosmospora perseae* sp. nov., causing trunk cankers on avocado in Italy. *Fungal Systematics and Evolution* 1: 131–140. <https://doi.org/10.3114/fuse.2018.01.06>
- Guarnaccia V., Polizzi G., Papadantonakis N., Gullino M.L., 2020. *Neofusicoccum* species causing branch cankers on avocado in Crete (Greece). *Journal of Plant Pathology* 102: 1251–1255. <https://doi.org/10.1007/s42161-020-00618-y>
- Guarnaccia V., Kraus C., Markakis E., Alves A., Armengol, J...Gramaje D., 2022a. Fungal trunk diseases of fruit trees in Europe: pathogens, spread and future directions. *Phytopathologia Mediterranea* 61: 563–599. <https://doi.org/10.36253/phyto-14167>
- Guarnaccia V., Aiello D., Papadantonakis N., Polizzi G., Gullino M.L., 2022b. First report of branch cankers on avocado (*Persea americana*) caused by *Neocosmospora* (syn. *Fusarium*) *perseae* in Crete (Greece). *Journal of Plant Pathology* 104: 419–420. <https://doi.org/10.1007/s42161-021-00983-2>
- Gusella G., Giambra S., Conigliaro G., Burruano S., Polizzi G., 2020. *Botryosphaeriaceae* species causing canker and dieback of English walnut (*Juglans regia*) in Italy. *Forest Pathology* 51: e12661. <https://doi.org/10.1111/efp.12661>
- Gusella G., Costanzo M.B., Aiello D., Polizzi G., 2021. Characterization of *Neofusicoccum parvum* causing canker and dieback on *Brachychiton* species. *European Journal of Plant Pathology* 161: 999–1005. <https://doi.org/10.1007/s10658-021-02379-5>
- Gusella G., Lawrence D.P., Aiello D., Luo Y., Polizzi G., Michailides T.J., 2022. Etiology of Botryosphaeria Panicle and Shoot Blight of Pistachio (*Pistacia vera*) caused by *Botryosphaeriaceae* in Italy. *Plant Disease* 106: 1192–1202. <https://doi.org/10.1094/PDIS-08-21-1672-RE>
- Hartill W.F.T., 1991. Post-harvest diseases of avocado fruits in New Zealand. *New Zealand Journal of Crop and Horticultural Science* 19: 297–304. <https://doi.org/10.1080/01140671.1991.10421814>
- Hartill W.F.T., Everett K.R., 2002. Inoculum sources and infection pathways of pathogens causing stem-end rots of ‘Hass’ avocado (*Persea americana*). *New Zealand Journal of Crop and Horticultural Science* 30: 249–260. <https://doi.org/10.1080/01140671.2002.9514221>
- Hernández-Rodríguez L., Mondino Hintz P., Alaniz-Ferro S., 2022. Diversity of *Botryosphaeriaceae* species causing stem canker and fruit rot in olive trees in Uruguay. *Journal of Phytopathology* 170: 264–277. <https://doi.org/10.1111/jph.13078>
- Inderbitzin P., Bostock R.M., Trouillas F.P., Michailides T.J., 2010. A six locus phylogeny reveals high species diversity in *Botryosphaeriaceae* from California almond. *Mycologia* 102: 1350–1368. <https://doi.org/10.3852/10-006>
- Ismail A.M., Cirvilleri G., Lombard L., Crous P.W., Groenewald J. Z., Polizzi, G., 2013. Characterisation of *Neofusicoccum* species causing mango dieback in Italy. *Journal of Plant Pathology* 549–557. <https://www.jstor.org/stable/23721576>
- Koike S.T., 2008. Crown rot of strawberry caused by *Macrophomina phaseolina* in California. *Plant Disease* 92: 1253–1253. <https://doi.org/10.1094/PDIS-92-8-1253B>

- Kumar S., Stecher G., Li M., Knyaz C., Tamura, K., 2018. MEGA X: Molecular evolutionary genetics analysis across computing platforms. *Molecular Biology and Evolution* 35: 1547–1549. <https://doi.org/10.1093/molbev/msy096>
- Larsson A., 2014. AliView: a fast and lightweight alignment viewer and editor for large datasets. *Bioinformatics* 30: 3276–3278. <https://doi.org/10.1093/bioinformatics/btu531>
- Linaldeddu B.T., Maddau L., Franceschini A., Alves A., Phillips A.J.L., 2016. *Botryosphaeriaceae* species associated with lentisk dieback in Italy and description of *Diplodia insularis* sp. nov. *Mycosphere* 7: 962–977. <https://doi.org/10.5943/mycosphere/si/1b/8>
- López-Herrera C.J., Melero-Vara J.M., 1992. Diseases of avocado caused by soil fungi in the southern Mediterranean coast of Spain. In: *Proceedings of Second World Avocado Congress 1992* (Lovatt CJ ed.), California Avocado Society, Orange, CA, USA, 119–121.
- Luo Y., Gu S., Felts D., Puckett R.D., Morgan D.P., Michailides T.J., 2017. Development of qPCR systems to quantify shoot infections by canker-causing pathogens in stone fruits and nut crops. *Journal of Applied Microbiology* 122: 416–428. <https://doi.org/10.1111/jam.13350>
- Luo Y., Lichtemberg P.S., Niederholzer F.J., Lightle D.M., Felts D.G., Michailides T.J., 2019. Understanding the process of latent infection of canker-causing pathogens in stone fruit and nut crops in California. *Plant Disease* 103: 2374–2384. <https://doi.org/10.1094/PDIS-11-18-1963-RE>
- Luo Y., Niederholzer F.J.A., Felts D.G., Puckett R.D., Michailides, T.J., 2020. Inoculum quantification of canker-causing pathogens in prune and walnut orchards using real-time PCR. *Journal of Applied Microbiology* 129:1337–1348. <https://doi.org/10.1111/jam.14702>
- Luo Y., Niederholzer F.J., Lightle D.M., Felts D., Lake J., Michailides T.J., 2021. Limited Evidence for Accumulation of Latent Infections of Canker-Causing Pathogens in Shoots of Stone Fruit and Nut Crops in California. *Phytopathology* 111: 1963–1971. <https://doi.org/10.1094/PHYTO-01-21-0009-R>
- Marsberg A., Kemler M., Jami F., Nagel J.H., Postma-Smidt A., ... Slippers B., 2017. *Botryosphaeria dothidea*: a latent pathogen of global importance to woody plant health. *Molecular Plant Pathology* 18: 477–488. <https://doi.org/10.1111/mpp.12495>
- Mathioudakis M.M., Tziros G.T., Kavroulakis N., 2020. First Report of *Diaporthe foeniculina* Associated with Branch Canker of Avocado in Greece. *Plant Disease* 104: 3057. <https://doi.org/10.1094/PDIS-04-20-0900-PDN>
- McDonald V., Eskalen A., 2011. *Botryosphaeriaceae* species associated with avocado branch cankers in California. *Plant Disease* 95: 1465–1473. <https://doi.org/10.1094/PDIS-02-11-0136>
- McDonald V., Lynch S., Eskalen A., 2009. First report of *Neofusicoccum australe*, *N. luteum*, and *N. parvum* associated with avocado branch canker in California. *Plant Disease* 93: 967. <https://doi.org/10.1094/PDIS-93-9-0967B>
- Migliore G., Farina V., Tinervia S., Matranga G., Schifani G., 2017. Consumer interest towards tropical fruit: factors affecting avocado fruit consumption in Italy. *Agricultural and Food Economics* 5: 1–12. <https://doi.org/10.1186/s40100-017-0095-8>
- Moral J., Morgan D., Trapero A., Michailides T.J., 2019. Ecology and epidemiology of diseases of nut crops and olives caused by *Botryosphaeriaceae* fungi in California and Spain. *Plant Disease* 103: 1809–1827. <https://doi.org/10.1094/PDIS-03-19-0622-FE>
- Ni H.F., Liou R.F., Hung T.H., Chen R.S., Yang H.R., 2009. First Report of a Fruit Rot Disease of Avocado Caused by *Neofusicoccum mangiferae*. *Plant Disease* 93: 760. <https://doi.org/10.1094/PDIS-93-7-0760B>
- Ni H., Chuang M., Hsu S., Lai S., Yang H., 2011. Survey of *Botryosphaeria* spp., Causal Agents of Postharvest Disease of Avocado, in Taiwan. *Journal of Taiwan Agricultural Research* 60: 157–166.
- Nouri M.T., Zhuang G., Culumber C.M., Trouillas F.P., 2018. First Report of *Macrophomina phaseolina* Causing trunk and cordon canker disease of grapevine in the United States. *Plant Disease* 103: 579. <http://dx.doi.org/10.1094/PDIS-07-18-1189-PDN>
- Nouri M.T., Lawrence D.P., Kallsen C.E., Trouillas F.P., 2020. *Macrophomina* crown and root rot of pistachio in California. *Plants* 9: 134. <https://doi.org/10.3390/plants9020134>
- Nylander J.A.A., 2004. MrModeltest v2. Program distributed by the author: Evolutionary Biology Centre, Uppsala University, Sweden.
- Osorio J.A., Crous C.J., De Beer Z.W., Wingfield M.J., Roux J., 2017. Endophytic *Botryosphaeriaceae*, including five new species, associated with mangrove trees in South Africa. *Fungal biology* 121: 361–393. <https://doi.org/10.1016/j.funbio.2016.09.004>
- Parkinson L.E., Shivas R.G., Dann, E.K., 2017. Pathogenicity of nectriaceous fungi on avocado in Australia. *Phytopathology* 107: 1479–1485. <https://doi.org/10.1094/PHYTO-03-17-0084-R>
- Pavlic-Zupanc D., Maleme H.M., Piškur B., Wingfield B.D., Wingfield M.J., Slippers B., 2017. Diversity, phylogeny and pathogenicity of *Botryosphaeriaceae* on non-native *Eucalyptus* grown in an urban environment: A case study. *Urban Forestry & Urban Greening* 26: 139–148. <https://doi.org/10.1016/j.ufug.2017.04.009>

- Pérez-Jiménez R.M., 2008. Significant avocado diseases caused by fungi and oomycetes. *The European Journal of Plant Science and Biotechnology* 2: 1–24.
- Peterson R.A., 1978. Susceptibility of Fuerte Avocado Fruit at Various Stages of Growth, to Infection by Anthracnose and Stem End Rot Fungi. *Australian Journal of Experimental Agriculture* 18: 158–160 <https://doi.org/10.1071/EA9780158>
- Phillips A.J.L., Alves A., Abdollahzadeh J., Slippers B., Wingfield M.J., ... Crous P.W., 2013. The *Botryosphaeriaceae*: genera and species known from culture. *Studies in Mycology* 76: 51–167. <https://doi.org/10.3114/sim0021>
- Poudel B., Shivas R.G., Adorada D.L., Barbetti M.J., Bithell S.L., ... Vaghefi N., 2021. Hidden diversity of *Macrophomina* associated with broadacre and horticultural crops in Australia. *European Journal of Plant Pathology* 161: 1–23. <https://doi.org/10.1007/s10658-021-02300-0>
- Qiu F., Tan X.H., Xie C.P., Xu G., Li X., ... Wang W.L., 2020. First report of *Lasiodiplodia theobromae* causing branch blight on avocado in China. *Plant Disease* 104: 2728–2728. <https://doi.org/10.1094/PDIS-03-20-0451-PDN>
- Rodríguez-Gálvez E., Guerrero P., Barradas C., Crous P.W., Alves A., 2017. Phylogeny and pathogenicity of *Lasiodiplodia* species associated with dieback of mango in Peru. *Fungal Biology* 121: 452–465. <https://doi.org/10.1016/j.funbio.2016.06.004>
- Rodríguez-Gálvez E., Hilário S., Batista E., Lopes A., Alves A., 2021. *Lasiodiplodia* species associated with dieback of avocado in the coastal area of Peru. *European Journal of Plant Pathology* 161: 219–232. <https://doi.org/10.1007/s10658-021-02317-5>
- Sarr M.P., Groenewald J.Z., Crous P.W., 2014. Genetic diversity in *Macrophomina phaseolina*, the causal agent of charcoal rot. *Phytopathologia Mediterranea* 53: 250. <https://www.jstor.org/stable/43871778>
- Sergeeva V., Tesoriero L., Spooner-Hart R., Nair N., 2005. First report of *Macrophomina phaseolina* on olives (*Olea europaea*) in Australia. *Australasian Plant Pathology* 34: 273–274. <https://doi.org/10.1071/AP05001>
- Sharma I., Kumari N., Sharma V., 2014. Defense gene expression in *Sorghum bicolor* against *Macrophomina phaseolina* in leaves and roots of susceptible and resistant cultivars. *Journal of Plant Interactions* 9: 315–323. <https://doi.org/10.1080/17429145.2013.832425>
- Slippers B., Wingfield M. J., 2007. *Botryosphaeriaceae* as endophytes and latent pathogens of woody plants: diversity, ecology and impact. *Fungal Biology Reviews* 21: 90–106. <https://doi.org/10.1016/j.fbr.2007.06.002>
- Smith H., Wingfield M.J., Coutinho T.A., Crous P.W., 1996. *Sphaeropsis sapinea* and *Botryosphaeria dothidea* endophytic in *Pinus* spp. and *Eucalyptus* spp. in South Africa. *South African Journal of Botany* 62: 86–88. [https://doi.org/10.1016/S0254-6299\(15\)30596-2](https://doi.org/10.1016/S0254-6299(15)30596-2)
- Swofford DL., 2002. PAUP*: Phylogenetic Analysis Using Parsimony (*and Other Methods); v 4.0a, build 169; Sinauer Associates: Sunderland, MA, USA. Available at: <https://paup.phylosolutions.com>.
- Tan Y. P., Shivas R.G., Marney T.S., Edwards J., Dearnaley J., ... Burgess T. I., 2019. Australian cultures of *Botryosphaeriaceae* held in Queensland and Victoria plant pathology herbaria revisited. *Australasian Plant Pathology* 48: 25–34. <https://doi.org/10.1007/s13313-018-0559-7>
- Tapia L., Larach A., Riquelme N., Guajardo J., Besoain X., 2020. First Report of *Neofusicoccum luteum* Causing Stem-End Rot Disease on Avocado Fruits in Chile. *Plant Disease* 104: 2027–2027. <https://doi.org/10.1094/PDIS-11-19-2299-PDN>
- Torres C., Camps R., Aguirre R., Besoain X., 2016. First report of *Diaporthe rudis* in Chile causing Stem-End rot on ‘hass’ avocado fruit imported from California. *Plant Disease*, 100: 1951–1951. <https://doi.org/10.1094/PDIS-12-15-1495-PDN>
- Twizeyimana M., Förster H., McDonald V., Wang D.H., Adaskaveg J.E., Eskalen A., 2013. Identification and pathogenicity of fungal pathogens associated with stem-end rot of avocado in California. *Plant Disease* 97: 1580–1584. <https://doi.org/10.1094/PDIS-03-13-0230-RE>
- Úrbez-Torres J.R., Leavitt G.M., Guerrero J.C., Guevara J., Gubler W.D., 2008. Identification and pathogenicity of *Lasiodiplodia theobromae* and *Diplodia seriata*, the causal agents of bot canker disease of grapevines in Mexico. *Plant Disease* 92: 519–529. <https://doi.org/10.1094/PDIS-92-4-0519>
- Úrbez-Torres J. R., Peduto F., Gubler W.D., 2010. First report of grapevine cankers caused by *Lasiodiplodia crassisporea* and *Neofusicoccum mediterraneum* in California. *Plant Disease* 94: 785–785. <https://doi.org/10.1094/PDIS-94-6-0785B>
- Valencia A. L., Gil P.M., Latorre B.A., Rosales I. M., 2019. Characterization and pathogenicity of *Botryosphaeriaceae* species obtained from avocado trees with branch canker and dieback and from avocado fruit with stem end rot in Chile. *Plant Disease* 103: 996–1005. <https://doi.org/10.1094/PDIS-07-18-1131-RE>
- van Dyk M., Spies C. F., Mostert L., Halleen F., 2021. Survey of trunk pathogens in South African olive nurseries. *Plant Disease* 105: 1630–1639. <https://doi.org/10.1094/PDIS-04-20-0798-RE>

- Vitale A., Aiello D., Guarnaccia V., Perrone G., Stea G., Polizzi G., 2012. First report of root rot caused by *Ilyonectria* (= *Neonectria*) *macrodidyma* on avocado (*Persea americana*) in Italy. *Journal of Phytopathology* 160: 156–159. <https://doi.org/10.1111/j.1439-0434.2011.01869.x>
- Wanjiku E.K., Waceke J.W., Wanjala B.W., Mbaka J.N., 2020. Identification and pathogenicity of fungal pathogens associated with stem end rots of avocado fruits in Kenya. *International Journal of Microbiology* 4063697. <https://doi.org/10.1155/2020/4063697>
- White T.J., Bruns T., Lee S., Taylor J., 1990. Amplification and direct sequencing of fungal ribosomal RNA genes for phylogenetics. In: *PCR protocols: A Guide to Methods and Applications* (Innis M.A., Gelfand D.H., Sninsky J.J., White T.J., ed.), Academic Press, San Diego, CA, USA, 315–322.
- Zea-Bonilla T., González-Sánchez M.A., Martín-Sánchez P.M., Pérez-Jiménez R.M., 2007. Avocado dieback caused by *Neofusicoccum parvum* in the Andalusia region, Spain. *Plant Disease* 91: 1052–1052. <https://doi.org/10.1094/PDIS-91-8-1052B>
- Zentmyer G.A., 1980. *Phytophthora cinnamomi* and the disease it causes. Monograph 10. American Phytopathological Society, St Paul, MN, USA, 96 pp.
- Zhang W., Groenewald J.Z., Lombard L., Schumacher R.K., Phillips A.J.L., Crous, P.W., 2021. Evaluating species in *Botryosphaeriales*. *Persoonia-Molecular Phylogeny and Evolution of Fungi* 46: 63–115. <https://doi.org/10.3767/persoonia.2021.46.03>
- Zwickl D.J., 2006. *Genetic Algorithm Approaches for the Phylogenetic Analysis of Large Biological Sequence Datasets Under the Maximum Likelihood Criterion*. Ph.D. dissertation, University of Texas, Austin, TX, USA.



Citation: A. Nabloussi, B. Pérez-Vich, L. Velasco (2023) Virulence, genetic diversity, and putative geographical origin of sunflower broomrape populations in Morocco. *Phytopathologia Mediterranea* 62(1): 65-72. doi: 10.36253/phyto-13948

Accepted: February 28, 2023

Published: May 8, 2023

Copyright: © 2023 A. Nabloussi, B. Pérez-Vich, L. Velasco. This is an open access, peer-reviewed article published by Firenze University Press (<http://www.fupress.com/pm>) and distributed under the terms of the Creative Commons Attribution License, which permits unrestricted use, distribution, and reproduction in any medium, provided the original author and source are credited.

Data Availability Statement: All relevant data are within the paper and its Supporting Information files.

Competing Interests: The Author(s) declare(s) no conflict of interest.

Editor: Maurizio Vurro, National Research Council, (CNR), Bari, Italy.

ORCID:

AN: 0000-0002-6125-1490

BP-V: 0000-0002-7085-5173

LV: 0000-0003-4998-9406

Research Papers

Virulence, genetic diversity, and putative geographical origin of sunflower broomrape populations in Morocco

ABDELGHANI NABLOUSSI¹, BEGOÑA PÉREZ-VICH², LEONARDO VELASCO^{2,*}

¹ Research Unit of Plant Breeding and Plant Genetic Resources Conservation, National Institute of Agricultural Research, Regional Center of Meknes, Morocco

² Institute for Sustainable Agriculture (IAS-CSIC), Córdoba, Spain

*Corresponding autor. E-mail: lvelasco@ias.csic.es

Summary. Sunflower broomrape (*Orobanche cumana* Wallr.) was detected for the first time parasitizing sunflower in Morocco in 2016. Seeds of three broomrape populations from two separate areas of Morocco, Souk Al Arbaa (populations SA1 and SA2) and Meknès (Population MK1) were collected. The populations' virulence, genetic diversity, and putative area of origin were examined. Race classification using a set of sunflower differential lines showed that MK1 was a race-E population, while SA1 and SA2 were race-G populations. The analysis with 192 SNP markers showed that SA1 and SA2 populations are genetically similar and very distant from the MK1 population. The three populations exhibited low intrapopulation diversity. Comparisons with populations from other areas showed that MK1 was introduced from a race-E population from the Guadalquivir Valley gene pool in Southern Spain, probably before 1988. Populations SA1 and SA2 showed close relationships with a population from Russia, although more exact knowledge of the origin of these populations requires further investigation. Since the SA and MK populations were collected from areas located approx. 100 km apart, the risks of mixing and recombining both gene pools to produce more virulent variants must be considered.

Keywords. Genetic diversity, parasitic weeds, SNP markers, virulence, plant introductions.

INTRODUCTION

Sunflower broomrape (*Orobanche cumana* Wallr.) is a parasitic plant naturally distributed in South-eastern Europe and Central Asia, where it parasitizes wild Compositae species (Beck-Mannagetta, 1930). Broomrape was first observed on sunflower in Russia in 1866 (Antonova, 2014), from where the parasite spread to sunflower crops in the Black Sea area, where it was first observed in 1935 (Batchvarova, 2014). By the middle 1950s, the main sunflower-producing areas in Russia, Ukraine, Kazakhstan, Moldavia, Romania, Bulgaria, Serbia, and Turkey had become infested by broomrape seeds, and sunflower production became dependent on the development of

resistant cultivars (Antonova, 2014; Kaya, 2014). The parasite was detected in 1958 in Spain (Molinero-Ruiz and Domínguez, 2014), in 1979 in China (Ma and Jan, 2014), in 2007 in France (Jestin *et al.*, 2014), in 2010 in Tunisia (Amri *et al.*, 2012), in 2016 in Morocco (Nabloussi *et al.*, 2018), and in 2017 in Portugal (González-Cantón *et al.*, 2019).

Sunflower broomrape is largely a self-pollinated plant, although it has some cross-pollination estimated to be up to 29% (Rodríguez-Ojeda *et al.*, 2013). In eastern Europe, where sunflower broomrape occurs in the wild and has been parasitizing sunflower since the introduction of this crop, intrapopulation diversity is typically large (Gagne *et al.*, 1998; Cvejić *et al.*, 2020). Broomrape plants produce thousands of seeds that are readily dispersed naturally by wind, water, and agricultural machinery and can be accidentally introduced into new areas as contaminants of sunflower seed (Fernández-Martínez *et al.*, 2015; Parker, 2016). Molecular genetic analyses of populations collected in Tunisia showed that some were most likely introduced from Eastern Europe (Jebri *et al.*, 2017). In Spain, two separate gene pools were initially detected in Central Spain and the Guadalquivir Valley in the south. Low genetic diversity in both indicated two separate introduction events and a founder effect (Pineda Martos *et al.*, 2013).

We have identified and collected sunflower broomrape populations from two separate locations in Morocco: Souk Al Arbaa (Rabat-Salé-Kénitra region) and Meknès (Fès-Meknès region), separated by approx. 100 km. The objective of the present research was to assess the virulence of the populations against a set of differential lines, evaluate their genetic variability with a set of molecular markers, and compare them with populations from other areas. This was to provide information on the introductions' putative origin(s).

MATERIALS AND METHODS

Sunflower broomrape populations

Seeds from two sunflower broomrape populations (designated as SA1 and SA2) were collected in two sunflower fields in Souk Al Arbaa, Rabat-Salé-Kénitra region of Morocco in 2016. These populations were named SA1 and SA2. Seeds from a third population (designated MK1) were collected in 2019 in a sunflower field of Meknès, Fès-Meknès region.

Several populations were used as controls, to test the putative areas of origin of the populations found in Morocco. These were populations OC94, SP, EK147, and EK21, with race E or race F virulence, and IN201,

with race G virulence, from the Guadalquivir Valley in Southern Spain; INA, EK37, and EK43, with race E or race F virulence, from the Cuenca province in Central Spain (Pineda-Martos *et al.*, 2013); OC1, with race E virulence, from Serbia; OC2, with race F virulence, from Romania; OC14, with race G virulence, from Russia; Boro-14, with race G virulence, from Turkey; Boro-19, with race F virulence, from Bulgaria (Pineda-Martos *et al.*, 2014a); and ORD, ORG, ORH, and ORK from Béja Governorate in Tunisia (Jebri *et al.*, 2017).

Sunflower differential lines

Seeds of the three Moroccan broomrape populations were tested against a set of eight differential sunflower lines: B117, with no resistant genes; J8281, resistant to broomrape races A and B; Record, resistant to races A to C; S1358, resistant to races A to D; NR5, resistant to races A to E; P96 and LP2, resistant to races A to F; and DEB2, resistant races A to G. B117 was developed from a confectionery landrace collected in Spain (Martín-Sanz *et al.*, 2016). J8281, Record, and S1358 were reported by Vranceanu *et al.* (1980). NR5 was a selection from line P-1380-2 reported by Vranceanu *et al.* (1980). P96 was developed by Fernández-Martínez *et al.* (2004). LP2 is a line containing the *Or7* gene isolated from the commercial sunflower hybrid PR64A95. DEB2 is a line developed by Velasco *et al.* (2012).

Phenotypic evaluation

Evaluation of the broomrape populations against the set of sunflower differential lines was conducted in two different experiments, because the broomrape populations were identified and collected in different years. Populations SA1 and SA2, for which seed availability was low, were evaluated in 2017 in multi-pot trays with pot volumes of 0.04 L, using two replications of ten plants for every combination of broomrape population and differential line. The experimental conditions were as described by Nabloussi *et al.* (2018). The pots were filled with a soil mixture of sand and peat (1:1 by volume) inoculated with broomrape seeds at 0.28 mg per g of soil. The evaluation was conducted in a growth chamber at 25/20°C (light/dark) and 16 h photoperiod. Population MK1 was evaluated in 2020 in a greenhouse with no temperature control using 6 L capacity pots and 12 plants per sunflower genotype. Sunflower seeds were germinated on moistened filter paper at 25°C in the dark for 48 h, then planted into pots (7 × 7 × 7 cm) filled with a mixture of sand and peat, each containing

approximately 30 mg of broomrape seeds. After 4 weeks in a growth chamber at 25°C/20°C (light/dark) and 16 h photoperiod, the plants were transplanted to 6 L capacity pots that each contained a mixture of sand, silt, and peat (2:1:1). In the multi-pot tray experiment, underground and emerged sunflower structures were counted as described by Nabloussi *et al.* (2018). In the pot experiment, emerged broomrape shoots were counted. ANOVA with Tukey's post hoc tests to compare means was carried out for data from each broomrape population, using IBM SPSS Statistics version 29.

Plant genotyping and diversity analyses

Apical tissues from 40 broomrape shoots parasitizing the susceptible line B117 were collected for each of the three Moroccan populations studied. The tissues were initially frozen at -80°C, then lyophilized and ground in a laboratory ball mill. DNA was extracted following an adaption of the protocol described by Pérez-Vich *et al.* (2004). For the other broomrape populations (controls), DNA from 15 to 48 individual plants was used, previously extracted and maintained at -80°C.

Genotyping of individual broomrape plants from the populations collected in Morocco and those used as controls was conducted with a set of 192 *O. cumana* SNP markers reported and mapped by Calderón-González *et al.* (2019), and KASP genotyping assays (LGC Biosearch Technologies).

Data were analyzed using GenAEx ver. 6.5. The following parameters of intrapopulation diversity were calculated: percentage of polymorphic loci (P), observed heterozygosity (Ho), expected heterozygosity (He), and Shannon's diversity index (I). Genetic distances between populations were estimated using Nei's unbiased genetic distance between pairs of populations (uNeiP), to provide a preliminary indication of the putative geographic areas of origin of the three populations found in Morocco.

The matrix of GST pairwise distances was used as an input for principal coordinates analysis (PCoA). To simplify the graph, the populations used to evaluate the relatedness of the Moroccan populations with other geographical areas were assessed in the following groups: Guadalquivir Valley races E and F, Guadalquivir Valley race G, Cuenca Province, Eastern Europe, and Tunisia. The Guadalquivir Valley populations were separated into two groups because a previous study (Martín Sanz *et al.*, 2016) showed that the race G populations exhibited increased intrapopulation diversity.

RESULTS

Race classification of the sunflower broomrape populations

Populations SA1 and SA2, collected in Souk Al Arbaa, showed a similar virulence pattern against the differential sunflower lines. They parasitized all lines with resistance to races A to E, producing from 5.7 to 9.8 nodules/shoots per plant for SA1, or from 6.7 to 17.6 nodules/shoots per plant for SA2. Parasitization of sunflower lines P96 and LP2 with resistance to race F was much less, respectively 0.3 and 0.8 nodules/shoots per plant for SA1 and 1.7 and 2.7 nodules/shoots per plant for SA2. However, no parasitization on sunflower line DEB2 (resistant to races A to G) was observed (Table 1). These results indicated that both populations are classified as race G. The virulence pattern of population MK1 was different. This population parasitized the differential lines Record (resistant to races A-C) and S1358 (resistant to races A-D) but not the lines J8281 (resistant to races A-B), NR5 (resistant to races A-E), P96, and LP2 (resistant to races A-F), and DEB2 (resistant to races A-G). Accordingly, the population is classified as race E. The absence of parasitization on line J8281 will be discussed below.

Table 1. Mean (numbers \pm standard errors) of broomrape nodules/shoots¹ for three broomrape populations collected in Morocco evaluated with a set of differential sunflower lines.

Differential line	Resistant to broomrape races	Sunflower broomrape populations ²		
		SA1	SA2	MK1
B117	None	13.2 \pm 1.5 d	17.2 \pm 2.2 e	24.6 \pm 2.6 c
J8281	A-B	8.8 \pm 0.7 bc	12.7 \pm 1.7 de	0.1 \pm 0.1 a
Record	A-C	5.7 \pm 0.7 b	6.7 \pm 0.9 bc	4.2 \pm 0.7 ab
S1358	A-D	7.3 \pm 0.9 bc	9.6 \pm 1.0 cd	8.9 \pm 1.9 b
NR5	A-E	9.8 \pm 1.1 cd	17.6 \pm 2.0 e	0.0 a
P96	A-F	0.3 \pm 0.1 a	1.7 \pm 0.4 ab	0.0 a
LP2	A-F	0.8 \pm 0.2 a	2.7 \pm 0.4 ab	0.0 a
DEB2	A-G	0.0 a	0.0 a	0.0 a

¹ Populations SA1 and SA2 were collected in 2016 and evaluated in an experiment in multi-pot trays in a growth chamber. The plants were uprooted, and nodules and developing shoots were assessed. Population MK1 was collected in 2019 and evaluated in a greenhouse experiment in 6 L capacity pots, where only emerged shoots were assessed.

² Values followed by the same letter within each column are not statistically significant at $\alpha=0.05$ based on Tukey's post hoc test.

Table 2. Genetic diversity parameters of the sunflower broomrape populations examined in this study. The populations were: SA1 and SA2 from Souk Al Arbaa, Rabat-Salé-Kénitra region, Morocco; MK1 from Meknès, Fès-Meknès region, Morocco; OC94, SP, EK147, EK21, and IN201 from the Guadalquivir Valley in Southern Spain; INA, EK37, and EK43, from the Cuenca province in Central Spain; OC1 from Serbia; OC2 from Romania; OC14 from Russia; Boro-14 from Turkey; Boro-19 from Bulgaria; ORD, ORG, ORH, and ORK from Béja Governorate, Tunisia.

Population	P	H _o (±SE)	He (±SE)	I (±SE)
SA1	0.66	0.00 ± 0.00	0.00 ± 0.00	0.00 ± 0.00
SA2	0.66	0.00 ± 0.00	0.00 ± 0.00	0.00 ± 0.00
MK1	0.66	0.01 ± 0.01	0.01 ± 0.00	0.00 ± 0.00
OC94	2.65	0.01 ± 0.01	0.00 ± 0.00	0.00 ± 0.00
SP	0.66	0.01 ± 0.01	0.00 ± 0.00	0.00 ± 0.00
EK147	1.99	0.01 ± 0.01	0.00 ± 0.00	0.00 ± 0.00
EK21	0.66	0.01 ± 0.01	0.00 ± 0.00	0.00 ± 0.00
IN201	50.33	0.05 ± 0.01	0.12 ± 0.01	0.54 ± 0.03
INA	0.00	0.00 ± 0.00	0.00 ± 0.00	0.00 ± 0.00
EK37	0.00	0.00 ± 0.00	0.00 ± 0.00	0.00 ± 0.00
EK43	0.66	0.00 ± 0.00	0.00 ± 0.00	0.00 ± 0.00
OC1	17.88	0.01 ± 0.00	0.06 ± 0.01	0.89 ± 0.02
OC2	66.89	0.02 ± 0.00	0.20 ± 0.01	0.89 ± 0.02
OC14	52.32	0.02 ± 0.01	0.16 ± 0.01	0.86 ± 0.03
Boro-14	17.88	0.01 ± 0.01	0.02 ± 0.00	0.82 ± 0.04
Boro-19	67.55	0.01 ± 0.01	0.17 ± 0.01	0.93 ± 0.02
ORD	47.68	0.00 ± 0.00	0.06 ± 0.01	0.00 ± 0.00
ORG	47.68	0.00 ± 0.00	0.06 ± 0.01	0.00 ± 0.00
ORH	48.34	0.00 ± 0.00	0.22 ± 0.02	0.00 ± 0.00
ORK	49.01	0.00 ± 0.00	0.24 ± 0.02	0.00 ± 0.00

P = percentage of polymorphic loci; H_o = observed heterozygosity; He = expected heterozygosity; I = Shannon's diversity index.

Intrapopulation diversity and relatedness to broomrape populations from other areas

Within the three broomrape populations SA1, SA2, and MK1, all the indexes of intrapopulation diversity (P, H_o, He), and Shannon's diversity index (I), indicated the absence of intrapopulation diversity (Table 2). Nei's unbiased genetic distance (uNeiP) between populations was zero between SA1 and SA2, and between MK1 and the four populations of the Guadalquivir Valley of races E and F. The genetic distance between SA1 and SA2, and MK1, was uNeiP = 0.71. The closest population to SA1 and SA2 was OC14 from Russia (uNeiP = 0.16), followed by OC2 from Romania (uNeiP = 0.43).

Relatedness of the Moroccan populations to those from other geographical areas is shown in the biplot of PCo1 and PCo2 (Figure 1), which explained 30.96% and 24.15%, respectively of the total variation. It can be observed how SA1 and SA2 are grouped together due to their null genetic

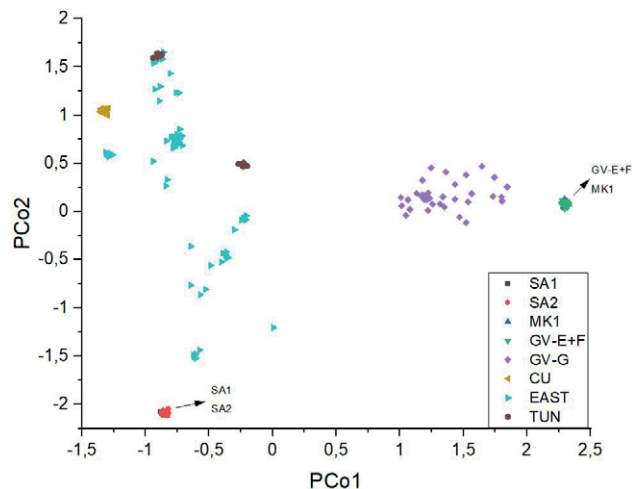


Figure 1. Principal coordinates analysis of four *Orobancha cumana* populations SA1, SA2, and MK1 collected in Morocco together with reference populations from the Guadalquivir Valley in Southern Spain, with virulence E and F (GV-E+F) or G (GV-G), Cuenca in Central Spain (CU), Eastern Europe (EAST) and Tunisia (TUN). The percentage of variation explained by each axis is given in parentheses.

distance. The same occurred for MK1 and the populations of races E and F of the Guadalquivir Valley.

DISCUSSION

This study has shown that the broomrape populations collected from sunflower in Morocco belong to two distant gene pools, which indicates two separate introduction events. The population MK1 collected in Meknès belongs to the classical gene pool of the Guadalquivir Valley in Southern Spain. Populations of this gene pool are genetically distant from the populations of Eastern Europe, and they are characterized by low intrapopulation genetic diversity (Pineda-Martos *et al.*, 2013). These Guadalquivir Valley populations were initially of race E until the second half of the 1990s, when a new race F emerged as a result of a point mutation, i.e., without alteration of the genetic structure of the populations (Pineda-Martos *et al.*, 2013). The mutation leading to race F virulence spread rapidly, due to selection pressure produced by the generalized cultivation of race-E resistant sunflower hybrids (Molinero-Ruiz and Domínguez, 2014). Molinero-Ruiz *et al.* (2008) found that all populations collected in the Guadalquivir Valley area in 1988 and 1989 already contained varying proportions of race-F individuals, and all these populations were infective to the sunflower differential line NR5. This line carries the *Or5* gene that confers resistance to race E but not to race F.

In the present research, population MK1 did not parasitize sunflower NR5, indicating that MK1 is a race E population. This, in turn, suggests that the broomrape seeds that founded this population were most likely introduced to Morocco before the generalized spread of race F in the Guadalquivir Valley, i.e., before 1988. This asks the question of why the population remained unobserved until 2016, when we detected it on broomrape plants in Meknès. There is no clear answer to this question, but it is important to note that an identical phenomenon occurred in the Castilla y León region in Northern Spain, where broomrape on sunflower was first observed in 2008 (Fernández-Escobar *et al.*, 2009). Evaluation of six populations collected in Castilla y León showed that three were race E of the Guadalquivir Valley gene pool (Malek *et al.*, 2017), like the MK1 population. Fernández-Escobar *et al.* (2009) suggested that the adaptation of populations to a new environment may provide an explanation for the long period that broomrape remained undetected, with low numbers of individuals each sunflower growing season.

The reaction of population MK1 with the set of differential lines requires further discussion. This population was avirulent on the race B resistant line J8281, while it was virulent on the race C differential line Record and the race D differential line S1358. This is a common behavior of race E and race F populations from the Guadalquivir Valley gene pool (Melero-Vara *et al.*, 2000). This is because the set of sunflower differential lines for races A to E was developed in Romania (Vranceanu *et al.*, 1980), and the gene pool of sunflower broomrape from the Guadalquivir Valley is genetically distant from the populations from eastern Europe (see Figure 1). Therefore, it is unsurprising that line S1358 has contrasting responses to sunflower broomrape populations from Romania and southern Spain. Despite this, we continue using this line in all studies on broomrape race classification to maintain a universal set of differential lines for use with broomrape populations from all geographical areas.

Populations SA1 and SA2 had similar virulence patterns, exhibiting race G virulence because they parasitized race F resistant sunflower lines P96 and LP2. The degree of attack of these populations on the host lines was low, which could be attributed to incomplete resistance of both lines to race G populations (Martín-Sanz *et al.*, 2016), and probably also to a low proportion of race G genotypes in the broomrape populations. SA1 and SA2 populations parasitizing line P96 indicates that they were most probably introduced from Eastern Europe, since the race G population from the Guadalquivir Valley has been shown to be avirulent on P96 (Martín-Sanz

Table 3. Nei's unbiased genetic distances (uNeiP) between the Moroccan broomrape populations SA1, SA2 and MK1 and other populations used in this study from diverse geographical areas.

Population and provenance	SA1	SA2	MK1
SA2	0.00		
MK1	0.71	0.71	
OC94 (Guadalquivir Valley, Spain)	0.70	0.70	0.00
SP (Guadalquivir Valley, Spain)	0.70	0.70	0.00
EK147 (Guadalquivir Valley, Spain)	0.70	0.70	0.00
EK21 (Guadalquivir Valley, Spain)	0.70	0.70	0.00
IN201 (Guadalquivir Valley, Spain)	0.52	0.52	0.12
INA (Cuenca, Spain)	0.60	0.60	0.85
EK37 (Cuenca, Spain)	0.60	0.60	0.85
EK43 (Cuenca, Spain)	0.60	0.60	0.85
OC1 (Serbia)	0.66	0.66	0.66
OC2 (Romania)	0.43	0.43	0.62
OC14 (Russia)	0.16	0.16	0.57
Boro-14 (Turkey)	0.59	0.59	0.91
Boro-19 (Bulgaria)	0.50	0.50	0.60
ORD (Tunisia)	0.68	0.68	0.66
ORG (Tunisia)	0.68	0.68	0.66
ORH (Tunisia)	0.60	0.60	0.55
ORK (Tunisia)	0.60	0.60	0.54

et al., 2016). This was further supported by the Nei's unbiased genetic distances (Table 3) and PCoA analysis (Figure 1), which showed that SA1 and SA2 populations were distant from to the Guadalquivir Valley gene pool, and were closer to some populations from Eastern Europe, particularly to population OC14 from Russia. The objectives of the present study did not include unequivocal identification of the origin of broomrape populations in Morocco. To do that for populations SA1 and SA2, it would be necessary to include many populations from several countries, which was beyond the scope of this study. The objective was to provide preliminary indication of the putative area of origin, and to conduct detailed studies in further research. For the MK1 population, the results indicated that the area of origin was the Guadalquivir Valley. For SA1 and SA2, the results indicate that these populations originated from Eastern Europe, most likely Russia, but this should be confirmed by expanding comparative analysis to a broad set of populations from that area. The origin of these populations in Russia or surrounding countries is not unexpected, since Russian sunflower cultivars such as Peredovik, or other cultivars developed from Russian or Ukrainian germplasm, are cultivated in Morocco (Nabloussi *et al.*, 2011). Therefore, broomrape seeds may have been introduced associated with imported sunflow-

er seed, which is one of the main modes of international broomrape dispersion (Fernández-Martínez *et al.*, 2015). Most relevant is that SA1 and SA2 populations were race G, which indicated that, unlike MK1, seed introduction was recent, as race G populations were not reported in Russia until 2013 (Antonova *et al.*, 2013).

Sunflower broomrape populations in Eastern Europe generally contain large intrapopulation diversity (Pineda-Martos *et al.*, 2014b; Bilgen *et al.*, 2019). This is partly due to co-existence in some areas of broomrape populations parasitizing sunflower crops and wild host species. Pineda-Martos *et al.* (2014b), documented gene flow between both types of populations, which contributed to increased genetic diversity in populations parasitizing on sunflower. Conversely, populations in areas where broomrape is not found in the wild, (e.g. Morocco and Spain) can exhibit no genetic diversity. This was the case for populations in Cuenca province in Central Spain and populations of races E and F from the Guadalquivir Valley in Southern Spain, which has been attributed to founder effects (Pineda-Martos *et al.*, 2014b). A similar situation in populations SA1 and SA2 in Morocco, where of numbers of seeds from a population from Eastern Europe has resulted in genetically homogeneous populations. For MK1, this population reproduces the absence of genetic variability of the original population from the Guadalquivir Valley.

Sunflower broomrape was considered to be an autogamous plant (Gagne *et al.*, 1998). However, several studies have shown cross fertilization in this species (Rodríguez-Ojeda *et al.*, 2013; Pineda-Martos *et al.*, 2013; Pineda-Martos *et al.*, 2014b; Martín-Sanz *et al.*, 2016). The appearance of race G populations in the Guadalquivir Valley area of Southern Spain was suggested to be due to mixture and subsequent genetic recombination between individuals of the two gene pools present in Spain (Martín-Sanz *et al.*, 2016). A similar situation may occur in Morocco if the individuals of the two gene pools identified in the present study come into contact and hybridize. Control measures are therefore required in Morocco to prevent introduction of new broomrape populations and expansion of existing ones, to limit the area infested by the parasite and to avoid creation of new populations with increased virulence, as has occurred in Southern Spain.

ACKNOWLEDGMENT

This study was funded by research project PID2020-117286RB-I00 of the Spanish Ministry of Economy and Innovation, and was co-funded with EU FEDER Funds.

LITERATURE CITED

- Amri M., Abbes Z., Youssef S.B., Bouhadida M., Salah H.B., Kharrat M., 2012. Detection of the parasitic plant, *Orobanche cumana* on sunflower (*Helianthus annuus* L.) in Tunisia. *African Journal of Biotechnology* 11: 4163–4167. <https://doi.org/10.5897/AJB11.3031>
- Antonova T., 2014. The history of interconnected evolution of *Orobanche cumana* Wallr. and sunflower in the Russian Federation and Kazakhstan. In: *Proceedings of the 3rd International Symposium on Broomrape (Orobanche spp.) in Sunflower*, International Sunflower Association, Paris, France, 57–64.
- Antonova T.S., Araslanova N.M., Strelnikov E.A., Ramazanov S.A., Guchetl S.Z., Chelyustnikova T.A., 2013. Distribution of highly virulent races of sunflower broomrape (*Orobanche cumana* Wallr.) in the southern regions of the Russian Federation. *Russian Agricultural Sciences* 39: 46–50. <https://doi.org/10.3103/S1068367413010023>
- Batchvarova R., 2014. Current situation of sunflower broomrape in Bulgaria. In: *Proceedings of the 3rd International Symposium on Broomrape (Orobanche spp.) in Sunflower*, International Sunflower Association, Paris, France, 51–54.
- Beck-Mannagetta G., 1930. Orobancheaceae. In: *Das Pflanzenreich Vol. IV* (A. Engler, ed.), Verlag von Wilhelm Engelmann, Leipzig, 1–348.
- Bilgen B.B., Barut A.K., Demirbaş S., 2019. Genetic characterization of *Orobanche cumana* populations from the Thrace region of Turkey using microsatellite markers. *Turkish Journal of Botany* 43: 3. <https://doi.org/10.3906/bot-1807-71>
- Calderón-González A., Pouilly N., Muñoz S., Grand X., Coque M., Velasco L., Pérez-Vich B., 2019. A SSR-SNP linkage map of the parasitic weed *Orobanche cumana* Wallr. including a gene for plant pigmentation. *Frontiers in Plant Science* 10: 797. <https://doi.org/10.3389/fpls.2019.00797>
- Cvejić, S., Radanović A., Dedić B., Jocković M., Jocić Miladinović D., 2020. Genetic and genomic tools in sunflower breeding for broomrape resistance. *Genes* 11: 152. <https://doi.org/10.3390/genes11020152>
- Fernández-Escobar J., Rodríguez-Ojeda M.I., Fernández-Martínez J.M., Alonso L.C., 2009. Sunflower broomrape (*Orobanche cumana* Wallr.) in Castilla-León, a traditionally non-broomrape infested area in Northern Spain. *Helia* 51: 57–64. <https://doi.org/10.2298/HEL0951057F>
- Fernández-Martínez J.M., Pérez-Vich B., Akhtouch B., Velasco L., Muñoz-Ruz J., Melero-Vara J.M., Domínguez J., 2004. Registration of four sunflower

- germplasm lines resistant to race F of broomrape. *Crop Science* 44: 1033–1034. <https://doi.org/10.2135/cropsci2004.1033>
- Fernández-Martínez J.M., Pérez-Vich B., Velasco L., 2015. Sunflower broomrape (*Orobanche cumana* Wallr.), in *Sunflower Oilseed. Chemistry, Production, Processing and Utilization* (E. Martínez-Force, N.T. Dunford, and B.K. Salas, eds.), AOC Press, Champaign, IL (USA), 129–156.
- Gagne G., Roeckel-Drevet P., Grezes-Besset B., Shindrova P., Ivanov P., ... Nicolas P., 1998. Study of the variability and evolution of *Orobanche cumana* populations infesting sunflower in different European countries. *Theoretical and Applied Genetics* 96: 1216–1222. <https://doi.org/10.1007/s001220050859>
- González-Cantón E., Velasco-Sanchez A., Velasco L., Martín-Sanz A., 2019. First report of sunflower broomrape (*Orobanche cumana* Wallr.) in Portugal. *Plant Disease* 103: 2143. <https://doi.org/10.1094/PDIS-10-18-1723-PDN>
- Jebri, M., Ben Khalifa M., Fakhfakh H., Pérez-Vich B., Velasco L., 2017. Genetic diversity and race composition of sunflower broomrape populations from Tunisia. *Phytopathologia Mediterranea* 56, 421–430. https://doi.org/10.14601/Phytopathol_Mediterr-20839
- Jestin C., Lecomte V., Duroueix F., 2014. Current situation of sunflower broomrape in France. In: *Proceedings of the 3rd International Symposium on Broomrape* (*Orobanche* spp.) in *Sunflower*, International Sunflower Association, Paris, France, 28–31.
- Kaya Y., 2014. Current situation of sunflower broomrape around the world. In: *Proceedings of the 3rd International Symposium on Broomrape* (*Orobanche* spp.) in *Sunflower*, International Sunflower Association, Paris, France, 9–18.
- Ma D.T., Jan C.C., 2014. Distribution and race composition of sunflower broomrape (*Orobanche cumana* Wallr.) in Northern China. In: *Proceedings of the 3rd International Symposium on Broomrape* (*Orobanche* spp.) in *Sunflower*, International Sunflower Association, Paris, France, 65–69.
- Malek J., del Moral L., Fernández-Escobar J., Pérez-Vich B., Velasco L., 2017. Racial characterization and genetic diversity of sunflower broomrape populations from Northern Spain. *Phytopathologia Mediterranea* 56: 70–76. https://doi.org/10.14601/Phytopathol_Mediterr-19163
- Martín-Sanz A., Malek J., Fernández-Martínez J.M., Pérez-Vich B., Velasco L., 2016. Increased virulence in sunflower broomrape (*Orobanche cumana* Wallr.) populations from Southern Spain is associated with greater genetic diversity. *Frontiers in Plant Science* 7: 589. <https://doi.org/10.3389/fpls.2016.00589>
- Melero-Vara J.M., Domínguez J., Fernández-Martínez J.M., 2000. Update on sunflower broomrape situation in Spain: Racial status and sunflower breeding for resistance. *Helia* 33: 45–56. <https://doi.org/10.1515/helia.2000.23.33.45>
- Molinero-Ruiz M.L., Domínguez J., 2014. Current situation of sunflower broomrape in Spain. In: *Proceedings of the 3rd International Symposium on Broomrape* (*Orobanche* spp.) in *Sunflower*, International Sunflower Association, Paris, France, 19–27.
- Molinero-Ruiz M.L., Pérez-Vich B., Pineda-Martos R., Melero-Vara J.M., 2008. Indigenous highly virulent accessions of the sunflower root parasitic weed *Orobanche cumana*. *Weed Research* 48: 169–178. <https://doi.org/10.1111/j.1365-3180.2007.00611.x>
- Nabloussi A., Fernández-Cuesta A., El-Fechтали M., Fernández-Martínez J.M., Velasco L., 2011. Performance and seed quality of Moroccan sunflower varieties and Spanish landraces used for confectionery and snack food. *Helia* 55: 75–82. <https://doi.org/10.2298/HEL1155075N>
- Nabloussi A., Velasco L., Assissel N., 2018. First report of sunflower broomrape, *Orobanche cumana* Wallr, in Morocco. *Plant Disease* 102, 457. <https://doi.org/10.1094/PDIS-06-17-0858-PDN>
- Parker C., 2016. *Orobanche cumana* (sunflower broomrape). In: *Invasive Species Compendium*. Wallingford, UK: CAB International. www.cabi.org/isc.
- Pérez-Vich B., Akhtouch B., Knapp S.J., Leon A.J., Velasco L., Fernández-Martínez J.M., Berry S.T., 2004. Quantitative trait loci analysis of broomrape (*Orobanche cumana* Wallr.) resistance in sunflower. *Theoretical and Applied Genetics* 109: 92–102. <https://doi.org/10.1007/s00122-004-1599-7>
- Pineda-Martos R., Velasco L., Fernández-Escobar J., Fernández-Martínez J.M., Pérez-Vich B., 2013. Genetic diversity of sunflower broomrape (*Orobanche cumana*) populations from Spain. *Weed Research* 53: 279–289. <https://doi.org/10.1111/wre.12022>
- Pineda-Martos R., Velasco L., Pérez-Vich B., 2014a. Identification, characterisation and discriminatory power of microsatellite markers in the parasitic weed *Orobanche cumana*. *Weed Research* 54: 120–132. <https://doi.org/10.1111/wre.12062>
- Pineda-Martos R., Pujadas-Salvà A.J., Fernández-Martínez J.M., Stoyanov K., Velasco L., Pérez-Vich B., 2014b. The genetic structure of wild *Orobanche cumana* Wallr. (*Orobanchaceae*) populations in Eastern Bulgaria reflects introgressions from weedy populations. *Scientific World Journal* 150432. <https://doi.org/10.1155/2014/150432>

- Rodríguez-Ojeda M.I., Fernández-Martínez J.M., Velasco L., Pérez-Vich B., 2013. Extent of cross-fertilization in *Orobancha cumana* Wallr. *Biologia Plantarum* 57: 559–562. <https://doi.org/10.1007/s10535-012-0301-1>
- Velasco, L., Pérez-Vich B., Yassein A.A.M., Jan C.C., Fernández-Martínez J.M., 2012. Inheritance of resistance to sunflower broomrape (*Orobancha cumana* Wallr.) in an interspecific cross between *Helianthus annuus* and *H. debilis* subsp. *tardiflorus*. *Plant Breeding* 131: 220–221. <https://doi.org/10.1111/j.1439-0523.2011.01915.x>
- Vrânceanu A.V., Tudor V.A., Stoenescu F.M., Pirvu N., 1980. Virulence groups of *Orobancha cumana* Wallr., differential hosts and resistance source genes in sunflower. In: *Proceedings of the 9th International Sunflower Conference*, International Sunflower Association, Paris, France, 74–82.



Citation: N. Bessadat, B. Hamon, N. Bataillé-Simoneau, N. Hamini-Kadar, M. Kihal, P. Simoneau (2023) Identification and characterization of fungi associated with leaf spot/blight and melting-out of turfgrass in Algeria. *Phytopathologia Mediterranea* 62(1): 73-93. doi: 10.36253/phyto-14169

Accepted: March 31, 2023

Published: May 8, 2023

Copyright: © 2023 N. Bessadat, B. Hamon, N. Bataillé-Simoneau, N. Hamini-Kadar, M. Kihal, P. Simoneau. This is an open access, peer-reviewed article published by Firenze University Press (<http://www.fupress.com/pm>) and distributed under the terms of the Creative Commons Attribution License, which permits unrestricted use, distribution, and reproduction in any medium, provided the original author and source are credited.

Data Availability Statement: All relevant data are within the paper and its Supporting Information files.

Competing Interests: The Author(s) declare(s) no conflict of interest.

Editor: Thomas A. Evans, University of Delaware, Newark, DE, United States.

ORCID:

NB: 0000-0001-7795-2606
BH: 0000-0001-5868-0676
NB-S: 0000-0001-6200-4259
NH-K: 0000-0002-3240-5913
MK: 0000-0003-2901-373X
PS: 0000-0002-3890-9848

Research Papers

Identification and characterization of fungi associated with leaf spot/blight and melting-out of turfgrass in Algeria

NABAHA BESSADAT^{1,2}, BRUNO HAMON¹, NELLY BATAILLÉ-SIMONEAU¹, NISSERINE HAMINI-KADAR², MABROUK KIHAL², PHILIPPE SIMONEAU^{1,*}

¹ Université Angers, Institut Agro, INRAE, UMR 1345 IRHS, SFR QUASAV, Beaucazoué, 49071, France

² Université Oran1 Ahmed Ben Bella, Laboratoire de Microbiologie Appliquée, BP1524 El M'naouer 31000 Oran, Algeria

*Corresponding author. E-mail: simoneau@univ-angers.fr

Summary. Symptoms of foliar blight were observed on turfgrass in Oran (Algeria), including yellow chlorotic patches on leaves during the 2020 summer (temperatures between 35 and 40°C). Symptoms extended downward from leaf tips and entire leaves became blighted, leading to irregular discoloured areas that later turned brown. Isolations from infected plants included 214 isolates identified as *Curvularia* or *Bipolaris*, based on morphological traits. Other isolates included *Fusarium*, *Myrothecium* and *Acremonium* spp. Three molecular loci, *ITS rDNA*, *gpd* and *tef1*, were amplified and sequenced. Morphological and multi-locus phylogenetic analyses revealed four fungal species viz. *B. sorokiniana*, *C. spicifera*, *C. verruculosa*, *C. geniculata*, and two additional *Curvularia* lineages, some of these fungi are reported as first records for Algeria. Koch's postulates were confirmed by inoculating potted turfgrass with spore suspensions of 16 isolates and re-isolating of the inoculated pathogens from symptomatic tissues. *Bipolaris sorokiniana* was the most virulent pathogen causing numerous foliar necrotic lesions similar to those observed in the field. Other isolates infected basal leaves only, and caused less severe symptoms. The results show that *Curvularia* species may be secondary pathogens infecting stressed plants, and that simultaneous occurrence of high temperatures and poor water quality have influenced disease progression. Correct identification of these pathogens is important for applying appropriate and timely disease management.

Keywords. *Bipolaris* spp., *Curvularia* spp., morphological characterization, multi-gene phylogeny, Koch's postulates.

INTRODUCTION

Turfgrass production and management are multibillion-dollar industries that provide safe playing surfaces for sports fields and outdoor recreation areas, as well as economic opportunities for seed and sod producers, lawn care operators and landscapers (Stackhouse *et al.*, 2020; Sithin, 2021).

Field turf is usually composed of two or more different grass species that may complement each other to provide functional and aesthetic improvements in turf quality (Zanelli *et al.*, 2021). Seed mixtures of perennial ryegrass (*Lolium perenne* L.), smooth-stalked meadow grass/Kentucky bluegrass (*Poa pratensis* L.), and red fescue (*Festuca rubra* L.) are widely used to establish football pitches in temperate climate zones (Sherratt *et al.*, 2017). These *Poaceae* are native to northern Africa, Europe and Asia, but are widely cultivated and naturalized around the world (Abdelguerfi and Abdelguerfi-Laouar, 2004; USDA-ARS, 2013). Some cultivars of these species have been shown to have good wintering, disease resistance and sodding characteristics (Wolski *et al.*, 2021; Zanelli *et al.*, 2021). In Algeria, these commercially available grass seed mixtures are imported from Europe, especially those used for the Oran Olympic Stadium playing field which was completed in 2019.

However, turfgrass production and use in sports fields are limited by several biotic stresses, with diseases being major limiting factors (Hatfield, 2017; Landschoot, 2021; Liu *et al.*, 2023). Several leaf spot- or blight-causing fungi have been reported from turf under wet and warm weather conditions, including *Bipolaris sorokiniana* (Sacc.) Shoemaker and *Curvularia* spp. (Nelson, 1992; Martinez *et al.*, 2020; Karunaratha, *et al.*, 2021). Increased incidence and severity of these diseases on lawn grasses have been associated with high temperatures, large amounts of nitrogen, low mowing height (Falloon, 1976; Martinez *et al.*, 2020; Landschoot, 2021), and other biotic stresses (Smiley *et al.*, 2005). Helminthosporioid fungi such as *Bipolaris* and *Drechslera* have been associated with *Curvularia* disease symptoms when climatic conditions are favourable (Nelson, 1992; Martinez *et al.*, 2020). These fungi cause root and crown rots which lead to “melting-out” symptoms in turf that typically follow the appearance of leaf spots (Martinez *et al.*, 2020). The fungi survive on plant debris and diseased tissues at the soil surface (Smiley *et al.*, 2005; Tan *et al.*, 2018; Chamekh *et al.*, 2019; Iturrieta-González *et al.*, 2020; Al-Sadi, 2021), and their spores can be air- or seed-borne (Nelson, 1992; Almaguer *et al.*, 2012; Santos *et al.*, 2018; Al-Sadi, 2021). The dark pigmentation of conidia makes the pathogens resistant to damage by ultraviolet radiation (Corwin *et al.*, 2007).

Bipolaris and *Curvularia* (*Pleosporaceae*, *Pleosporales*) include pathogens of many plants, particularly cereals and grasses with wide distribution, including bluegrass, maize, and oats (Sivanesan, 1987; Manamgoda *et al.*, 2014; Marin Felix *et al.*, 2017; Farr and Rossman, 2022). Many species of these genera are emerging opportunistic pathogens of animals and humans (Khan

et al., 2000; Madrid *et al.*, 2014; Manamgoda *et al.*, 2015; Iturrieta-González *et al.*, 2020; Pham *et al.*, 2022; Thekkedath *et al.*, 2022). Some species of *Bipolaris* and *Curvularia* are anamorphs of *Cochliobolus* (Sivanesan, 1987; Marin-Felix *et al.*, 2020). They are characterized by septate and erect conidiophores, with sympodially proliferating conidiogenous cells, and pigmented phragmospores (Zhang *et al.*, 2012). These fungi can be distinguished by conidial morphology (hila, septa, septum ontogeny, and wall structure) (Sivanesan, 1987).

Several methods have been used for diagnosing fungal pathogens of turfgrasses. Traditional diagnostic methods included symptomology, morphology, and microscopical identifications (Sivanesan, 1987). These have been augmented by nucleic acid detection such as PCR-based technologies (Stackhouse *et al.*, 2020), since this group of fungi is not reliably identifiable using traditional techniques (Tan *et al.*, 2018; Bhunjun *et al.*, 2020). Variation in cultural and morphological characteristics, such as size and shape of conidia, and colony growth rate of isolates due to culture conditions, have been reported (Sun *et al.*, 2003; Santos *et al.*, 2018). These variations may lead to inaccurate pathogen identification (Manamgoda *et al.*, 2015). In addition, phylogenetics studies based on the *ITS rDNA* region have limited utility for species identifications, especially among members of the *Pleosporales*. This marker provided little resolution for closely related *Curvularia* and *Bipolaris* species (Madrid *et al.*, 2014; Bhunjun *et al.*, 2020), indicating that additional markers are required for accurate identification within this group of fungi.

Berbee *et al.* (1999) conducted phylogenetic analyses of the *ITS rDNA* region and glyceraldehyde 3-phosphate dehydrogenase (*gpd*) gene sequences to assess the evolutionary relationships of *Cochliobolus*, *Pseudocochliobolus*, *Curvularia*, and *Bipolaris*. These phylogenies were later confirmed using additional loci such as the large subunit (LSU) and translation elongation factor (*tef1*) (Manamgoda *et al.*, 2012). Two main monophyletic groups were then established. *Bipolaris* and *Cochliobolus* spp. were clustered in group 1. In group 2, species previously considered to be *Bipolaris*, *Cochliobolus*, or *Pseudocochliobolus* were reclassified as *Curvularia* (Manamgoda *et al.*, 2012), with the most common species causing diseases on grasses. Some *Bipolaris* species were later reclassified as *Curvularia* (Jeon *et al.*, 2015; Manamgoda *et al.*, 2015; Marin-Félix *et al.*, 2020). The *Curvularia*-*Bipolaris* complex currently comprises *Curvularia*, *Bipolaris*, *Cochliobolus*, and *Pseudocochliobolus* (Manamgoda *et al.*, 2012; 2015; Deng *et al.*, 2015; Marin-Félix *et al.*, 2017), and the recently confirmed two species of *Exserohilum* in *Curvularia* (Hernández-Restrepo

et al., 2018; Marin-Félix *et al.*, 2020). Currently, there are 45 accepted species of *Bipolaris* and more than 105 of *Curvularia* (Marin Felix *et al.*, 2017; 2020; Bhunjun *et al.*, 2020).

These fungi cause different symptoms depending on the host grass species (Landschoot, 2021), and some signs and symptoms of different pathogens may be similar, making diagnoses difficult. There are also several pathogens causing a disease with one name, allowing confusion when referring to fungicide resistances (Stackhouse *et al.*, 2020). For example, turfgrass diseases related to leaf spots and leaf blights were formerly described as “Helminthosporium leaf spots and blights” or “Cochliobolus Diseases” (Nelson, 1992).

In Algeria, there is little information on occurrence of pathogens on cultivated grasses, and none on their presence in sports playing fields. For this reason, isolation and identification studies were carried out on the fungi found on symptomatic turfgrass at the Oran Olympic stadium. This research included pathogenicity tests to obtain basic data for development of effective disease management.

MATERIALS AND METHODS

Fungal isolates

Severe leaf blight and melting-out symptoms of turfgrass were observed in the Olympic stadium located in the Bir El Djir suburb of Oran, Algeria, during the summer of 2020. The turfgrass was composed by *Lolium perenne*, *Festuca rubra* and *Poa pratensis*. Suspected fungal causal agents were isolated from leaves, roots, stems, or seeds. Plant tissues were first immersed in water and then added to 2% sodium hypochlorite solutions for 2 min, followed by sterile distilled water for 5 min, and dried on sterilized paper towels. The tissue pieces were then placed onto potato carrot agar (PCA) or Czapek’s agar and incubated at room temperature (24–28°C). Isolations from rhizosphere soil were carried out by the dilution plate method. Rhizosphere soil was separated from roots using a brush and was collected in a Petri dish. Dried soil (1 g) was then added to 9 mL of distilled water and vortex-homogenized for 5 min, and 1 mL of the mixture was then transferred into test tubes each containing 9 mL of sterilized distilled water. This operation was repeated twice. A 100 µL volume of a 1:1000 soil dilution suspension was then spread on Czapek’s agar. Recovered fungi were examined using a stereo microscope, and fungal spores from mature colonies were transferred to PCA. Pure cultures of the fungi were prepared from hyphal tips. Fungus isolates were main-

tained on potato dextrose agar (PDA) slants at 4°C, and were preserved in 30% glycerol stock cultures in a deep freeze (-80°C) in the COMIC culture collection, Université d’Angers, France.

Morphology of isolated fungi

Microscopic features of 25 isolates (20 *Curvularia*, five *Bipolaris*), representing different morphological types, were examined by making direct mounts in 85% lactic acid from 5 to 12 d-old PCA cultures. Using a light microscope (Optika 190-B) and a calibrated micrometer, the lengths and width of approx. 50 conidia and 30 conidiophores of each isolate were assessed, together with other relevant morphological features. Preliminary identifications were made using the available literature (Sivanesan, 1987; Manamgoda *et al.*, 2012; Madrid *et al.*, 2014; Jeon *et al.*, 2015). Colony features were studied on PDA, PCA, Czapek’s agar and Malt extract agar (MEA), after growth at 25°C. Mycelial agar discs (5 mm diam.) were removed from edges of 6-d-old, actively growing cultures, and were inoculated centrally into 90 mm diam. agar plates each containing 15 mL of the respective media. The inoculated plates were kept in the dark at 4, 20, 25, 30, 35 or 40°C ($\pm 0.1^\circ\text{C}$) for 7 days. The resulting colony colours were determined as described in *Methuen Handbook of Colour* (Kornerup and Wanscher, 1978). Radial colony growth rates were determined for each representative isolate. Two measurements of each colony were made at right angles to each other, and treatments were replicated three times for each of the four culture media.

DNA extraction and PCR amplification from representative isolates

DNA was isolated from pure fungal cultures grown on PDA for 7 to 14 d, using the microwave method of Goodwin and Lee (1993). The *ITS rDNA* region, partial fragments of the glyceraldehyde-3-phosphate dehydrogenase (*gpd*) and the translation elongation factor 1- α (*tef1*) genes were amplified, respectively, using fungal primers ITS1 and ITS4 (White *et al.*, 1990), *gpd1-gpd2* (Berbee *et al.*, 1999), and EF1-983F-EF1-2218R (Rehner and Buckley, 2005). PCR amplifications of the extracted DNA (2 µL) was performed in a 50 µL reaction mixture containing: 75 mM Tris-HCl pH 9.0, 20 mM (NH₄)₂SO₄, 0.01% (w/v) Tween 20, 1.5 mM MgCl₂, 200 µM of each deoxyribonucleotide triphosphate, 1 unit of thermostable DNA polymerase (GoTaq, Promega), and 400 nM of each relevant oligonucleotide primer. The reactions

were conducted in a T100™ thermal cycler (Bio-Rad), and thermal cycling parameters were as described in the above references. After complete amplification, the PCR products were analyzed with gel electrophoresis, using 1.2% agarose gel in 0.5× TBE buffer and ethidium bromide (0.5 µg mL⁻¹) as the staining agent. Successful products were sequenced by GATC Company (Germany). The obtained sequences were deposited in GenBank and accession numbers assigned.

Phylogenetic analyses

DNA sequences of eleven isolates and of related species retrieved from GenBank were concatenated and aligned using the MUSCLE algorithm in MEGA 7 (Kumar *et al.*, 2016). Two datasets (sequences from *Curvularia* spp. or *Bipolaris* spp.) were made to perform separate phylogenetic analyses. The first set included five isolates pre-identified in *Bipolaris*, and in 34 *Bipolaris* species for which sequences at the three loci were available in GenBank. The second dataset included six isolates pre-identified in *Curvularia*, and in 98 *Curvularia* species for which sequences at the three loci were available in GenBank. Phylogenetic analyses were carried out using the maximum likelihood (ML) approach and IQTree v.1.6 software (Nguyen *et al.*, 2015). The best evolutionary history of the fungi for each dataset was calculated using ModelFinder (Kalyaanamoorthy *et al.*, 2017) and the Bayesian Information Criterion (BIC) selection procedure. The most suitable nucleotide substitution model for the “*Bipolaris*” dataset was TIM3 + F + I + G4, and for “*Curvularia*” was TIM2e + R4. The ML analyses were carried out with 1000 ultrafast bootstrap replicates, and only values above 70% were considered significant.

Pathogenicity tests

Pathogenicity of eleven morphologically distinct isolates was tested on potted turfgrass plants. Other isolates, including three of *Myrothecium*, one of *Fusarium* and one of *Acremonium*, were included to the tests for comparisons. A seed mixture (Rocalba®), containing 50% *Lolium perenne* (var. Jubilee), 35% *Festuca rubra rubra* (var. Relevant), and 15% *Poa pratensis* (var. Sunbeam) was sown into 10 cm diam. pots containing a 3:1 mixture of sterilized universal potting soil (Fertiplus®) and 25% sterilized sand. The pots with turfgrasses were maintained for 8 weeks in a greenhouse (nighttime 23–28°C, daytime 27–38°C). Each fungal isolate was grown on PCA for 14 d at room temperature. Conidia were removed from the surface of fungal colonies with 10 mL of sterile distilled

water using a sterile glass rod. A 15 mL conidium suspension adjusted to 10⁴ conidia mL⁻¹ was then inoculated onto each pot of turfgrass, using a laboratory atomizer. Three replicates were used for each isolate treatment. Control pots of turfgrass were sprayed with sterile distilled water. The inoculated plants were covered with polyethylene plastic bags for 48 h to maintain high relative humidity (80–92%), and the bags were opened every second day for a few hours. The proportions (%) of necrotic leaf area (n. l. a.) were calculated after visual rating at 7 and 14 d, using the 0 to 9 disease severity scale of Falloon (1976). The experiment was repeated once, and the results presented are the averages of the two repeats, each with three replicates. Re-isolations from inoculated plants were carried out on PCA medium as described above, and isolates were compared to original cultures, providing evidence for fulfilment of Koch’s postulates.

RESULTS

Foliar disease symptoms on the playing field in the Oran Olympic stadium were first observed at the beginning of July in the summer of 2020. Initially, symptomatic leaf blades appeared as off-colour and yellow, with dark brown to black spots. Symptoms extended downward from the tips of leaf blades and eventually blighted entire leaves, leading to irregular discoloured areas that later turned brown. By August, when temperatures ranged between 35 and 40°C, disease thinned the turf in large sections. Almost all the sampled plants showed two types of lesions characteristic of leaf blight and spot symptoms (Figure 1a). Leaf blight included elongated, large, brown/tan necroses generally on lower leaves of the infected plants (Figure 1 b and d), and leaf spots were small on leaf blades (Figure 1 e).

A total of 230 symptomatic samples were collected from damaged and healthy-appearing areas on borders and centre of the field. Numerous conidiophores and conidia were produced on lesions after 48 h of incubation on Czapek’s agar at room temperature (24–26°C) (Figure 1c). Through isolation and microscope observations, 214 of 320 fungal colonies recovered from infected plants were identified as *Curvularia* or *Bipolaris*. *Curvularia* was isolated at high incidence (combined mean data for leaves, stems and roots, 54%), an *Bipolaris* was recovered from crowns and leaves at lower frequency (3%). *Fusarium* spp. were co-isolated with *Curvularia* and *Bipolaris* spp., representing 31% of isolates. Several other fungi were also isolated from symptomatic turfgrass tissues, and were considered as either saprophytes or as minor pathogens. These included *Myrothecium*

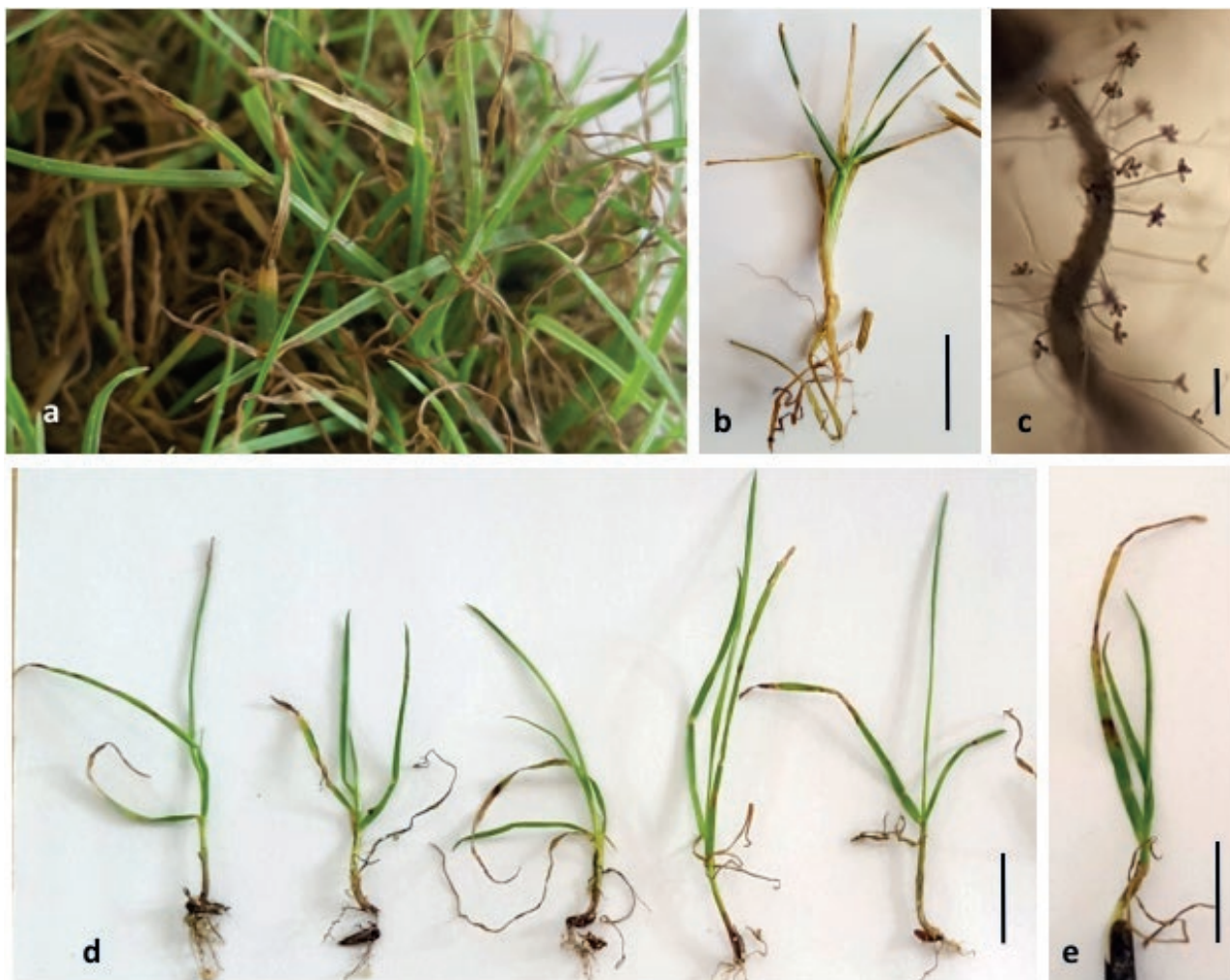


Figure 1. a, Leaf spot and melting out damage on field turfgrasses. b, tan to yellow crown and cut leaves. c, *Curvularia* conidia and conidiophores on dead leaves and stalks. d and e, black leaf spot and brown tip symptoms on naturally infected turfgrass. Scale bars: 50 µm (c); 10 mm (b, d and e).

spp., *Chaetomium* spp., *Penicillium* spp., *Trichoderma* spp. (10%), and *Acremonium* sp. (3%). All the fungi isolated from turfgrass rhizospheres were also isolated from aerial parts of turfgrass plants. Fewer *Bipolaris* spp. isolates were obtained from leaves, suggesting that the incubation temperature may have influenced their development and may have favoured proliferation of *Curvularia* spp. For this reason, growth assessments of different isolates were carried out on culture media under several different controlled temperatures.

Species identification

Twenty-five of 214 isolates with *Curvularia* and *Bipolaris* characteristics obtained from turfgrass tissues

(leaves, roots, crowns, or seeds) and rhizospheres were purified, and these pure culture isolates were further characterized (Tables 1 and 2). Micromorphological data showed a distinct variation among the isolates based on conidium length and width (23–86 µm × 10–22 µm; n = 1250). The number of septa ranged between three and eight. The isolates had straight to curved conidia with variable hila. The presence or absence of protuberant hila was dependent on the conidium age; the hila were conspicuous on old conidia but not on young conidia. Macro-morphological characterization (colony texture), showed little variation between cottony and velvety, and colony pattern was either glabrous or raised.

Isolates were classified into groups of close resemblance (Table 2), and 11 morphologically distinct isolates

Table 1. Details of the isolates used in this study, including GenBank accession numbers of the generated sequences of the ribosomal DNA region ITS, and the protein-coding genes *gpd* and *tef1*.

Isolate	Organ/ substrate	Species	GenBank accession numbers		
			ITS	<i>gpd</i>	<i>tef1</i>
NB838	Crown	<i>Bipolaris sorokiniana</i>	OP703618	OP709928	OP709939
NB839	Crown	<i>B. sorokiniana</i>	OP703619	OP709929	OP709940
NB840	Crown	<i>B. sorokiniana</i>	OP703620	OP709930	OP709941
NB841	Crown	<i>B. sorokiniana</i>	OP703621	OP709931	OP709942
NB842	Crown	<i>B. sorokiniana</i>	OP703622	OP709932	OP709943
NB843	Crown	<i>Curvularia spicifera</i>	OP703625	OP709933	OP709944
NB844	Crown	<i>C. spicifera</i>	OP703626	OP709934	OP709945
NB851	Leaf	<i>Curvularia</i> sp.	NA	NA	NA
NB853	Root	<i>Curvularia</i> sp.	NA	NA	NA
NB855	Rhizosphere	<i>Curvularia</i> sp.	OP703627	OP709935	OP709946
NB860	Leaf	<i>Myrothecium</i> sp.	NA	NA	NA
NB861	Leaf	<i>Myrothecium</i> sp.	NA	NA	NA
NB862	Leaf	<i>Myrothecium</i> sp.	NA	NA	NA
NB864	Leaf	<i>C. verruculosa</i>	OP703628	OP709936	OP709947
NB865	Leaf	<i>Curvularia</i> sp.	NA	NA	NA
NB866	Leaf	<i>Curvularia</i> sp.	NA	NA	NA
NB867	Leaf	<i>Curvularia</i> sp.	NA	NA	NA
NB870	Leaf	<i>Acremonium</i> sp.	NA	NA	NA
NB871	Root	<i>C. geniculata</i>	OP703629	OP709937	OP709948
NB872	Root	<i>Curvularia</i> sp.	NA	NA	NA
NB873	Root	<i>Curvularia</i> sp.	NA	NA	NA
NB874	Root	<i>Curvularia</i> sp.	OP703630	OP709938	OP709949
NB875	Leaf	<i>Fusarium</i> sp.	NA	NA	NA
NB876	Leaf	<i>Curvularia</i> sp.	NA	NA	NA
NB877	Leaf	<i>Curvularia</i> sp.	NA	NA	NA
NB878	Leaf	<i>Curvularia</i> sp.	NA	NA	NA
NB879	Leaf	<i>Curvularia</i> sp.	NA	NA	NA
NB880	Leaf	<i>Curvularia</i> sp.	NA	NA	NA
NB883	Seed	<i>Curvularia</i> sp.	NA	NA	NA
NB884	Seed	<i>Curvularia</i> sp.	NA	NA	NA

were selected among the groups for further molecular characterization. A phylogenetic tree from the combined dataset of ITS rDNA, *tef1* and *gpd* sequences indicated more precise relationships and similarities with related sequences from recognized species within *Bipolaris* (Figure 2) and *Curvularia* (Figure 3).

Based on the combination of morphological characteristics and sequence data, six different lineages were distinguished, including *Bipolaris sorokiniana*, *Curvularia spicifera*, *C. verruculosa*, *C. geniculata* and two *Curvularia* spp., one related to *C. verruculosa* and the other to *C. mossaddeghii*. From available literature, *C. verruculosa* and *C. geniculata* are new records for fungi of Algeria. These species are described below, in alphabetic order.

Bipolaris sorokiniana (Sorokin) Shoemaker 1959

Five isolates (NB838, NB839, NB840, NB841, and NB842) exhibited similar colony morphology and colour. Colonies on PDA were velvety and radially creased, reaching 46.9 ± 7.5 mm diam. after 7 d, olive brown (4D4/4E7), with fluffy white mycelium and irregular white margins (Figure 4 a); reverse yellowish brown (5F4). Sporulation sparse until hyphae disturbed. Abundant, elevated aerial hyphae around colony margins and sparse aerial hyphae at colony centres were observed upon aging. On PCA, cottony, 68.5 ± 9.3 mm diam., olive (3D3) to olive brown (4D3), with abundant aerial mycelium with grayish surfaces and sometimes white patches (Figure 4 b); reverse olive brown (4D4/4F7). Colonies on Czapek's agar were velvety, 76.9 ± 3.4 mm diam., grayish yellow (4C7) to olive brown (4E6/

Table 2. Morphological characteristics of *Bipolaris* and *Curvularia* isolates obtained from turfgrass.

Isolate	Colony colour ^a	Conidium ^b				Conidiophore ^b				Molecular identification
		Mean length (µm) x ± SD	Mean width (µm) x ± SD	Septation	Shape	Mean length (µm) x ± SD	Mean width (µm) x ± SD	Septation		
NB838		86.3 ± 4.9	21.9 ± 1.4	4-8		81.5 ± 15.4	7.1 ± 0.6	2.0-6	<i>B. sorokiniana</i>	
NB842		67.9 ± 5.9	21.4 ± 1.4	3-8		75.4 ± 16.3	6.8 ± 0.5	2.0-6	<i>B. sorokiniana</i>	
NB841	Grayish yellow (4C7) to olive brown (4E6/ 4D7)	64.3 ± 5.4	20.4 ± 1.5	5-8	Straight. ellipsoidal to cylindrical	87.1 ± 25.8	7.1 ± 0.5	2.0-8	<i>B. sorokiniana</i>	
NB840		66.7 ± 4.4	20.9 ± 1.1	4-7		113.5 ± 35.8	7.9 ± 0.6	2.0-9	<i>B. sorokiniana</i>	
NB839		81.0 ± 7.0	22.9 ± 1.5	6-8		58.0 ± 12.3	6.9 ± 0.7	1.0-4	<i>B. sorokiniana</i>	
NB844	Brownish orange (5C4/6B3)	29.9 ± 3.8	10.0 ± 0.8	3-4.0	Straight. obovoid to ellipsoidal	67.6 ± 15.0	5.6 ± 0.4	4.0-9	<i>C. spicifera</i>	
NB843		31.9 ± 0.8	10.3 ± 3.0	3-4.0		75.6 ± 17.5	5.4 ± 0.6	5.0-10	<i>C. spicifera</i>	
NB866		30.5 ± 2.4	12.1 ± 1.2	3		89.2 ± 20.2	5.8 ± 1.0	3.0-8	ND	
NB864	Olive (3E7/3F6) or Light brown (6D4)	25.6 ± 2.0	10.3 ± 0.9	3	Ellipsoidal. unequal sided. straight to slightly curved	122.8 ± 22.2	5.9 ± 0.6	5.0-12	<i>C. verruculosa</i>	
NB873		30.4 ± 2.0	12.0 ± 1.0	3		107.5 ± 25.1	5.5 ± 0.9	4.0-12	ND	
NB878		30.9 ± 3.0	12.0 ± 1.0	3		165.8 ± 84.9	4.9 ± 0.7	6.0-28	ND	
NB874	Olive (2E2/ 2F3) or olive yellow (3C7/ 3 8D)	23.0 ± 1.2	12.2 ± 0.8	3	Ovoid. distinctly curved and ellipsoidal	130.7 ± 25.6	5.0 ± 0.2	6.0-12	<i>Curvularia</i> sp.	
NB853		23.7 ± 1.9	11.5 ± 0.7	3		120.7 ± 29.2	4.2 ± 0.5	5.0-11	ND	
NB884		28.0 ± 3.0	12.3 ± 0.8	3		96.7 ± 17.2	4.6 ± 0.6	4.0-10	ND	
NB867		34.0 ± 6.8	10.4 ± 1.2	(3) 4 (5) (6)		61.6 ± 29.0	4.2 ± 0.6	3.0-10	ND	
NB876	Grayish orange (5B3) to Light brown (6D6)	32.9 ± 3.4	10.3 ± 0.8	4 (5)	Ellipsoidal. slightly curved	76.7 ± 14.7	4.5 ± 0.6	3.0-8	ND	
NB871		35.4 ± 5.0	11.2 ± 0.8	4 (5-6)		79.4 ± 21.1	4.2 ± 0.5	4.0-10	<i>C. geniculata</i>	
NB872		30.0 ± 2.3	10.7 ± 0.9	(3) 4 (5)		98.5 ± 25.5	4.8 ± 0.4	4.0-12	ND	
NB877		26.8 ± 2.1	12.0 ± 1.3	3	Distinctly curved	78.5 ± 12.2	5.0 ± 0.0	3.0-6	ND	
NB880		27.9 ± 1.7	13.3 ± 1.1	3		128.1 ± 39.6	4.8 ± 0.4	4.0-11	ND	
NB879	Light brown (6D5) to olive brown (4D5 / 4D6)	30.1 ± 2.7	11.3 ± 1.0	3	Ellipsoidal to ovoid. straight to slightly curved	61.5 ± 18.8	4.8 ± 0.5	3.0-7	ND	
NB883		26.6 ± 1.3	12.1 ± 1.0	3		156.7 ± 46.5	5.1 ± 0.4	5.0-17	ND	
NB855		26.0 ± 2.3	12.0 ± 1.0	3 (4)		134.9 ± 38.1	5.2 ± 0.4	4.0-13	<i>Curvularia</i> sp.	
NB851		24.9 ± 1.9	11.1 ± 1.0	3 (5)		105.6 ± 30.2	4.9 ± 0.6	5.0-14	ND	
NB865		27.0 ± 2.0	12.3 ± 0.9	3		126.6 ± 39.4	5.7 ± 0.7	4.0-21	ND	

^a: Characteristics on Czapek's agar. ^b: Microscopic features on PCA; ND, not determined.

4D7) (Figure 4 c), reverse same colour. On MEA, colony diam. 32.7 ± 6.3 mm, with cottony dense white margins; other characteristics same as PDA (Figure 4d). Conidiophores were simple, rarely branched, septate, (40) 83–201 μ m long and 6–8 μ m thick, pale to medium brown, occasionally with series of 2–4 geniculate, sympodial proliferations, bearing 1–3 conidia. Conidia formed singly at the tips of conidiogenous cells, and were pale to dark brown, mostly straight, ellipsoidal to cylindrical, rounded at the bases and apices, mostly with 5–6 (8) transverse septa, smooth walled, (47) 64–86 (98) μ m long and (15) 21–27 μ m wide (Figure 4, e to h). Germination was observed

from only one distal cell on each conidium (Figure 3 g). Microconidiation was rarely observed, and these were hyaline, spherical cells at the extremities of conidia. Sexual morph not observed. Conidiophores emerging from the surfaces of dead infected plants, were rigid, brown, clustered or scattered, each with three conidiogenous loci, 77–143 μ m long and 7–10 μ m wide (Figure 4, h and i). Most conidia had 6–8 transverse septa, 65–75 μ m. Other morphologies were as for growth on PCA.

Curvularia geniculata (Tracy & Earle) Boedijn 1933

Isolate NB871 formed velvety colonies on PDA, reach-



Figure 2. Phylogenetic tree reconstructed using the maximum likelihood method, from the alignment of *ITS rDNA*, *gpd* and *tef1* sequences of *Bipolaris* isolates. The tree was rooted with *Curvularia verruculosa* CBS 150.63. Bootstrap support values greater than 0.7 are indicated by arrows near nodes. The scale bar indicates the expected number of substitutions per position.

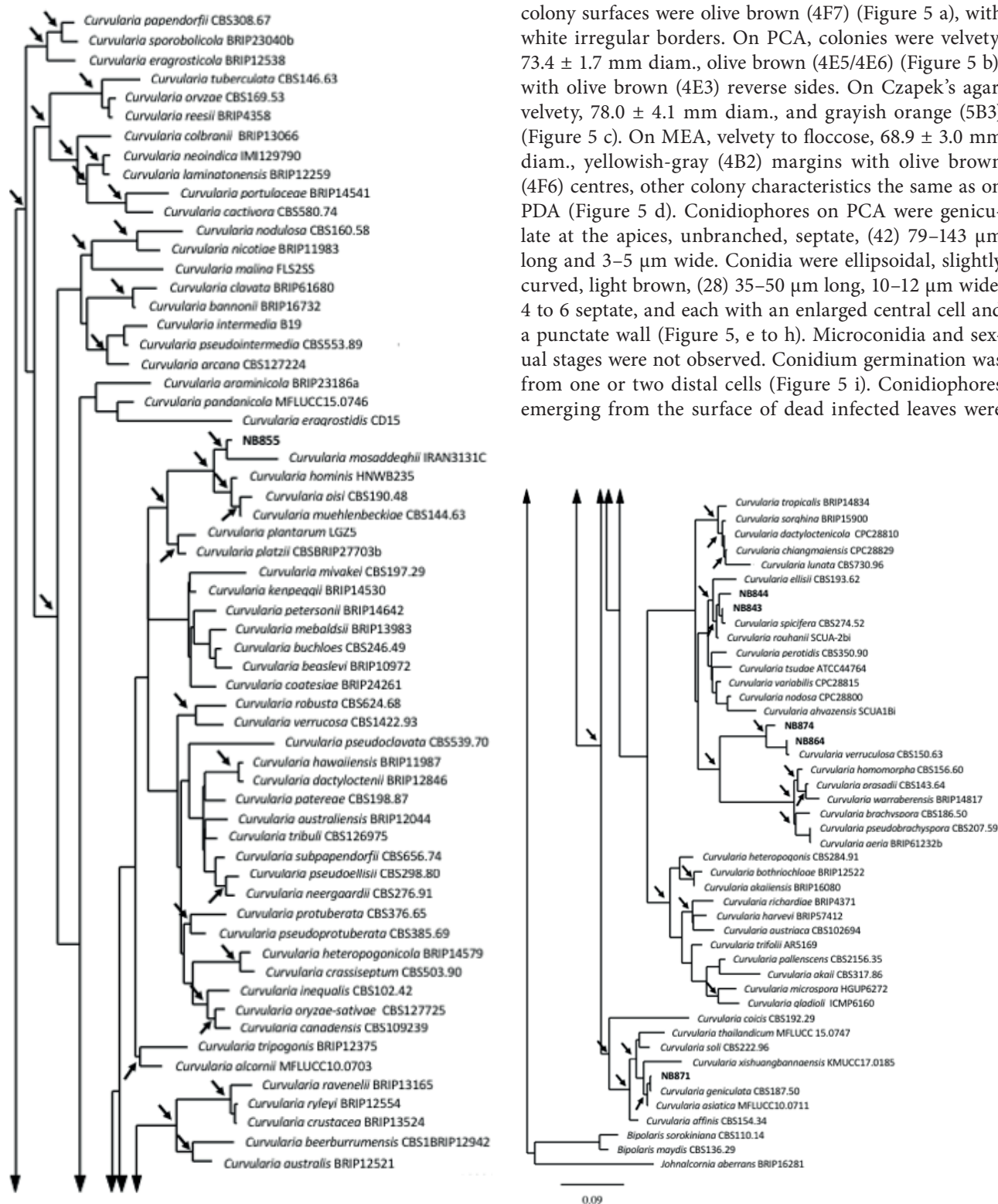


Figure 3. Phylogenetic tree reconstructed using the maximum likelihood method, from the alignment of *ITS rDNA*, *gpd* and *tef1* sequences of *Curvularia* isolates. The tree was rooted with *Bipolaris* and *Johnalcornia* spp. Bootstrap support values greater than 0.7 are indicated by arrows near nodes. The scale bar indicates the expected number of substitutions per position.

ing 56.9 ± 2.8 mm diam., after 7 d at 25°C. The upper colony surfaces were olive brown (4F7) (Figure 5 a), with white irregular borders. On PCA, colonies were velvety, 73.4 ± 1.7 mm diam., olive brown (4E5/4E6) (Figure 5 b), with olive brown (4E3) reverse sides. On Czapek's agar, velvety, 78.0 ± 4.1 mm diam., and grayish orange (5B3) (Figure 5 c). On MEA, velvety to floccose, 68.9 ± 3.0 mm diam., yellowish-gray (4B2) margins with olive brown (4F6) centres, other colony characteristics the same as on PDA (Figure 5 d). Conidiophores on PCA were geniculate at the apices, unbranched, septate, (42) 79–143 μ m long and 3–5 μ m wide. Conidia were ellipsoidal, slightly curved, light brown, (28) 35–50 μ m long, 10–12 μ m wide, 4 to 6 septate, and each with an enlarged central cell and a punctate wall (Figure 5, e to h). Microconidia and sexual stages were not observed. Conidium germination was from one or two distal cells (Figure 5 i). Conidiophores emerging from the surface of dead infected leaves were

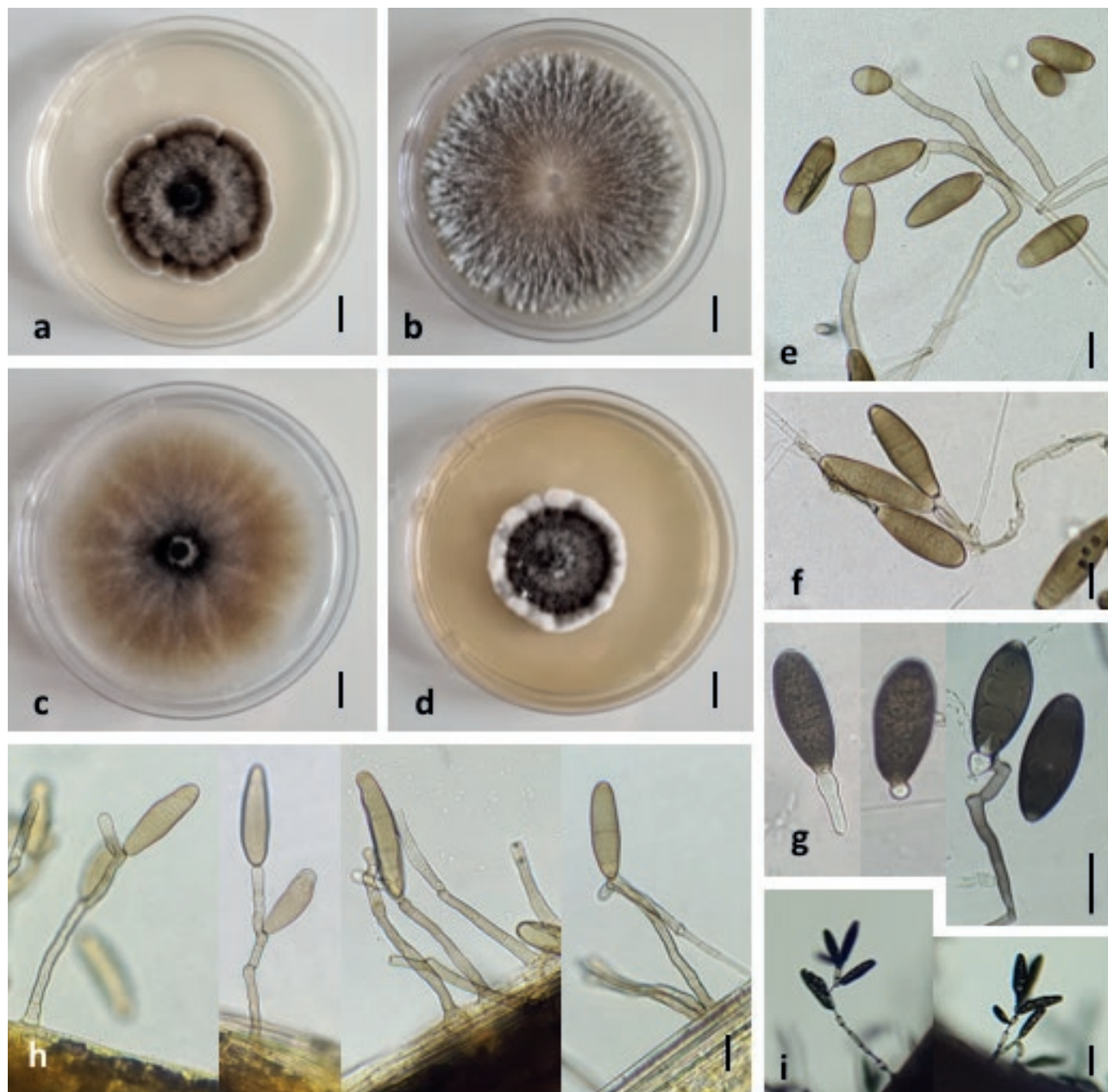


Figure 4. *Bipolaris sorokiniana*. Colony on: a, PDA, b, PCA, c, Czapek's agar, d, MEA. e and f, conidiophores and conidia on PCA. g, germinating conidia. h, conidiophores and conidia produced on leaf host. i, conidiophore proliferation on host tissue 21 days after inoculation. Scale bars: 10mm (a to d); 25 μ m (e to h); 50 μ m (i).

rigid, brown, scattered, each with 3–7 (15) conidiogenous loci, 67–99 (133) μ m long and 3.8–5.5 μ m wide (Figure 5 j). Most conidia had 4–5 transverse septa, were 33–44 μ m long and 9–13 μ m wide. Hila were not protuberant.

Curvularia spicifera (Bainier) Boedijn 1933

Colonies of two isolates (NB843, NB844), were velvety with cottony centres, 56.6 \pm 1.1 mm diam. after 7 d at

25°C, irregular, olive brown (4F7), and slightly white at the margins (Figure 6 a), sporulating abundantly when grown on PDA at 25°C; reverse sides yellowish brown (5F4). Colonies on PCA were velvety to floccose and olive (3F3/ 3F7), 65.4 \pm 2.2 mm diam. (Figure 6b). On Czapek's agar, velvety with glabrous irregular margins, 65.4 \pm 4.8 mm diam., brownish to grayish orange (5C4/6B3) (Figure 6 c); reverse sides same color. On

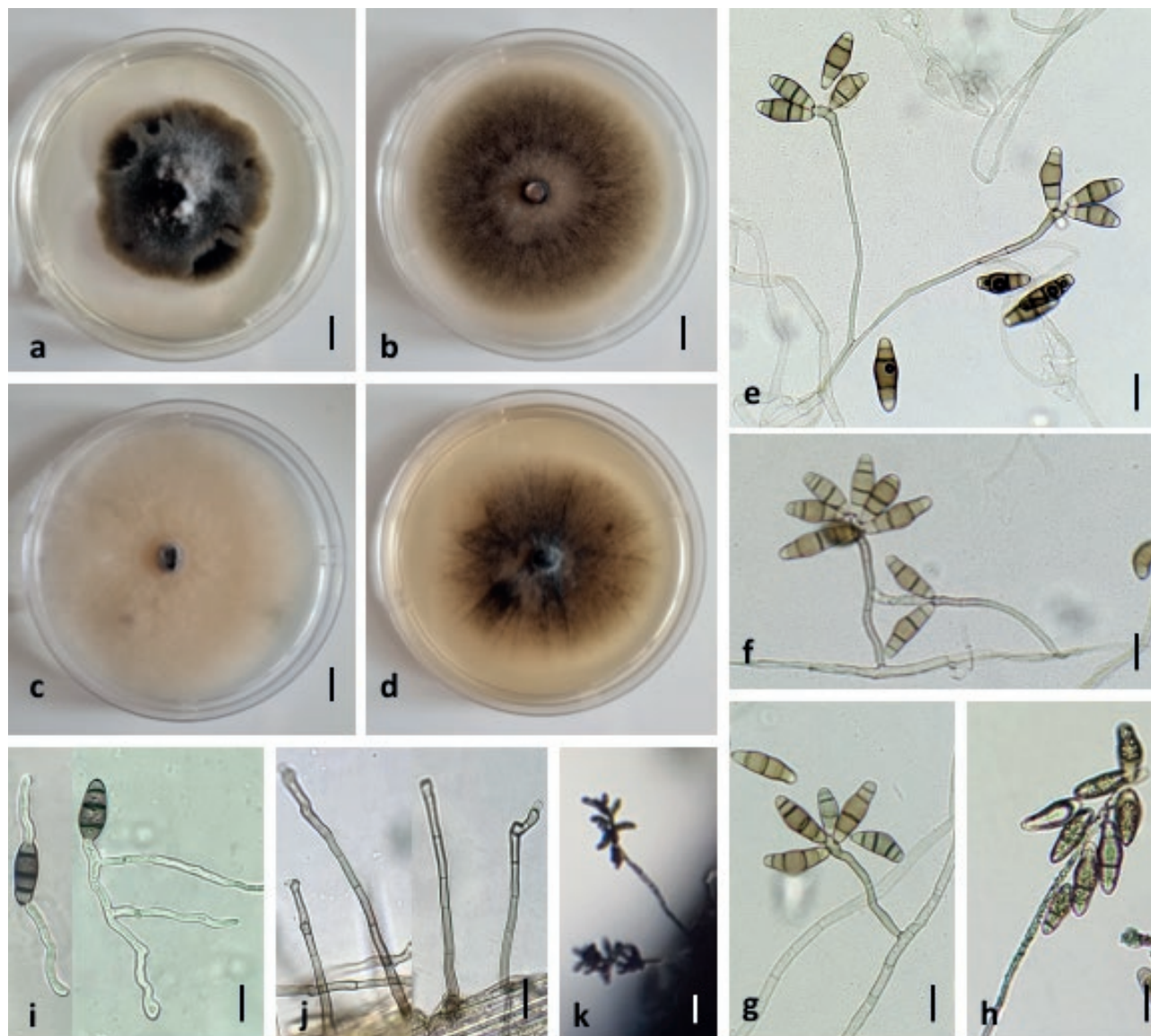


Figure 5. *Curvularia geniculata* (NB871). Colony on: **a**, PDA, **b**, PCA, **c**, Czapek's agar, **d**, MEA. **e–g**, conidiophores and conidia on PCA. **h**, conidia and conidiophore ornamentation. **i**, conidia germination. **j** and **k**, conidiophores and sporulation pattern on leaf host 21 days after inoculation. Scale bars 10 mm (**a** to **d**); 25 μ m (**e–j**); 50 μ m (**k**).

MEA, cottony compact, 58.4 ± 1.3 mm diam., grayish green (27F5) with dull green (27D3) margins (Figure 6 d), reverse sides yellowish brown (5E5/ 5F4). Conidiophores on PCA were erect, mostly straight, rarely geniculate in the upper parts, (42) 71–120 long \times 4–6 μ m wide, brown at the base, paler towards the apices, septate with cell walls thicker than those of vegetative hyphae. Conidiogenous cells were integrated, terminal or intercalary, with sympodial proliferations (15–25), pale brown to brown, with darkened scars (Figure 6 e and k). Conidia obovoid to ellipsoid, straight, (23) 30–40

μ m long and 8–12 μ m wide, terminal cells usually light brown at the apices, third cells often more swollen, 3 distoseptate with punctate cell walls (Figure 6 g); hila not protuberant. Sexual morph not observed. Microconidiation was observed as forming hyaline, spherical cells at the ends of phragmoconidia (Figure 6, f to j). Conidiophores emerging from the surfaces of dead infected leaves, rigid, brown, scattered, with 3–7 (15) conidiogenous loci, 67–99 (133) μ m long and 3.8–5.5 μ m wide. Most conidia with 4–5 transverse septa were 33–44 μ m long and 9–13 μ m wide (Figure 6, h and i).

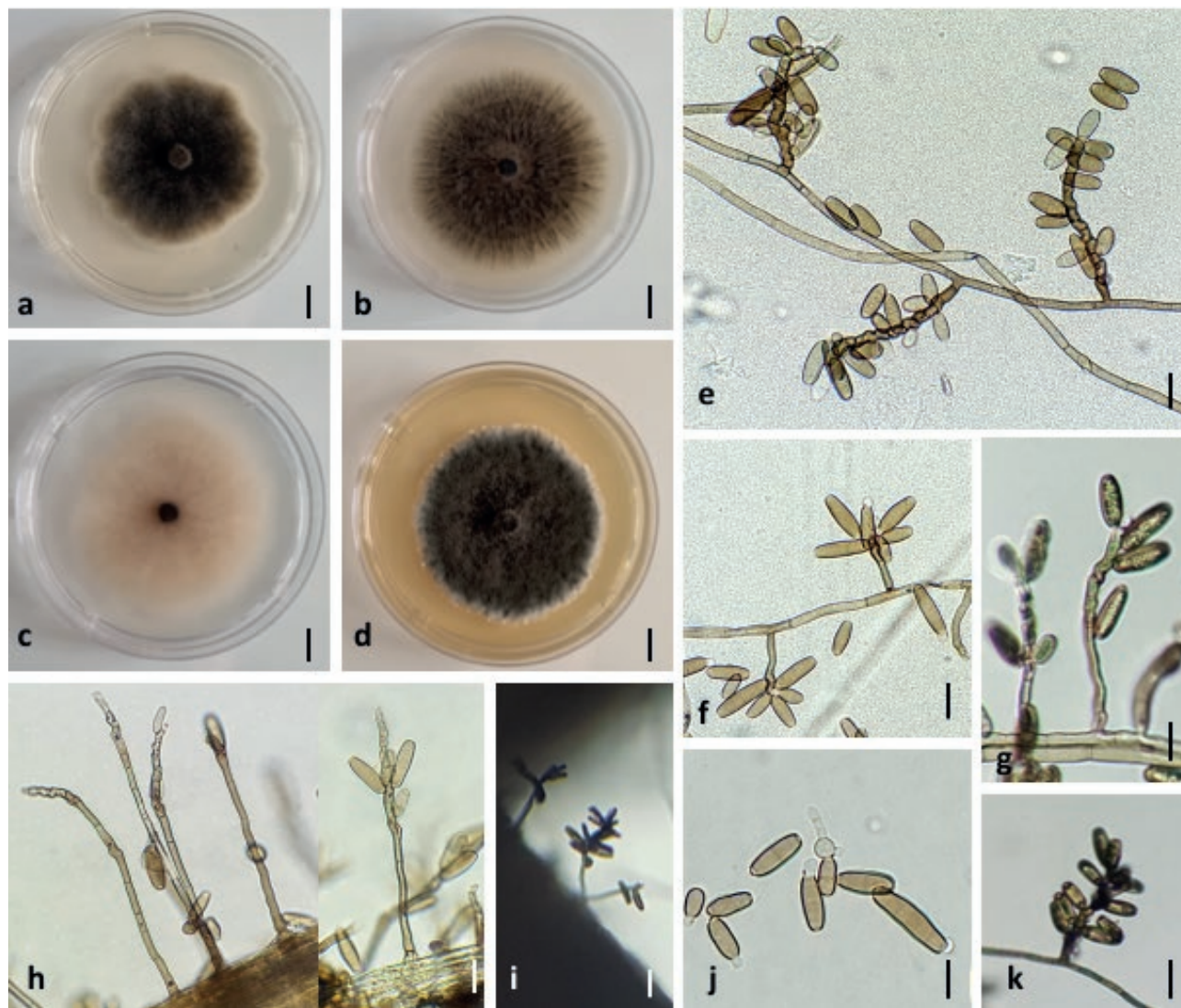


Figure 6. *Curvularia spicifera*. Colony on: **a**, PDA, **b**, PCA, **c**, Czapek's agar, **d**, MEA. **e**, conidiophores, conidiogenous cells and conidia on PCA. **f** and **j**, microconidiation and conidia germination. **g**, conidia ornamentation. **h** and **i**, conidiophores and conidia on leaf host. **k**, sporulation pattern on center of 7 days PCA colony. Scale bars: 10 mm (**a** to **d**); 25 μ m (**e**, **f**, **g**, **h** and **j**); 50 μ m (**i** and **k**).

Curvularia verruculosa Tandon & Bilgrami ex M.B. Ellis 1962

Isolate NB864 produced powdery colonies that developed gentle radial folds as they aged, reaching 34.8 ± 2.2 mm diam. after 7 d at 25°C on PDA (Figure 7 a); reverse sides olive brown (4F8). On PCA, glabrous to velvety, flattened olive (3F6), 71.5 ± 1.3 mm diam. (Figure 7 b), and reverse sides olive (3F3). On Czapek's agar, glabrous with irregular margins, 59.8 ± 1.3 mm diam., olive (3E7/3F6) (Figure 7 c); reverse sides same colour. On MEA, 35 ± 0.7 mm diam., grayish green (28E4/ 28F6), reverse sides brownish gray (6F2), other characteristics as on PDA (Figure 7 d). Conidiophores on PCA were septate, simple but rarely

branched, erect or curved, pale, geniculate close to the apices, thick-walled, (85) 122 to 155 μ m long and 5 to 6 μ m wide. Conidia were each ellipsoidal, unequal sided, straight to slightly curved, three-septate, rounded at both ends, with a rough verrucose wall, (21) 25–30 μ m long and (8) 10–12 μ m wide, light to dark brown, the subterminal third cell larger and darker than other cells (Figure 7, e and f). Microconidial and sexual stages were not observed. Germination was from two distal cells (Figure 7 g). Conidiophores emerged from the surfaces of dead infected leaves, and were rigid, brown, clustered, with 4–15 conidiogenous loci, 134–268 μ m long and 6–10 μ m wide (Figure 7 i). Most conidia with 2–3 transverse septa,

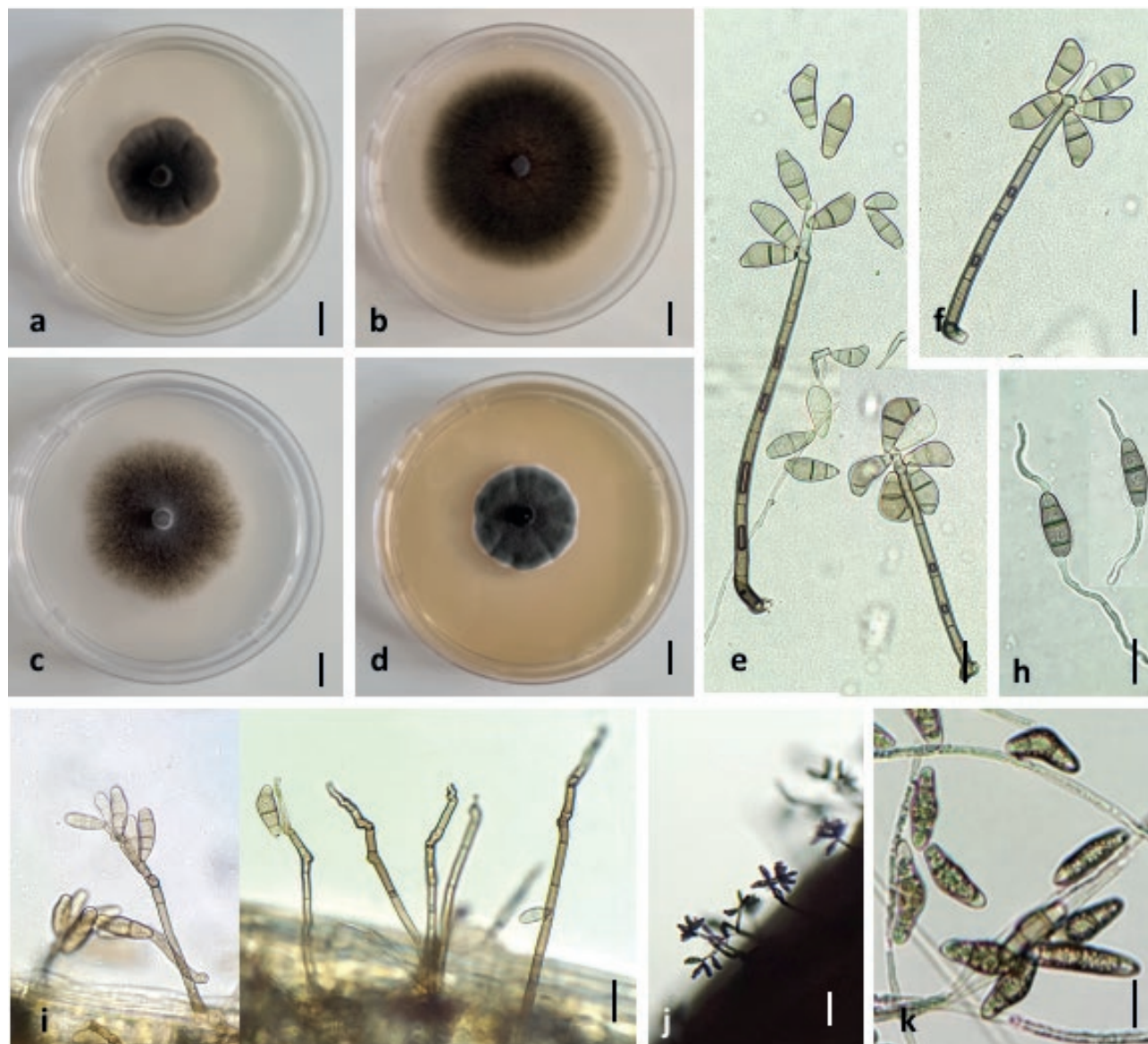


Figure 7. *Curvularia verruculosa* (NB864). Colony on: **a**, PDA, **b**, PCA, **c**, Czapek's agar, **d**, MEA. **e** and **f**, conidiophores, conidia and sporulation pattern on PCA. **g**, conidia germination, **h**, conidiophores and conidia formed on leaf host. **i** and **j**, sporulation on leaf host. **k**, conidia and hypha ornamentation. Scale bars 10 mm (**a** to **d**); 25 μ m (**e**, **f**, **h**, **i**, **j** and **k**); 50 μ m (**g**).

27–38 μ m long and 11–15 μ m wide. Hila not protuberant. The conidium terminal cells were paler and less verrucose than the central cells (Figure 7 k).

Curvularia spp. morphological group IV

One isolate (NB874) formed olive brown (4E5), velvety to powdery and folded colonies on PDA. reaching 66.5 ± 1.7 mm diam. after 7 d at 25°C. The colonies were circular, gray at the centres (3B2), effuse and white (3B1) towards the periphery, with fimbriate margins (Figure 8 a); reverse sides olive brown (4F8/ 4E3). On PCA, $71.5 \pm$

1.3 mm diam., olive (3F4), velvety (Figure 8 b); reverse sides olive (3F4) to olive gray (3E2). On Czapek's agar, glabrous with velvety centres, 44.8 ± 1.7 mm diam., olive (2E2/2F3) (Figure 8 c); reverse sides the same colour. On MEA, 73.8 ± 0.5 mm diam., and colony characteristics as on PDA (Figure 8 d). Conidiophores on PCA usually simple, straight or slightly geniculate, brown, with cell walls often thicker than those of the vegetative hyphae, (85) 130–193 μ m long and 4–5 μ m wide. Conidiogenous cells intercalary, polytretic, proliferating sympodially (Figure 8, e and f), slightly swollen. Conidia ovoid, ellip-

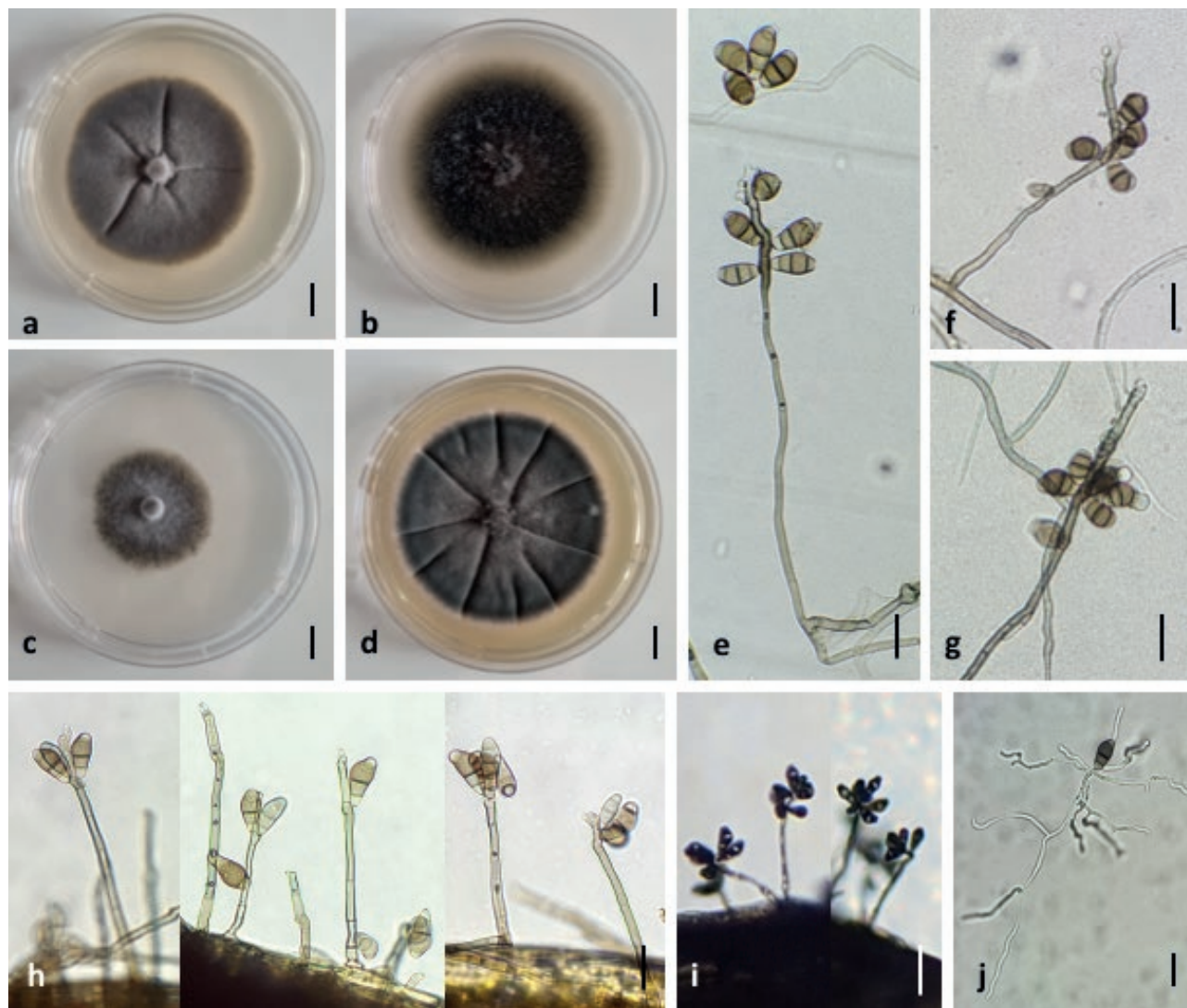


Figure 8. *Curvularia* sp. morphotype group IV (NB874). Colony on: **a**, PDA, **b**, PCA, **c**, Czapek's agar, **d**, MEA. **e** and **f**, conidiophores, conidiogenous cells and conidia on PCA. **g**, microconidiation. **h**, conidia and conidiophores on leaf host. **i**, sporulation pattern on leaf host 21 days after inoculation. **j**, conidium germination. Scale bars 10 mm (**a** to **d**); 25 μ m (**e**, **f**, **g**, **h** and **j**); 50 μ m (**i**).

tical, smooth-walled and curved at the subterminal cells, three septate, four celled, 20–25 μ m long and 10–13 μ m wide, brown, with each third cell unequally sided and larger than the others, apical and basal cells subhyaline. Hila non-protruding. Microconidiation observed, forming pale brown, globose cells at the upper parts of conidia (Figure 8 g). Sexual morph not observed. Conidiophores emerging from the surfaces of dead infected leaves, rigid, brown, scattered, with 2–5 conidiogenous loci, 105–288 μ m long and 5–7 μ m wide. Most of conidia with 3 transverse septa were 27–33 μ m long and 10–15 μ m wide (Figure 8, h and i). Germination was observed from one or two distal cells of conidia (Figure 8 j). Hila were protuberant on mature conidia. Based on the mul-

tilocus phylogeny, this isolate was strongly related to *C. verruculosa* but was significantly separated from this species. *gpd* and *ITS rDNA* sequences were similar to that of *C. americana*, but no *tef1* sequence is available for this species in GenBank.

***Curvularia* spp. morphological group VI**

Isolate NB855 had velvety, olive brown (4E5) with grayish beige (4C3) colony surfaces, which were 77.3 ± 1.7 mm diam. on PDA after 7 d at 25°C (Figure 9 a). The periphery of each colony was floccose and olive with a fimbriate margin; reverse sides olive brown (4F5). Colonies on PCA were funiculose, olive (3F5), and were 76 ± 0.8 mm diam. (Figure 9 b), with reverse sides olive (3F4).

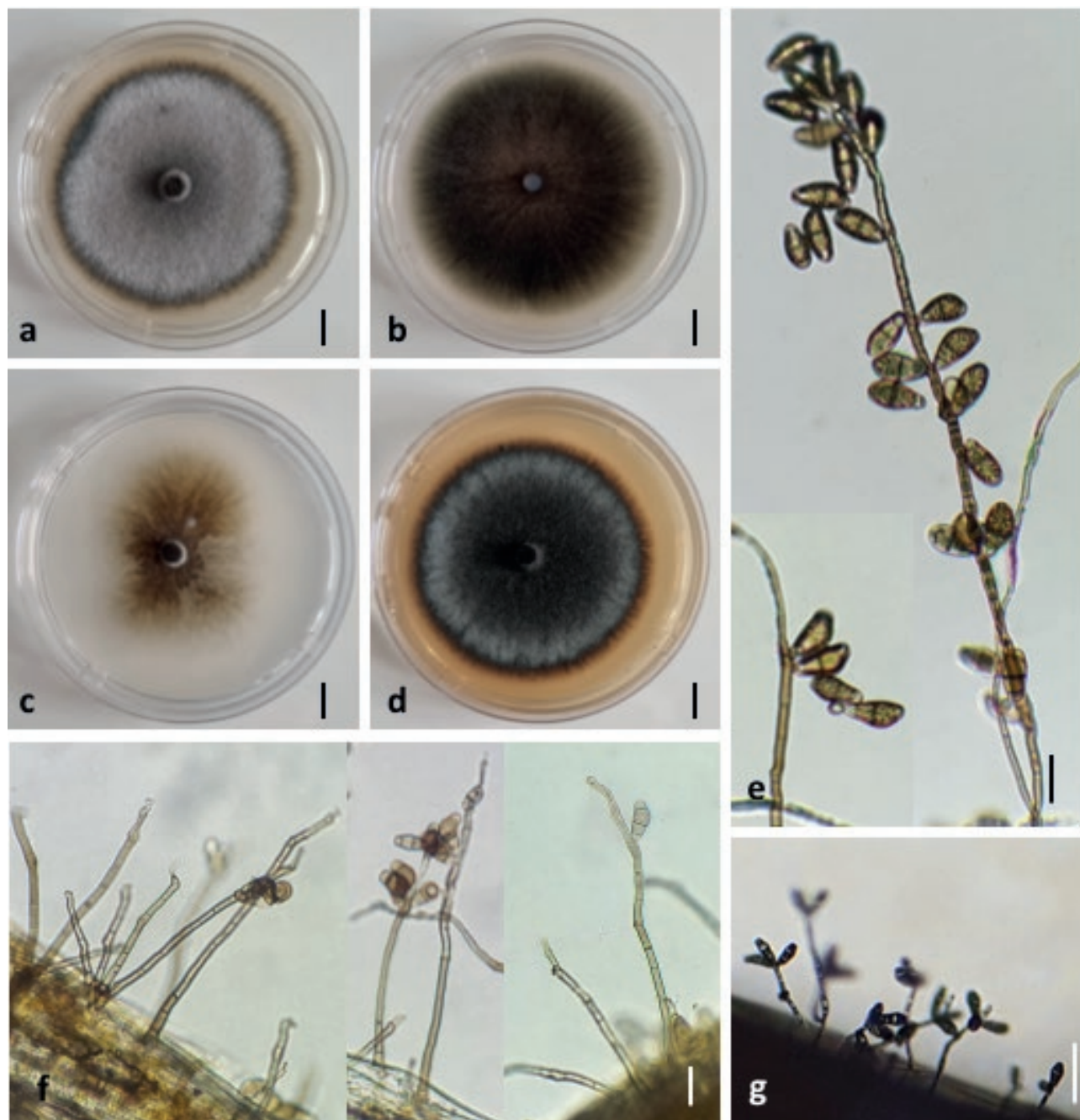


Figure 9. *Curvularia* sp. morphotype group VI (NB855). Colony on: a, PDA, b, PCA, c, Czapek's agar, d, MEA. e, Conidiophores and conidia ornamentation on PCA. f, conidia and conidiophores on leaf host. g, sporulation pattern on leaf host 21 days after inoculation. Scale bars 10mm (a to d); 25µm (e-f); 50µm (g).

On Czapek's agar, glabrous, and olive brown (4D5/4D6) with irregular transparent margins, and 67.8 ± 3.8 mm diam. (Figure 9 c); reverse sides same colour. On MEA, 72.8 ± 0.5 mm diam., brownish gray (5D2) centres and yellowish brown (5F5) margins (Figure 9 d), and other characteristics same as on PDA. Conidiophores on PCA

were simple or branched, geniculate towards the apices, brown, septate, with cell walls thicker than those of the vegetative hyphae, (78) $135\text{--}263$ µm long and $5\text{--}6$ µm wide. Conidiogenous cells intercalary, polytretic, proliferating sympodially, subcylindrical to irregular with dark conidiogenous loci. Conidia ellipsoid to ovoid,

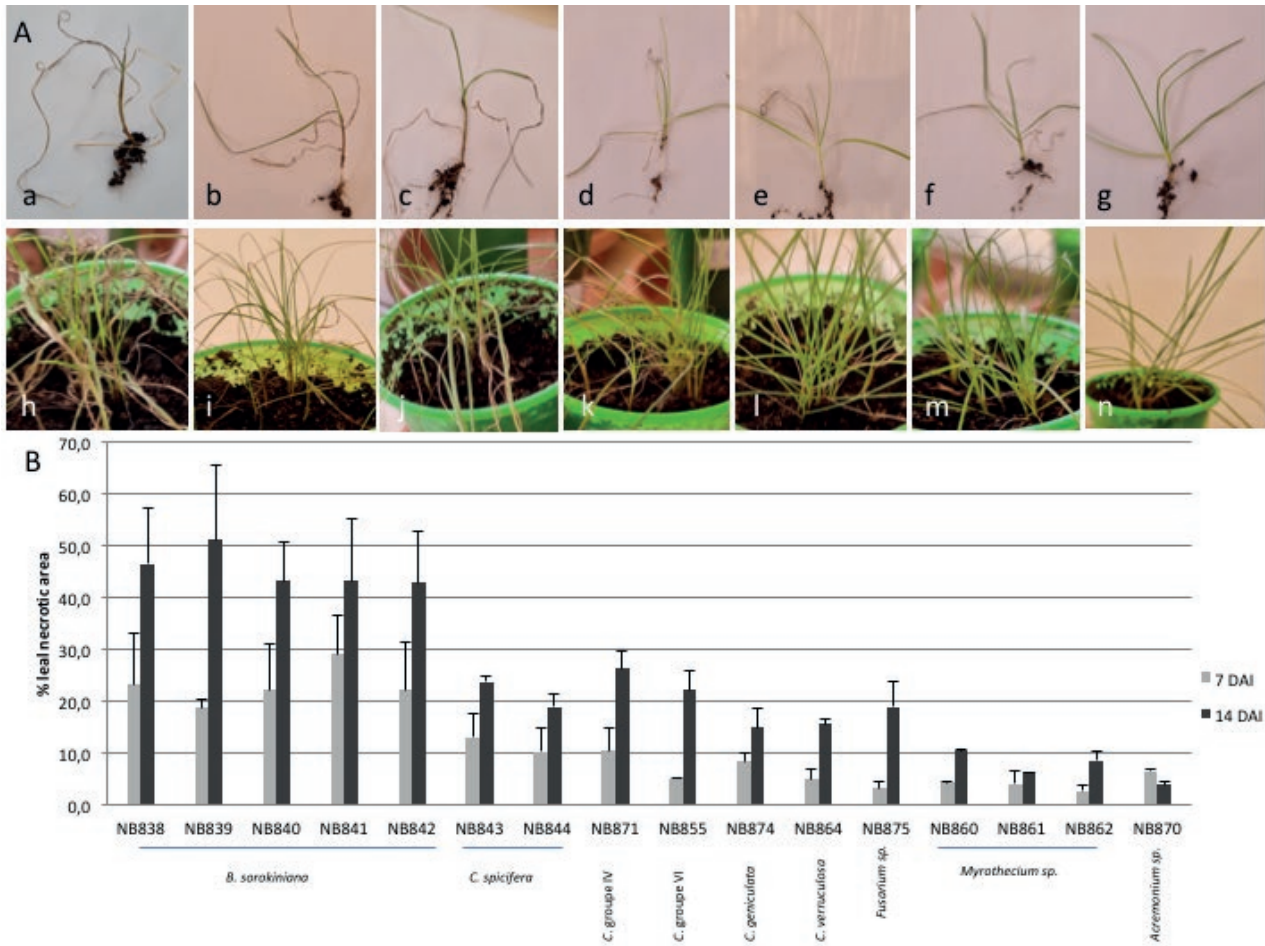


Figure 10. A, leaf spot and blight symptoms on six-week-old turfgrass leaves under greenhouse conditions 14 days after inoculation with: a and h, *Bipolaris sorokiniana* (NB840), b and i, *C. spicifera* (NB843), c and j, *C. geniculata* (NB871), d and k, *Curvularia* group IV (NB874), e and l, *Curvularia* group VI (NB855), f and m, *C. verruculosa* (NB864). g and n, negative control. B, percentage of leaf necrotic area recorded at 7 and 14 DAI on potted turfgrass.

straight to slightly curved, (21) 26–30 μm long and (10) 12–14 μm wide, 3–4 celled, each with the third intermediate cells usually verruculose and darker than the others, brown, and apical and basal cells pale brown (Figure 9 e). Microconidial and sexual stages were not observed. Conidiophores emerging from the surfaces of dead infected leaves, rigid, brown, scattered or clustered, with 3–11 conidiogenous loci, 87–150 (188) μm long and 5–8 μm wide (Figure 9, f and g). Most conidia with 3 transverse septa, 22–30 μm long and 8–14 μm wide. Hila sometimes slightly protuberant. The multilocus phylogeny showed that this strain grouped closely to *C. mosad-deghii*, but formed a separate branch.

Three *Curvularia* isolates (NB869, NB873, and NB877) produced sexual morphs on PDA after 4 weeks at 20°C. Sterile ascomata were solitary or arising in

groups, immersed or erumpent, dark brown or black, and were 600–950 (1050) μm long and 200–400 (550) μm wide, thick-walled, surrounded by hyphae and conidiophores arising in groups from the bodies and necks. The internal cells were angular to globose, and hyaline.

Colony radial growth assessments at different temperatures for representative isolates from each of the six morphological groups showed that the optimum temperature ranges of *B. sorokiniana* were 25–30°C, but *C. spicifera* and *Curvularia* group IV grew most rapidly between 25 and 35°C. The other morphological groups had maximum growth at 30°C. *Curvularia* morphotype group VI strain NB855 displayed more rapid growth than other species groups. None of the isolates exhibited radial growth at 4°C after 7 d incubation. At 40°C, mycelial growth was less rapid than at the other temperatures for all the assessed isolates.

Pathogenicity assessments

Under greenhouse conditions, turfgrass plants inoculated with *Curvularia* spp. and *Bipolaris* conidium suspensions developed small brown spots on leaves 7 d after inoculation (DAI). These spots enlarged with time, and closely resembled disease lesions observed in the field. At 14 DAI, *Curvularia* isolates induced leaf tip dieback and chlorosis, mostly on basal leaves (Figure 10 A). *Bipolaris sorokiniana* isolates produced dark, irregular brown spots that increased in size and coalesced, leading to an extensive blighting of entire leaf blades and tillers that turned tan and brown (Figure 10 A, a to h). At 21 DAI, leaves inoculated with *B. sorokiniana* isolates began disintegrating (“melting”), and thereafter infections spread to the crown and root areas, which induced the “melting out” phase of the plants.

Results presented in Figure 10 B showed that *B. sorokiniana* isolates were more aggressive than the other inoculated isolates. Mean proportions of leaf necrotic area ranged from 43.3% to 51.3% (overall mean = $45.5 \pm 3.5\%$) for plants inoculated with *B. sorokiniana*, and from 14.9% to 26.3% (overall mean = $20.3 \pm 4.6\%$) for *Curvularia* spp. inoculations. Minor symptoms ranging from 3.9% to 19% (overall mean = $7.3 \pm 5.8\%$) were induced by isolates of *Myrothecium*, *Fusarium*, or *Acremonium*. Little difference was detected in aggressiveness among the *B. sorokiniana* isolates. Sporulation was observed in the host lesions after 7 to 14 d, and the respective pathogens were reisolated from 90 to 100% of diseased leaves sampled from each trial. Plants sprayed with sterile distilled water remained symptomless (Figure 10 A, g and n).

DISCUSSION

Accurate identification of *Bipolaris* and *Curvularia* species causing leaf spots and blight of turfgrass is important, due to potential species level variations in pathogenicity characteristics. Overall, using characteristics of conidia, *Curvularia* sp. isolates were easily distinguished from *B. sorokiniana* isolates, and from *C. spicifera* that had atypical, straight, short conidia that were similar to those of *Bipolaris*. *Curvularia* is characterized by conidia with enlarged intermediate cells that contribute to the characteristic curvatures, while in *Bipolaris* conidia curvature is continuous throughout conidium lengths. Conidia of *Bipolaris* are also usually longer than those of *Curvularia* (Marin-Felix *et al.*, 2017). Krizsan *et al.* (2015) showed that the most important discriminative features between species were the shapes and septation

of the conidia. However, some *Curvularia* species have short and straight conidia with intermediate conidial characteristics, making species identification difficult. These species may seem different from the type genus *Curvularia* that has euseptate and curving conidia.

Morphological variation was demonstrated when conidia are produced on different substrates (Sivanesan, 1987; Sun *et al.*, 2003). Presence or absence of protuberant hila within the one species has been observed in relation to conidium age (Santos *et al.*, 2018). In addition, Differences in mycelium colour can also occur when comparing subcultures from one colony. This shows that colony colour alone should not be a characteristic for species identification (Santos *et al.*, 2018). Due to ambiguities in morphological characteristics, DNA sequences of multiple loci are widely used for accurate species identification, and determining new species (Jeon *et al.*, 2015; Tan *et al.*, 2018; Marin-Félix *et al.*, 2017, 2020; Iturrieta-González *et al.*, 2020; Zhang *et al.*, 2020; Connally *et al.*, 2021). These studies have shown that morphological criteria of several species do not correlate with molecular identification, highlighting the usefulness of combining sequence data from *ITS rDNA*, *gpd* and *tef1* to correctly delineate species within *Curvularia* and *Bipolaris* genera (Marin-Félix *et al.*, 2017; 2020). Using this set of sequences, the present study confirmed that some of the isolates from the Oran Olympic stadium turfgrass corresponded to *B. sorokiniana* and *C. spicifera*, and other isolates were of four other *Curvularia* species, i.e., *C. geniculata*, *C. verruculosa* and two undetermined *Curvularia* species.

The presence of *Curvularia* spp. associated with grass diseases has been reported world-wide. These fungi have been found in Argentina and the United States of America (Roane and Roane, 1997; Goldring *et al.*, 2007; Roberts and Tredway, 2008; Martinez and Pearce 2020); in Europe, in Portugal (Sivanesan, 1987; Coelho *et al.*, 2020); in Asia, including Iran and China (Ahmadpour *et al.*, 2013; Xin-hua *et al.*, 2019); in Oceania, including New Zealand and Australia (Falloon 1976; McKenzie 1978; Pennycook, 1989; Tan *et al.*, 2018); and in Southern Africa, in: Zimbabwe (Sivanesan, 1987). *Bipolaris sorokiniana* is a plurivorous species, and has been reported as a phytopathogen of almost a hundred *Poaceae*, including cultivated and wild species (Farr and Rossman, 2022), and from different countries (Karunarathna *et al.*, 2021). In Algeria, *B. sorokiniana* has been isolated from leaves of lentil (El Amine *et al.*, 2021) and maize (Zibani *et al.*, 2022).

Bipolaris sorokiniana was found in small proportions of turfgrass crowns samples in the present study. The low frequency of isolation of this pathogen may be

related to the incubation conditions that were applied, and to strong competition with the fast growing *Curvularia* species. Temperature is an important environmental factor that affects fungal activity and pathogenicity. There is an optimal level at which the growth and activity of fungi are greatest; above and below that level, growth and activity are reduced. In the present study experiments, optimum growth of *Curvularia* was at 30 – 35°C, whereas *B. sorokiniana* isolates grew most rapidly at 25 – 30°C. Rapid colonization of substrates *Curvularia* probably hampered development of *B. sorokiniana*. This indicates that alternative methods (e.g. nucleic acid-based detection from symptomatic plants) should be used for precise and rapid disease diagnoses.

Although six species of fungi were identified on turfgrass, the presence of a pathogen alone does not denote disease. Differences in pathogenicity among these species was detected in the present study, Koch's postulates were fulfilled. Plant trials indicated that *Curvularia* species are likely to be minor turfgrass pathogens, in contrast to *B. sorokiniana*. *Curvularia* spp. are typically considered to be weak pathogens of several plant hosts, or as saprobes (Smiley *et al.*, 2005; Manamgoda *et al.*, 2012; Ayoubi *et al.*, 2017).

Simultaneous occurrence of high temperatures and poor water quality may influence disease progression. Incidence of lawn blight diseases can be ascribed to environmental factors (climate, atmospheric pollution, soil texture), mineral supply, water quality, and plant factors (growth stage sensitivity, varietal response to the stress). The Mediterranean climate is characterized by long drought periods that occur in the North (Margat and Vallé, 2000). The results of the present study are consistent with those of Dicklow and Madeiras (2021). They reported *Curvularia* as a stress pathogen of turf resulting from high temperatures or summer stress, which may be secondary to other pathogens or caused by poor cultural practices. A possible explanation is that lesions caused by *B. sorokiniana* are invaded by *Curvularia* which is aggressive at high temperatures. The occurrence of these fungi together causes greater disease than with one species alone.

The present study has confirmed that *B. sorokiniana* is a potential threat for production of animal fodder and in rangeland grasses, where pathogen damage can severely affect pasture and lawn quality. In sports fields specifically, assessments for this pathogen may allow for disease prevention. This will aid appropriately swift disease management to be applied, as different pathogens and their strains can respond differently to chemical treatments. This will prevent further spread of disease, and reduce losses due to diseases.

LITERATURE CITED

- Abdelguerfi A., Abdelguerfi-Laouar M., 2004. Répartition de la fétuque, du dactyle et de Lolium en fonction de quelques facteurs du milieu, en Algérie. In: *Réhabilitation des Pâturages et des Parcours en Milieux Méditerranéens* Ferchichi A. (comp.), Ferchichi A. (collab.). CIHEAM (Cahiers Options Méditerranéennes; n. 62), Zaragoza, Spain, 43–46.
- Ahmadpour A., Heidarian Z., Karami S., Tsukiboshi T., Zhang M., Javan-Nikkhah M., 2013. New species of *Bipolaris* and *Curvularia* on Grass species in Iran. *Rostaniha* 14 (2): 216–228. <https://doi.org/10.22092/BOTANY.2014.101288>
- Almaguer M., Rojas T.I., Dobal V., Batista A., Aira M.J., 2012. Effect of temperature on growth and germination of conidia in *Curvularia* and *Bipolaris* species isolated from the air. *Aerobiologia* 29: 13–20. <https://doi.org/10.1007/s10453-012-9257-z>
- Al-Sadi AM., 2021. *Bipolaris sorokiniana*-Induced Black Point, Common Root Rot, and Spot Blotch Diseases of Wheat: A Review. *Frontiers in Cellular and Infection Microbiology* 11: 584899. <https://doi.org/10.3389/fcimb.2021.584899>
- Ayoubi N., Mohammad S., Rasoul Z., Doustmorad Z., 2017. First report of *Curvularia inaequalis* and *C. spicifera* causing leaf blight and fruit rot of strawberry in Iran. *Nova Hedwigia* 105(1). https://doi.org/10.1127/nova_hedwigia/2017/0402
- Berbee M.L., Pirseyedi M., Hubbard S., 1999. *Cochliobolus* phylogenetics and the origin of known, highly virulent pathogens, inferred from ITS and glyceraldehyde-3-phosphate dehydrogenase gene sequences. *Mycologia* 91: 964–77.
- Bhunjun C.S., Dong Y., Jayawardena R.S., Jeewon R., Phukhamsakda C., ... Sheng J., 2020. A polyphasic approach to delineate species in *Bipolaris*. *Fungal Diversity* 102: 225–256.
- Boedijn KB., 1933. Über einige phragmosporen dematiaceen. *Bulletin du Jardin Botanique de Buitenzorg* 13: 120–134.
- Chamekh R., Deniel F., Donot C., Jany J.L., Nodet P., Belabid L., 2019. Isolation, Identification and Enzymatic Activity of Halotolerant and Halophilic Fungi from the Great Sebkhah of Oran in Northwestern of Algeria. *Mycobiology* 47(2): 230–241. <https://doi.org/10.1080/12298093.2019.1623979>
- Coelho L., Borrero C., Bueno-Pallero F., Guerrero C., Fonseca, F., ... Dionisio L., 2020. First report of *Curvularia trifolii* causing Curvularia blight in *Agrostis stolonifera* in south of Portugal. *Plant Disease* 104(1): 292.

- Connally A., Smith D., Marek S., Wu Y., Walker N., 2021. Phylogenetic evaluation of *Bipolaris* and *Curvularia* species collected from turfgrasses. *International Turfgrass Society Research Journal* 14: 916-930. <https://doi.org/10.1002/its2.16>
- Corwin B., Tisserad N., Fresenburg B., 2007. *Identification and Management of Turfgrass Diseases - Integrated Pest Management*. College of Agriculture, Food and Natural Resources, University of Missouri, IPM1029 Columbia, United States of America, 55 pp.
- Deng H., Tan Y.P., Shivas R.G., Niu Y.C., 2015. *Curvularia tsudae* comb. nov. et nom. nov., formerly *Pseudocochliobolus australiensis*, and a revised synonymy for *Curvularia australiensis*. *Mycoscience* 56: 24–8.
- Dicklow M.B., Madeiras A., 2021. Leaf Spot Diseases of Turf- UMass Extension Turf Program. Consulted 26/08/2022. <https://ag.umass.edu/turf/fact-sheets/leaf-spot-diseases-of-turf>
- El Amine Kouadri M., Amine Bekkar A., Zaim S., 2021. First report of *Bipolaris sorokiniana* causing spot blotch of lentil in Algeria. *New Disease Reports* 43(2): e12009.
- Falloon R.E., 1976. *Curvularia trifolii* as a high-temperature turfgrass pathogen, *New Zealand Journal of Agricultural Research* 19(2), 243–248. <https://doi.org/10.1080/00288233.1976.10426773>
- Farr D.F., Rossman A.Y., 2022. Fungal Databases, U.S. National Fungus Collections, ARS, USDA. Retrieved September 7, 2022, from <https://nt.ars-grin.gov/fungal-databases/>
- Goodwin D.C., Lee S.B., 1993. Microwave miniprep of total genomic DNA from fungi, plants, protists and animals for PCR. *BioTechniques* 15: 438–444.
- Goldring L.V., Lacasa M., Wright E.R., 2007. *Curvularia* blight on *Lolium perenne* on turfgrasses in Argentina. *Plant Disease* 91: 323.
- Hatfield J., 2017, Turfgrass and Climate Change. *Agronomy Journal* 109: 1708-1718. <https://doi.org/10.2134/agnonj2016.10.0626>
- Hernández-Restrepo M., Madrid H., Tan Y.P., da Cunha K.C., Gené J., ... Crous P.W., 2018 Multi-locus phylogeny and taxonomy of *Exserohilum*. *Persoonia* 41:71–108. <https://doi.org/10.3767/persoonia.2018.41.05>
- Iturrieta-González I., Gené J., Wiederhold N., García D., 2020. Three new *Curvularia* species from clinical and environmental sources. *MycKeys* 68: 1–21. <https://doi.org/10.3897/mycokeys.68.51667>
- Jeon S.J., Nguyen T.T., Lee H.B., 2015. Phylogenetic Status of an Unrecorded Species of *Curvularia*, *C. spicifera*, Based on Current Classification System of *Curvularia* and *Bipolaris* Group Using Multi Loci. *Mycobiology* 43(3): 210–217. <https://doi.org/10.5941/MYCO.2015.43.3.210>
- Kalyaanamoorthy S., Minh B., Wong T., von Haeseler A., Jeremiin, L.S., 2017. ModelFinder: fast model selection for accurate phylogenetic estimates. *Nature Methods* 14: 587–589. <http://doi.org/10.1038/nmeth.4285>
- Karunaratna A., Tibpromma S., Jayawardena R.S., Nanayakkara C., Asad S., ... Kumla J., (2021) Fungal Pathogens in Grasslands. *Frontiers in Cellular Infection Microbiology* 11:695087. <https://doi.org/10.3389/fcimb.2021.695087>
- Khan J.A., Hussain S.T., Hasan S., McEvoy P., Sarwari A., 2000. Disseminated *Bipolaris* infection in an immunocompetent host: an atypical presentation. *Journal of Pakistan Medical Association* 50:68–71.
- Kornerup A., Wanscher J.H., 1978. *Methuen Handbook of Colour*, 3rd ed. Methuen, London, United Kingdom, 252 pp.
- Krizsan K., Papp T., Palanisamy M., Shobana C., Muthusamy C., ... Kredics, L., 2015. Clinical Importance of the Genus *Curvularia*. In: *Medical Mycology: Current Trends and Future Prospects* (M. Razzaghi-Abyaneh, M. Shams-Ghahfarokhi, M. Rai ed.), CRC Press, Boca Raton, Florida, United States of America, 147–204. <https://doi.org/10.1201/b18707-10>
- Kumar S., Stecher G., Tamura K., 2016. MEGA 7: Molecular evolutionary genetics analysis version 7.0 for bigger datasets. *Molecular Biology and Evolution* 33: 1870–1874. <https://doi.org/10.1093/molbev/msw054>
- Landschoot P., 2021. *Turfgrass Diseases: Leaf Spot and Melting-Out Diseases (Causal Fungi: Bipolaris and Drechslera spp.)*. University Park, The Pennsylvania State University, United States of America, 5 pp. <https://extension.psu.edu>
- Liu H., Todd J.L., Luo H., 2023. Turfgrass Salinity Stress and Tolerance—A Review. *Plants* 12, 925. <https://doi.org/10.3390/plants12040925>
- Madrid H., da Cunha K.C., Gené J., Dijksterhuis J., Cano J., ..., Crous P.W., 2014. Novel *Curvularia* species from clinical specimens. *Persoonia* 33:48–60. <https://doi.org/10.3767/003158514X683538>
- Manamgoda D.S., Cai L., McKenzie E.H.C., Crous P.W., Madrid H., Chukeatirote E., Shivas R.G., Tan Y.P., Hyde K.D., 2012. A phylogenetic and taxonomic re-evaluation of the *Bipolaris* - *Cochliobolus* - *Curvularia* complex. *Fungal Diversity* 56:131–144.
- Manamgoda D.S., Rossman A.Y., Castlebury L.A., Crous P.W., Madrid H., ... Hyde K.D., 2014. The genus *Bipolaris*. *Studies in Mycology* 79: 221–288. <https://doi.org/10.1016/j.simyco.2014.10.002>

- Manamgoda D.S., Rossman A.Y., Castlebury L.A., Chuke-atirote E., Hyde K.D., 2015. A taxonomic and phylogenetic re-appraisal of the genus *Curvularia* (Pleosporaceae): human and plant pathogens. *Phytotaxa* 212: 175–198. <https://doi.org/10.11646/phytotaxa.212.3.1>
- Margat J., Vallée D., 2000. *Mediterranean vision on water, population and environment for the 21st century*. Blue Plan, Valbonne, France, 62 pp.
- Marin-Felix Y., Senwantha C., Cheewangkoon R., Crous P.W., 2017. New species and records of *Bipolaris* and *Curvularia* from Thailand. *Mycosphere* 8: 1556–1574.
- Marin-Felix Y., Hernández-Restrepo M., Crous P. W., 2020. Multi-locus phylogeny of the genus *Curvularia* and description of ten new species. *Mycological Progress* 19: 559–588. <https://doi.org/10.1007/s11557-020-01576-6>
- Martinez A., Pearce M., Burpee L., 2020. *Turfgrass Diseases in Georgia: Identification and Control*. UGA Cooperative Extension Bulletin 1233, The University of Georgia, United States of America, 12pp.
- McKenzie E.H.C., 1978. Occurrence of *Drechslera* and *Curvularia* on grass seed in New Zealand, *New Zealand Journal of Agricultural Research* 21(2): 283–286. <https://doi.org/10.1080/00288233.1978.10427412>
- Nelson E.B., 1992. Late summer leaf spots and leaf blights. An independent newsletter for cool season turf managers. *Turf GrassTrends* 4: 12 pp.
- Nguyen L.T., Schmidt H.A., von Haeseler A., Minh B.Q., 2015. IQ-Tree: a fast and effective stochastic algorithm for estimating maximum likelihood phylogenies. *Molecular Biology and Evolution* 32: 268–274.
- Pennycook S.R., 1989. *Plant Diseases Recorded in New Zealand*. 3 Vol. Plant Diseases Division, D.S.I.R., Auckland, New Zealand.
- Pham j., Kulla B., McKenna J., 2022. Invasive fungal infection caused by *Curvularia* species in a patient with intranasal drug use: A case report, *Medical Mycology Case Reports* 37: 1–3. <https://doi.org/10.1016/j.mmcr.2022.05.005>
- Rehner S.A., Buckley E., 2005. A *Beauveria* phylogeny inferred from nuclear ITS and EF1- α sequences: evidence for cryptic diversification and links to *Cordyceps* teleomorphs. *Mycologia*, 84–98. 97pp.
- Roane C.W., Roane M.K., 1997. Graminicolous Fungi of Virginia: Fungi associated with genera *Echinochloa* to *Zizania*. *Virginia J. Sci.* 48: 11–46.
- Delgado, G. 2011. Nicaraguan fungi: a checklist of hyphomycetes. *Mycotaxon* 115: 534.
- Roberts J.A., Tredway L.P., 2008. First Report of *Curvularia* Blight of Zoysiagrass Caused by *Curvularia lunata* in the United States. *Plant Disease* 92(1):173. <https://doi.org/10.1094/PDIS-92-1-0173B>
- Santos P.R.R.D., Leão E., Aguiar R., Melo M., Santos G., 2018. Morphological and molecular characterization of *Curvularia lunata* pathogenic to andropogon grass. *Bragantia*, <https://doi.org/77.10.1590/1678-4499.2017258>
- Sherratt P.J., Street J.R., Gardner D., 2017. Cool-Season Turfgrasses for Sports Fields and Recreational Areas. Agriculture and Natural Resources. [https://ohioline.osu.edu/factsheet/str1#:~:text=The%20recommended%20species%20are%3A,Tall%20fescue%20\(Lolium%20arundinaceum\)](https://ohioline.osu.edu/factsheet/str1#:~:text=The%20recommended%20species%20are%3A,Tall%20fescue%20(Lolium%20arundinaceum)). Visited 30/08/2022
- Shoemaker A., 1959. Nomenclature of *Drechslera* and *Bipolaris*, grass parasites segregated from ‘*Helminthosporium*’. *Canadian Journal of Botany* 37: 879–887.
- Sithin M., 2021. Role of Turfgrass in Urban Landscapes. *Journal of Plant Development Sciences* 13: 247–255.
- Sivanesan A., 1987. Graminicolous species of *Bipolaris*, *Curvularia*, *Drechslera*, *Exserohilum* and their teleomorphs. *Mycological Papers* 158: 1–261.
- Smiley R.W., Dernoeden P.H., Clarke B.B., 2005. *Compendium of Turfgrass Diseases*, 3rd ed. The American Phytopathological Society, Minnesota, United States of America, 167 pp. <https://doi.org/10.1094/9780890546154>
- Stackhouse T., Martinez-Espinoza A.D., Ali M.E., 2020. Turfgrass Disease Diagnosis: Past, Present, and Future. *Plants* 9(11): 1544. <https://doi.org/10.3390/plants9111544>
- Sun G., Oide S., Tanaka E., Shimizu K., Tanaka C., Tsuda M., 2003. Species separation in *Curvularia* “geniculata” group inferred from Brn1 gene sequences. *Mycoscience* 44: 239–244. <https://doi.org/10.1007/s10267-003-0104-5>
- Tan Y.P., Crous P.W., Shivas R.G., 2018. Cryptic species of *Curvularia* in the culture collection of the Queensland Plant Pathology Herbarium. *MycKeys* 35: 1–25. <https://doi.org/10.3897/mycokeys.35.25665>
- Tandon, R.N., Bilgrami, K.S., 1962. A new pathogenic species of genus *Curvularia*. *Current Science* 31: 254–254.
- Thekkedath E., Burden Z., Steinberg S., Cury J., 2022. *Curvularia pneumonia* Presenting as a Mass-Like Lesion. *Cureus* 14(6): e25933. <https://doi.org/10.7759/cureus.25933>
- USDA-ARS, 2013. Germplasm Resources Information Network (GRIN). Online Database. Beltsville, Maryland, USA: National Germplasm Resources Laboratory. <https://npgsweb.ars-grin.gov/gringlobal/taxon/taxonomysimple.aspx>
- White T. J., Bruns, T., Lee S. Taylor J., 1990. Amplification and direct sequencing of fungal ribosomal RNA genes for phylogenetics. In: *PCR Protocols: A Guide*

- to *Methods and Applications*; M.A. Innis D.H., Gelfand J.J., Sninsky T.J., White T. J., Eds., Academic Press, San Diego, CA, 315–322pp.
- Wolski K., Markowska J., Radkowski A., Brennenstul M., Sobol Ł., ... Khachatryan K., 2021. The influence of the grass mixture composition on the quality and suitability for football pitches. *Scientific Reports* 11(1). <https://doi.org/11.10.1038/s41598-021-99859-9>
- Xin-hua W., Jin-xin G., Shi-gang G., Tong L., Zhi-xiang L., ... Jie C., 2019. Research progress on maize *Curvularia* leaf spot caused by *Curvularia lunata*. *Acta Phytopathologica Sinica* 49: 433–444. <https://doi.org/10.13926/j.cnki.apps.000394>
- Zanelli B., Vidrih M., Bohinc T., Trdan S., 2021. Impact of fertilisers on five turfgrass mixtures for football pitches under natural conditions. *Horticultural Science* 48: 190–204.
- Zhang Q., Yang Z-F., Cheng W., Wijayawardene N.N., Hyde K.D., ... Wang Y., 2020. Diseases of *Cymbopogon citratus* (*Poaceae*) in China: *Curvularia nanningensis* sp. nov. *MycKeys* 63: 49–67. <https://doi.org/10.3897/mycokeys.63.49264>
- Zhang Y., Crous P.W., Schoch C.L., Hyde K.D., 2012. Pleosporales. *Fungal Diversity* 53: 1–221. <https://doi.org/10.1007/s13225-011-0117-x>
- Zibani A., Ali S., Benslimane H., 2022. Corn diseases in Algeria: first report of three *Bipolaris* and two *Exserohilum* species causing leaf spot and leaf blight diseases. *Cereal Research Communications* 50: 449–461. <https://doi.org/10.1007/s42976-021-00192-8>



Citation: S. Campigli, S. Luti, T. Martellini, D. Rizzo, L. Bartolini, C. Carrai, J. Baskarathevan, L. Ghelardini, F. Peduto Hand, G. Marchi (2023) TaqMan qPCR assays improve *Pseudomonas syringae* pv. *actinidiae* biovar 3 and *P. viridiflava* (PG07) detection within the *Pseudomonas* sp. community of kiwifruit. *Phytopathologia Mediterranea* 62(1):95-114. doi:10.36253/phyto-14400

Accepted: April 20, 2023

Published: May 8, 2023

Copyright: © 2023 S. Campigli, S. Luti, T. Martellini, D. Rizzo, L. Bartolini, C. Carrai, J. Baskarathevan, L. Ghelardini, F. Peduto Hand, G. Marchi. This is an open access, peer-reviewed article published by Firenze University Press (<http://www.fupress.com/pm>) and distributed under the terms of the Creative Commons Attribution License, which permits unrestricted use, distribution, and reproduction in any medium, provided the original author and source are credited.

Data Availability Statement: All relevant data are within the paper and its Supporting Information files.

Competing Interests: The Author(s) declare(s) no conflict of interest.

Editor: Roberto Buonaurio, University of Perugia, Italy.

ORCID:

SC: 0000-0001-7231-535X
SL: 0000-0001-7050-6590
DR: 0000-0003-2834-4684
JB: 0000-0002-5389-2570
LG: 0000-0002-3180-4226
FPH: 0000-0002-5553-0370
GM: 0000-0002-2937-3500

Research Papers

TaqMan qPCR assays improve *Pseudomonas syringae* pv. *actinidiae* biovar 3 and *P. viridiflava* (PG07) detection within the *Pseudomonas* sp. community of kiwifruit

SARA CAMPIGLI^{1,*}, SIMONE LUTI², TOMMASO MARTELLINI¹, DOMENICO RIZZO³, LINDA BARTOLINI³, CLAUDIO CARRAI³, JEYASEELAN BASKARATHEVAN⁴, LUISA GHELARDINI¹, FRANCESCA PEDUTO HAND⁵, GUIDO MARCHI¹

¹ Department of Agriculture, Food, Environment and Forestry, University of Florence, Ple delle Cascine 18, Florence, 50144, Italy

² Department of Experimental and Clinical Biomedical Sciences, University of Florence, Viale Morgagni 50, Florence, 50134, Italy

³ Regione Toscana, Servizio Fitosanitario Regionale e di Vigilanza e Controllo Agroforestale, Via A. Manzoni 16, Florence, 50121, Italy

⁴ Plant Health & Environment Laboratory, Diagnostic and Surveillance Services, Biosecurity New Zealand, Ministry for Primary Industries, PO Box 2095, Auckland, 1140, New Zealand

⁵ Department of Plant Pathology, The Ohio State University, Columbus, OH 43220, U.S.A.

*Corresponding author. E-mail: sara.campigli@unifi.it

Summary. Kiwifruit is inhabited by a heterogeneous community of bacteria belonging to the *Pseudomonas syringae* species complex (Pssc). Only a few of its members, such as the specialist *Pseudomonas syringae* pv. *actinidiae* biovar 3 (Psa3), are known as pathogens, but for most of the species, such as *P. viridiflava* (Pv), a generalist with high intraspecific variation, the nature of their relationship with kiwifruit is unclear. Currently, no culture independent molecular diagnostic assay is available for Pv. In this study we validated two TaqMan qPCR diagnostic assays adopting a strategy that for the first time widely focuses on the *Pseudomonas* sp. community associated to kiwifruit in Tuscany (Italy). Primers and probes were designed based on the sequence of the *lscy* gene of Psa3 (qPCR_{Psa3}) and the *rpoD* gene of Pv phylogroup 7 (qPCR_{Pv7}). Both qPCR assays have a LOD of 60 fg of DNA. By using reference strains along with 240 strains isolated from kiwifruit and characterized *ad hoc* as *Pseudomonas* sp., specificity was proven for members of six of the 13 Pssc phylogroups. Moreover, to evaluate the possible effects of seasonal variations in the *Pseudomonas* sp. community composition on assay specificity, the assays were tested on naturally infected leaves and canes sampled from different orchards throughout a growing season. At last, by proving qPCR's capacity to detect latent infections in artificially inoculated leaves, their potential usefulness in surveillance programs and for epidemiological studies was verified.

Keywords: *Actinidia* sp., orchard variability, *Pseudomonas syringae* species complex, specificity.

INTRODUCTION

It has long been assumed that the bacterium *Pseudomonas syringae* (Ps) has evolved in association with plants, on which it forms populations dominated by a few pathogenic strains with narrow host ranges (Dye *et al.*, 1980; Hirano and Upper, 2000; Morris *et al.*, 2010). In the last two decades however, compelling evidence was gained that members of what is currently termed as the *Pseudomonas syringae* species complex (Pssc, Gardan *et al.*, 1999), are ubiquitous bacteria, widespread in all continents both in agricultural and non-agricultural settings, which may live in association with substrates other than plants and take advantage of the water cycle for dissemination (Morris *et al.*, 2007; 2008; 2010; Berge *et al.*, 2014). Primary studies aimed at establishing the phylogenetic structure of the Pssc, used a MLST (Multi Locus Sequence Typing) approach based on seven core genome genes. This allowed delineation of four main phylogroups (PGs). More recently, the existence of seven and then 13 PGs was proposed based on the polymorphisms observed in the sole *rpoD* and *cts* gene sequences, respectively (Sarkar and Guttman, 2004; Parkinson *et al.*, 2011; Berge *et al.*, 2014; Baltrus *et al.*, 2017). However, the relationship between these phylogenetic patterns and the traits required to occupy different ecological niches are still unknown. Many members of the Pssc isolated from water or healthy plant tissues have typical plant pathogenic traits, such as a canonical Type Three Secretion System (TTSS), ability to induce Hypersensitive Response (HR) on tobacco, to produce phytotoxins and effectors, and, most of all, to cause disease in many different hosts at least under experimental conditions (Morris *et al.*, 2019). At the same time, strains that cluster in different PGs and cause disease to the same host plants are known to exist (Morris *et al.*, 2007; Mohr *et al.*, 2008; Bartoli *et al.*, 2014; Dillon *et al.*, 2019).

The first reports of damage to kiwifruit (*Actinidia* spp.) plants caused by members of the Pssc were recorded in New Zealand (Wilkie *et al.*, 1973) followed by Japan, Korea, Italy, and China between the mid 1980s and early 1990s. To date, reports have concerned Ps (unknown PG), Ps pv. *syringae* (Psyr; PG02), *P. savastanoi* (Psav; PG03), Ps pv. *actinidifoliorum* (Pfm, PG01), Ps pv. *actinidiae* (Psa, PG01/b) and *P. viridiflava* (Pv). Pssc strains belonging to either PG7 or PG08 are currently, referred to as *P. viridiflava* nomenespecies (Bull and Koike, 2015). While Ps, Psyr, Pv, Psav, and Pfm have been mostly, but not exclusively, reported as leaf spot and bud rot agents in kiwifruit orchards, Psa also causes shoot dieback and cane and trunk cankers (Vanneste, 2017). Sufficient variability was found in Psa to justify its

further differentiation into five biovars, also distinguishable based on virulence traits. A specific lineage of biovar-3 (Psa3) is currently considered the most aggressive and responsible for the bacterial canker pandemic that is threatening kiwifruit production in all countries where this host is grown (McCann *et al.*, 2017; Vanneste, 2017; Sawada and Fujikawa, 2019). Recent studies, however, have pointed out that the phylloplane of kiwifruit hosts a much more variegated Pssc community than previously thought (Bartoli *et al.*, 2015; Straub *et al.*, 2018). In southeastern France, PG01 and PG13 phylotypes are the most widespread, but PG02, PG03, PG07, PG08, PG09, and PG10 also occur, although at much lower frequencies (Borschinger *et al.*, 2016). In just two New Zealand orchards, Straub *et al.* (2018) reported that kiwifruit leaves were commonly inhabited by multiple phylotypes of PG01, PG02, and PG03, the latter being by far the most abundant, but rarely inhabited by PG05 and never by PG07. It was also observed that genetic diversity of the Pssc community was strongly affected by the presence or absence of disease, host genotype (cultivar), as well as environmental factors, including humidity, nutrient availability, UV radiation and orchard management practices (Straub *et al.*, 2018).

Given the importance of kiwifruit production worldwide (approx. 4.4M tons produced in 2020; FAOSTAT, 2020), great emphasis has been given to understanding the life cycle of Psa on this host, and to developing reliable and selective assays for rapid routine diagnoses (Vanneste, 2017; Donati *et al.*, 2020). Most assays are PCR based (simplex, nested, multiplex, and Real-Time) and their pros and cons have been assessed through an interlaboratory comparison (Loreti *et al.*, 2018). Among major findings were: i) isolation on semi-selective media followed by bacterial characterization, although having limited sensitivity, had very reliable specificity compared to several PCR methods; and ii) high risks of false positives or inconclusive PCR results came from testing bacterial cultures of phylogenetically closely related *Pseudomonas* sp. or kiwifruit-associated bacteria. In view of these findings, the EPPO international standard recommends that both PCR and isolation are performed for “critical” symptomatic samples and for all asymptomatic samples (EPPO PM 7/120 [2], 2021). To date, no culture independent molecular diagnostic assay is available for Pv.

The present study outlines two novel TaqMan Real-Time PCR assays (qPCR) for specific detection of Psa3 and Pv belonging to PG07 (Pv7) on kiwifruit, and the strategy implemented to verify their specificity against the *Pseudomonas* sp. community that was associated with kiwifruit during a growing season in Tuscany, Italy.

MATERIAL AND METHODS

Bacterial strains

Fifty-seven Pssc reference strains and 21 plant associated bacteria from national and international collections, were used for initial testing of qPCR assays' specificity (Table 1). The phylogenetic position of reference strains within the Pssc complex was determined based on partial *cts* (citrate synthase) and *rpoD* (RNA polymerase sigma factor) genes sequence analysis according to Berge *et al.* (2014) and Parkinson *et al.* (2011), respectively.

All strains were grown on Nutrient Agar (NA) at 27°C and were preserved in 30% glycerol at -80°C.

Plant material and bacteria isolation procedures

To verify the specificity of the qPCR assays against the cultivable *Pseudomonas* sp. kiwifruit-associated microflora, bacteria were isolated from *A. chinensis* var. *deliciosa* cv. Hayward (AcdH) plants from Tuscany (Italy) from 2014 to 2020. With the exception of 2016, when plant samples were collected from one orchard in the province of Lucca and one in Pistoia, all other tested samples were collected from six orchards in Lutirano (province of Florence), the only kiwifruit growing area of Tuscany where the presence of Psa3 has been officially confirmed (DDR n.512/2013). All orchards were planted in the 1990s, except for orchard No. 6 in Lutirano, which was 3 years old in 2018 (Supplementary Figure S1). Most isolates were obtained from fully expanded kiwifruit leaf blades, but isolations from host sap (2017) and canes showing dieback symptoms (2014 and 2018) were also carried out (Figure 1). In 2016 and 2020, bacteria were also isolated from leaves collected from nursery potted plants.

All samples were transported to the laboratory on ice and were processed within 24 h. For bacterial isolation from leaves, approx. 1 g of fully expanded leaf blade was crushed in a universal extraction bag (480100, BIOREBA, Reinach, Switzerland) using a hammer, and was then homogenized under a laminar flow hood by adding 7 mL of sterile saline solution (0.85% NaCl) and incubated for 5 min at room temperature. Twenty cm dieback cane sections were thoroughly washed under tap water and air dried. After soaking in 70% ethanol for 5 min, segments were each decorticated, superficially disinfested by wiping with a sterilized paper towel soaked with 50% ethanol, and then air dried inside a laminar flow hood. After removing 5 cm of tissue from each end using flame disinfested shears, approx. 0.5 g of wood chips were aseptically excised with a sterile scalpel and were then macerated in 7

mL of saline solution for 1 h with gentle shaking at room temperature. Five mL of xylem sap were collected according to Biondi *et al.* (2013), diluted 1:2 (v:v) with saline solution and thoroughly vortexed. Isolations from leaf and cane macerates or from sap were carried out by dilution-plate on modified King's B semi-selective agar medium (KBCA), as outlined by the EPPO standard for Psa3 (King *et al.*, 1954; Mohan and Schaad, 1987; EPPO PM7\120[2], 2021). For bacterial isolation from artificially inoculated nursery potted plants, Nutrient Sucrose Agar supplemented with 5% sucrose (NSA) amended with 60 mg L⁻¹ cycloheximide was also used (Figure 1). All isolation plates were incubated for 96 h at 27°C, checked daily, and the most represented bacterial morphotypes were selected and streaked twice on NSA to ensure purity. All isolates were stored in 30% glycerol at -80°C until further use.

Nucleic acid extraction procedures from plant tissues and purified bacteria

Leaf tissues

Total nucleic acids were extracted from naturally and artificially infected as well as non-infected kiwifruit (AcdH) and tobacco (*Nicotiana tabacum* cv. Virginia Bright) leaves, or from a cell suspension of the culturable microbial community growing on NSA plates (Figure 1), using CTAB buffer [100 mM Tris, pH 8.0, 1.4 M NaCl, 20 mM EDTA, pH 8.0, 2.5% (w:v) CTAB, 2.5% (w:v) polyvinylpyrrolidone (PVP-40)]. For non-infected or naturally infected leaves, approx. 1 g of each leaf blade was crushed using a hammer, in a universal extraction bag. Seven mL of CTAB buffer were directly added to the bag and, after 5 min incubation, 500 µL were transferred to a 1.5 mL capacity microcentrifuge tube. For artificially inoculated leaves, 1 mL of leaves macerates (1 g) in 7 mL of saline solution, or of a cell suspension of the culturable microbial community growing on NSA plates obtained by washing plates with 3 mL of the same solution, were centrifuged for 5 min at 17089 × g in a 1.5 mL microcentrifuge tubes. After removing the supernatant, the resulting pellet was re-suspended in 500 µL of CTAB buffer. In all cases, after incubating for 30 min at 65°C, purification was carried out according to Angelini *et al.* (2001). Nucleic acids were re-suspended in 100 µL of Tris HCl (10mM, pH 8) and stored at -20°C until further use.

Cane tissues

Total nucleic acids were extracted from non-infected or naturally infected kiwifruit canes (Figure 1), or from

Table 1. Bacterial reference strains used in qPCR assays deployed in this study, along with their geographic origins and hosts of isolation as indicated by the collection curators. For strains that were included in phylogenetic analyses, their classification phylogroups (PG) and subclades are also indicated.

Bacterial species ^a	Strain ^b	Host plant/matrix	Geographic origin	Year of isolation	Phylogroup/subclade	
					<i>cts</i> ^c	<i>rpoD</i> ^d
<i>Agrobacterium radiobacter</i>	C58	<i>Prunus avium</i>	USA	1958	- ^e	-
<i>Allorhizobium vitis</i>	ICMP 11960	<i>Vitis vinifera</i>	France	1985	-	-
<i>A. vitis</i>	CG 628	<i>V. vinifera</i>	USA	1983	-	-
<i>A. vitis</i>	CG 634	<i>V. vinifera</i>	USA	1983	-	-
<i>Pantoea agglomerans</i>	PVFi FL1	<i>Olea europaea</i>	Italy	2002	-	-
<i>P. agglomerans</i>	NCCPB 653	<i>Pyrus communis</i>	United Kingdom	1958	-	-
<i>P. agglomerans</i>	NCCPB 656	<i>Malus sylvestris</i>	United Kingdom	1959	-	-
<i>P. agglomerans</i> pv. <i>gypsophila</i>	824/1	<i>Gypsophila paniculata</i>	Israel	1991	-	-
<i>Pectobacterium carotovorum</i>	PVFi Pcc7	<i>Zantedeschia aethiopica</i>	Italy	2012	-	-
<i>P. carotovorum</i>	PVFi PCC23	<i>Z. aethiopica</i>	Italy	2013	-	-
<i>Pseudomonas amygdali</i>	NCCPB 2607	<i>Prunus dulcis</i>	Greece	1967	-	-
<i>P. amygdali</i>	NCCPB 2608	<i>P. dulcis</i>	Greece	1967	-	-
<i>P. amygdali</i>	NCCPB 2610	<i>P. dulcis</i>	Greece	1967	-	-
<i>P. cichorii</i>	ICMP 5707	<i>Cichorium endivia</i>	Germany	1929	-	-
<i>P. corrugata</i>	C2P1	<i>Chrysanthemum morifolium</i>	Italy	1990	-	-
<i>P. mediterranea</i>	C5P1-rad1	<i>C. morifolium</i>	Italy	1990	-	-
<i>P. savastanoi</i> pv. <i>nerii</i>	ITM 510	<i>Nerium oleander</i>	Italy	1983	-	-
<i>P. savastanoi</i> pv. <i>phaseolicola</i>	CFBP 1390	<i>Phaseolus vulgaris</i>	Canada	1949	-	-
<i>P. savastanoi</i> pv. <i>phaseolicola</i>	NCCPB 2571	<i>P. vulgaris</i>	United Kingdom	1974	-	-
<i>P. savastanoi</i> pv. <i>phaseolicola</i>	RW60	<i>Lablab purpureus</i>	Ethiopia	1985	-	-
<i>P. savastanoi</i> pv. <i>savastanoi</i>	PVFi MLLI2	<i>O. europaea</i>	Italy	2001	-	-
<i>P. savastanoi</i> pv. <i>savastanoi</i>	PVBa 229	<i>O. europaea</i>	Italy	1968	-	-
<i>P. syringae</i>	ICMP 11292	<i>Actinidia deliciosa</i>	New Zealand	1991	PG01/a	PG01
<i>P. syringae</i>	CFBP 8517	Lake water	France	2006	PG09/a	und ^f
<i>P. syringae</i>	CFBP 8514	Stream water	France	2007	PG09/b	und
<i>P. syringae</i>	CFBP 8512	River water	France	2011	PG09/c	und
<i>P. syringae</i> pv. <i>aceris</i>	CFBP 2339	<i>Acer</i> sp.	USA	1970	-	-
<i>P. syringae</i> pv. <i>actinidiae</i> - Biovar 1	ICMP 9617	<i>A. deliciosa</i> cv. Hayward	Japan	1984	PG01/b	PG01
<i>P. syringae</i> pv. <i>actinidiae</i> - Biovar 1	ICMP 9853	<i>A. deliciosa</i> cv. Hayward	Japan	1984	PG01/b	PG01
<i>P. syringae</i> pv. <i>actinidiae</i> - Biovar 1	ICMP 19069	<i>A. deliciosa</i>	Japan	1984	PG01/b	PG01
<i>P. syringae</i> pv. <i>actinidiae</i> - Biovar 2	ICMP 19072	<i>A. chinensis</i>	Korea	1997	PG01/b	PG01
<i>P. syringae</i> pv. <i>actinidiae</i> - Biovar 3	ICMP 18708	<i>A. chinensis</i> var. <i>chinensis</i>	New Zealand	2010	PG01/b	PG01
<i>P. syringae</i> pv. <i>actinidiae</i> - Biovar 3	ICMP 18884	<i>A. deliciosa</i>	New Zealand	2010	PG01/b	PG01
<i>P. syringae</i> pv. <i>actinidiae</i> - Biovar 3	ICMP 19076	<i>A. deliciosa</i>	New Zealand	2011	PG01/b	PG01
<i>P. syringae</i> pv. <i>actinidiae</i> - Biovar 3	CFBP 7286	<i>A. chinensis</i> cv. HORT16A	Italy	2008	PG01/b	PG01
<i>P. syringae</i> pv. <i>actinidiae</i> - Biovar 3	CFBP 7906	<i>A. deliciosa</i> cv. Summer	France	2011	PG01/b	PG01
<i>P. syringae</i> pv. <i>actinidiae</i> - Biovar 3	CFBP 8302	<i>A. deliciosa</i>	Chile	2011	PG01/b	PG01
<i>P. syringae</i> pv. <i>actinidiae</i> - Biovar 5	CFBP 8414	<i>A. chinensis</i>	Japan	2012	PG01/b	PG01
<i>P. syringae</i> pv. <i>actinidifoliorum</i>	ICMP 18804	<i>A. chinensis</i>	New Zealand	2010	PG01/a	PG01
<i>P. syringae</i> pv. <i>maculicula</i>	NCCPB 1777	<i>Brassica oleracea</i>	United Kingdom	1965	-	-
<i>P. syringae</i> pv. <i>miricae</i>	CFBP 2897	<i>Myrica rubra</i>	Japan	1978	-	-
<i>P. syringae</i> pv. <i>miricae</i>	MAFF 302457	<i>M. rubra</i>	Japan	1984	-	-
<i>P. syringae</i> pv. <i>photinae</i>	CFBP 2899	<i>Photinia glabra</i>	Japan	1976	-	-
<i>P. syringae</i> pv. <i>primulae</i>	CFBP 1660	<i>Primula</i> sp.	USA	1939	PG07/a	PG07
<i>P. syringae</i> pv. <i>ribicola</i>	CFBP 2348	<i>Ribes aureum</i>	unknown	1946	PG07/a	PG07

(Continued)

Table 1. (Continued).

Bacterial species ^a	Strain ^b	Host plant/matrix	Geographic origin	Year of isolation	Phylogroup/subclade	
					<i>cts</i> ^c	<i>rpoD</i> ^d
<i>P. syringae</i> pv. tabaci	GSPB 1209	<i>Nicotiana tabacum</i>	Germany	unknown	-	-
<i>P. syringae</i> pv. theae	CFBP 2353	<i>Thea sinensis</i>	Japan	1970	PG01/b	PG01
<i>P. syringae</i> pv. tomato	IPV-BO 1544	<i>Solanum lycopersicum</i>	Italy	1989	-	-
<i>P. syringae</i> pv. viburni	CFBP 1702	<i>Viburnum</i> sp.	USA	1931	PG01/b	PG01
<i>P. viridiflava</i>	ICMP 9274	<i>A. deliciosa</i> cv. Hayward	New Zealand	1985	PG07/a	PG07
<i>P. viridiflava</i>	ICMP 11289	<i>A. deliciosa</i> cv. Hayward	New Zealand	1991	PG07/a	PG07
<i>P. viridiflava</i>	ICMP 13105	<i>A. deliciosa</i>	France	1985	PG02/d	PG02
<i>P. viridiflava</i>	ICMP 13110	<i>A. deliciosa</i>	France	1985	PG02/d	PG02
<i>P. viridiflava</i>	ICMP 13302	<i>A. chinensis</i> cv. Earligold	New Zealand	1996	und	PG03
<i>P. viridiflava</i>	ICMP 13303	<i>A. chinensis</i> cv. Earligold	New Zealand	1996	PG03	PG03
<i>P. viridiflava</i>	CFBP 8506	Stream water	France	2007	PG07/a	PG07
<i>P. viridiflava</i>	CFBP 8511	Channel water	France	2011	PG08	und
<i>P. viridiflava</i>	CFBP 1590	<i>Prunus cerasus</i>	France	1974	PG07/a	PG07
<i>P. viridiflava</i>	CFBP 2107	<i>Phaseolus</i> sp.	Switzerland	1927	PG07/a	PG07
<i>P. viridiflava</i>	CFBP 8559	Biofilm on stone	France	2006	PG07/a	PG07
<i>P. viridiflava</i>	CFBP 8508	<i>A. deliciosa</i>	Italy	2012	PG07/a	PG07
<i>P. viridiflava</i>	CFBP 8509	<i>Primula</i> sp.	France	2007	PG07/a	PG07
<i>P. viridiflava</i>	CFBP 6890	<i>Raphanus sativus</i>	France	2004	PG07/a	PG07
<i>P. viridiflava</i>	CFBP 4476	<i>A. deliciosa</i>	New Zealand	1984	PG02	PG02
<i>P. viridiflava</i>	UCR-1	<i>Vitis</i> sp.	USA	2002	PG07/a	PG07
<i>P. viridiflava</i>	TOMA 3-02	<i>S. lycopersicum</i>	USA	2002	PG01/a	PG01
<i>P. viridiflava</i>	TOME 9-02	<i>S. lycopersicum</i>	USA	2002	PG01/a	PG01
<i>P. viridiflava</i>	TOMP 2-02	<i>S. lycopersicum</i>	USA	2002	PG07/b	und
<i>P. viridiflava</i>	TOMU 4-02	<i>S. lycopersicum</i>	USA	2002	PG01/a	PG01
<i>P. viridiflava</i>	OrSU-MM	unknown	USA	unknown	PG03	PG03
<i>Xanthomonas arboricola</i> pv. pruni	PVFi KVPT2A	<i>A. deliciosa</i>	Italy	2016	-	-
<i>X. arboricola</i> pv. pruni	PVFi L1	<i>Prunus laurocerasus</i>	Italy	2010	-	-
<i>X. citri</i> pv. citri	CFBP 3369	<i>Citrus aurantifolia</i>	USA	1989	-	-
<i>X. euvesicatoria</i>	PVFi Xe1	<i>Capsicum annum</i>	Italy	2017	-	-
<i>X. euvesicatoria</i>	PVFi 49	unknown	unknown	unknown	-	-
<i>X. phaseoli</i>	CFBP 8462	<i>P. vulgaris</i>	USA	unknown	-	-
<i>Xylella fastidiosa</i> subsp. <i>multiplex</i>	PVFi Ma29	<i>P. dulcis</i>	Italy	2019	-	-
<i>X. fastidiosa</i> subsp. <i>pauca</i>	Salento2	<i>O. europaea</i>	Italy	2015	-	-

^a Bacterial nomenclature is according to the Comprehensive List of Names of Plant Pathogenic Bacteria, 1980-2007 published by the International Society of Plant Pathology Committee on the Taxonomy of Plant Pathogenic Bacteria (https://www.isppweb.org/about_tppb_names.asp).

^b ICMP: International Collection of Micro-organisms from Plants, Auckland, New Zealand.

CFBP: Collection Francaise de Bacteries Phytopathogenes, Angers, France.

NCPPB: National Collection of Plant Pathogenic Bacteria, York, United Kingdom.

IPV-BO: Culture Collection of Istituto di Patologia Vegetale, Università di Bologna, Italy.

ITM: Culture collection of Istituto Tossine e Micotossine da Parassiti vegetali, C.N.R., Bari, Italy.

PVBa: Culture collection of Dipartimento di Patologia vegetale, Università degli Studi, Bari, Italy.

PVFi: Culture collection of Dipartimento di Biotecnologie Agrarie-Patologia vegetale, Università degli Studi, Firenze, Italy.

GSPB : Göttinger Sammlung Phytopathogener Bakterien, University of Göttingen, Germany.

MAFF: Genetic Resources Center, National Agriculture and Food Research Organization (NARO), Japan.

The whole genomic DNA of *Xylella fastidiosa* subsp. *pauca* Salento2 was provided by Dr. Gianluca Bleve.

^c According to Berge *et al.*, 2014.

^d According to Parkinson *et al.*, 2011.

^e Not tested.

^f Undetermined.

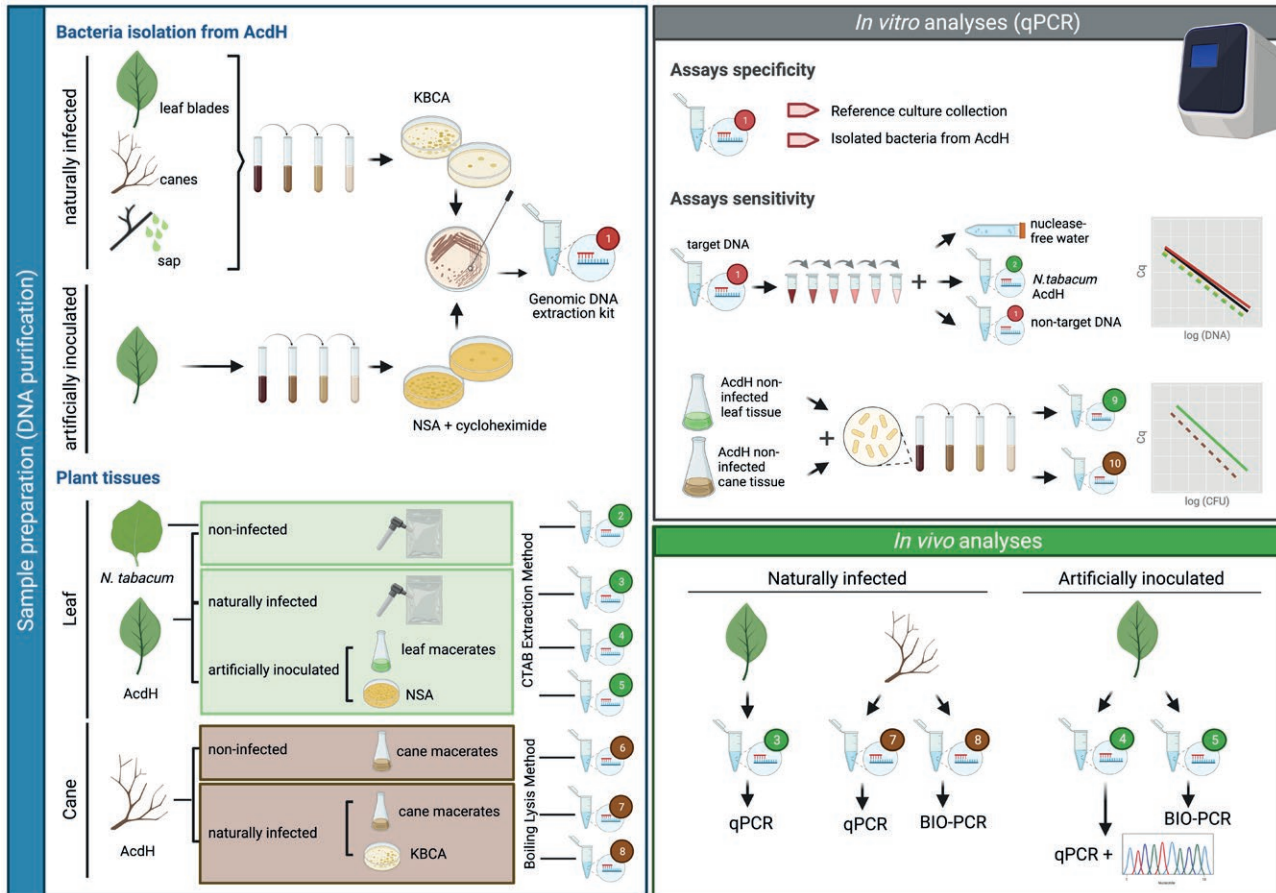


Figure 1. Summary of DNA extraction procedures and *in vitro* and *in vivo* analyses carried out to validate the qPCR assays developed in this study. Sample preparation (DNA purification): PCR templates included total nucleic acids extracted from (1) purified bacteria isolated from different *Actinidia chinensis* var. *deliciosa* cv. Hayward (AcdH) tissues and reference strains from national and international culture collections; (2) non-infected tobacco and kiwifruit leaves; (3) naturally infected or (4) artificially inoculated kiwifruit leaves; (5) culturable bacterial community from artificially inoculated kiwifruit leaves growing on NSA plates; (6) non-infected or (7) naturally infected kiwifruit canes; and (8) culturable bacterial community on KBCA from naturally infected kiwifruit canes. *In vitro* analyses (qPCR): Assays specificity (qPCR_{Psa3} and qPCR_{Pv}) were assessed using DNA extracted from reference bacterial strains and purified isolates from AcdH (1). Assays sensitivity was assessed using serial dilutions of target genomic DNA (1) in either nuclease-free water, plant DNA extracted from non-infected tobacco or kiwifruit leaf tissues (2), or DNA extracted from non-target bacteria (1). Additionally, non-infected kiwifruit leaf or cane tissues were spiked with 10-fold serial dilutions of Psa3KL103 and PvKL5 cells prior to DNA extraction using CTAB (9, leaf) or boiling lysis (10, cane) methods. *In vivo* analyses: Assays specificity (qPCR_{Psa3} and qPCR_{Pv}) was evaluated on total nucleic acids extracted from kiwifruit leaf (3, 4) or cane (7) tissues. BIO-PCR assays (BIO-PCR_{Psa3} and BIO-PCR_{Pv}) were used on the total nucleic acids extracted from the culturable fraction of the microorganisms that were infecting kiwifruit canes or artificially inoculated leaves and that were able to grow on KBCA (8) or NSA (5) plates. To verify the *in vivo* specificity of the two qPCRs, a selection of the amplicons produced from nucleic acids extracted from artificially inoculated leaves (4) was Sanger sequenced. Image created with BioRender.com.

the microbial community growing on KBCA plates, following the boiling lysis procedure (Moore *et al.*, 2004; Tyson *et al.*, 2012) with some modifications. Briefly, 1.5 mL of the suspension obtained by macerating 0.5 g of wood chips in 7 mL of saline for 1 h or of KBCA plates washings with 3 mL of the same solution, were centrifuged (as above) in 2 mL microcentrifuge tubes. The supernatant was removed, and the resulting pellet resuspended in 70 μ L of 1 mM EDTA, boiled for 5 min,

cooled at room temperature on ice and immediately used in PCR experiments.

Bacterial strains and isolates

Total nucleic acids were extracted from 1 mL of Nutrient Broth cultures of reference bacterial strains or purified isolates grown for 48 h at 27°C, using the Bac-

terial Genomic DNA Isolation Kit (Norgen Biotek Corporation, Thorold, Canada) according to manufacturer's instructions (Figure 1).

Bacterial isolates characterization

Identification and phylogenetic affiliation of all bacterial isolates obtained from kiwifruit between 2014 and 2020 was tentatively determined based on partial *cts* gene sequence analysis according to Berge *et al.* (2014) (Supplementary Table S1). PCR reagents' mix composition was as described herein: 1 × PCR Green Buffer (Thermo Scientific, Waltham, MA, USA), 0.2 mM of each dNTP (Thermo Scientific), 1.25 U of DreamTaq (Thermo Scientific), 0.2 μM of each primer (Table 2) and approx. 5 ng of genomic DNA. PCR reactions were carried out in a T professional trio thermocycler (Biometra, Göttingen, Germany). Thermal cycling consisted of 3 min at 95°C for initial denaturation, 35 cycles of denaturation at 95°C for 30 s, annealing at 57 °C for 30 s, extension at 72°C for 30 s, followed by a final extension of 10 min at 72°C. All PCR products were visualized after electrophoresis in 1.5 % agarose gels (Genaxxon bioscience GmbH, Ulm, Germany) in 1 × Tris–acetate–EDTA buffer (Invitrogen, Waltham, MA, USA) and staining with Midori Green (0.06 μL mL⁻¹; Nippon Genetics Europe GmbH, Düren, Germany). Amplicons

were purified using FastAP and Exonuclease I (Thermo Scientific), and Sanger sequenced using primer *cts*-Rp (Table 2). Nucleotide sequences were visualized and checked for quality using CHROMAS LITE 2.01 (Technelysium, South Brisbane, QLD, Australia), trimmed to 409 bp length and aligned using MUSCLE as implemented in MEGAX (Kumar *et al.*, 2018). Each *cts* sequence that differed from the rest of the sequences by one or more nucleotides was assigned a different allele number. To classify the bacterial isolates according to their phylogroup (PG) of affiliation within the Pssc, a cladogram using the Neighbor Joining (NJ) method and the Maximum Composite Likelihood model of evolution, was constructed using MEGAX. The 64 homologous nucleotide sequences representative of the 13 recognized phylogroups of the Pssc according to Berge *et al.* (2014) and those of 41 Pssc strains used in this study were included in the analysis for comparative purposes.

To confirm identifications based on *cts* sequence analysis, bacteria ascribed to Pssc PG01/b and PG07 were subjected to further molecular analyses (Table 2). The DNA of all isolates allocated within PG01/b, was tested using the Psa specific protocol developed by Gallelli *et al.* (2011), and by analyzing the sequence of a fragment of the *pfk* gene reported as useful to discriminate between biovars 1, 2 and 3 of Psa, and Pfm (Chapman *et al.*, 2012). Bacteria ascribed to PG07 were investigated using the

Table 2. List of PCR primers and probes used or developed in this study, along with their nucleotide sequences.

Primers/Probe	Sequence (5'-3')	Genomic target	Specificity	Expected product size (bp)	Reference
Plasm L1	TCGGCGCCATTTTCGATTG				
Plasm R1	ATAACCGACCAGCCGTTGA	<i>lscy</i> (levansucrase γ)	Psa3	231	Luti <i>et al.</i> , 2021
Plasm P1	FAM-GCCGCTACATCTAGCAGGTA-TAMRA				
Pvir 1L	GAAGAATCGGCAGACGCTTC				
Pvir 4RD	GCCGAAGCGCTGTGCA	<i>rpoD</i> (RNA polymerase sigma 70 factor)	Pv7	81	this study
Pvir 2P	FAM-AGAAGACGAAGTCGAAAGCG-TAMRA				
<i>cts</i> -Fp	AGTTGATCATCGAGGGCGCWGCC	<i>cts</i> (citrate synthase)	<i>Pseudomonas</i> sp.	480	Sarkar and Guttman, 2004
<i>cts</i> -Rp	TGATCGGTTTGATCTCGCACGG				
PsrhoD FNP1	TGAAGGCGARATCGAAATCGCCAA	<i>rpoD</i> (RNA polymerase sigma 70 factor)	<i>Pseudomonas</i> sp.	700	Parkinson <i>et al.</i> , 2011
PsrhoDnprpcr1	YGCMGWCAGCTTYTGCTGGCA				
<i>pfk</i> -Fp	ACCMTGAACCKKGCCTGGA	<i>pfk</i> (phosphofructokinase)	<i>P. syringae</i>	850	Sarkar and Guttman, 2004
<i>pfk</i> -Rp	ATRCCGAAVCCGAHCTGGGT				
KN-F	CACGATACATGGGCTTATGC	<i>ompP1</i> (outer membrane protein P1)	Psa	492	Koh and Nou, 2002
KN-R	CTTTTCATCCACACTCCG				
AvrDdpx-F	TTTCGGTGGTAACGTTGGCA	<i>avrD1</i> (avirulence gene D1)	Psa	226	Gallelli <i>et al.</i> , 2011
AvrDdpx-R	TTCCGCTAGGTGAAAATGGG				
ORF1/2-Fw	CGACCTGCTTTCGATCA	T-PAI	Pssc PG07/08	900	Bartoli <i>et al.</i> , 2014
ORF1/2-Rv	TCAATACTCTGGAGATCAG				

rpoD based phylogenetic scheme developed by Parkinson *et al.* (2011) and by sequencing a fragment of a Pv7 characteristic pathogenicity island (T-PAI) described by Araki *et al.* (2006) and Bartoli *et al.* (2014). At last, isolates that according to molecular analyses could be identified as Psa3 and Pv7 were further characterized using the LOPAT scheme (Lelliott and Stead, 1987) and additional biochemical tests according to Berge *et al.* (2014) and Schaad *et al.*, (2001): aesculin degradation, acidification of sucrose, and utilization of D(-) tartrate, mannitol or glucose as sole carbon sources.

The gene sequences analyzed in this study are available in GenBank under the following accession numbers: MW701434 to MW701442, MW716007-15, MW716028-39, MW716040, MW727267, MW814986-92, MW826360 and MW826361.

Primers and TaqMan probes design, PCR approaches and amplification conditions

Primers and probe for Psa3 were previously used by Luti *et al.*, (2021) to study *in vitro* expression of a functional levansucrase coding gene, *lscy*, is located on a non-self-transmissible low copy plasmid (NZ_CP012180.1) in the Psa3 ICMP 18708 genome. In the present study, the identification of a specific genome sequence used to design a PCR assay for Pv7, was obtained by a close evaluation of nucleotide variability existing among Pssc members in the *rpoD* housekeeping gene (HK) (Table 2 and Supplementary Figure S2a and b). All primers and probes were synthesized by Eurofins GmbH. Probes were labeled with 6-carboxyfluorescein (FAM) as the fluorescent reporter dye and 5-Carboxy-tetramethylrhodamine (TAMRA) as the quencher dye.

Primers/probe sets were used in two types of TaqMan based PCR approaches: qPCR and BIO-PCR (i.e., “biological amplification of PCR targets prior to their enzymatic amplification”; Schaad *et al.*, 1999). TaqMan qPCR was used to index for Psa3 (qPCR_{Psa3}) and Pv7 members (qPCR_{Pv7}) in different AcdH tissues. The assays were run from total nucleic acids extracted from kiwifruit leaf and cane tissues, and total genomic DNA from bacterial reference strains and purified isolates from this study (Figure 1). TaqMan BIO-PCR was used to verify the presence living cells of Psa3 (BIO-PCR_{Psa3}) and Pv7 (BIO-PCR_{Pv7}) within the culturable bacteria growing on isolation plates. The assays were run on total nucleic acids extracted from the cultivable fraction of the microorganisms that were infecting/contaminating canes or artificially inoculated leaves and that were able to grow on KBCA (canes) or NSA (leaves) plates within 96 h at 27°C.

qPCRs and BIO-PCRs reactions each contained 2 × GoTaq® Probe qPCR Master Mix (Promega Corporation, Madison, Wisconsin, USA), 0.5 μM of each primer and 0.3 μM of probe. One μL of total nucleic acids from isolation plates (BIO-PCR) or of bacterial genomic DNA, or 3 μL of total nucleic acids extracted from kiwifruit leaves or canes washings, were used as template, respectively. Nuclease-free water was added to a final volume of 15 μL. All reactions were carried out in the CFX96™ Real-Time PCR Detection System (Bio-Rad Laboratories, Hercules, California, USA).

The thermal cycling conditions included a denaturation step at 95°C for 5 min, followed by 40 cycles at 95°C for 15 s and 62°C for 1 min. Detection and quantification of fluorescence were read after every cycle and data were assembled using the CFX Manager Software (Bio-Rad Laboratories). In all PCR experiments, a positive control (Psa3KL103 or KL318; Pv7aKL5 or KL317) and three non-template controls (NTC) were included to test PCR performance: water, nucleic acids extracted from non-infected plant tissues (leaf or cane), and a non-target bacterial strain (Psa3 or Pv7a). Signal threshold levels were set automatically by the system.

In vitro determination of qPCR assays specificity and sensitivity

Specificity of the qPCR assays was assessed using reference bacterial strains and purified isolates listed in Table 1 and Supplementary Table S1.

DNA concentration was measured using a picodrop (Picodrop Ltd, Cambridge, England). A serial dilution of each Pv7aKL5 and Psa3KL103 genomic nucleic acids ranging from 60 ng to 6 fg μL⁻¹ was used to evaluate the sensitivity and linearity of the qPCR assays in: i) nuclease-free water, ii) 4 ng of DNA extracted from strains Pv7aKL5 (qPCR_{Psa3}) or Psa3KL103 (qPCR_{Pv7}), or iii) 4 ng of DNA extracted from non-infected AcdH (host) or tobacco (non-host) leaves (qPCR_{Psa3} and qPCR_{Pv7}) (Figure 1). Each dilution series always included plant, bacterial DNA, and no-DNA negative controls. Additionally, 10-fold serial dilutions of Psa3KL103 and Pv7aKL5 cells, ranging from 10⁸ to 10² CFU mL⁻¹ of saline (as determined by colony counting on NA plates) were added to AcdH leaf or cane tissues prior to DNA extraction. Briefly, 1 mL of each bacterial suspension was added to 1 g of healthy AcdH crushed leaf blade homogenized in 4 mL of saline solution, or to 0.5 g of wood chips in 6 mL saline (Figure 1). Nucleic acids extraction and qPCR testing were performed as previously described.

In all experiments, qPCR reactions were carried out in quadruplicate, and the limit of detection (LOD) for

each substrate was defined as the lowest target amount giving a positive qPCR result in at least three of the four reactions. The mean values of the quantification cycle (Cq) obtained were plotted against the logarithm of each the DNA or CFU concentration in the reactions, to calculate the slopes (k) and intercepts (q) of the standard regression lines using Excel (Microsoft). Relationships between Cq and target copy numbers were evaluated by calculating the coefficient of determination (R^2). The slopes of the standard regression lines were used to calculate amplification efficiency (E) using the equation $E = 10^{-1/\text{slope}} - 1$ (Bustin *et al.*, 2009; Bustin and Huggett, 2017). All experiments were conducted at least twice.

In vivo assessment of specificity and sensitivity of qPCR assays

Naturally infected leaves and canes

Leaf samples were collected during the 2018 vegetative season from six AcdH orchards in Lutirano, at 21 (May), 57 (June), 92 (July), 162 (September) and 190 (October) days after bud break (dabb), which occurred on 16 April 2018 in orchard No. 1. In each orchard, seven contiguous plants along a row were arbitrarily chosen 2 weeks prior to bud break, and one leaf was collected from each plant at each sampling time. At each sampling, plants were carefully inspected for presence of leaf symptoms (ts) previously described as typical of kiwifruit bacterial canker (Vanneste *et al.*, 2011) or of bacterial blight (Young *et al.*, 1988), i.e., brown angular lesions surrounded by a distinct yellow halo that becomes narrow and faded on aged leaves. If no leaves showing ts could be found, plants were screened again for presence of generic bacterial canker spots (gs) on leaves, i.e., necrotic spots brown to dark brown in color, size varying from pinpoint to large, and elliptical, angular, or irregular shaped without yellow halos (Serizawa *et al.*, 1989; Vanneste *et al.*, 2011). If no symptoms were present, an asymptomatic leaf (al) was collected (Supplementary Figure S3). Total nucleic acids were directly extracted and indexed using qPCR_{Psa3} and qPCR_{Pv7}, as indicated above using two replications. At each sampling time, bacterial isolation was also carried out from one of the seven leaves collected in each orchard, by dilution-plate on KBCA followed by isolate purification and characterization as described above (Figure 1).

Canes showing symptoms of dieback were selected during winter pruning (26 March 2018) in orchard No. 3 (Supplementary Figure S3) and sectioned in 20 cm fragments. Twenty sections were immediately taken to the laboratory while 60 sections were placed in four

gauze-enclosed frames (15 sections/frame) and buried 5 cm deep into the ground along four different plant rows as described by Tyson *et al.*, (2012). Forty-two (May), 77 (June) and 117 (July) days after pruning (dap), 20 sections (five sections/frame) were retrieved from the orchard floor. Bacterial isolation on KBCA, total nucleic acids extractions, BIO-PCRs and qPCRs were performed as described above (Figure 1). Two replications per each DNA sample were used.

Chi-square contingency table (2X2) analysis was performed to examine differences in the distribution of Psa3 and Pv7 across the different types of leaf symptoms (ts, gs, al), or for each of the two bacteria, according to the indexing methodology (qPCR vs. dilution plating or qPCR vs. BIO-PCR). Yates correction for continuity was applied (Zar, 1999).

Artificially inoculated leaves

In May 2020 (bud break occurred on 30 March), presence of Psa3 and Pv in the leaves of six, 4-year-old female potted plants of AcdH maintained at the University of Florence was assessed using the two qPCR protocols, and by isolation onto KBCA and NSA amended with 60 mg L⁻¹ cycloheximide. In June, strains Pv7aKL317 and Psa3KL318, which had been isolated from the same leaf in 2018 at Lutirano (Supplementary Table S1), were grown for 72 h on NA plates at 27°C, suspended in sterile distilled water to a concentration of 10⁸ CFU mL⁻¹, and individually inoculated (on 8 June 2020) onto 40 leaves of each of two plants per bacterial strain. Each leaf was inoculated by rubbing two 10 µL droplets of bacterial suspension on the two opposite sides of the adaxial midrib of a fully expanded leaves using gloved fingers (Renzi *et al.*, 2012). The rubbed area was labeled with a marker, and two control plants were inoculated in a similar manner with sterile distilled water. Each leaf was then enclosed in a plastic bag for 24 h, and all plants were then maintained outdoor and watered daily. The plants were sprayed once a month with boscalid (Cantus®, BASF, Italy) from June to September as a prophylactic treatment for gray mold disease (*Botrytis cinerea*). Four, 11, 18 (June), 42 (July) and 85 (September) days after inoculation (dai), 12 leaves from each treatment were inspected for symptoms (ts, gs) and were then collected. Approx. 1 g of leaf blade tissue including the labeled areas of inoculation, was excised with a sterile scalpel inside a laminar flow hood, and isolation on NSA, total nucleic acids extraction from growth plates and BIO-PCR indexing, were performed as described above. Nucleic acids extraction from the leaves and qPCR indexing were carried out as previous-

ly described (Figure 1). Two replications per each total nucleic acid sample were used. To verify that sequence amplicons of qPCR for Psa3 and Pv7 corresponded to their target, the respective amplification products were purified from a selection of qPCR reactions showing different Cqs, and these were Sanger sequenced in forward and reverse (Figure 1). Sequence identity (%) was evaluated by comparison with the homologous sequences of strains Pv7aKL317 and Psa3KL318.

RESULTS

Phylogeny of the Pseudomonas sp. community inhabiting AcdH in Tuscany (Italy)

cts sequence comparison of the 240 isolates recovered from kiwifruit on KBCA between 2014 and 2020 showed the existence of 73 alleles (Supplementary Table 1). Neighbor joining analysis indicated that 45 alleles (169 strains) could be ascribed to the Pssc, and 30 of these could be classified both to PG and subclade level according to Berge *et al.*, (2014). These were: PG01 (three alleles in clade b), PG02 (14 alleles of which one was in clade a, nine in clade b, one in clade c and three in clade d), PG07 (four in clade a), PG12 (two alleles in clade b) and PG13 (seven alleles in clade a). For alleles-18 and -19, the subclade of classification within PG02 could not be determined. Neighbor joining analysis indicated that 13 alleles, although ascribable to the Pssc following the procedure of Berge *et al.*, (2014), could not be allocated into canonical PGs (Supplementary Table 1). Overall, among the *cts* alleles found within the Pssc associated with kiwifruit in Tuscany, 23 were novel (based on GenBank database searches, <https://www.ncbi.nlm.nih.gov/genbank>), 18 were found in only one of the Pssc strains that were typed. Allele-1 was the most common, being shared by 24 strains isolated from five of six orchards at Lutirano in different years, seasons, and from different plant tissues. Based on the *Pseudomonas sp.* used as reference in the *cts* identification scheme, 20 of the remaining 28 alleles could be ascribed to this genus (59 strains). The remaining eight alleles (12 strains) were distantly related to the references included in the analyses, although results of identity searches carried out in GenBank indicated closest similarities to *Pseudomonas* (data not shown). Altogether, 24 alleles that we ascribed to *Pseudomonas sp.* were new, 18 were found only in one kiwifruit strain, and one (allele-50), within 14 strains isolated from kiwifruit leaves in different years and orchards, was the most prevalent. Evidence was found showing that members of six of the 13 phylogroups forming the Pssc, were associated to AcdH in Tuscany.

qPCRs specificity testing

Of the 78 reference strains used in this study (Table 1), 57 of which were Pssc, only Psa3 strains (ICMP 18708, ICMP 18884, ICMP 19076, CFBP 7286, CFBP 7906 and CFBP 8302) were successfully amplified with the qPCR_{Psa3} assay, indicating 100% specificity. When qPCR_{Pv7} was used, only the DNA of the Pv and Ps strains that belong to PG07/a and 07/b according to *cts*, or to PG07 according to *rpoD* analysis results (Table 1), could be amplified. Indeed, no qPCR_{Pv7} signal was obtained from strains ICMP 13105 (PG02), ICMP 13110 (PG02), ICMP 13302 (PG03), ICMP 13303 (PG03), CFBP 4476 (PG02), TOMA3-02 (PG01), TOME9-02 (PG01), TOMU4-02 (PG01) and OrSU-MM (PG03), although all of these are all classified as Pv in their respective collections of origin. Since the DNA of Pv CFBP 8511 (PG08) was also discriminated, the qPCR_{Pv7} assay is considered to be 100% specific for Pv members of the PG07 clade.

To accurately assess specificity against the background *Pseudomonas sp.* community associated with kiwifruit in Tuscany, qPCR assays were used on the DNA extracted from 240 strains isolated from AcdH leaves (143 isolates), sap (23) and canes (74), on KBCA between 2014 and 2020 and on NSA in 2020 (Supplementary Table S1). When tested with the qPCR_{Psa3} assay, only the DNA from 24 strains isolated from leaves (22) or canes (two) in different years and orchards at Lutirano, could be amplified. For all of these isolates, *cts* and *pfk* gene sequence analyses showed 100% identity with the homologous sequences of the Psa3 pathotype strain (ICMP 9617). Moreover, they all tested positive to the Psa-specific PCR protocol developed by Gallelli *et al.* (2011), their LOPAT profile was Ia, they all weakly hydrolyzed aesculin, produced acid from sucrose, did not produce fluorescence on KB, and grew with mannitol and glucose but not with D(-) tartrate as sole carbon sources (data not shown). Based on these results, analytical specificity of the qPCR_{Psa3} assay was 100% also when tested against representative isolates of the cultivable fraction of the *Pseudomonas sp.* community associated to kiwifruit in Tuscany.

For the qPCR_{Pv7} assay, only the DNA of nine strains that were isolated in different years and orchards at Lutirano, was amplified. Seven strains were isolated from leaf tissues and two from canes after 77 days of permanence in orchard No. 3 floor. These strains were the only ones that, according to *cts* (four alleles in clade a) and *rpoD* (four alleles) NJ analyses, belong to PG07/a and PG07, respectively (Supplementary Table 1 and Figure S4). With the exception of strains UCR-1 (PG07/a)

and TOMP2-02 (PG07/b), a Pv T-PAI fragment (Bartoli *et al.*, 2014), was successfully amplified from the PG07 strains used in the present study. Sequencing of these products confirmed the existence of high variability, not only between Pv reference strains, which were collected from different hosts and from different continents, but also within the Pv7a population resident in Lutirano. These strains were placed in seven clades by NJ analysis, with the five strains that shared the *cts* allele-24 partitioned in four of them (Supplementary Figure S5). In accordance with *P. viridiflava*, all PG07 strains isolated at Lutirano hydrolyzed aesculin, did not produce acid from sucrose, and grew with mannitol, glucose and D(-) tartrate as sole carbon source (data not shown). At last, according to the LOPAT scheme, strains KL24, KL48, KL317, KL396 and KL397 (*cts*-allele 24) can be ascribed to group II (*P. viridiflava*), while strains KL5, KL6, KL332 and KL345 (*cts* allele-23, -21, -22) could not, since they did not induce HR on tobacco (Lelliot and Stead, 1987).

Based on strains and isolates characterization carried out herein, qPCR_{Pv7} assays has a theoretical 100% analytical specificity for Pv7.

In vitro sensitivity of the qPCR assays

When adding Psa3KL103 or Pv7aKL5 DNA to either water, a background (4 ng) of non-target bacterial DNA (Psa3KL103 or Pv7aKL5), or non-target nucleic acids extracted from plant (AcdH or *N. tabacum*), the LOD was 60 fg for both qPCR_{Psa3} and qPCR_{Pv7} (Table 3). In general, addition of non-target nucleic acids (non-target bacteria or plants) increased the sensitivity of qPCRs,

with the exception of when either type of plant DNA was added to qPCR_{Psa3}. For both qPCR assays, R^2 values were greater than 0.997 in all reaction conditions, while E varied in a range from 99.3% (qPCR_{Psa3} with presence of AcdH nucleic acids) to 113.1% (qPCR_{Pv7} with presence of Psa3KL103 DNA).

When leaf or cane tissues were spiked with Pv7aKL5 or Psa3KL103 cells and total nucleic acids co-extracted using CTAB (leaf) or boiling lysis (canes) methods (Table 4), the derived R^2 values indicated that both assays were suitable for quantifying the bacterial targets ($R^2 > 0.980$; Bustin and Huggett, 2017), showing linearity over the nominal range of 10^8 to $10^4/10^3$ CFU g⁻¹. However, while both assays had good amplification efficiency (within the 95–105% range; Bustin and Huggett, 2017) for nucleic acids extracted from leaf tissues using CTAB, the efficiency of both assays decreased when applied to nucleic acids extracted from cane tissues using boiling lysis (Table 4).

In vivo sensitivity and specificity of the qPCR assays

Naturally infected leaves

A total of 210 leaves were collected from the six kiwifruit orchards that were monitored during the 2018 growing season. Of these, 39 were recorded as ts, 85 as gs, and 86 were al. At the first sampling time, approx. 21 d from bud break, no ts symptoms could be found in any orchard and the incidence of gs was low (four leaves out of 42) (Table 5). In subsequent samplings, the presence of ts or gs was always observed, albeit their relative abundance varied between orchards (data not shown).

Table 3. Limit of detection of the qPCR assays developed in this study on Psa3KL103 and Pv7aKL5 nucleic acids in different substrate backgrounds.

Substrate ^a	Range ^b (fg/reaction)		qPCR _{Psa3}						qPCR _{Pv7}					
			LOD ^c		Linear regression ^e				LOD		Linear regression			
	From	To	Cq ^d	SD	k	q	E	R ²	Cq	SD	k	q	E	R ²
water	6*10 ⁶	60	35.88	±1.4	-3.323	41.6	99.93	0.999	35.36	±0.6	-3.282	41.09	101.6	0.999
bacterium	6*10 ⁶	60	34.78	±1.1	-3.077	40.6	111.3	0.997	35.06	±0.7	-3.043	40.31	113.1	0.998
AcdH	6*10 ⁶	60	38.35	±0.3	-3.338	44.1	99.32	0.999	34.57	±0.5	-3.308	40.49	100.5	0.999
Nt	6*10 ⁶	60	38.30	±0.4	-3.209	43.9	104.9	0.999	34.21	±0.4	-3.160	39.94	107.2	0.999

^a Background substrate of water, 4 ng of non-target bacterial DNA (Pv7aKL5, qPCR_{Psa3}; Psa3KL103, qPCR_{Pv7}), 4 ng of non-infected kiwi (AcdH) or tobacco (Nt) leaf nucleic acids.

^b Psa3KL103 or Pv7aKL5 DNA per 15 µL reaction mixture.

^c Limit of Detection.

^d Average Cq values were calculated for four PCRs from the lowest bacterial concentration detected.

^e Linear regression of all positive samples: k and q, slope and intercept of the standard regression line; E, average efficiency of amplification; R², coefficient of determination.

Table 4. Limit of detection of qPCR analyses of kiwifruit leaf and cane extracts, spiked with bacterial cell suspensions of Psa3KL103 or Pv7aKL5 prior to nucleic acids extraction using the CTAB (leaves) or boiling lysis (canes) methods .

PCR	Spiked leaves								Spiked canes							
	Range ^a (CFU g ⁻¹)		LOD ^b		Linear Regression ^d				Range (CFU g ⁻¹)		LOD		Linear Regression			
			Cq ^c	SD	k	q	E	R ²			Cq	SD	k	q	E	R ²
qPCR _{Psa3}	10 ⁸	10 ³	37.99	±0.5	-3.419	40.20	96.08	0.999	10 ⁸	10 ⁴	37.17	±0.8	-3.957	44.40	78.94	0.989
qPCR _{Pv7}	10 ⁸	10 ³	35.72	±0.3	-3.308	37.44	100.5	0.999	10 ⁸	10 ³	38.05	±0.2	-3.078	39.39	111.2	0.992

^a Concentration of Psa3KL103 or Pv7aKL5 cells per 1 g of healthy leaf or cane tissue, added prior to DNA extraction.

^b Limit Of Detection.

^c Average Cq values were calculated for four PCRs from the lowest bacterial concentration detected.

^d Linear regressions of all positive samples: k and q, slopes and intercepts of the standard regression lines; E, average efficiencies of amplification; R², coefficients of determination.

Table 5. Analyses of symptomatic and asymptomatic kiwifruit leaves collected from six orchards during the 2018 vegetative season 21, 57, 92, 162 or 190 days after bud break (DABB). At each time point from each of seven plants in a row/orchard, one leaf was collected, scored as asymptomatic (al) or symptomatic (ts, typical symptoms, gs, generic symptoms; see Figure S3 and text for description). Presence of Psa3 and Pv7 was verified using qPCR, and by dilution plating of plant tissue extracts on KBCA followed by purification and characterization of single bacterial colonies (one leaf/orchard/time point).

DABB	Numbers of positive leaves /total numbers of leaves analyzed					
	qPCR			Isolates characterization		
	ts	gs	al	ts	gs	al
<i>Psa3</i>						
21	0/0	1/4	1/38	0/0	0/0	0/6
57	13/14	4/12	0/16	3/4	0/1	0/1
92	12/15	0/9	0/18	2/2	0/3	0/1
162	5/8	2/26	0/8	1/1	1/5	0/0
190	2/2	0/34	0/6	0/0	0/6	0/0
TOTAL	32/39	7/85	1/86	6/7	1/15	0/8
<i>Pv7</i>						
21	0/0	1/4	11/38	0/0	0/0	0/6
57	7/14	3/12	7/16	1/4	0/1	0/1
92	5/15	1/9	1/18	0/2	1/3	0/1
162	0/8	1/26	1/8	0/1	0/5	0/0
190	0/2	2/34	1/6	0/0	0/6	0/0
TOTAL	12/39	8/85	21/86	1/7	1/15	0/8

Ts symptoms were most commonly observed at 57 dabb (June) and 92 dabb (July), while gs symptoms were greatest toward the end of the season, at 162 and 190 dabb.

Based on qPCR_{Psa3} results, 40 leaves (19%) were positive for Psa3 throughout the season. Of these, 32 and seven were recorded as ts or gs, respectively. Only

one leaf was scored as asymptomatic. According to qPCR_{Pv7}, 41 leaves were positive for the presence of Pv7 DNA. Of these, 12 and eight were showing ts or gs, respectively, while 21 were asymptomatic. The overall frequency of detection differed ($P < 0.001$) significantly between Psa3 and Pv7 in ts leaves, as well as in asymptomatic leaves, but not in leaves showing gs ($P > 0.50$).

Results obtained from dilution plating on KBCA followed by strain typing were in agreement ($P > 0.90$) with those obtained by qPCR_{Psa3}. Twenty-two out of 30 leaves were negative and six were positive in both procedures, one leaf was positive to qPCR_{Psa3} only, and one leaf was positive only in Psa3 standard isolation. The results of the two approaches were also in agreement for Pv7 ($P > 0.05$). Twenty-three leaves tested positive and two leaves were negative, from both procedures, five leaves tested positive to qPCR_{Pv7} only, and no leaves were positive for isolation only (Supplementary Table S2).

Naturally infected canes

qPCR_{Psa3} results confirmed the widespread presence of Psa3 in symptomatic canes (bc) collected in Luti-rano at the time of winter pruning, with 19 out of 20 segments testing positive (Table 6). Thereafter, a sharp decrease in the frequency of Psa3 positive samples was recorded during the permanence of canes in the orchard floor, until the DNA of the bacterium became undetectable 117 dap. Selection and characterization results of the most common bacterial colony morphotypes, indicated that pruning was the only time at which Psa3 could be separated from the rest of the microorganisms that grew on KBCA plates. Nevertheless, when the same plates were washed and the growing microbial mass was analyzed with BIO-PCR_{Psa3} (culturable cells), evidence of Psa3 presence in the isolation plates was found until

Table 6. Analyses of dieback cane sections collected in orchard No. 3 at pruning time (0) or 42, 77 or 117 days after pruning (DAP), during which time cane sections were maintained buried at 5 cm depth in the orchard soil. Presence of Psa3 and Pv7 was verified using qPCR, and by dilution plating of the extracts on KBCA followed by BIO-PCR or by purification and characterization of single bacterial colonies.

DAP	Numbers positive sections/total numbers of sections analyzed					
	Psa3			Pv7		
	qPCR	BIO-PCR	Isolates characterization	qPCR	BIO-PCR	Isolates characterization
0	19/20	13/20	1/20	15/20	1/20	0/20
42	4/20	2/20	0/20	10/20	4/20	0/20
77	5/20	5/20	0/20	5/20	5/20	2/20
117	0/20	0/20	0/20	5/20	3/20	0/20
TOTAL	28/80	20/80	1/80	35/80	13/80	2/80

77 dap (Table 6). Overall frequencies of Psa3 detection were not statistically different ($P > 0.1$) between qPCR-Psa3 (viable, culturable, and dead cells) and BIO-PCR-Psa3 (culturable cells).

According to qPCR-Pv7, Pv7 was also a common inhabitant of bc canes at the time of pruning, as 15 out of 20 assessed cane sections were found positive. As for Psa3, the concentration of Pv7 DNA decreased, although less steeply, during the permanence of the canes in the orchard floor, but unlike Psa3, Pv7 remained detectable until 117 dap, when five out of 20 assessed cane sections tested positive. Only at the 77 dap time point, Pv7 colonies were successfully separated from the bacterial mass growing on KBCA plates, although BIO-PCR-Pv7 indi-

cated that culturable Pv7 was occasionally present in the plates from pruning time (one section out of 20) to the end of the trial. Overall frequency of Pv7 detection by qPCR-Pv7 was significantly different ($P < 0.001$) from that obtained with BIO-PCR-Pv7.

Artificially inoculated leaves

Nucleic acids extracted from leaves of six AcdH potted plants in May 2020, just prior to inoculation with Psa3KL318 and Pv7aKL317, tested negative in the qPCR and BIO-PCR assays. However, standard isolation on both NSA and KBCA followed by isolate characterization at that time indicated the presence of bacteria belonging to PG02/b and PG02/d of Pssc (Supplementary Table S1). None of the inoculated or non-inoculated leaves showed bacterial disease symptoms throughout the trial. Taking into account their respective LOD values estimated *in vitro* ($C_q=37.99$, qPCR-Psa3; $C_q=35.72$, qPCR-Pv7a), when qPCR-Psa3 and qPCR-Pv7 were applied to the nucleic acids extracted from leaves, the frequency of detection of the two bacteria (Table 7) was greatest at 4 dai (six leaves tested positive to qPCR-Psa3 and ten leaves were positive for qPCR-Pv7). Thereafter, detection decreased until the end of the trial (85 dai), when none (qPCR-Psa3) or one (qPCR-Pv7) of the sampled leaves tested positive. According to qPCR-Psa3 and qPCR-Pv7, the amounts of the two bacteria per g of leaf, when detected, were stable and similar until 42 dai, varying from 3.96 to 3.83 log CFU g⁻¹ for Psa3 and 4.3 to 3.5 log CFU g⁻¹ for Pv7.

Results obtained by selection and identification of colony morphotypes growing on NSA plates showed only three leaves as infected with Psa3 (two sampled at

Table 7. Analyses of artificially infected leaves from kiwi potted plants, 4, 11, 18, 42 or 85 days after inoculation (DAI) with strains Psa3KL318 or Pv7aKL317. Presence of Psa3 and Pv7 was verified using qPCR, and by dilution plating of the extracts on NSA followed by BIO-PCR or by purification and characterization of single bacterial colonies.

DAI	Psa3					Pv7a				
	No. positive leaves/total No. of leaves analyzed			C_q^a (SD)	Log CFU g ⁻¹ _b (SD)	No. positive leaves/total No. of leaves analyzed			C_q (SD)	Log CFU g ⁻¹ (SD)
	Isolates characterization	BIO-PCR	qPCR			Isolates characterization	BIO-PCR	qPCR		
4	0/12	1/12	6/12	35.45 (±1.68)	3.96 (±0.46)	0/12	1/12	10/12	31.71 (±2.01)	4.30 (±0.59)
11	0/12	3/12	2/12	36.36 (±2.19)	3.65 (±0.59)	2/12	11/12	8/12	33.53 (±1.46)	3.77 (±0.47)
18	2/12	9/12	2/12	35.68 (±1.34)	3.93 (±0.27)	3/12	12/12	5/12	34.52 (±0.46)	3.48 (±0.10)
42	0/12	7/12	1/12	36.1 (-)	3.83 (-)	0/12	6/12	5/12	34.54 (±1.22)	3.49 (±0.40)
85	1/12	3/12	0/12	-	-	0/12	6/12	1/12	31.96 (-)	4.18 (-)
TOTAL	3/60	23/60	11/60			5/12	36/60	29/60		

18 dai; one at 85 dai) and five leaves infected with Pv7 (two sampled at 11 dai; three at 18 dai). Nevertheless, according to BIO-PCR_{Psa3} and BIO-PCR_{Pv7}, the two viable bacteria were often present on/in the sampled leaves, being culturable on NSA isolation plates. The frequency of leaves from which Psa3 and Pv7 could be cultured was minimum at four dai, increased until 18 dai, and then decreased until the end of the trial (85 dai). Based on overall detection frequencies, sensitivities of qPCR_{Psa3} ($P < 0.025$) and qPCR_{Pv7} ($P > 0.05$) were, respectively, less than and equal to that of their BIO-PCR variant, but greater than isolate characterization following dilution plating on NSA ($P < 0.001$). When qPCR amplicons were sequenced to test the specificity of qPCR_{Psa3} (eight amplicons; Cq range from 33.4 to 36.6) and qPCR_{Pv7} (eight amplicons; Cq range from 29.8 to 36.5), 100% identity was found with the respective homologous sequences of Psa3_{KL318} and Pv7a_{KL317} (Supplementary Table S3).

DISCUSSION

In this work we present two new TaqMan qPCR-based approaches for sensitive and accurate detection of Psa3 (qPCR_{Psa3}) and Pv PG07 (qPCR_{Pv7}) in kiwifruit, and the procedure followed for their validation against the *Pseudomonas* sp. background microflora of kiwifruit.

The lineage of Psa3 responsible for the bacterial canker pandemic, is pathogenic to *Actinidia* sp. and possibly few other species (Liu *et al.*, 2016), and has just recently started to diversify (McCann *et al.*, 2017; Firrao *et al.*, 2018). In pursuing the development of a new specific test for the detection of the Psa3 pandemic lineage, the recently characterized *lscy* gene was targeted. The gene codes for a functional levansucrase with a peculiar signature of 15 amino acids at the N-terminal region, which, based on whole genome comparisons, has only been found in pandemic isolates of the bacterium (Luti *et al.*, 2021). More challenging was development of a qPCR assay for Pv. This bacterium is a heterogenic saprophyte, is prone to recombination, and has a complex evolutionary history, being currently allocated in PGs 7 and 8, of Pssc (Billing, 1970; Goss *et al.*, 2005; Bartoli *et al.*, 2014; Bull and Koike, 2015). To account for intrataxon variability, the present study focused on developing an assay for PG07 (Pv7), which represents most of the strains classified as *P. viridiflava* in previous studies (Berge *et al.*, 2014; Lipps and Samac, 2022), and exploited the polymorphisms of the HK *rpoD* gene.

In vitro analyses showed that both assays were sensitive and specific. However, when qPCR_{Pv7} was tested

against a collection of 78 reference bacterial strains from kiwifruit and other hosts, the DNAs of 10 strains catalogued as "*P. viridiflava*" in their collections of origin, failed to give the expected signal. Further *cts* and *rpoD* sequence analyses indicated that none of them belonged to PG07, confirming the robustness of the protocol for discriminating within the Pssc complex according to the *rpoD* phylogenetic signal (Parkinson *et al.*, 2011). For a more *ad hoc* verification, the two approaches were assessed on the DNA of 240 *Pseudomonas* sp. strains that we isolated in different years, seasons and from different kiwifruit tissues, 169 of which could be classified within the Pssc complex (PGs 01, 02, 03, 07, 12 and 13) according to their *cts* derived phylogeny. Both assays were highly specific as they distinguished Psa3 (24 isolates) and Pv7 (nine isolates).

To properly evaluate these results, it is important to recall that the range of Pssc PGs and subclades that has been found associated to kiwifruit worldwide, is much vaster than what detected in the present study. For example, the presence of PG5 and PG10 has been detected in orchards in France, but never in Tuscany (Italy). Similarly, PG03, which was very rarely isolated from kiwifruit in Tuscany in the present study, is widespread in New Zealand where it causes bacterial blight (Young *et al.*, 1997).

Phylogeographic structuring possibly exists in the Pssc metapopulation associated to *Actinidia* sp. (Bastardo *et al.*, 2017), but there is also circumstantial evidence that the decision to use a semi-selective medium (KBCA) to set-up the reference collection may have led to underestimate the variability of the *Pseudomonas* sp. community in Tuscany. KBCA was originally developed to isolate *Ps. syringae*, tomato and pisi (Mohan and Schaad, 1987). Since bacterial isolation may be difficult without the use of a semi-selective media, use of KBCA has become a common practice to investigate the composition of Pssc in different environmental samples, as well as a standard when indexing for Psa3 (Riffaud and Morris, 2002; Morris *et al.*, 2008; Loreti *et al.*, 2018; Parisi *et al.*, 2019). Keeping in mind that also "all-purpose" media are selective to some extent, NSA and KBA amended only with cycloheximide (King *et al.*, 1954) were used in the preliminary phases of the present study to isolate Pssc bacteria from naturally infected leaves and canes. However the mass of microorganisms growing in the first 72 h of culturing was often so abundant that isolation of Pv, and especially of Psa3, was strongly hindered (data not shown). Although the use of KBCA reduced this problem, the trade-off was possibly a data bias towards a simplified *Pseudomonas* sp. population structure (i.e. underestimation of variability), as has

been previously shown for Pssc and specifically for Pv (Gitaitis *et al.*, 1997; Morris *et al.*, 2008). The present study then evaluated the effective degree of specificity of the two assays in three validation experiments, using plant tissues that contained natural or artificial populations of the target organisms as well as of their background microflora. These tissues included naturally infected leaves or canes collected in different orchards during the vegetative growth season, or artificially infected leaves of nursery plants.

Results from orchard leaves obtained by means of qPCRs or dilution plating on KBCA followed by isolate typing (*cts*, *rpoD* and *pfk* genes) were in good agreement and indicated that during the 2018 vegetative season in Tuscany there was an association of Psa3, but not of Pv7a, with leaves showing ts symptoms. Previous research has indicated that these symptoms can be caused by both target bacteria (Young *et al.*, 1988, 1997; Serizawa *et al.*, 1989; Balestra *et al.*, 2009; Vanneste *et al.*, 2011). As previously reported in New Zealand and Japan, the frequency of ts leaves in Lutirano (Tuscany) greatly increased from late spring (3 weeks after bud break), when leaves were nearly all asymptomatic, to mid-summer, and then progressively decreased until the end of the kiwifruit growing season (late Autumn in Tuscany). In contrast, frequency of gs increased and of asymptomatic leaves decreased with leaf aging (Vanneste *et al.*, 2011). Accordingly, qPCRPs3 results indicated that the bacterium was significantly associated to ts leaves, rarely to gs leaves, and never with asymptomatic leaves, highlighting the specificity of the assay also when tested against the kiwifruit leaves background microflora present in each orchard.

Pv is a common member of the Pssc associated with kiwifruit phylloplane in Central Italy, where its population reaches a major peak in spring and a secondary one in autumn (Balestra and Varvaro, 1998). However, the capability of Pv to induce ts symptoms on kiwifruit leaves is controversial. In California and in Central Italy, Pv (LOPAT II), together with *P. syringae* (LOPAT Ia), is reported as the agent of kiwifruit bacterial blight, a disease characterized by the development of ts leaf spots and flower bud rot. In New Zealand, after further characterization of the pathogenic isolates, it was concluded that the agent of bacterial blight, a bacterium with a LOPAT II profile, was misidentified as Pv and should be classified in the PG03, *P. savastanoi*, of the Pssc (Conn *et al.*, 1993; Young *et al.*, 1997; Hu *et al.*, 1999; Visnovsky *et al.*, 2019). Based on qPCR Pv7 results the present study confirmed that Pv7 is a common inhabitant of kiwifruit leaves in Tuscany. However, the present study data also show that in the Tuscan environment, in

contrast to Psa3, Pv7 is a leaf saprophyte rather than a pathogen, since: i) its frequency in/on the sampled leaves was high 21 days after bud break when nearly all leaves were asymptomatic; ii) its frequency in/on ts leaves was approximately 1/3 of that of Psa3; and iii) as for Psa3, its presence in/on leaves showing generic spot symptoms (gs) was only sporadic.

Following a procedure that was previously used in New Zealand orchards (Tyson *et al.*, 2012), in the second validation experiment we monitored the fate of Psa3 and, for the first time of Pv7, in pruned canes with symptoms of dieback after burying them to 5 cm depth in the orchard soil.

Since attempts to purify and characterize colony morphotypes from KBCA was hampered by the abundance of the growing microbial mass, we verified the presence of Psa3 and Pv7 in the plates by BIO-PCR, an approach that enhances likelihood of detecting the bacterial target, if in a culturable state (Schaad *et al.*, 1995, 1999). Although, with the exception of pruning time, Psa3 could not be recovered according to isolate typing results, we found that this bacterium was often effectively growing in the isolation plates, and that qPCRPs3 and BIO-PCRPs3 results were overall in strict agreement. While Psa3 was widely colonizing the woody tissues at pruning, thereafter Psa3 population rapidly diminished and became undetectable by both detection methods after approximately 4 months in the orchard floor. These results are concordant with previous findings by Tyson *et al.* (2012) using BIO-PCR in New Zealand, which showed that in early spring nearly all symptomatic canes were systematically infected, and that viable Psa could be detected only until 11 weeks of permanence of canes in the orchard floor. The present study gave similar results using BIO-PCRPs3 and qPCRPs3 at 77 dap (June). In the case of Pv7, which was recently found associated with canker tissues of plum and apricot (Parisi *et al.*, 2019; Bophela *et al.*, 2020), the qPCR Pv7 and BIO-PCR Pv7 approaches gave conflicting results at pruning. With qPCR Pv7, 75% of the cane sections were infected by the bacterium, while according to BIO-PCR Pv7, culturable Pv7 was nearly absent (5%), in accordance with isolate typing results. Over successive sampling dates, qPCR Pv7 and BIO-PCR Pv7 results were in closer agreement, with both methods indicating that 15% of cane sections were infected at 77 dap and 25% were infected at 117 dap. These results indicate that at pruning, nearly all Pv7 cells in the sampled canes were dead or were non-culturable on KBCA (low frequencies of positive according to BIO-PCR Pv7), although their DNA recovered from woody tissues was amplifiable (high frequencies of infected canes according to qPCR Pv7). Subsequently, however, either

the original Pv7 population found suitable conditions to proliferate in the decaying tissues, or the canes became re-infected. Pv is a water cycle-related bacterium, so spring rains, which are frequent and abundant in Luti-rano, could have easily dispersed Pv inoculum from the phylloplane, where the bacterium was present in 2018 at least since May, to the soil surface. Then, water movements on/in the soil, where there is circumstantial evidence that this bacterium can survive, may have facilitated its contact with the buried canes and their subsequent infection (Gitaitis *et al.*, 1997; Bartoli *et al.*, 2015; Borshinger *et al.*, 2016). Of course, Psa3 could have used the same route to reach the canes but, even so, our data indicate that the dead tissues were not a substrate where its proliferation was possible.

In the final *in vivo* experiment, fully expanded kiwifruit leaves were inoculated at the end of spring, with the aim of evaluating usefulness of the two qPCR assays for detecting asymptomatic infections. Susceptibility of kiwifruit leaves to Psa1 in Japan and to Psa3 in New Zealand, was strongly correlated with leaf age, being maximum when leaves reached 2 cm in length or are 1-3 weeks old, and then decreased progressively during aging. Spray-inoculated 7-week-old cv. Hayward leaves never showed spots or fleck symptoms (Serizawa and Ichikawa, 1993; Tyson *et al.*, 2015). Petriccione *et al.* (2014) showed that after inoculation of Psa3 CRA-FRU 8.43 on fully expanded AcdH leaves, the bacterium entered a biotrophic phase (asymptomatic) that may last several weeks, during which it was unable, at least temporarily, to overcome plant host defenses. This impedes infection progress, as indicated by stable Psa3 population in leaf apoplast, as well as absence of disease symptoms (necrotrophic phase). More recently, the infection threshold value for the transition from epiphytic phase to apoplastic invasion on AcdH leaves by Psa3 (CFBP7286), was estimated to be 4.4×10^4 CFU g^{-1} of leaf blade tissues (Donati *et al.*, 2020). The present results confirm these previous observations for Psa3KL318, but also show that Pv7aKL317 behaved in a similar fashion. Although both strains did not cause leaf symptoms throughout the trial, both survived in/on aging leaves during summer, as indicated by BIO-PCR and, for Psa3, by re-isolating the bacterium 85 dai.

The inability of Psa3KL318 to progress from biotrophic to necrotrophic phases in order to grow and multiply at higher densities in host leaves, was also evident by interpolating qPCR Cq values against the corresponding standard curves developed in this study. The average population of Psa3KL318 per leaf was nearly constant and never exceeded 10^4 CFU g^{-1} , which is in the order of magnitude of population densities reached

by Psa3 CRA-FRU 8.43 in asymptomatic leaves (Petriccione *et al.*, 2014). Keeping in mind that Pv7aKL317 and Psa3KL318 were co-infecting the same leaf in early spring of 2018, the finding that Pv7aKL317 can also sustain itself on the phylloplane at a density of 10^4 to 10^3 CFU g^{-1} , confirms that the kiwifruit phyllosphere is a niche that *Pseudomonas* spp. bacteria cohabit under a wide range of environmental conditions. Given the apparently common presence of this heterogenic community worldwide, its existence should be fully accounted for when developing specific culture-independent diagnostic assays for *Pseudomonas* sp. on kiwifruit.

In conclusion, this research has demonstrated the usefulness of TaqMan-based qPCR for sensitive and specific detection of Pv7 and Psa3 from symptomatic and asymptomatic kiwifruit tissues. Several molecular diagnostic assays for Psa3 have been previously developed, including two SYBR green qPCR protocols. The qPCR-Psa3 described here will be a valuable alternative for confirmatory analyses as it is based on different genomic targets (Gallelli *et al.*, 2014; Andersen *et al.*, 2018; EPPO PM7\120[2], 2021). Due to their reliability as monitoring tools to estimate target populations in the phyllosphere, qPCR-Psa3 and qPCR-Pv7, which represent the first molecular assays specifically developed for PG07, should facilitate future studies on colonization and survival of these pathogens in orchard conditions.

ACKNOWLEDGMENTS

The authors declare no conflict of interest. We thank Dr. Sally Miller (OSU), Dr. Caroline Roper (UCR), and Dr. Melodie Putnam (OrSU) who generously provided strains for this study, and two anonymous reviewers for their valuable input and constructive criticism.

FUNDING

This study was supported by the Phytosanitary Service of the Tuscany Region (Italy).

CREDIT AUTHORSHIP CONTRIBUTION STATEMENT

Sara Campigli: Conceptualization, Data curation, Investigation, Writing-original draft; **Simone Luti:** Investigation, Methodology; **Tommaso Martellini:** Investigation; **Domenico Rizzo:** Formal analysis, Review; **Linda Bartolini:** Investigation; **Claudio Carrai:** Formal analysis, Funding acquisition; **Jeyaseelan**

Baskarathevan: Resources, Review; **Luisa Ghelardini:** Conceptualization, Review & editing; **Francesca Peduto Hand:** Supervision, Writing, Review & editing; **Guido Marchi:** Conceptualization, Data curation, Supervision, Writing, Review & editing.

LITERATURE CITED

- Andersen M.T., Templeton M.D., Rees-George J., Van-neste J.L., Cornish D.A., ... Rikkerink E.H.A., 2018. Highly specific assays to detect isolates of *Pseudomonas syringae* pv. *actinidiae* biovar 3 and *Pseudomonas syringae* pv. *actinidifoliorum* directly from plant material. *Plant Pathology* 67: 1220–1230. <https://doi.org/10.1111/ppa.12817>
- Angelini E., Clair D., Borgo M., Bertaccini A., Boudon-Padieu E., 2001. Flavescence dorée in France and Italy—Occurrence of closely related phytoplasma isolates and their near relationships to Palatinate grapevine yellows and an alder yellows phytoplasma. *Vitis* 40: 79–86. <https://doi.org/10.5073/vitis.2001.40.79-86>
- Araki H., Tian D., Goss E.M., Jakob K., Halldorsdottir S.S.,... Bergelson J., 2006. Presence/absence polymorphism for alternative pathogenicity islands in *Pseudomonas viridiflava*, a pathogen of *Arabidopsis*. *Proceedings of the National Academy of Sciences* 103: 5887–5892. <https://doi.org/10.1073/pnas.0601431103>
- Balestra G.M., Mazzaglia A., Quattrucci A., Renzi M., Rossetti A., 2009. Occurrence of *Pseudomonas syringae* pv. *actinidiae* in Jin Tao kiwi plants in Italy. *Phytopathologia Mediterranea* 48: 299–301. DOI: 10.14601/Phytopathol_Mediterr-2821
- Balestra G.M., Varvaro L., 1998. Seasonal fluctuations in kiwifruit phyllosphere and ice nucleation activity of *Pseudomonas viridiflava*. *Journal of Plant Pathology* 80: 151–156. <http://dx.doi.org/10.4454/jpp.v80i2.812>
- Baltrus D.A., McCann H.C., Guttman D.S., 2017. Evolution, genomics and epidemiology of *Pseudomonas syringae*: challenges in bacterial molecular plant pathology. *Molecular Plant Pathology* 18: 152–168. <https://doi.org/10.1111/mpp.12506>
- Bartoli C., Berge O., Monteil C.L., Guilbaud C., Balestra G.M., ... Morris C.E., 2014. The *Pseudomonas viridiflava* phylogroups in the *P. syringae* species complex are characterized by genetic variability and phenotypic plasticity of pathogenicity-related traits. *Environmental Microbiology* 16: 2301–2315. <https://doi.org/10.1111/1462-2920.12433>
- Bartoli C., Lamichhane J.R., Berge O., Varvaro L., Morris C.E., 2015. Mutability in *Pseudomonas viridiflava* as a programmed balance between antibiotic resistance and pathogenicity. *Molecular Plant Pathology* 16: 860–869. <https://doi.org/10.1111/mpp.12243>
- Bastardo A., Balboa S., Romalde J.L., 2017. From the Gene Sequence to the Phylogeography through the Population Structure: The Cases of *Yersinia ruckeri* and *Vibrio tapetis*. In: *Genetic Diversity* (L. Bitz ed.), InTech, Rijeka, Croatia, Chapter 4, 57–87 <http://dx.doi.org/10.5772/67182>
- Berge O., Monteil C. L., Bartoli C., Chandeysson C., Guilbaud C., ... Morris C.E., 2014. A User's Guide to a Data Base of the Diversity of *Pseudomonas syringae* and Its Application to Classifying Strains in This Phylogenetic Complex. *PLoS ONE* 9: e105547. doi:10.1371/journal.pone.0105547
- Billing E., 1970. *Pseudomonas viridiflava* (Burkholder, 1930; Clara 1934). *Journal of Applied Microbiology* 33: 492–500. <https://doi.org/10.1111/j.1365-2672.1970.tb02225.x>
- Biondi E., Galeone A., Kuzmanović N., Ardizzi S., Lucchese C., Bertaccini A., 2013. *Pseudomonas syringae* pv. *actinidiae* detection in kiwifruit plant tissue and bleeding sap. *Annals of Applied Biology* 162: 60–70. <https://doi.org/10.1111/aab.12001>
- Bophela K.N., Petersen Y., Bull C.T., Coutinho T.A., 2020. Identification of *Pseudomonas* isolates associated with bacterial canker of stone fruit trees in the Western Cape, South Africa. *Plant Disease* 104: 882–892. <https://doi.org/10.1094/PDIS-05-19-1102-RE>
- Borschinger B., Bartoli C., Chandeysson C., Guilbaud C., Parisi L., ... Morris C.E., 2016. A set of PCRs for rapid identification and characterization of *Pseudomonas syringae* phylogroups. *Journal of Applied Microbiology* 120: 714–723. <https://doi.org/10.1111/jam.13219>
- Bull C.T., Koike S.T., 2015. Practical benefits of knowing the enemy: modern molecular tools for diagnosing the etiology of bacterial diseases and understanding the taxonomy and diversity of plant-pathogenic bacteria. *Annual Review of Phytopathology* 53: 157–180. <https://doi.org/10.1146/annurev-phyto-080614-120122>
- Bustin S.A., Benes V., Garson J.A., Hellems J., Huggett J., ... Wittwer C.T., 2009. The MIQE Guidelines: Minimum Information for Publication of Quantitative Real-Time PCR Experiments. *Clinical Chemistry* 55: 611–622. <https://doi.org/10.1373/clinchem.2008.112797>
- Bustin S., Huggett J., 2017. qPCR primer design revisited. *Biomolecular Detection and Quantification* 14: 19–28. <https://doi.org/10.1016/j.bdq.2017.11.001>
- Chapman J.R., Taylor R.K., Weir B.S., Romberg M.K., Vanneste J.L., ... Alexander B.J.R., 2012. Phylogenetic relationships among global populations of *Pseu-*

- domonas syringae* pv. *actinidiae*. *Phytopathology* 102: 1034–1044. <https://doi.org/10.1094/PHYTO-03-12-0064-R>
- Conn K.E., Gubler W.D., Hasey J.K., 1993. Bacterial blight of kiwifruit in California. *Plant Disease* 77: 228–230. DOI: 10.1094/PD-77-0228.
- Dillon M.M., Thakur S., Almeida R N., Wang P.W., Weir B.S., Guttman D.S., 2019. Recombination of ecologically and evolutionarily significant loci maintains genetic cohesion in the *Pseudomonas syringae* species complex. *Genome Biology* 20: 1–28. <https://doi.org/10.1186/s13059-018-1606-y>
- Donati I., Cellini A., Sangiorgio D., Vanneste J.L., Scortichini M., ... Spinelli F., 2020. *Pseudomonas syringae* pv. *actinidiae*: Ecology, infection dynamics and disease epidemiology. *Microbial Ecology* 80: 81–102. <https://doi.org/10.1007/s00248-019-01459-8>
- Dye D.W., Bradbury J., Goto M., Hayward A.C., Lelliott R.A., Schroth M.N., 1980. International standards for naming pathovars of phytopathogenic bacteria and a list of pathovar names and pathotype strains. *Review of Plant Pathology* 59: 153–168.
- EPPO Bulletin 2021. Volume 51, Issue 3, PM 7/120 (2) *Pseudomonas syringae* pv. *actinidiae*. EPPO STANDARD – DIAGNOSTICS. DOI: 10.1111/epp.12782
- FAOSTAT, 2020. Food and Agriculture Organization of the United Nations. Available at: <http://www.fao.org/faostat/en/#home>. Accessed March 16, 2021.
- Firrao G., Torelli E., Polano C., Ferrante P., Ferrini F., ... Ermacora P., 2018. Genomic structural variations affecting virulence during clonal expansion of *Pseudomonas syringae* pv. *actinidiae* biovar 3 in Europe. *Frontiers in Microbiology* 9: 656. <https://doi.org/10.3389/fmicb.2018.00656>
- Gallelli A., Talocci S., LAurora A., Loreti S., 2011. Detection of *Pseudomonas syringae* pv. *actinidiae*, causal agent of bacterial canker of kiwifruit, from symptomless fruits and twigs, and from pollen. *Phytopathologia Mediterranea* 50: 462–472.
- Gallelli A., Talocci S., Pilotti M., Loreti S., 2014. Real-time and qualitative PCR for detecting *Pseudomonas syringae* pv. *actinidiae* isolates causing recent outbreaks of kiwifruit bacterial canker. *Plant Pathology* 63: 264–276. <https://doi.org/10.1111/ppa.12082>
- Gardan L., Shafik H., Belouin S., Broch R., Grimont F., Grimont P.A.D., 1999. DNA relatedness among the pathovars of *Pseudomonas syringae* and description of *Pseudomonas tremiae* sp. nov. and *Pseudomonas cannabina* sp. nov. (ex Sutic and Dowson 1959). *International Journal of Systematic and Evolutionary Microbiology* 49: 469–478. <https://doi.org/10.1099/00207713-49-2-469>
- Gitaitis R., Sumner D., Gay D., Smittle D., McDonald G., ... Hung Y., 1997. Bacterial streak and bulb rot of onion: I. A diagnostic medium for the semiselective isolation and enumeration of *Pseudomonas viridiflava*. *Plant Disease* 81: 897–900. <https://doi.org/10.1094/PDIS.1997.81.8.897>
- Goss E.M., Kreitman M., Bergelson J., 2005. Genetic diversity, recombination and cryptic clades in *Pseudomonas viridiflava* infecting natural populations of *Arabidopsis thaliana*. *Genetics* 169: 21–35. <https://doi.org/10.1534/genetics.104.031351>
- Hirano S.S., Upper C.D., 2000. Bacteria in the leaf ecosystem with emphasis on *Pseudomonas syringae*—a pathogen, ice nucleus, and epiphyte. *Microbiology and Molecular Biology Reviews* 64: 624–653. DOI: 10.1128/MMBR.64.3.624-653.2000
- Hu F.P., Young J.M., Jones D.S., 1999. Evidence that bacterial blight of kiwifruit, caused by a *Pseudomonas* sp., was introduced into New Zealand from China. *Journal of Phytopathology* 147: 89–97.
- King E.O., Ward M.K., Raney D.E., 1954. Two simple media for the demonstration of pyocyanin and fluorescin. *Journal of Laboratory and Clinical Medicine* 44: 301–307.
- Kumar S., Stecher G., Li M., Knyaz C., Tamura K., 2018. MEGA X: Molecular Evolutionary Genetics Analysis across computing platforms. *Molecular Biology and Evolution* 35: 1547–1549. <https://doi.org/10.1093/molbev/msy096>
- Lelliott R.A., Stead D.E., 1987. *Methods for the Diagnosis of Bacterial Diseases of Plants*. Blackwell Scientific Publications, Oxford, United Kingdom, 162 pp.
- Lipps S.M., Samac D.A., 2022. *Pseudomonas viridiflava*: An internal outsider of the *Pseudomonas syringae* species complex. *Molecular Plant Pathology* 23: 3–15. <https://doi.org/10.1111/mpp.13133>
- Liu P., Xue S., He R., Hu J., Wang X., ... Zhu L., 2016. *Pseudomonas syringae* pv. *Actinidiae* isolated from non-kiwifruit plant species in China. *European Journal of Plant Pathology* 145: 743–754. DOI 10.1007/s10658-016-0863-4
- Loreti S., Cuntly A., Pucci N., Chabirand A., Stefani E., ... Poliakoff F., 2018. Performance of diagnostic tests for the detection and identification of *Pseudomonas syringae* pv. *actinidiae* (Psa) from woody samples. *European Journal of Plant Pathology* 152: 657–676. <https://doi.org/10.1007/s10658-018-1509-5>
- Luti S., Campigli S., Ranaldi F., Paoli P., Pazzagli L., Marchi G., 2021. Lsc β and lsc γ , two novel levansucrases of *Pseudomonas syringae* pv. *actinidiae* biovar 3, the causal agent of bacterial canker of kiwifruit, show different enzymatic properties. *International*

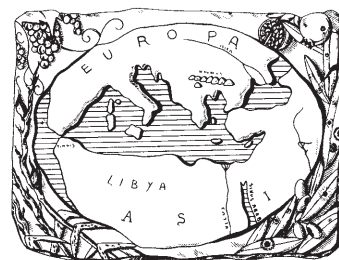
- Journal of Biological Macromolecules* 179: 279–291. <https://doi.org/10.1016/j.ijbiomac.2021.02.189>
- McCann H.C., Li L., Liu Y., Li D., Pan H., ... Huang H., 2017. Origin and evolution of the kiwifruit canker pandemic. *Genome Biology and Evolution* 9: 932–944. <https://doi.org/10.1093/gbe/evx055>
- Mohan S.K., Schaad N.W., 1987. An improved agar plating assay for detecting *Pseudomonas syringae* pv. *syringae* and *P. s.* pv. *phaseolicola* in contaminated bean seed. *Phytopathology* 77: 1390–1395.
- Mohr T.J., Liu H., Yan S., Morris C.E., Castillo J.A., ... Vinatzer B.A., 2008. Naturally occurring nonpathogenic isolates of the plant pathogen *Pseudomonas syringae* lack a type III secretion system and effector gene orthologues. *Journal of Bacteriology* 190: 2858–2870. <https://doi.org/10.1128/JB.01757-07>
- Moore E., Arnscheidt A., Krüger A., Strömpl C., Mau M., 2004. Simplified protocols for the preparation of genomic DNA from bacterial cultures. *Molecular Microbial Ecology Manual* 1: 3–18.
- Morris C.E., Kinkel L.L., Xiao K., Prior P., Sands D.C., 2007. Surprising niche for the plant pathogen *Pseudomonas syringae*. *Infection, Genetics and Evolution* 7: 84–92. <https://doi.org/10.1016/j.meegid.2006.05.002>
- Morris C.E., Sands D.C., Vinatzer B.A., Glaux C., Guilbaud C., ... Thompson B.M., 2008. The life history of the plant pathogen *Pseudomonas syringae* is linked to the water cycle. *The ISME journal* 2: 321–334. DOI: 10.1038/ismej.2007.113
- Morris C.E., Sands D.C., Vanneste J.L., Montarry J., Oakley B., ... Glaux C., 2010. Inferring the evolutionary history of the plant pathogen *Pseudomonas syringae* from its biogeography in headwaters of rivers in North America, Europe, and New Zealand. *MBio* 1: 00107–00110. <https://doi.org/10.1128/mBio.00107-10>
- Morris C.E., Lamichhane J.R., Nikolić I., Stanković S., Moury B., 2019. The overlapping continuum of host range among strains in the *Pseudomonas syringae* complex. *Phytopathology Research* 1: 1–16. <https://doi.org/10.1186/s42483-018-0010-6>
- Parisi L., Morgaint B., Blanco-Garcia J., Guilbaud C., Chan-deysson C., ... Morris C.E., 2019. Bacteria from four phylogroups of the *Pseudomonas syringae* complex can cause bacterial canker of apricot. *Plant Pathology* 68: 1249–1258. <https://doi.org/10.1111/ppa.13051>
- Parkinson N., Bryant R., Bew, J., Elphinstone J., 2011. Rapid phylogenetic identification of members of the *Pseudomonas syringae* species complex using the *rpoD* locus. *Plant Pathology* 60: 338–344. <https://doi.org/10.1111/j.1365-3059.2010.02366.x>
- Petriccione M., Salzano A. M., Di Cecco I., Scaloni A., Scortichini M., 2014. Proteomic analysis of the *Actinidia deliciosa* leaf apoplast during biotrophic colonization by *Pseudomonas syringae* pv. *actinidiae*. *Journal of Proteomics* 101: 43–62. <https://doi.org/10.1016/j.jprot.2014.01.030>
- Renzi M., Copini P., Taddei A. R., Rossetti A., Gallipoli L., ... Balestra G.M., 2012. Bacterial canker on kiwifruit in Italy: anatomical changes in the wood and in the primary infection sites. *Phytopathology* 102: 827–840. <https://doi.org/10.1094/PHYTO-02-12-0019-R>
- Riffaud C.H., Morris C.E., 2002. Detection of *Pseudomonas syringae* pv. *aptata* in irrigation water retention basins by immunofluorescence colony-staining. *European Journal of Plant Pathology* 108: 539–545. <https://doi.org/10.1023/A:1019919627886>
- Sarkar S.F., Guttman D.S., 2004. Evolution of the core genome of *Pseudomonas syringae*, a highly clonal, endemic plant pathogen. *Applied and Environmental Microbiology* 70: 1999–2012. DOI:10.1128/AEM.02553-07
- Sawada H., Fujikawa T., 2019. Genetic diversity of *Pseudomonas syringae* pv. *actinidiae*, pathogen of kiwifruit bacterial canker. *Plant Pathology* 68: 1235–1248. <https://doi.org/10.1111/ppa.13040>
- Schaad N.W., Cheong S.S., Tamaki S., Hatziloukas E., Panopoulos N.J., 1995. A combined biological amplification (BIO-PCR) technique to detect *Pseudomonas syringae* pv. *phaseolicola* in bean seed extracts. *Phytopathology* 85: 243–248. DOI: 10.1094/Phyto-85-243
- Schaad N.W., Berthier-Schaad Y., Sechler A., Knorr D., 1999. Detection of *Clavibacter michiganensis* subsp. *sepedonicus* in potato tubers by BIO-PCR and an automated real-time fluorescence detection system. *Plant Disease* 83: 1095–1100. DOI: 10.1094/PDIS.1999.83.12.1095
- Schaad N.W., Jones J.B., Chun W., 2001. *Laboratory Guide for the Identification of Plant Pathogenic Bacteria*. 3th ed. American Phytopathological Society (APS Press), USA, 373 pp.
- Serizawa S., Ichikawa T., Takikawa Y., Tsuyumu S., Goto M., 1989. Occurrence of bacterial canker of kiwifruit in Japan. *Japanese Journal of Phytopathology* 55: 427–436 (in Japanese). <https://doi.org/10.3186/jjphytopath.55.427>
- Serizawa S., Ichikawa T., 1993. Epidemiology of bacterial canker of kiwifruit. 2. The most suitable times and environments for infection on new canes. *Annals of the Phytopathological Society of Japan* 59: 460–468 (in Japanese). DOI 10.3186/jjphytopath.59.460
- Straub C., Colombi E., Li L., Huang H., Templeton M.D., ... Rainey P.B., 2018. The ecological genetics of *Pseudomonas syringae* from kiwifruit leaves. *Environmental Microbiology* 20: 2066–2084. <https://doi.org/10.1111/1462-2920.14092>

- Tyson J.L., Rees-George J., Curtis C.L., Manning M.A., Fullerton R.A., 2012. Survival of *Pseudomonas syringae* pv *actinidiae* on the orchard floor over winter. *New Zealand Plant Protection* 65: 25–28. <https://doi.org/10.30843/nzpp.2012.65.5420>
- Tyson J.L., Horner I.J., Curtis C.L., Blackmore A., Manning M.A., 2015. Influence of leaf age on infection of *Actinidia* species by *Pseudomonas syringae* pv *actinidiae*. *New Zealand Plant Protection* 68: 328–331. <https://doi.org/10.30843/nzpp.2015.68.5829>
- Vanneste J.L., Yu J., Cornish D.A., Max S., Clark G., 2011. Presence of *Pseudomonas syringae* pv *actinidiae* the causal agent of bacterial canker of kiwifruit on symptomatic and asymptomatic tissues of kiwifruit. *New Zealand Plant Protection* 64: 241–245. <https://doi.org/10.30843/nzpp.2011.64.5948>
- Vanneste J.L., 2017. The scientific, economic, and social impacts of the New Zealand outbreak of bacterial canker of kiwifruit (*Pseudomonas syringae* pv. *actinidiae*). *Annual Review of Phytopathology* 55: 377–399. <https://doi.org/10.1146/annurev-phyto-080516-035530>
- Visnovsky S.B., Marroni M.V., Pushparajah S., Everett K.R., Taylor R.K., ... Pitman A.R., 2019. Using multilocus sequence analysis to distinguish pathogenic from saprotrophic strains of *Pseudomonas* from stone fruit and kiwifruit. *European Journal of Plant Pathology* 155: 643–658. <https://doi.org/10.1007/s10658-019-01799-8>
- Wilkie J.P., Dye D.W., Watson D.R.W., 1973. Further hosts of *Pseudomonas viridiflava*. *New Zealand Journal of Agricultural Research* 16: 315–323. <https://doi.org/10.1080/00288233.1973.10421110>
- Young J.M., Cheesmur G.J., Welham F.V., Henshall W.R., 1988. Bacterial blight of kiwifruit. *Annals of Applied Biology* 112: 91–105. <https://doi.org/10.1111/j.1744-7348.1988.tb02044.x>
- Young J.M., Gardan L., Ren X.Z., Hu F.P., 1997. Genomic and phenotypic characterization of the bacterium causing blight of kiwifruit in New Zealand. *Plant Pathology* 46: 857–864. <https://doi.org/10.1046/j.1365-3059.1997.d01-72.x>
- Zar J.H., 1999. *Biostatistical Analysis*, 4th ed. Prentice-Hall International, London, UK, 663 pp.

Finito di stampare da
Logo s.r.l. - Borgoricco (PD) - Italia

Mediterranean Phytopathological Union

Founded by Antonio Ciccarone



The Mediterranean Phytopathological Union (MPU) is a non-profit society open to organizations and individuals involved in plant pathology with a specific interest in the aspects related to the Mediterranean area considered as an ecological region. The MPU was created with the aim of stimulating contacts among plant pathologists and facilitating the spread of information, news and scientific material on plant diseases occurring in the area. MPU also intends to facilitate and promote studies and research on diseases of Mediterranean crops and their control.

The MPU is affiliated to the International Society for Plant Pathology.

MPU Governing Board

President

DIMITRIOS TSITSIGIANNIS, Agricultural University of Athens, Greece – E-mail: dimtsi@aua.gr

Immediate Past President

ANTONIO F. LOGRIECO, National Research Council, Bari, Italy – E-mail: antonio.logrieco@ispa.cnr.it

Board members

BLANCA B. LANDA, Institute for Sustainable Agriculture-CSIC, Córdoba, Spain – E-mail: blanca.landa@csic.es

ANNA MARIA D' ONGHIA, CIHEAM/Mediterranean Agronomic Institute of Bari, Valenzano, Bari, Italy – E-mail: donghia@iamb.it

DIMITRIS TSALTAS, Cyprus University of Technology, Lemesos, Cyprus – E-mail: dimitris.tsaltas@cut.ac.cy

Honorary President - Treasurer

GIUSEPPE SURICO, DAGRI, University of Florence, Firenze, Italy - E-mail: giuseppe.surico@unifi.it

Secretary

ANNA MARIA D' ONGHIA, CIHEAM/Mediterranean Agronomic Institute of Bari, Valenzano, Bari, Italy – E-mail: donghia@iamb.it

Affiliated Societies

ARAB SOCIETY FOR PLANT PROTECTION (ASPP), <http://www.asplantprotection.org/>

FRENCH SOCIETY FOR PHYTOPATHOLOGY (FSP), <http://www.sfp-asso.org/>

HELLENIC PHYTOPATHOLOGICAL SOCIETY (HPS), <http://efe.aua.gr/>

ISRAELI PHYTOPATHOLOGICAL SOCIETY (IPS), <http://www.phytopathology.org.il/>

ITALIAN PHYTOPATHOLOGICAL SOCIETY (SIPAV), <http://www.sipav.org/>

PORTUGUESE PHYTOPATHOLOGICAL SOCIETY (PPS), <http://www.sffitopatologia.org/>

SPANISH SOCIETY FOR PLANT PATHOLOGY (SEF), <http://www.sef.es/sef/>

2023 MPU MEMBERSHIP DUES

INSTITUTIONAL MPU MEMBERSHIP: : € 200.00 (college and university departments, libraries and other facilities or organizations). Beside the open-access on-line version of *Phytopathologia Mediterranea*, the print version can be received with a € 50 contribution to mail charges (total € 250,00 to receive the print version). Researchers belonging to an Institution which is a member of the Union are entitled to publish with a reduced page contribution, as the Individual Regular members.

INDIVIDUAL REGULAR MPU MEMBERSHIP*: € 50.00 (free access to the open-access on-line version of *Phytopathologia Mediterranea* and can get the print version with a contribution to mail charges of € 50 (total € 100,00 to receive the print version).

*Students can join the MPU as a Student member on the recommendation of a Regular member. Student MPU members are entitled to a 50% reduction of the membership dues (proof of student status must be provided).

Payment information and online membership renewal and subscription at www.mpunion.com

For subscriptions and other information visit the MPU web site:

www.mpunion.com

or contact us at: Phone +39 39 055 2755861/862 – E-mail: phymed@unifi.it

Phytopathologia Mediterranea

Volume 62, April, 2023

Contents

- Identification of multi-race *Fusarium* wilt resistance in chickpea (*Cicer arietinum* L.) using rapid hydroponic phenotyping
J. Jorben, A. Rao, S. Nagappa Chowluru, S. Tomar, N. Kumar, C. Bharadwaj, B. Siddanagowda Patil, K. Ram Soren 3
- First report of *Leptosphaeria maculans* and *Leptosphaeria biglobosa* causing blackleg disease of oilseed rape in Tunisia
E. Maghrebi, O. Beldi, T. Ochi, B. Koopmann, H. Chaabane, B.A. Bahri 17
- First report of tomato leaf curl New Delhi virus in *Lagenaria siceraria* var. *longissima* in Italy
E. Troiano, G. Parrella 25
- Virulence of *Puccinia triticina* and *Puccinia tritici-duri* on durum wheat in southern Spain, from 2020 to 2022
J.N. Rodríguez-Vázquez, K. Ammar, I. Solís, F. Martínez-Moreno 29
- Colletotrichum* infections during flower development and fruit ripening in four olive cultivars
V. Moreira, M.J. Carbone, P. Mondino, S. Alaniz 35
- Diversity of *Botryosphaeriaceae* species associated with canker and dieback of avocado (*Persea americana*) in Italy
A. Fiorenza, G. Gusella, L. Vecchio, D. Aiello, G. Polizzi 47
- Virulence, genetic diversity, and putative geographical origin of sunflower broomrape populations in Morocco
A. Nabloussi, B. Pérez-Vich, L. Velasco 65
- Identification and characterization of fungi associated with leaf spot/blight and melting-out of turfgrass in Algeria
N. Bessadat, B. Hamon, N. Bataillé-Simoneau, N. Hamini-Kadar, M. Kihal, P. Simoneau 73
- TaqMan qPCR assays improve *Pseudomonas syringae* pv. actinidiae biovar 3 and *P. viridiflava* (PG07) detection within the *Pseudomonas* sp. community of kiwifruit
S. Campigli, S. Luti, T. Martellini, D. Rizzo, L. Bartolini, C. Carrai, J. Baskarathevan, L. Ghelardini, F. Peduto Hand, G. Marchi 95

Phytopathologia Mediterranea is an Open Access Journal published by Firenze University Press (available at www.fupress.com/pm/) and distributed under the terms of the Creative Commons Attribution 4.0 International License (CC-BY-4.0) which permits unrestricted use, distribution, and reproduction in any medium, provided you give appropriate credit to the original author(s) and the source, provide a link to the Creative Commons license, and indicate if changes were made.

The Creative Commons Public Domain Dedication (CC0 1.0) waiver applies to the data made available in this issue, unless otherwise stated.

Copyright © 2023 Authors. The authors retain all rights to the original work without any restrictions.

Phytopathologia Mediterranea is covered by AGRIS, BIOSIS, CAB, Chemical Abstracts, CSA, ELFIS, JSTOR, ISI, Web of Science, PHYTOMED, SCOPUS and more